EXPLOITING ANTHRACYCLINE-DNA ADDUCT FORMATION TO ENHANCE ANTHRACYCLINE ANTICANCER ACTIVITY

Submitted by Michal Ugarenko Bachelor of Medical Science with Honours

A thesis submitted in total fulfillment of the requirements for the degree of Doctor of Philosophy

> La Trobe Institute for Molecular Science Faculty of Science, Technology and Engineering La Trobe University Bundoora, Victoria 3086 Australia

> > September 2012

TABLE of CONTENTS

Table of Contents	i
Abstract	viii
Acknowledgements	
Statement of Authorship	xi
Abbreviations	xii

General Introduction 1
1.1 Basic Aspects of Cancer
1.2 Cancer Treatment
1.2.1 Surgery
1.2.2 Radiotherapy
1.2.3 Chemotherapy
1.2.3.1 Combination Chemotherapy
1.3 Anthracyclines
1.4 Doxorubicin
1.4.1 Discovery 11
1.4.2 Clinical Use 11
1.4.3 Mechanisms of Action 12
1.4.3.1 Topoisomerase-II Poisoning 13
1.4.3.2 DNA Adduct Formation
1.5 Formaldehyde
1.5.1 Endogenous Formaldehyde17
1.5.2 Formaldehyde from Doxorubicin
1.6 Formaldehyde-Releasing Prodrugs
1.6.1 AN-9
1.6.1.1 History
1.6.1.2 Anticancer Activity
1.6.1.3 Mouse Studies and Clinical Trials
1.6.2 Other Formaldehyde-Releasing Prodrugs

1.7 Combination of Anthracyclines with Formaldehyde-Releasing Prodrugs	. 23
1.7.1 In vitro studies	. 23
1.7.2 Mouse Studies	. 23
1.7.3 Pre-Activated Anthracyclines	. 24
1.8 DNA Adduct Formation vs. Topoisomerase-II Poisoning	. 26
1.9 Cellular Consequences of Anthracycline-DNA Adduct Formation	. 26
1.10 Limitations of Anthracyclines	. 28
1.10.1 Cardiotoxicity	. 30
1.10.2 Acquired Resistance	. 31
1.10.3 Intrinsic Resistance	. 32
1.11 Apoptosis	. 33
1.11.1 Apoptotic Pathways	. 33
1.11.2 Bcl-2 Family Proteins	. 35
1.11.2.1 Bax / Bak	. 37
1.11.2.2 BH3-Only Proteins	. 37
1.11.2.3 Anti-Apoptotic Proteins	. 38
1.11.3 Bcl-2 Family Interactions	. 38
1.12 Inhibiting Anti-Apoptotic Proteins	. 42
1.12.1 ABT-737 / ABT-263	. 43
1.13 Tumour Targeting	. 43
1.13.1 Drug Delivery	. 44
1.13.2 Targeting Signalling Pathways	. 45
1.14 Research Objectives	. 46

Materials and Methods 4	19
2.1 Cell Lines	50
2.2 Drugs and Compounds	51
2.2.1 Anthracyclines and Related Compounds 5	51
2.2.2 Formaldehyde-Releasing Prodrugs 5	52
2.2.3 Other Compounds	52
2.3 Immunoblotting 5	53
2.3.1 Preparation of Whole Cell Lysates	53

2.3.2 Determination of Protein Concentration and SDS-PAGE	
2.5.2 Determination of Freem Concentration and SDS FFEED	53
2.3.3 Western Transfer	53
2.3.4 Immunoprobing	54
2.4 Growth Inhibition Assay	54
2.5 Cell Viability Assays	57
2.5.1 Sub-G1 FACS Assay	57
2.5.2 Caspase-3 Activation Assay	57
2.5.3 Apoptotic Morphology Assay	59
2.5.3.1 Mitotic Catastrophe	60
2.5.4 Propidium Iodide Uptake Assay	60
2.6 Alkaling Cornet Assess (single call cal alectrophonesis)	
2.6 Alkaline Comet Assay (single cell gel electrophoresis)	62
2.6 Alkanne Comet Assay (single cell gel electrophoresis) 2.7 Nash Assay	
	63
2.7 Nash Assay	63 64
 2.7 Nash Assay 2.8 [¹⁴C]-Doxorubicin DNA Adduct Levels 	63 64 65
 2.7 Nash Assay 2.8 [¹⁴C]-Doxorubicin DNA Adduct Levels 2.9 siRNA Knockdown of Mcl-1 	63 64 65 67
 2.7 Nash Assay 2.8 [¹⁴C]-Doxorubicin DNA Adduct Levels 2.9 siRNA Knockdown of Mcl-1 2.10 Anti-FLAG Co-Immunoprecipitation 	63 64 65 67 68
 2.7 Nash Assay 2.8 [¹⁴C]-Doxorubicin DNA Adduct Levels 2.9 siRNA Knockdown of Mcl-1 2.10 Anti-FLAG Co-Immunoprecipitation 2.11 Mass Spectrometry 	 63 64 65 67 68 70
 2.7 Nash Assay 2.8 [¹⁴C]-Doxorubicin DNA Adduct Levels 2.9 siRNA Knockdown of Mcl-1 2.10 Anti-FLAG Co-Immunoprecipitation 2.11 Mass Spectrometry 2.12 Detection of the β3 Integrin Subunit by Flow Cytometry 	 63 64 65 67 68 70 71
 2.7 Nash Assay 2.8 [¹⁴C]-Doxorubicin DNA Adduct Levels 2.9 siRNA Knockdown of Mcl-1 2.10 Anti-FLAG Co-Immunoprecipitation	 63 64 65 67 68 70 71 72

ABT-737 Overcomes Bcl-2 Mediated Resistance to Doxorubicin-DNA Adducts	75
3.1 Introduction	76
3.1.1 Bcl-2	76
3.1.2 Targeting Anti-Apoptotic Proteins	77
3.1.2.1 Antisense-Based Strategies	77
3.1.2.2 BH3 Mimetics / Small Molecule Inhibitors	77
3.1.3 ABT-737	80
3.1.3.1 Discovery and Mechanism	80
3.1.3.2 Anticancer Activity	82
3.1.3.3 In vivo Studies	83
3.1.4 ABT-263	84

3.1.5 Mcl-1 Mediated Resistance to ABT-737 and ABT-263 85
3.1.6 Project Objectives
3.2 Results
3.2.1 Bcl-2 overexpressing HL-60 cell model
3.2.2 ABT-737 is cytotoxic as a single agent in HL-60 cells
3.2.3 Overexpression of Bcl-2 confers resistance to doxorubicin/AN-9 DNA-adduct
forming treatments
3.2.4 Nanomolar levels of ABT-737 overcomes Bcl-2 mediated resistance to
doxorubicin/AN-9 treatment
3.2.5 The triple treatment is synergistic in three independent apoptosis assays 100
3.2.6 Cell kill induced by the triple treatment is dependent on caspase-mediated apoptosis
3.2.7 Identifying the molecular mechanisms responsible for the synergy induced by the
triple treatment
3.2.7.1 The triple treatment does not affect Bcl-2 protein levels
3.2.7.2 Control compounds demonstrate that cell death induced by the triple treatment is
dependent on doxorubicin-DNA adduct formation116
3.2.7.3 Cell kill induced by the triple treatment is independent of topoisomerase-II
poisoning122
3.2.7.4 Increasing formaldehyde levels increases DNA adduct formation and apoptosis
3.2.8 ABT-737 is synergistic with doxorubicin as a single agent
3.2.9 ABT-737 overcomes Bcl-2 mediated resistance to etoposide
3.2.10 The triple treatment is synergistic in other cancer cell lines
3.2.11 Mcl-1 knockdown increases ABT-737 sensitivity in HCT116 cells 137
3.3 Discussion
3.3.1 Overexpression of Bcl-2 confers chemoresistance
3.3.2 ABT-737 as a single agent
3.3.3 ABT-737 overcomes Bcl-2 mediated chemoresistance to doxorubicin-DNA adduct
forming treatments
3.3.4. Identifying the molecular mechanisms responsible for the synergy induced by the
triple treatment
3.3.5 Mcl-1 mediated resistance to ABT-737 154

3.3.6 Clinical implications of ABT-737 and the triple treatment	. 156
3.3.7 Conclusions	158

Using Doxazolidine to Demonstrate That Bcl-2 Overexpression Provides Only Short-
Term Resistance to Doxorubicin-DNA Adducts in HL-60 Cells 159
4.1 Introduction
4.1.1 Pre-Activated Anthracyclines
4.1.1.1 Barminomycin
4.1.1.2 Doxoform and Doxazolidine
4.1.2 Project Objectives
4.2 Results
4.2.1 Doxazolidine displays much greater cytotoxicity than doxorubicin and the
combination of doxorubicin with AN-9 in cancer cells
4.2.2 Overexpression of Bcl-2 confers resistance to short-term doxazolidine treatments in
HL-60 cells which can be overcome by ABT-737 166
4.2.3 Bcl-2 overexpressing HL-60 cells become sensitive to doxazolidine treatment over
time
4.2.4 The increase in sensitivity of Bcl-2 overexpressing HL-60 cells to doxazolidine
appears to be mediated by apoptosis and not other forms of cell death 173
4.2.5 Bcl-2 mediated resistance is also overcome in response to longer-term doxorubicin
and doxorubicin/AN-9 treatments
4.2.6 Investigating the mechanism/s responsible for overcoming Bcl-2 mediated resistance
in HL-60 cells
4.2.6.1 Is apoptosis induced by Rad9/Bcl-2 interactions?
4.2.6.2 Using mass spectrometry to identify Bcl-2 binding partners
4.3 Discussion
4.3.1 Doxazolidine induces rapid cell kill without the requirement of formaldehyde 193
4.3.2 Targeting doxorubicin-formaldehyde conjugates
4.3.3 Bcl-2 mediated resistance to doxazolidine treatment is short-lived 197
4.3.4 Short-lived Bcl-2 mediated resistance is not just limited to doxazolidine treatment199
4.3.5 What is the mechanism responsible for overcoming Bcl-2 mediated resistance? 201
4.3.6 Conclusions

Assessment of the $\alpha v\beta 3$ Integrin as a Method of Targeting Doxorubicin-DNA Adducts
to Tumours
5.1 Introduction
5.1.1 Targeting Angiogenesis and Metastasis
5.1.2 Integrins
5.1.2.1 Integrin Structure
5.1.2.2 Ligand Binding
5.1.2.3 Integrin Activation (Inside-Out Signalling)
5.1.2.4 Integrin Function (Outside-In Signalling)
5.1.2.5 Integrins and Cancer
5.1.3 The αvβ3 Integrin
5.1.4 Targeting the αvβ3 Integrin
5.1.4.1 Antibodies
5.1.4.2 RGD Peptides
5.1.5 Project Objectives
5.2 Results
5.2.1 αvβ3 integrin expressing cell models
5.2.2 The $\alpha\nu\beta$ 3 integrin does not affect doxorubicin-DNA adduct formation
5.2.3 Doxorubicin-DNA adduct-forming treatments cause synergistic cell death in highly
invasive, αvβ3 integrin expressing cancer cells
5.2.4 The $\alpha\nu\beta3$ integrin promotes adhesion and invasion of 66cl4 and 4T1.2 cancer cells
5.2.5 The c(RGDfK) peptide inhibits the ability of the $\alpha\nu\beta3$ integrin to promote adhesion
5.2.6 The c(RGDfK) peptide does not interfere with doxorubicin/AN-9 mediated cell kill
5.2.7 Mouse studies highlight the potential of targeting doxorubicin-DNA adducts to $\alpha\nu\beta3$
integrin expressing tumours
5.3 Discussion
5.3.1 The αvβ3 integrin is a highly suitable anti-cancer target
5.3.2 Doxorubicin-DNA adduct formation and resulting cytotoxicity is unaffected by $\alpha v\beta 3$
integrin levels

5.3.3 RGD peptides can effectively inhibit $\alpha\nu\beta3$ integrin function without	affecting
doxorubicin/AN-9 induced apoptosis	259
5.3.4 Using a mouse model to evaluate the potential success of targeting doxorubi	cin-DNA
adducts to $\alpha v\beta 3$ integrin expressing tumours	260
5.3.5 Clinical implications of RGD peptide-based targeting strategies	263
5.3.5.1 RGD peptides display a dual response	263
5.3.5.2 RGD peptide-based targeting of chemotherapeutics	264
5.3.6 Conclusions	266

General Discussion and Future Directions	
6.1 General Discussion	
6.1.1 Advantages of Anthracycline-DNA Adduct Formation	
6.1.1.1 Cardiotoxicity	
6.1.1.2 Resistance	270
6.1.2 Overcoming Bcl-2 Mediated Resistance	270
6.1.3 Targeting Anthracycline-DNA Adducts to Tumours	272
6.2 Conclusions	
6.3 Future Directions	
6.3.1 Overcoming Bcl-2 Resistance with ABT-737 / ABT-263	278
6.3.2 Short-Lived Bcl-2 Mediated Resistance	
6.3.3 RGD-Based Targeting of DNA Adduct Forming Treatments to $\alpha\nu\beta3$	Expressing
Cancer Cells	

References

ABSTRACT

The anthracycline anticancer agent doxorubicin functions primarily as a topoisomerase-II poison, but forms more cytotoxic DNA adducts in the presence of formaldehyde. The combination of formaldehyde-releasing prodrugs (such as AN-9) with doxorubicin has been shown to result in synergistic DNA adduct formation and synergistic levels of cell kill in a wide range of cancer cells, thus, providing a new avenue for enhancing the anticancer efficacy of doxorubicin. However, as with most chemotherapeutic treatments, the therapeutic potential of anthracycline-DNA adduct forming treatments may be limited by tumour cell resistance and adverse side-effects. The overall aim of this project was to assess potential methods of overcoming these limiting factors.

Many cancer types express high levels of anti-apoptotic proteins such as Bcl-2 which confer resistance to chemotherapeutics, including anthracycline-DNA adduct forming treatments. The Bcl-2 inhibitor ABT-737 was shown to be highly synergistic with doxorubicin/AN-9 short-term (<8 hr) treatments in Bcl-2 overexpressing HL-60 cancer cells, completely overcoming resistance. Therefore, the addition of ABT-737 to form a 'triple treatment' of doxorubicin/AN-9/ABT-737 may render previously resistant cancer cells sensitive to anthracycline-DNA adduct forming treatments. Over longer treatment times, however, Bcl-2 overexpressing HL-60 cells became increasingly sensitive to apoptosis resulting from doxorubicin-DNA adduct forming treatments. The mechanisms involved in overcoming this resistance are unclear but may involve Bcl-2 interactions with pro-apoptotic proteins which tip the balance in favour of apoptosis. This suggests that the DNA damage caused by these anthracycline treatments may be sufficient to overcome Bcl-2 mediated resistance.

Targeting anthracycline-DNA adduct formation to the tumour site can potentially allow more specific cancer cell kill to reduce adverse side-effects and reduce drug doses. The $\alpha\nu\beta3$ integrin is highly expressed on invasive cancer cells and is a suitable candidate to target. Doxorubicin/AN-9 treatments were shown to be cytotoxic to mouse mammary epithelial cancer cells expressing high levels of $\alpha\nu\beta3$ integrin *in vitro*, and to reduce tumour size *in vivo* in a high $\alpha\nu\beta3$ integrin expressing mouse model. RGD peptides inhibit $\alpha\nu\beta3$ integrin activity

and may therefore be used to target DNA adduct forming treatments to invasive cancer cells expressing high levels of $\alpha v\beta 3$ integrin.

Overall, the findings from this project illustrate that anthracycline-DNA adduct forming treatments possess a high degree of anticancer potential, which may be enhanced further by overcoming Bcl-2 mediated resistance and/or developing tumour-specific targeting strategies.

ACKNOWLEDGEMENTS

First of all I would like to greatly thank my supervisors Suzi Cutts and Don Phillips for their continual support, encouragement, scientific discussions, and words of wisdom over the years. It has been a privilege and honour to perform my studies in your laboratory. The SMC/DRP laboratory has been such a great environment and I have made many friends over the years, so I'd like to thank all current (Dave, Paul, Jelena) and previous members (Rob, Benny, Oula, Bec, Lonnie, Kate, Damian, and Jeffri) of the lab for making it such a relaxed and friendly place to do a PhD.

The Biochemistry Department at La Trobe University has been an inspirational place with people full of advice, knowledge and character, so thankyou to all my colleagues who helped me along the way in my research, as well as providing many social memories.

Finally, I'd like to thank my parents for their amazing support throughout life and always encouraging me to do my best.

STATEMENT of AUTHORSHIP

Except where reference is made in the text of the thesis, this thesis contains no material published elsewhere or extracted in whole or in part from a thesis submitted for the award of any other degree or diploma.

No other person's work has been used without due acknowledgment in the main text of the thesis.

The thesis has not been submitted for the award of any degree of diploma in any other tertiary institution.

Signed

Michal Ugarenko

ABBREVIATIONS

ALL	Acute lymphoblastic leukemia				
ATM	Ataxia telangiectasia mutated				
ATR	Ataxia telangiectasia and Rad3 relate				
AML	Acute myeloid leukemia				
AMS	Accelerator mass spectrometry				
BSA	Bovine serum albumin				
CLL	Chronic lymphocytic leukemia				
Co-IP	Co-immunoprecipitation				
DISC	Death-inducing signalling complex				
DMSO	Dimethyl sulphoxide				
DNA	Deoxyribonucleic acid				
DOX	Doxorubicin				
DOXAZ	Doxazolidine				
DTT	Dithiothreitol				
DXZ	Doxazolidine				
ECM	Extracellular matrix				
EDTA	Ethylenediaminetetraacetic acid				
EGFR	Epidermal growth factor receptor				
EPR	Enhanced penetration and retention				
FACS	Fluorescence-activated cell sorting				
FADD	Fas-associated death domain				
FBS	Fetal bovine serum				
FDA	Food and drug administration				
FGF	Fibroblast growth factor				
FITC	Fluorescein isothiocyanate				
FL	Follicular lymphoma				
HDAC	Histone deacetylase				
HR	Homologous recombination				
HSA	Human serum albumin				
IC ₅₀	50% growth inhibitory concentration				

IMD	Integrin-mediated death					
LF	Lipofectamine					
MALDI	Matrix assisted laser desorption ionization					
MEM	Minimal essential medium					
MOMP	Mitochondrial outer membrane permeabilization					
MS	Mass spectrometry					
MTS	3-(4,5-dimethylthiazol-2-yl)-5-(3-carboxymethoxyphenyl)-2-(4-sulfophenyl)-					
	2H-tetrazolium, inner salt					
NER	Nucleotide excision repair					
NMR	Nuclear magnetic resonance					
NSCLC	Non-small cell lung carcinoma					
OTM	Olive tail moment					
PAGE	Polyacrylamide gel electrophoresis					
PBMC	Peripheral blood mononuclear cells					
PBS	Phosphate-buffered saline					
P-gp	Permeability-glycoprotein					
PI	Propidium iodide					
PMS	Phenazine methosulfate					
PMSF	Phenylmethylsulphonyl fluoride					
PPD	Pentyl-PABC-DOXAZ					
pRS	pRetroSuper					
PVDF	Polyvinylidene fluoride					
RIP1	Receptor-interacting protein 1					
RNA	Ribonucleic acid					
ROS	Reactive oxygen species					
SCID	Severe combined immunodeficiency					
SCLC	Small cell lung carcinoma					
SDS	Sodium dodecyl sulphate					
TBS	Tris-buffered saline					
TE	Tris-EDTA					
THRAP3	Thyroid hormone receptor-associated protein 3					
TOF	Time of flight					
VEGF	Vascular endothelial growth factor					

VEGFR2 Vascular endothelial growth factor receptor-2

WT Wild-type

Chapter 1

GENERAL INTRODUCTION

1.1 BASIC ASPECTS OF CANCER

At the cellular level a variety of normal regulatory processes exist which are fundamental in controlling cell behaviour, including proliferation, motility and death. Cancer is recognized as a state where these regulatory processes are upset, leading to uncontrolled growth and division of cells. Genetic alterations in the form of mutations and chromosomal damage initiate the onset of cancer by transforming normal cells into invasive, malignant cancer cells. These altered cells divide uncontrollably to form a colony of cancer cells resulting in the formation of a tumour. Tumours can be classified as either benign where the disease remains localized, or malignant where the disease invades surrounding tissues and metastasizes to other sites in the body, forming secondary areas of proliferation. When the disease metastasizes to other tissues and organs it is associated with a poor prognosis since this has the greatest impact on the patient's health and can lead to organ failure and death. The leading cancer types for new cases and deaths in the USA for 2012 are shown in Figure 1.1.

Cancer formation is generally considered to be a multi-step process requiring an accumulation of genetic alterations over the lifetime of an individual (Ruddon, 2007). Typically, a series of mutations in multiple genes that play important roles in normal cellular regulation are necessary to progressively drive a cell to become cancerous. For example, it is well established that colorectal cancer arises from mutations that occur in a defined order, thus providing evidence for the requirement of 'multiple-hits' for cancer development (Fearon and Vogelstein, 1990). Most cancers typically arise later in life for the reason that these mutations often take years to accumulate after a lifetime's exposure to various carcinogens. These mutations occur mainly in somatic cells and not in germ-line cells and therefore are not passed on to future generations, although there are exceptions such as familial breast cancer (Ford *et al.*, 1998).

Hanahan and Weinberg (2000) proposed that as normal, healthy cells are subjected to 'multiple hits', six essential cellular physiological processes become altered that enable the cells to progressively become cancerous. These processes called the six hallmarks of cancer are shown in Figure 1.2A and include; sustaining proliferative signalling, evading growth suppressors, activating invasion and metastasis, enabling replicative immortality, inducing

			Males	Female	95		
Prostate	241,740	29%			Breast	226,870	29%
Lung & bronchus	116,470	14%			Lung & bronchus	109,690	14%
Colon & rectum	73,420	9%		T	Colon & rectum	70,040	9%
Urinary bladder	55,600	7%			Uterine corpus	47,130	6%
Melanoma of the skin	44,250	5%			Thyroid	43,210	5%
Kidney & renal pelvis	40,250	5%			Melanoma of the skin	32,000	4%
Non-Hodgkin lymphoma	38,160	4%			Non-Hodgkin lymphoma	31,970	4%
Oral cavity & pharynx	28,540	3%			Kidney & renal pelvis	24,520	3%
Leukemia	26,830	3%			Ovary	22,280	3%
Pancreas	22,090	3%			Pancreas	21,830	3%
All Sites	848,170	100%			All Sites	790,740	100%
All Sites	848,170	100%	Males	Female		790,740	100%
	848,170 87,750	100% 29%	Males	Female		790,740 72,590	100% 26%
mated Deaths			Males	Female	28		26%
mated Deaths Lung & bronchus	87,750	29%	Males	Female	2 S Lung & bronchus	72,590	26% 14%
mated Deaths Lung & bronchus Prostate	87,750 28,170	29% 9%	Males	Female	25 Lung & bronchus Breast	72,590 39,510	26% 14% 9%
mated Deaths Lung & bronchus Prostate Colon & rectum	87,750 28,170 26,470	29% 9% 9%	Males	Female	25 Lung & bronchus Breast Colon & rectum	72,590 39,510 25,220	26% 14% 9% 7%
mated Deaths Lung & bronchus Prostate Colon & rectum Pancreas	87,750 28,170 26,470 18,850	29% 9% 9% 6%	Males	Female	es Lung & bronchus Breast Colon & rectum Pancreas	72,590 39,510 25,220 18,540	26% 14% 9% 7% 6%
mated Deaths Lung & bronchus Prostate Colon & rectum Pancreas Liver & intrahepatic bile duct	87,750 28,170 26,470 18,850 13,980	29% 9% 9% 6% 5%	Males	Female	25 Lung & bronchus Breast Colon & rectum Pancreas Ovary	72,590 39,510 25,220 18,540 15,500	26% 14% 9% 7% 6% 4%
mated Deaths Lung & bronchus Prostate Colon & rectum Pancreas Liver & intrahepatic bile duct Leukemia	87,750 28,170 26,470 18,850 13,980 13,500	29% 9% 9% 6% 5% 4%	Males	Female	25 Lung & bronchus Breast Colon & rectum Pancreas Ovary Leukemia	72,590 39,510 25,220 18,540 15,500 10,040	26% 14% 9% 7% 6% 4% 3%
mated Deaths Lung & bronchus Prostate Colon & rectum Pancreas Liver & intrahepatic bile duct Leukemia Esophagus	87,750 28,170 26,470 18,850 13,980 13,500 12,040	29% 9% 9% 6% 5% 4%	Males	Female	2S Lung & bronchus Breast Colon & rectum Pancreas Ovary Leukemia Non-Hodgkin lymphoma	72,590 39,510 25,220 18,540 15,500 10,040 8,620	26% 14% 9% 7% 6% 4% 3% 3%
mated Deaths Lung & bronchus Prostate Colon & rectum Pancreas Liver & intrahepatic bile duct Leukemia Esophagus Urinary bladder	87,750 28,170 26,470 18,850 13,980 13,500 12,040 10,510	29% 9% 6% 5% 4% 3%	Males	Female	25 Lung & bronchus Breast Colon & rectum Pancreas Ovary Leukemia Non-Hodgkin lymphoma Uterine Corpus	72,590 39,510 25,220 18,540 15,500 10,040 8,620 8,010	

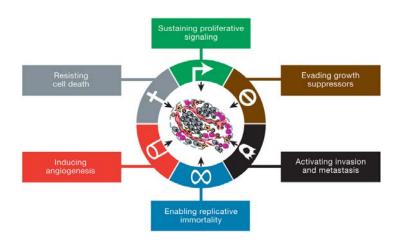
Figure 1.1. The ten leading cancer types for estimated new cases and deaths by sex in the USA for 2012 (Siegel *et al.*, 2012).

angiogenesis, and resisting cell death. Since these six hallmarks were proposed, continual research has allowed a greater understanding of cancer progression and as such additional hallmarks have been proposed which are outlined in Figure 1.2B (Hanahan and Weinberg, 2011). Developing specific drugs and strategies that prevent cells from acquiring these hallmarks is crucial to stop tumour growth and cancer progression. Figure 1.2B also lists classes of compounds that have been identified to target the pathways and proteins that are implicated in each of the hallmarks of cancer.

Mutations in two classes of genes, namely oncogenes and tumour-suppressor genes have been implicated in the onset of cancer and the acquisition of the hallmarks of cancer (DeVita *et al.*, 2005). Proto-oncogenes are genes that are involved in promoting cell growth and proliferation and can be converted into cancer-inducing oncogenes by mutations or increased expression of the gene product. Examples of proto-oncogenes that undergo a 'gain in function' to become oncogenes include transcription factors such as myc, and anti-apoptotic proteins such as Bcl-2. Tumour-suppressor genes on the other hand are genes that contribute to cancer progression when they undergo a 'loss of function'. The best studied example is the p53 gene which is mutated in approximately half of all cancers (Levine, 1997).

Mutations in proto-oncogenes and tumour-suppressor genes may arise from exposure to various chemicals and ultraviolet radiation. While spontaneous mutations arising from inherent errors in DNA replication and repair may contribute to cancer, numerous types of cancers are linked to exposure to industrial pollutants, chemicals in cigarettes, radiation from sunlight, and dietary factors (Ruddon, 2007). For example, the incidence of lung cancer in both males and females is strongly linked to cigarette smoking (Boyle and Maisonneuve, 1995), and cancers of the mouth, larynx, pharynx and esophagus have also been correlated with tobacco use (Stellman and Resnicow, 1997). Skin cancer is also directly linked to the amount of sunlight exposure (Peto, 2001).

Most of the major cancer risk factors including smoking, alcohol consumption and exposure to sunlight are avoidable, and the correlation of these risk factors with cancer has lead to a decline in cancer death rates over the last 20 years (Jemal *et al.*, 2010). Despite this, the global death rate due to cancer in 2008 was estimated to be greater than 7 million people with over 12 million new cases diagnosed (Ferlay *et al.*, 2010), and it is predicted that one in



B

Α

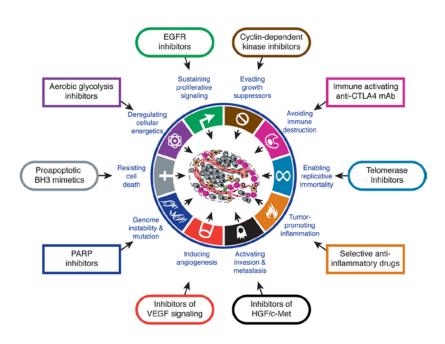


Figure 1.2. The hallmarks of cancer.

The original six hallmarks of cancer (A) proposed in 2000 (taken from Hanahan and Weinberg, 2011), and (B) the revised hallmarks of cancer (Hanahan and Weinberg, 2011). Classes of compounds that are aimed at targeting each of the hallmarks are also shown.

every three people will develop cancer at some stage during their life-time. Therefore, it is without doubt that ongoing research is required to better understand the basis of cancer in the hope of developing improved therapies.

1.2 CANCER TREATMENT

1.2.1 Surgery

Surgery can be a safe treatment method especially with advances in surgical techniques to cure cancer patients with confined solid tumours. For example, surgery alone is used to treat skin cancer patients with primary melanomas resulting in a 90% cure rate (DeVita *et al.*, 2005). However, since a high percentage of cancer patients with solid tumours will have already developed secondary metastases, surgery is often used to resect the bulk of the tumour and is combined with other treatment modalities to control the remaining disease (McCarter and Fong, 2001). Another limitation is that surgery cannot be used to treat non-solid tumours such as leukemias and lymphomas. The use of surgery does have other benefits, especially laparoscopic surgery which is used by surgeons for visual diagnosis and monitoring of several cancer types (DeVita *et al.*, 2008).

1.2.2 Radiotherapy

Radiotherapy, which is used in approximately half of all cancer patients, involves the use of high-energy waves (including gamma rays, X-rays and charged particles) to induce DNA damage and kill tumour cells (Samant and Gooi, 2005). Most of the DNA damage occurs via indirect ionization which in the presence of oxygen leads to the formation of free radicals that react with DNA and cause DNA strand breaks. Normal cells are also susceptible to damage induced by radiation therapy and therefore to reduce side-effects the treatment is fractionated to allow normal cells to repair damage and recover (Rice, 1997). Radiotherapy is commonly used to treat breast, prostate, lung, and gastrointestinal cancers, and is effective against painful bone metastases and spinal cord compression due to tumour growth, however, it is limited if there is extensive involvement of critical organs such as liver or lung metastases

(Samant and Gooi, 2005). Since solid tumours consist of hypoxic regions and due to the importance of cellular oxygen in inducing the DNA damage, tumour cells can be resistant to radiotherapy (Harrison *et al.*, 2002).

1.2.3 Chemotherapy

Chemotherapy involves the use of drugs (either natural or synthetic) to destroy cancer cells, for example by damaging DNA or affecting mitosis, and setting off a cascade of events that eventually leads to cell death. Virtually all chemotherapeutic drugs once administered act non-specifically and exert their effects on rapidly growing and dividing cells, including cancer cells which proliferate uncontrollably. However, actively growing normal cells of the body (including cells lining the gastrointestinal tract and bone marrow cells) are also susceptible and this leads to unwanted side-effects which limit the therapeutic potential of many anticancer drugs. Normal cells do however have the ability to recover from exposure to DNA-damaging anticancer drugs since the mechanisms involved in DNA repair and cell-cycle arrest are intact in comparison to cancer cells. Chemotherapeutics are often divided into classes based on their mechanism of action. These classes include the alkylating agents, antimetabolites, anti-microtubule agents, topoisomerase inhibitors and anti-hormonal agents, and examples of drugs in each of these classes are outlined in Table 1.1.

One of the major advantages of chemotherapy over other treatment modalities is that it is given systemically and therefore can be effective against non-solid tumours and can be used to treat metastatic disease. Chemotherapy is also often combined with surgery and radiotherapy to maximize the potential to eradicate the cancer. In neoadjuvant chemotherapy, the cancer is initially treated with chemotherapy to reduce the size of the tumour and make it easier to treat via other modalities. In adjuvant chemotherapy, anticancer drugs are used after surgery or radiation to eliminate the remaining cancer cells.

1.2.3.1 Combination Chemotherapy

Single agent chemotherapy very rarely leads to a complete cure of cancer due to the presence of drug-resistant cancer cells in the tumour population. Therefore, anticancer drugs are more **Table 1.1**. Major classes of clinically used chemotherapeutics (based on Brighton and Wood,2005).

Class of chemotherapeutics	Examples in clinical use
Alkylating agents	Melphalan, cyclophosphamide, chlorambucin Platinum-containing drugs – cisplatin, carboplatin
Anti-metabolites	5-fluorouracil, cytarabine, methotrexate, gemcitabine
Anti-microtubule agents	Taxanes – paclitaxel, docataxel Vinca alkaloids – vincristine, vinblastine
Topoisomerase inhibitors	Anthracyclines - doxorubicin, daunorubicin Anthracenediones – mitoxantrone Camptothecins – topotecan, irinotecan
Anti-hormonal agents	Tamoxifen

commonly utilized in combination chemotherapy where two or more drugs are used in an attempt to minimize the development of resistant cancer cells and maximize tumour cell kill. In order to achieve this, the drugs used should be partially effective against the particular tumour, have different mechanisms of action, and have minimal overlapping toxicities. Preclinical testing on cancer cells in culture and animal models can reveal synergistic drug combinations which can then be applied in a clinical setting to determine if the new combination is more effective than the single agents. For example, breast cancer is commonly treated with the CMF (cyclophosphamide, methotrexate and 5-fluorouracil) combination regimen (Bonadonna *et al.*, 2005). In certain circumstances it is more beneficial to use alternating or sequential regimens rather than simultaneous regimens to allow higher drug doses to be used (Crown *et al.*, 2004). With greater understanding of the pathways affected in cancer cells and a greater understanding of the mechanisms of anticancer drugs, optimal combinations of drugs can be chosen to treat a particular cancer to achieve a maximal effect.

1.3 ANTHRACYCLINES

The anthracyclines are a group of anticancer drugs that have been used in the clinic since the 1960's and today have one of the widest ranges of therapeutic use of any class of chemotherapeutics. The first anthracycline was discovered in 1958 after isolation from a new species of soil bacterium, *Streptomyces peucetius* (Di Marco *et al.*, 1964). The bacterium produced a red antibiotic which was purified independently by two separate groups in Italy and France and was named daunorubicin (Weiss, 1992). This compound displayed antibacterial and antifungal effects, but also was found to be active against a number of murine tumours (Di Marco *et al.*, 1964). In 1964, clinical trials of daunorubicin began and the compound was found to be especially effective against acute leukemia (Tan *et al.*, 1967), for which it is still used today (DeVita *et al.*, 2005). The most clinically useful anthracyclines used currently are daunorubicin, doxorubicin, idarubicin and epirubicin, and the structures of these drugs are shown in Figure 1.3. All the anthracyclines consist of a rigid, planar four-

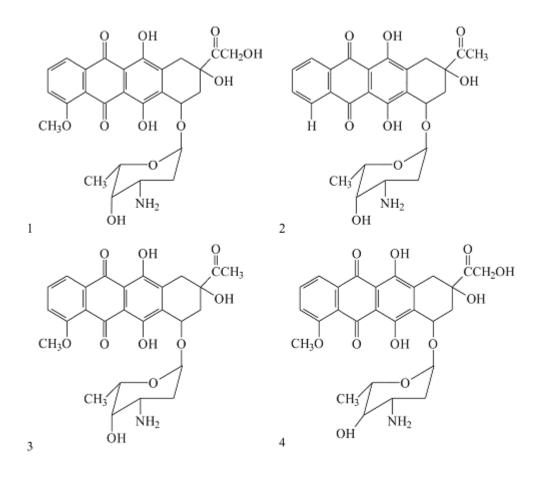


Figure 1.3. Structures of four clinically important anthracyclines: (1) doxorubicin, (2) idarubicin, (3) daunorubicin, and (4) epirubicin.

membered ring system containing an anthraquinone chromophore linked by a glycosidic bond to a daunosamine sugar group (DeVita *et al.*, 2005).

1.4 DOXORUBICIN

1.4.1 Discovery

Following the discovery that daunorubicin displayed anticancer properties, there was a search to find more active derivatives of the compound. Arcamone and colleagues (1969) subjected the daunorubicin producing Streptomyces bacterium to the mutagen N-nitroso-N-methyl urethane which generated a mutant strain, *Streptomyces peucetius* var *caesius* (Arcamone *et al.*, 1969). This mutant strain was discovered to produce a modified antibiotic with a slightly altered structure. The compound was called Adriamycin and was later given the international non-propriety name of doxorubicin (from this point on the name doxorubicin will be used). As depicted in Figure 1.3, the structure of doxorubicin differs by only a single hydroxyl group from daunorubicin. Despite the minor difference in structure, doxorubicin was shown to have greater activity against murine tumours (Di Marco *et al.*, 1969), and was shown to display a wider spectrum of activity against human tumours (Bonadonna *et al.*, 1970; Tan *et al.*, 1973), and in 1974 was approved for clinical use.

1.4.2 Clinical Use

While the use of daunorubicin is currently limited to treatment of acute myelocytic and lymphocytic leukemias, doxorubicin is effective against a broad range of cancers, and is commonly utilized in combination chemotherapy with drugs that have a complimentary mechanism of action (Stathopoulos *et al.*, 1995; Pawlicki *et al.*, 2002). Doxorubicin is particularly effective against solid tumours including breast, lung, ovarian, liver and thyroid carcinomas, as well as Hodgkin's and non-Hodgkin's lymphomas, multiple myeloma and myelogenous and lymphoid leukemias (DeVita *et al.*, 2005).

Doxorubicin is most often administered to patients as an intravenous injection and has a triphasic elimination profile. As the drug rapidly concentrates into tissues and cells around the body it has an initial distribution half-life of 5-10 minutes, followed by a secondary half-life of 1-3 hours, and a terminal elimination half-life of 24-50 hours (Camaggi *et al.*, 1988; DeVita *et al.*, 2005). The plasma concentration of doxorubicin after bolus administration generally falls in the range of 1-2 μ M and quickly declines to nanomolar concentrations within 1 hour (Gewirtz, 1999). Therefore, potential mechanisms of doxorubicin action studied *in vitro* should reflect submicromolar concentrations. The clearance of doxorubicin from the body occurs predominantly by metabolism and biliary excretion (DeVita *et al.*, 2005). In the liver, doxorubicin is rapidly converted to metabolites, with the major metabolite being the less active doxorubicinol (Vaclavikova *et al.*, 2008). The majority of the administered doxorubicin and the metabolites are then excreted in the bile and faeces with a smaller amount being excreted in urine (Seyffart, 1991; DeVita *et al.*, 2005).

As with most chemotherapeutics, the use of doxorubicin in the clinic has limitations, the most significant being cardiotoxic side effects, and the development of resistance in the tumour population (these limitations will be discussed in more detail in Section 1.10). Due to the effectiveness of doxorubicin against many cancer types there has been a worldwide effort to develop doxorubicin analogues that are less cardiotoxic and more active against doxorubicin resistant tumours. Over the years more than 2,000 analogues have been developed, but to this day doxorubicin remains as the most widely used anthracycline in the clinic (Weiss, 1992).

1.4.3 Mechanisms of Action

The exact mechanisms of action of doxorubicin (and other anthracyclines) are still being resolved, but are likely to involve multiple different pathways. Potential targets for doxorubicin mechanism of action have been reviewed in detail elsewhere (Gewirtz, 1999; Minotti *et al.*, 2004), although only the mechanisms occurring at clinical concentrations of doxorubicin are of relevance. Doxorubicin rapidly enters cells via passive diffusion and appears to exert its major effects in the nucleus (Gigli *et al.*, 1988; Coley *et al.*, 1993). The primary target of doxorubicin action is DNA, as highlighted by the finding that >99% of the

drug in the nucleus is associated with DNA (Gigli *et al.*, 1988), and a study of human tumour biopsies showing that over 80% of the drug is associated with DNA (Cummings and McArdle, 1986). Due to its rigid planar structure, doxorubicin is able to intercalate between DNA base pairs with the daunosamine sugar group fitting into the minor groove (Manfait *et al.*, 1982). There appears to be two distinct interactions of doxorubicin with DNA that relate to the cytotoxicity of the drug at pharmacologically relevant doses: (1) impairment of the action of the enzyme topoisomerase-II, and (2) the formation of doxorubicin-DNA adducts.

1.4.3.1 Topoisomerase-II Poisoning

The primary action of doxorubicin and other anthracyclines appears to be the poisoning of the enzyme topoisomerase-II which regulates the degree of supercoiling in double-stranded DNA, and is especially important for DNA replication and transcription (Wang, 1996). Studies in the late 1970's and early 1980's showed that treatment with doxorubicin resulted in DNA strand breaks (Ross et al., 1978; Ross and Bradley, 1981), and in 1984 the enzyme topoisomerase-II was identified as being the target for doxorubicin action (Tewey et al., 1984). Topoisomerase-II cleaves double stranded DNA and facilitates the passage of another segment of DNA through the break in an energy-dependent reaction (Liu et al., 1980; Liu et al., 1983). The two strands are then re-ligated and the enzyme dissociates from the double helix which now has an altered topological state and allows access for DNA and RNA polymerases (Corbett and Osheroff, 1993). Doxorubicin interferes with this process by intercalating into DNA, leading to the formation of ternary drug-DNA-topoisomerase-II cleavable complexes (Tewey *et al.*, 1984). The presence of these cleavable complexes stalls topoisomerase-II enzymatic activity preventing the re-ligation step, and the DNA remains cleaved, resulting in double-stranded DNA breaks (Tewey et al., 1984). Ultimately, an accumulation of double-stranded DNA breaks leads to cell-cycle arrest and cell death via apoptosis (Bellarosa et al., 2001; Swift et al., 2006). There is strong evidence to indicate that topoisomerase-II poisoning is a major mechanism of doxorubicin action *in vivo* including findings that the resulting DNA damage occurs at clinical levels of the drug (Tewey et al., 1984; Bellarosa et al., 2001), and that some types of resistant tumour cells have reduced levels or altered activity of topoisomerase-II (Deffie et al., 1989; Webb et al., 1991). Despite this evidence, it has been demonstrated that doxorubicin is able to kill cancer cells via another mechanism as outlined in the next section (Cutts et al., 2001; Swift et al., 2006).

1.4.3.2 DNA Adduct Formation

Over the past 20 years the Cutts/Phillips laboratory have been instrumental in demonstrating that doxorubicin functions via another mechanism - the formation of covalent adducts with DNA. Evidence that doxorubicin is able to form adducts with DNA evolved in the early 1980's (Sinha, 1980; Sinha and Gregory, 1981; Sinha *et al.*, 1984), and in 1990 *in vitro* transcriptional footprinting studies showed that these adducts form predominantly at 5'-GC-3' sequences on DNA since long-lived transcription blockages were detected at these sites (Cullinane and Phillips, 1990). Subsequently, it was demonstrated that doxorubicin-DNA adducts form optimally at 37 °C and pH 7 (Cullinane *et al.*, 1994). An important discovery in the mid-1990's was that the buffer (Tris/DTT) used in earlier *in vitro* studies where doxorubicin-DNA adduct formation was reported, released formaldehyde and that formaldehyde appeared to be critical in the formation of DNA adducts (Taatjes *et al.*, 1997a).

The structure of the doxorubicin-DNA adduct has been characterized *in vitro* by 2D NMR (Zeman et al., 1998) and mass spectrometry (Taatjes et al., 1996; Taatjes et al., 1997b), and was consistent with an earlier X-ray crystal structure of a daunorubicin-DNA adduct (Wang et al., 1991). The 2D NMR structure of the doxorubicin-DNA adduct is shown in Figure 1.4. The doxorubicin chromophore intercalates between C and N of 5'-GCN-3' sequences (Zeman et al., 1998), and the doxorubicin sugar group (daunosamine) projects into the DNA minor groove (Wang et al., 1991). The daunosamine sugar group is connected to the N-2 amino of guanine via a single N-C-N (aminal) covalent bond (Wang et al., 1991; Zeman et al., 1998). It has been unambiguously demonstrated that the central carbon atom from the aminal bond originates from formaldehyde, hence formaldehyde is a necessity for adduct formation (Taatjes et al., 1996; Taatjes et al., 1997b; Zeman et al., 1998). The most direct evidence comes from NMR studies using isotopically labeled [¹³C]-formaldehyde which showed the labeled carbon atom to be incorporated into the aminal linkage (Zeman et al., 1998). This was confirmed using $[{}^{3}H]$ -formaldehyde in breast cancer cells in culture (Taatjes *et al.*, 1999b). Formaldehyde reacts with the N-3' group of daunosamine to produce a reactive Schiff base which then forms the aminal link with the N-2 amino of guanine (Zeman et al., 1998). The N-3' daunosamine group has been shown to be critical for adduct formation since anthracycline derivatives that lack this group are unable to form adducts with DNA (Leng et al., 1996).

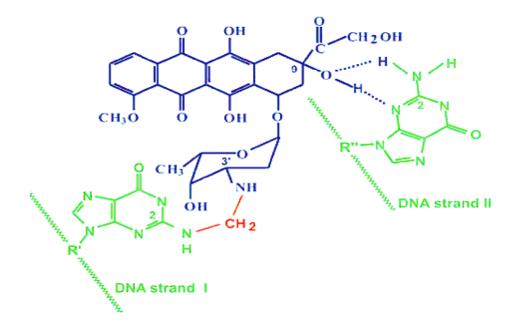


Figure 1.4. Structure of the doxorubicin-DNA adduct obtained by 2D NMR.

Doxorubicin is linked to guanine via a covalent aminal (N-C-N) linkage between the N-3' of daunosamine and the N-2 of guanine. The central carbon atom shown in red is derived from formaldehyde. Dashed lines represent hydrogen bonding of doxorubicin with the second strand of DNA (Zeman *et al.*, 1998).

The end result is the formation of a drug-DNA monoadduct which is further stabilized through intercalation and non-covalent hydrogen-bonding interactions with the second DNA strand (Zeman *et al.*, 1998). These non-covalent interactions stabilize the DNA sufficiently to enable them to function as 'virtual cross-links' and allows them to be detected *in vitro* by denaturation-based crosslinking assays (Cutts and Phillips, 1995; Cullinane *et al.*, 2000). The aminal linkage itself however is characteristically unstable and as such doxorubicin-DNA adducts have been shown to be both heat and alkali labile (van Rosmalen *et al.*, 1995), and possess a limited stability. Early studies demonstrated that doxorubicin-DNA adducts display a half-life ranging between 5-40 hours at 37 °C (Cutts and Phillips, 1995; van Rosmalen *et al.*, 1995; Moufarij *et al.*, 2001). More recently however, a study employing the extremely sensitive technique of accelerator mass spectrometry (AMS) and using clinically relevant levels of doxorubicin, showed that the half-life of DNA adducts was 13 hours at 37 °C, and approximately 50% of these adducts persisted up to 12 days in breast cancer cells (Coldwell *et al.*, 2008).

The clinical relevance of formaldehyde-dependent doxorubicin-DNA adduct formation as a mechanism of action was unclear until AMS was used to demonstrate that approximately 1300 DNA adducts per cell were detected in MCF-7 breast cancer cells using just 25 nM of doxorubicin (Coldwell *et al.*, 2008). These adducts were formed utilizing only endogenous levels of formaldehyde present within cells and/or formaldehyde produced from doxorubicin redox cycling (see Section 1.5 below) and emphasize that even without the use of exogenous formaldehyde, the formation of DNA adducts is likely to be a clinically relevant mechanism of action of anthracyclines. Evidence has also shown that doxorubicin-DNA adducts formed in cells display the same characteristics as those formed in Cell-free systems (Cutts *et al.*, 2003). In particular, doxorubicin-DNA adducts formed in IMR-32 neuroblastoma cells shared the same 5'-GC-3' DNA sequence specifity and had a similar melting temperature and half-life as observed for adducts in cell-free systems, indicating that the lesions are identical (Cutts *et al.*, 2003).

1.5 FORMALDEHYDE

1.5.1 Endogenous Formaldehyde

Formaldehyde is a highly reactive compound found in the environment as a pollutant from various sources, and exposure to formaldehyde can result in irritation and acute toxic effects on the eyes, skin, respiratory tract, and central nervous system (Solomons and Cochrane, 1984). Potential carcinogenic effects of formaldehyde have been documented for many years (Solomons and Cochrane, 1984; Hauptmann et al., 2004) and recently formaldehyde has been classified as an environmental human carcinogen (Cogliano et al., 2005). The toxic and carcinogenic effects of formaldehyde are likely due to its ability to readily react with cellular components, including proteins and DNA, resulting in the formation of intra- and intermolecular crosslinks (Casanova et al., 1991; Shaham et al., 1996). Although exposure to exogenous formaldehyde can be detrimental to human health, formaldehyde is produced in all cells and tissues (Kalasz, 2003; Taatjes et al., 1997a), and together with its main metabolite (formate) is involved in various essential pathways including the production of purines, thymidine, and several amino acids (Neuberger, 1981). The metabolism of formaldehyde occurs rapidly and involves several enzymes (Teng et al., 2001; Golden et al., 2006) which maintain low endogenous levels of formaldehyde, however, when the intracellular concentration of formaldehyde is greater than can be metabolized, formaldehyde-induced toxicity can occur (Golden et al., 2006).

Intracellular formaldehyde levels in various cancer cells lines have been reported to range between 0-4 μ M (Kato *et al.*, 2001). There has been a growing body of evidence suggesting a positive correlation between formaldehyde levels and tumour burden. Studies have shown that lymphocytic leukemia cells produce more formaldehyde than normal lymphocytes (Thorndike and Beck, 1977), and tumour-bearing transgenic mice exhaled higher levels of formaldehyde compared to tumour-free control mice (Ebeler *et al.*, 1997). Furthermore, higher levels of formaldehyde have been detected in urine from bladder and prostate cancer patients compared to control patients (Spanel *et al.*, 1999). This evidence suggests that higher levels of DNA adducts may potentially be formed following doxorubicin treatment in tumour cells, thus, providing some degree of selectivity over normal healthy cells.

1.5.2 Formaldehyde from Doxorubicin

Evidence has shown that doxorubicin itself can lead to an increase in formaldehyde production within cells. Treatment of MCF-7 breast cancer cells with doxorubicin and physiological levels of daunorubicin (0.5-1 μ M) resulted in higher levels of intracellular formaldehyde production compared to untreated cells (Kato et al., 2000). Higher levels of formaldehyde have also been detected in the urine of rats following intravenous (3.3-fold increase after 6 hr treatment) and oral treatment (2.7-fold increase after 24 hr treatment) with doxorubicin (10 mg/kg) relative to untreated rats (Bagchi et al., 1995). This increase in formaldehyde is believed to be due to doxorubicin undergoing redox cycling, resulting in the production of superoxide and hydrogen peroxide which can lead to the production of formaldehyde via Fenton chemistry (which requires a redox active metal catalyst such as iron or copper) (Myers et al., 1982; Taatjes et al., 1997a; Kato et al., 2000). The redox cycling of doxorubicin is also linked to cardiotoxicity which is explained in detail in Section 1.10.1. The ability of doxorubicin to chelate iron (Myers *et al.*, 1982) may allow the Fenton reaction to occur in close proximity to the drug, thus allowing doxorubicin to react with the formaldehyde produced to form DNA adducts. Therefore, formaldehyde may be available in cells either from endogenous sources or as metabolic products of doxorubicin itself and can facilitate DNA adduct formation within cells.

1.6 FORMALDEHYDE-RELEASING PRODRUGS

Once it was established that formaldehyde was required for doxorubicin-DNA adduct formation, there was considerable interest in enhancing the formation of adducts by the use of elevated levels of formaldehyde. Since formaldehyde itself is highly reactive and toxic, a delivery mechanism is required to safely administer formaldehyde intracellularly. DNA adduct levels can be increased in cells with the use of formaldehyde-releasing prodrugs, such as AN-9, in combination with doxorubicin (Cutts *et al.*, 2001).

1.6.1 AN-9

AN-9 (pivaloyloxymethyl butyrate), the most extensively studied formaldehyde-releasing prodrug, undergoes intracellular esterase-mediated hydrolysis to release formaldehyde, pivalic acid (which is inert) and butyric acid, as depicted in Figure 1.5A.

1.6.1.1 History

AN-9 was originally designed and synthesized by Nudelman and colleagues (1992) as part of a series of acyloxyalkyl ester prodrugs in an attempt to deliver butyric acid into cells. Butyric acid (a naturally occurring fatty acid) has been shown to display anticancer properties *in vitro* by inducing growth arrest, differentiation, and inhibiting proliferation in a variety of cancer cell lines (Leder and Leder, 1975; Prasad, 1980; Januszewicz et al., 1988), as well as modulating the expression of both oncogenes and tumour-suppressor genes (Toscani et al., 1988). These anticancer effects of butyric acid stem from its ability to act as a histone deacetylase (HDAC) inhibitor (Candido et al., 1978; Vidali et al., 1978). Inhibition of HDACs leads to hyperacetylation of histones which results in relaxation of chromatin and can increase the accessibility of transcription factors to DNA, causing changes in gene expression (Glaser *et al.*, 2003). Despite the promising *in vitro* anticancer effects of butyric acid, in patients (in the form of sodium butyrate) it proved to be ineffective, mainly due to its rapid metabolism and excretion (Miller et al., 1987; Daniel et al., 1989). In order to overcome these disadvantages and increase the intracellular concentration of butyric acid, a panel of butyrate-releasing prodrugs were synthesized, of which AN-9 displayed the greatest anticancer activity and was subjected to further analysis (Nudelman et al., 1992).

1.6.1.2 Anticancer Activity

AN-9, like butyric acid, has been shown induce differentiation, inhibit proliferation, and inhibit colony formation of cancer cells *in vitro* (Rephaeli *et al.*, 1991; Nudelman *et al.*, 1992). AN-9 has also been shown to modulate the expression of the several genes including the early regulatory genes c-myc and c-jun which have important roles in the differentiation pathway (Rabizadeh *et al.*, 1993). AN-9 treatment has been shown to cause cell death via classical hallmarks of apoptosis (Kasukabe *et al.*, 1997; Zimra *et al.*, 1997) and is

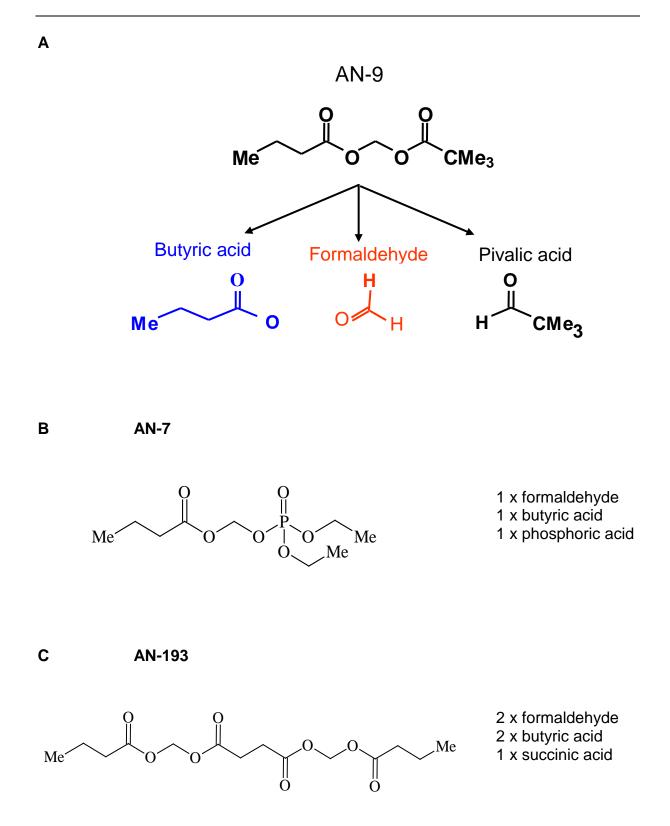


Figure 1.5. Structures of the formaldehyde-releasing prodrugs (A) AN-9 (pivaloyloxymethyl butyrate), (B) AN-7, and (C) AN-193, and the products released upon esterase mediated hydrolysis (Me = CH_3 group).

accompanied by a reduction in the expression of the anti-apoptotic protein Bcl-2 (Zimra *et al.*, 1997; Rabizadeh *et al.*, 2001). When AN-9 was evaluated against a panel of primary human tumours it displayed greater inhibition against melanoma, breast, ovarian, colorectal, and non-small cell lung carcinoma (NSCLC) colony-forming units compared to butyric acid (Siu *et al.*, 1998). AN-9 has also been shown to inhibit neovascularization *in vitro* and *in vivo*, and reduce expression levels of pro-angiogenic markers, indicating that the prodrug possesses antiangiogenic properties (Blank-Porat *et al.*, 2007; Tarasenko *et al.*, 2008).

The effects of AN-9 were shown to occur at much lower concentrations (approximately 10fold lower) and at a much faster rate (approximately 100-fold faster) compared to butyric acid (Rephaeli et al., 1991; Rabizadeh et al., 1993; Zimra et al., 1997). The activity of AN-9 was originally believed to be due mostly to the released butyric acid and its ability to act as a HDAC inhibitor, and indeed AN-9 was shown to cause transient hyperacetylation of histones at a concentration one order of magnitude lower than butyric acid (Aviram et al., 1994). However, based on recent structure-activity relationship studies using a range of butyric acid releasing prodrugs in a range of cell lines, it was revealed that prodrugs that release formaldehyde are much more active than those that release acetaldehyde (irrespective of the level of released butyric acid) in terms of inhibiting proliferation, inducing differentiation, and apoptosis (Nudelman et al., 2005). These findings reflect a pivotal importance on the released formaldehyde for mediating the activity of AN-9. The anticancer activity of AN-9 can therefore be attributed to both the released butyric acid which most likely plays a minor role by acting as a HDAC inhibitor and inducing histone acetylation and promoting differentiation, and the released formaldehyde which plays a dominant role in inhibiting proliferation, promoting differentiation, and inducing apoptosis. The mechanism by which the released formaldehyde exerts these effects may involve the ability of formaldehyde to reduce glutathione levels and increase the level of reactive oxygen species (ROS), subsequently leading to oxidative damage (Levovich et al., 2008).

1.6.1.3 Mouse Studies and Clinical Trials

AN-9 possesses low toxicity and was shown to reduce tumour size and/or prolong the survival of mice with different types of tumours (Rephaeli *et al.*, 1991; Nudelman *et al.*, 1992; Kasukabe *et al.*, 1997; Entin-Meer *et al.*, 2005; Tarasenko *et al.*, 2008). AN-9 also

decreased lung tumour burden in mice injected with highly metastatic subclones of Lewis lung carcinoma (Rephaeli *et al.*, 1991), and melanoma (Nudelman *et al.*, 1992). Following promising results in mouse models, AN-9 entered clinical trials. In a Phase I clinical study where AN-9 (in a lipid emulsion labelled Pivanex) was administered daily to patients with advanced solid malignancies, the highest dose that could be administered was $3.3 \text{ g/m}^2/\text{day}$ (Patnaik *et al.*, 2002). The dose-limiting toxicity could not be reached since dose escalation was limited by the volume of intralipid vehicle that could be administered and not by drug-induced side-effects. A Phase II trial of AN-9 (Pivanex) was conducted in 47 patients with NSCLC in which AN-9 was well tolerated and three patients displayed a partial response to treatment (Reid *et al.*, 2004). The most common side-effects observed in patients treated with AN-9 included nausea, vomiting, fatigue, weight loss, and other mild to moderate symptoms which were reversible (Patnaik *et al.*, 2002; Reid *et al.*, 2004). A Phase IIb trial of AN-9 in combination with docetaxel in patients with NSCLC was terminated due to undisclosed safety issues.

1.6.2 Other Formaldehyde-Releasing Prodrugs

While AN-9 demonstrated promising *in vitro* anticancer activity, its highly lipophilic nature means that it possesses low water solubility and requires non-aqueous media for clinical formulation. For this reason, derivatives containing water solubilizing functional groups were designed and synthesized to make formaldehyde-releasing prodrugs more amenable to clinical use (Nudelman *et al.*, 2001). The lead compound, AN-7 (butyroyloxymethyl-diethyl phosphate) releases formaldehyde, butyric acid, and phosphoric acid upon esterase hydrolysis (Figure 1.5B), and has high aqueous solubility and is orally bioavailable while still retaining anticancer activity (Nudelman *et al.*, 2001; Rephaeli *et al.*, 2005). *In vivo*, AN-7 was shown to reduce tumour growth, inhibit metastasis, and increase survival without any adverse effects in mice bearing human prostate tumours (Rephaeli *et al.*, 2005), and was also shown to reduce lung metastases in mice implanted with highly metastatic Lewis lung carcinoma cells (Rephaeli *et al.*, 2005). Prodrugs that release two molecules of formaldehyde upon esterase hydrolysis (Type-II prodrugs including AN-193, Figure 1.5C) have also been developed and demonstrated enhanced efficacy compared to AN-9 in cell culture studies (Cutts *et al.*, 2005; Nudelman *et al.*, 2005).

1.7 COMBINATION OF ANTHRACYCLINES WITH FORMALDEHYDE-RELEASING PRODRUGS

1.7.1 In vitro Studies

The combination of doxorubicin with various formaldehyde-releasing prodrugs, including AN-9 and AN-7 has been shown to elicit a synergistic response in several cancer cell lines (Kasukabe et al., 1997; Niitsu et al., 2000; Cutts et al., 2001; Cutts et al., 2005; Engel et al., 2006; Swift et al., 2006). The level of doxorubicin-DNA adducts formed in cancer cells is greatly enhanced (up to 10-fold within a few hours) with the co-administration of formaldehyde-releasing prodrugs (Cutts et al., 2001; Cutts et al., 2005), and this in turn leads to synergistic cancer cell death (Rabizadeh et al., 2001; Swift et al., 2006). Evidence has clearly demonstrated that this synergy in cancer cells is due to the released formaldehyde from the prodrugs. Prodrugs that released acetaldehyde instead of formaldehyde did not potentiate DNA adduct formation (Cutts et al., 2001; Cutts et al., 2005), and the addition of sodium butyrate did not lead to an enhancement of adduct levels (Cutts et al., 2001). Moreover, DNA adduct levels were reduced and cell viability increased with the use of semicarbazide, a formaldehyde-sequestering agent (Cutts et al., 2001), further highlighting the importance of formaldehyde for covalent doxorubicin-DNA adduct formation and the resulting synergy. Other clinically relevant anthracyclines, daunorubicin and idarubicin (but not epirubicin), have also been shown to display synergy when combined with AN-9 due to the potentiation of DNA adduct levels (Cutts et al., 2007). The Type-II prodrug AN-193, which releases two molecules of formaldehyde upon esterase hydrolysis, enhances doxorubicin-DNA adduct formation to at least twice the level compared to Type-I prodrugs (Cutts et al., 2005).

1.7.2 Mouse Studies

Kasukabe and colleagues (1997) demonstrated that the combination of AN-9 and daunorubicin significantly increased the survival time of mice inoculated with monocytic leukemia cells in comparison to either agent alone. Based on the results of the Kasukabe and colleagues (1997) *in vivo* study and years of promising *in vitro* studies in various cancer cells, a collaboration was set up with Dr. Cullinane at the Peter MacCallum Cancer Institute

(Melbourne, Australia) to perform pre-clinical testing of the combination of doxorubicin with formaldehyde-releasing prodrugs in mouse models. Nude mice were implanted with MDA-MB-231 breast cancer cells and treated with doxorubicin (intravenous tail vein injection), AN-9, AN-193, and the combination of doxorubicin with either prodrug, twice weekly for three weeks. Initially the prodrugs were administered via intraperitoneal injection, however, the combination treatments did not differ in response (tumour volume) compared to the single agent treatments. In a subsequent study the formaldehyde-releasing prodrugs were administered by intratumoural injection to maximize formaldehyde release at the tumour site. The results of this study (Figure 1.6, Cutts et al., unpublished data) showed that the combination treatments significantly inhibited tumour volume compared to the single agent treatments, indicating that doxorubicin-DNA adduct formation is the major mechanism of tumour volume reduction. The mice tolerated the combination treatments without displaying any weight loss. This study provides a proof of principle that when the levels of formaldehyde-releasing prodrugs are high at the tumour site, the antitumour effects mediated by doxorubicin-DNA adduct formation are much greater than doxorubicin as a single agent. While intratumoural injections are not a favourable route of administration in the clinic, in the future, targeting strategies may be employed to deliver high levels of formaldehyde specifically at the tumour site.

1.7.3 Pre-Activated Anthracyclines

While the combination of anthracyclines with formaldehyde-releasing prodrugs has provided promising anti-cancer efficacy both *in vitro* and *in vivo*, the use of compounds that are able to form DNA adducts without the requirement of endogenous or exogenous formaldehyde would be deemed to possess even greater potential. Two "pre-activated" anthracycline compounds, barminomycin and doxoform/doxazolidine, are able to form covalent DNA adducts as single agents and display much greater cytotoxic activity compared to doxorubicin (Uchida *et al.*, 1988; Fenick *et al.*, 1997; Taatjes *et al.*, 1998; Perrin *et al.*, 1999; Moufarij *et al.*, 2001; Post *et al.*, 2005). Greater detail on the characteristics and activity of pre-activated anthracyclines is provided in Section 4.1.

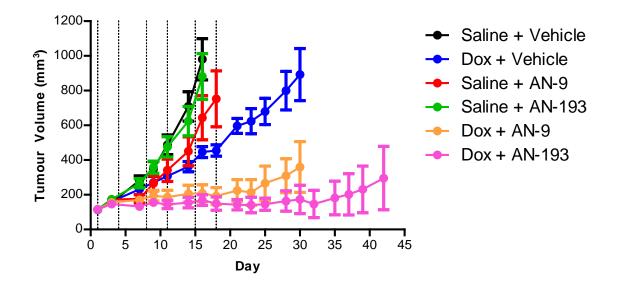


Figure 1.6. Effect of doxorubicin in combination with AN-9 or AN-193 on MDA-MB-231 tumour growth in a Balb/c nude mouse model.

Female Balb/c nude mice were inoculated subcutaneously on the flank with MDA-MB-231 cells and after 15 days were randomized into groups (8 mice per group). Mice were treated with the compounds twice weekly until an ethical end point was reached. Drug concentrations were 2 mg/kg doxorubicin and 100 mg/kg AN-9 and AN-193. Data represents the mean tumour volume from each group and error bars represent the standard error of the mean (Cutts *et al.*, unpublished data).

1.8 DNA ADDUCT FORMATION vs. TOPOISOMERASE-II POISONING

Evidence strongly indicates that the formation of doxorubicin-DNA adducts is a completely independent mechanism of action to that of formation of double stranded DNA breaks induced by doxorubicin poisoning of topoisomerase-II (Swift *et al.*, 2006). It has been shown in HL-60 promyelocytic leukemic cells that as the level of doxorubicin-DNA adducts increases with increasing AN-9, the level of topoisomerase-II mediated DNA damage decreases (Swift *et al.*, 2006). Furthermore, the use of topoisomerase-II catalytic inhibitors and topoisomerase-II defective cell lines did not affect DNA adduct levels or the resulting apoptotic response. Doxorubicin-DNA adducts are also substantially more cytotoxic than topoisomerase-II induced DNA damage with high levels of apoptosis occurring after only a few hours. The independence of these lesions can also be inferred by the fact that they take place at different sequences of DNA (Capranico *et al.*, 1990; Cullinane and Phillips, 1990). Therefore, as illustrated in Figure 1.7, the presence of formaldehyde appears to switch the mechanism of doxorubicin action from topoisomerase-II impairment to the formation of more cytotoxic DNA adducts.

1.9 CELLULAR CONSEQUENCES OF ANTHRACYCLINE-DNA ADDUCT FORMATION

The formation of multiple, bulky drug-DNA lesions would be expected to affect critical cellular processes, including DNA replication and transcription. Indeed, evidence has shown that anthracycline-DNA adduct formation impedes the binding of DNA-interacting proteins, including transcription factors and RNA polymerase (Cutts *et al.*, 1996), leading to the formation of stalled replication forks and blocked transcription. While the exact cellular responses to anthracycline-DNA adducts have not been fully elucidated it is evident that a complex interplay of repair and DNA damage response pathways act together to process the damage (Spencer *et al.*, 2008; Forrest, 2010).

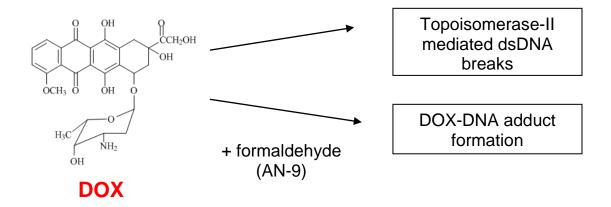


Figure 1.7. Formaldehyde switches the mechanism of action of doxorubicin.

Doxorubicin primarily functions as a topoisomerase-II poison resulting in double-strand DNA breaks. However, in the presence of formaldehyde (or formaldehyde-releasing prodrugs) the mechanism of action of doxorubicin is switched to more cytotoxic DNA adduct formation.

Various DNA repair pathways exist in cells to process and repair different types of endogenous and exogenous DNA damage. Studies utilizing cells with deficiencies in DNA repair pathways demonstrated that nucleotide excision repair (NER) and homologous recombination (HR) are the important pathways involved in the processing of anthracycline-DNA adducts (Spencer et al., 2008). A model for the processing of anthracycline-DNA adducts has been proposed (Figure 1.8) where adducts can be detected during transcription by the stalling of RNA polymerase by transcription-coupled NER, or during replication by the stalling of replication forks (Bilardi, 2010; Forrest, 2010). In both cases double-stranded DNA breaks may occur which subsequently triggers the activation of a number of proteins involved in the damage response pathway (Ciccia and Elledge, 2010). Two proteins identified as playing key roles in the DNA damage signal response to anthracycline-DNA adducts are the serine/threonine protein kinases ATM (ataxia telangiectasia mutated) and ATR (ataxia telangiectasia and Rad3 related; Li and Zou, 2005; Jackson and Bartek, 2009). It is proposed that the formation of transcription-coupled double-stranded DNA breaks in response to anthracycline-DNA adducts leads to recruitment of ATM (in the G1 phase of the cell cycle), while the formation of replication-coupled double-stranded DNA breaks leads to recruitment of ATR (in the S/G2phase of the cell cycle; Forrest, 2010; Forrest et al., 2012). These proteins in turn can activate other proteins to initiate further signalling events leading to cell cycle arrest, DNA repair by HR, or cell death (Forrest, 2010). Cell death which occurs in response to DNA-adduct forming treatments typically involves DNA fragmentation (Swift et al., 2006) and nuclear condensation (Cutts et al., 2007), and is inhibited by Bcl-2 overexpression (Swift *et al.*, 2006), thus reflecting a classical apoptotic response.

1.10 LIMITATIONS OF ANTHRACYCLINES

The major problems confronting the use of chemotherapy in the clinic are severe side-effects and induced or intrinsic chemoresistance. Although doxorubicin is one of the most widely used chemotherapeutics in the clinic its use is limited by these factors.

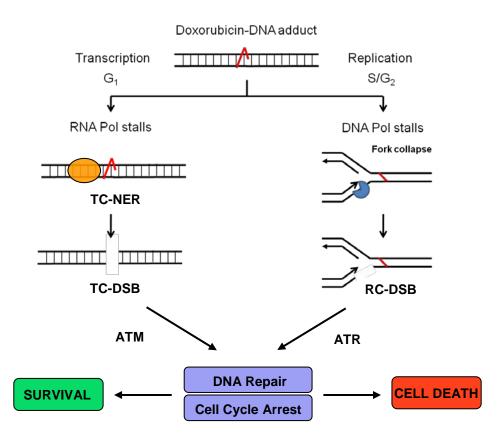


Figure 1.8. Proposed model for the processing of doxorubicin-DNA adducts.

Doxorubicin-DNA adducts can be detected and processed during transcription by NER or during DNA replication. Both processes result in the formation of double-stranded DNA breaks (DSB; transcription coupled and replication coupled are abbreviated to TC and RC respectively) which leads to the initiation of DNA damage response pathways signalled either by ATM or ATR. These proteins can activate DNA repair and cell cycle arrest which can lead to cell survival, or cell death if the damage is too great (adapted from Forrest, 2010).

1.10.1 Cardiotoxicity

As with all chemotherapeutics, doxorubicin affects normal replicating cells leading to sideeffects which include hair loss, gastrointestinal toxicities, and myelosupression (DeVita *et al.*, 2008). While most side-effects are mild to moderate and easily manageable, doxorubicin (and all anthracycline) treatment is restricted by severe cardiotoxic side-effects (Von Hoff *et al.*, 1979). Acute cardiotoxicity manifested by hypotension and arrhythmias can occur during or shortly after doxorubicin treatment and is reversible, however, cumulative doxorubicin treatment can result in chronic cardiotoxic effects which are irreversible and can lead to fatal cardiomyopathy and congestive heart failure (as reviewed by Minotti *et al.*, 2004; Ferreira *et al.*, 2008; Simunek *et al.*, 2009), even years after cessation of chemotherapy (Steinherz and Steinherz, 1991). These chronic cardiotoxic effects limit the total cumulative lifetime dose of doxorubicin to 450-600 mg/m² and daunorubicin to 550 mg/m² (Minotti *et al.*, 2004), which may lead to a reduction in the duration and success of treatment.

Many factors are likely to contribute to anthracycline-induced cardiotoxicity (as reviewed by Ferreira et al., 2008; Simunek et al., 2009), but the principle cause is believed to involve the redox cycling of the drugs and the subsequent generation of ROS. The quinone structure of anthracyclines allows them to undergo redox cycling via several enzymes resulting in the generation of semiquinone radicals which can react further with oxygen, generating an array of highly reactive species including superoxides, hydrogen peroxide, and hydroxyl radicals (Goodman and Hochstein, 1977; Bachur et al., 1982; Kalyanaraman et al., 1984; Doroshow and Davies, 1986). Due to their high reactivity these species are able to cause damage to various cellular components including nucleic acids and lipid membranes (Myers et al., 1977; Monti et al., 1995), however, the damage can be minimized via the action of several detoxifying enzymes including superoxide dismutase, catalase, and glutathione peroxidase (Blokhina et al., 2003). Redox cycling of anthracyclines in cardiac cells has been shown to primarily involve mitochondria (Davies and Doroshow, 1986; Wang et al., 2001), and due to the high energy demand of cardiac cells they are rich in mitochondria and therefore generate high levels of ROS. Cardiac cells are even more susceptible to ROS induced damage since they contain low levels of catalase and other radical detoxifying enzymes (Doroshow et al., 1980). In addition, doxorubicin itself has been shown to downregulate glutathione peroxidase (Doroshow et al., 1980). Taken together, all of these factors make cardiac cells especially

vulnerable to ROS-induced damage and help explain the sensitivity of the heart to the effects of anthracycline treatment.

Due to the severity of anthracycline cardiotoxicity, various strategies have been developed in an attempt to improve their therapeutic use, including the synthesis of new derivatives. The most clinically notable analogue developed is the anthracenedione mitoxantrone. Mitoxantrone also functions as a topoisomerase-II poison (Smith et al., 1990), and is able to form DNA adducts in the presence of formaldehyde (Parker et al., 1999), but due to differences in its structure it does not undergo redox cycling to the same extent as doxorubicin and as such is less cardiotoxic (Koutinos et al., 2002). Anthracyclines have also been combined with numerous antioxidants in an attempt to reduce the levels of ROS generated, including probucol (Siveski-Iliskovic et al., 1995; Iliskovic and Singal, 1997; Walker et al., 2011), and the FDA approved cardioprotective agent dexrazoxane (ICRF-187) which has been shown to reduce anthracycline-induced cardiotoxicity in clinical trials (Speyer et al., 1992; Swain et al., 1997) without compromising anticancer activity (Swain and Vici, 2004). Another strategy to reduce cardiotoxicity involves the use of drug delivery systems such as liposomes to encapsulate doxorubicin, thus reducing the exposure of normal cells to the drug (as reviewed by Rahman et al., 2007). Some of these encapsulated doxorubicin formulations including Doxil have shown promising results in clinical trials and are discussed in more detail in Section 1.13.1.

1.10.2 Acquired Resistance

Due to the genetic instability of cancer cells they generally have a high spontaneous rate of mutation which can allow them to develop resistance to chemotherapeutics over time (i.e. acquired resistance). The most commonly reported mechanism involved in acquired resistance to anthracyclines is the overexpression of membrane efflux pumps (as reviewed by Den Boer *et al.*, 1998). The membrane efflux pumps, permeability-glycoprotein (P-gp) and multidrug-resistance-associated protein (MRP1) are ATP binding cassette transporter proteins that form pores in the plasma membrane and actively transport a range of substances out of cells (Gottesman *et al.*, 2002). The overexpression of these proteins in cancer cells enables the cells to pump out chemotherapeutic drugs during treatment, thus reducing the

intracellular drug concentration (Taatjes *et al.*, 1999b) and preventing cell kill (Berman and McBride, 1992). Treatment with one type of chemotherapeutic drug can lead to resistance to multiple drugs since these pumps can transport a range of drugs out of cells including anthracyclines, vinca alkaloids, and the epipodophyllotoxins – this is termed the multidrug resistance phenotype (Ueda *et al.*, 1987; Grant *et al.*, 1994). Continual exposure of cancer cells to anthracyclines can result in the overexpression of these membrane efflux pumps (Slovak *et al.*, 1988) which confers resistance to anthracycline treatment (Cutts *et al.*, 2005; Cutts *et al.*, 2007). Other membrane pumps such as breast cancer resistance protein 1 (BCRP1) also confers resistance to anthracyclines and other chemotherapeutics (Doyle *et al.*, 1998).

Another commonly reported anthracycline resistance mechanism is the alteration of the drug target topoisomerase-II (as reviewed by Den Boer *et al.*, 1998). The cytotoxicity of anthracyclines depends on their ability to poison the enzyme topoisomerase-II, therefore, reduced availability or accessibility of this target can compromise the activity of the drugs (Hofmann and Mattern, 1993). Studies have demonstrated that cell lines with decreased expression and activity of topoisomerase-II are associated with anthracycline resistance (Deffie *et al.*, 1989; de Jong *et al.*, 1990; Cutts *et al.*, 2005; Swift *et al.*, 2006).

1.10.3 Intrinsic Resistance

Some tumours are intrinsically resistant prior to chemotherapy due to gene mutations and altered gene expression profiles. For example, the tumour suppressor protein p53 is mutated in over half of all human tumours (Levine, 1997), and since it functions as a transcription factor that upregulates genes leading to cell cycle arrest or apoptosis, mutations in p53 are often implicated in intrinsic chemoresistance to a range of drugs (DeVita *et al.*, 2005). One of the main forms of inherent chemoresistance is the ability of tumour cells to evade the apoptotic mechanisms responsible for killing tumour cells upon exposure to chemotherapeutics. In fact, it is well documented that many human tumours are inherently resistant to chemotherapy (including doxorubicin treatment) due to the overexpression of anti-apoptotic proteins such as Bcl-2 and Bcl-xL (Schmitt *et al.*, 2000; Panaretakis *et al.*, 2002; DeVita *et al.*, 2005).

1.11 APOPTOSIS

Apoptosis or programmed cell death is a regulated process that is important during embryonic development and throughout the life of multicellular organisms. In order to maintain normal cell numbers and composition, unwanted or surplus cells are safely eliminated via apoptosis which is characterized by a well-defined sequence of morphological changes. The hallmarks of apoptosis include cytoplasmic condensation, cell shrinkage, chromatin condensation and DNA fragmentation, and membrane blebbing, before the cell begins to break apart forming apoptotic bodies which are ingested and degraded by macrophages (Ziegler and Groscurth, 2004; Fadeel and Orrenius, 2005). The highly regulated and controlled process of apoptosis is distinct from another form of cell death termed necrosis in which cells typically swell and burst, releasing their intracellular contents which can damage surrounding cells and result in inflammation (Fadeel and Orrenius, 2005). Disregulation of apoptosis can lead to severe consequences. Increased apoptosis can exacerbate conditions such as AIDS, Alzheimer's disease, and Huntington's disease, while inadequate apoptosis is implicated in autoimmune diseases and cancer (Fadeel and Orrenius, 2005). In fact, evasion of apoptosis is one of the hallmarks of cancer and is essential for tumour growth (Hanahan and Weinberg, 2000).

1.11.1 Apoptotic Pathways

There are two main apoptotic pathways – the extrinsic and intrinsic pathways (Figure 1.9; reviewed by Fadeel and Orrenius, 2005; Fulda and Debatin, 2006). The extrinsic pathway involves the binding of pro-apoptotic extracellular ligands such as FAS ligand, TRAIL or TNF to death receptors (members of the tumour necrosis factor receptor family) on the cell surface. Ligand binding induces death receptor clustering and the recruitment of the adapter protein FADD (Fas-associated death domain), which in turn leads to recruitment of procaspase-8 or -10 forming the death-inducing signalling complex (DISC). Formation of the DISC leads to the autocatalytic activation of caspase-8 or -10 which is then able to activate the effector caspases.

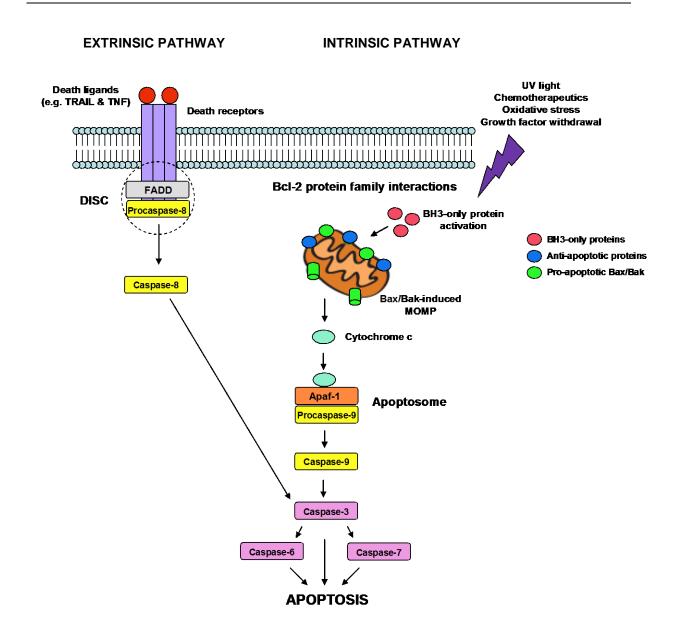


Figure 1.9. Extrinsic and intrinsic apoptotic pathways.

The extrinsic pathway involves the binding of extracellular ligands (such as TRAIL and TNF) to death receptors on the cell surface, while the intrinsic pathway involves interactions between Bcl-2 protein family members in response to certain death signals leading to mitochondrial outer membrane permeabilization (MOMP). Both pathways lead to the activation of initiator caspases which in turn cleave and activate effector caspases (caspases-3-6-7) which destroy various essential proteins and cellular components leading to cell death.

The intrinsic pathway involves mitochondria and is activated by cellular stress caused by factors including DNA damage (from UV light, chemicals and chemotherapeutics), as well as growth factor withdrawal and ROS. The pathway is regulated by members of the Bcl-2 protein family and it is the relative ratios of these proteins which dictates whether apoptosis occurs or not. Certain members of the Bcl-2 protein family become activated in response to cellular stress and interact with each other, eventually leading to Bax/Bak-mediated pore formation in the outer mitochondrial membrane and the release of cytochrome c (and other proteins such as pro-apoptotic Smac/DIABLO) into the cytoplasm. Once released, cytochrome c interacts with the adapter protein Apaf-1 in the cytosol, leading to the formation of an oligomer complex called the apoptosome. This leads to the recruitment of procaspase-9 which becomes activated within the complex and in turn cleaves and activates effector caspases.

Both of the apoptotic pathways lead to the induction of a caspase cascade. Caspases are a group of cysteine proteases that upon activation cleave a multitude of other cellular proteins (Degterev *et al.*, 2003; Lavrik *et al.*, 2005). They are divided into initiator caspases (for example caspases-8-9-10) which cleave and activate the effector caspases (caspases-3-6-7). The effector caspases cleave and destroy various essential cellular proteins leading to the characteristic morphological changes associated with apoptosis and ultimately cell death (Degterev *et al.*, 2003; Lavrik *et al.*, 2005).

1.11.2 Bcl-2 Family Proteins

The intrinsic apoptotic pathway is regulated by the Bcl-2 family proteins which are subdivided into three groups – the anti-apoptotic proteins (Bcl-2, Bcl-xL, Bcl-w, Mcl-1 and A1), the multidomain pro-apoptotic proteins (Bax, Bak, and Bok), and the BH3-only pro-apoptotic proteins (Bim, Bid, Bad, Bik, Noxa, Puma, Bmf, Hrk). Regulation of the intrinsic pathway is based on specific interactions between Bcl-2 family members which share homology in up to four regions called BH domains (Figure 1.10A; Giam *et al.*, 2008). The BH1-3 domains of the anti-apoptotic and multidomain pro-apoptotic proteins fold together to form a hydrophobic groove (Petros *et al.*, 2004). The BH3 domain of the BH3-only proteins forms a short amphipathic alpha-helix which is able to fit into the hydrophobic grooves of

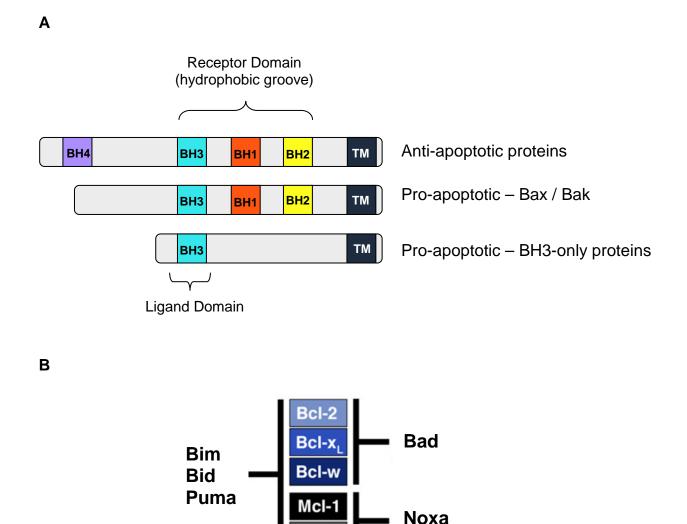


Figure 1.10. Bcl-2 protein family homology domain composition and interactions between BH3-only proteins with anti-apoptotic proteins.

(A) Bcl-2 family proteins share homology in up to four BH domains where the BH1-3 domains come together to form the hydrophobic groove that interacts with the BH3 domain of pro-apoptotic proteins (TM – transmembrane domain; adapted from Giam *et al*, (2008)).
(B) The BH3-only proteins can be divided into promiscuous binders (Bim, Bid, and Puma) which are able to interact with all anti-apoptotic proteins, while Bad and Noxa are selective binders since their BH3 domains can only interact with a subset of anti-apoptotic proteins (adapted from van Delft *et al.*, 2006).

specific multidomain family members (Petros *et al.*, 2004; Giam *et al.*, 2008). The BH4 domain of the anti-apoptotic proteins stabilizes the hydrophobic groove and as such the BH3 domain cannot interact with other proteins (Conus *et al.*, 2000; Kirkin *et al.*, 2004). The BH3 domain of pro-apoptotic Bax and Bak on the other hand is less packed into the groove and as such is able to interact with the hydrophobic grooves of other family members (Kirkin *et al.*, 2004).

1.11.2.1 Bax / Bak

The multidomain pro-apoptotic proteins Bax and Bak are ubiquitously expressed in almost all cell types and are absolutely essential for apoptosis to occur since Bax/Bak double knockout cells are unable to undergo apoptotic cell death (Zong *et al.*, 2001; Willis *et al.*, 2007). Single knockouts of Bax or Bak however can be compensated for reflecting functional redundancy (Lindsten *et al.*, 2000). In healthy cells, Bax is primarily located as a monomer in the cytosol (or loosely attached to the outer mitochondrial membrane), while Bak is an integral membrane protein on the outer mitochondrial membrane (Kirkin *et al.*, 2004; Giam *et al.*, 2008). Upon apoptotic signals, Bax translocates to the outer mitochondrial membrane (Wolter *et al.*, 1997), and both Bax and Bak undergo conformational changes leading to their activation (Kirkin *et al.*, 2004). Once activated, Bax and Bak form oligomers and aggregates on the outer mitochondrial membrane and induce mitochondrial outer membrane permeabilization (MOMP) and cytochrome c release, although the precise details on how MOMP is achieved is unclear (Antonsson *et al.*, 2001; Kirkin *et al.*, 2004; Giam *et al.*, 2008).

1.11.2.2 BH3-Only Proteins

The BH3-only proteins are kept inactive in healthy cells, but upon apoptotic signals they become activated to trigger Bax/Bak mediated MOMP and cell death. In response to certain apoptotic signals the BH3-only proteins are transcriptionally up-regulated, post-translationally modified, or relocalized to become activated. For example, Bim is kept inactive by sequestration to dynein light chains and becomes released upon apoptotic stimuli (Puthalakath *et al.*, 1999), while Noxa (Oda *et al.*, 2000) and Puma (Nakano and Vousden, 2001) are upregulated via p53 mediated transcription in response to DNA damage. Once activated, the BH3-only proteins are able to insert their alpha helices into the hydrophobic

grooves of anti-apoptotic proteins (Giam *et al.*, 2008). As depicted in Figure 1.10B, some BH3-only proteins (Bid, Bim, and Puma) are promiscuous binders and can interact with all anti-apoptotic proteins, while other BH3-only proteins are selective binders, including Bad (which cannot bind to Mcl-1 or A1) and Noxa (which cannot bind to Bcl-2, Bcl-xL, and Bcl-w; Chen *et al.*, 2005; Certo *et al.*, 2006). Therefore, the promiscuous binders (Bad, Bim, and Puma) are more potent in inducing cell death compared to the selective binders (Chen *et al.*, 2005).

1.11.2.3 Anti-Apoptotic Proteins

The anti-apoptotic proteins are predominantly located on the outer mitochondrial membrane and function to prevent Bax/Bak activation and subsequent cell death (Kirkin *et al.*, 2004). These proteins are vital for embryonic development and survival as demonstrated by knockout studies in mice (Nakayama *et al.*, 1994; Kamada *et al.*, 1995; Motoyama *et al.*, 1995; Rinkenberger *et al.*, 2000). While a lack of anti-apoptotic proteins is clearly detrimental, an overexpression of these proteins is evident in a range of human tumours and is implicated in tumour growth and progression. Overexpression of Bcl-2 is common in many cancer types including follicular lymphoma, chronic and acute leukemia, small cell lung carcinoma (SCLC), prostate, renal, colorectal, melanoma, myeloma, and non-Hodgkin's lymphoma (as reviewed by Kirkin *et al.*, 2004). Furthermore, increased Bcl-xL is seen in hepatocellular and renal carcinoma (Gobe *et al.*, 2002; Watanabe *et al.*, 2002), as well as pancreatic cancer (Ghaneh *et al.*, 2002). Increased Bcl-w is commonly implicated in colorectal adenocarcinomas (Wilson *et al.*, 2000), and Mcl-1 is overexpressed in a number of hematopoietic and lymphoid cancers (Warr and Shore, 2008).

1.11.3 Bcl-2 Family Interactions

There are two models as to how BH3-only proteins interact with other Bcl-2 family members to activate Bax and Bak – the direct and indirect activation models. In the direct activation model (Figure 1.11A) the BH3-only proteins are divided into activators (Bim, Bid, and possibly Puma) and sensitizers (Bad and Noxa) (Letai *et al.*, 2002; Cartron *et al.*, 2004; Kim *et al.*, 2006). The activator BH3-only proteins directly bind to Bax/Bak and promote their

activation while the anti-apoptotic proteins sequester the activators to prevent Bax/Bak activation and apoptosis (Desagher *et al.*, 1999; Walensky *et al.*, 2006). The sensitizer BH3-only proteins bind to the anti-apoptotic proteins with higher affinity and displace the anti-apoptotic proteins, allowing the released activators to promote apoptosis (Letai *et al.*, 2002). Therefore, in this model apoptosis only occurs in the presence of activator BH3-only proteins (Kuwana *et al.*, 2005; Kim *et al.*, 2006).

More recent evidence however, has demonstrated that apoptosis is not dependent on direct activation of Bax/Bak by BH3-only proteins (Willis et al., 2007). In the indirect activation model (Figure 1.11B), BH3-only proteins (once activated) function only to bind to antiapoptotic proteins which sequester Bax/Bak. Hence, the BH3-only proteins do not directly activate Bax/Bak but instead do so indirectly by engaging the multiple anti-apoptotic proteins that constrain them. Bak is held in check only by Bcl-xL and Mcl-1, therefore, in order to completely release Bak and trigger apoptosis, both of these anti-apoptotic proteins need to be neutralized (Willis et al., 2005). Studies have demonstrated that expression of both of the selective BH3-only proteins Bad and Noxa (to release Bak from Bcl-xL and Mcl-1 respectively) is required for Bak-mediated apoptosis (Willis et al., 2005; Uren et al., 2007). Bax on the other hand is held in check by multiple anti-apoptotic proteins including Bcl-2 (Willis et al., 2007). Once the anti-apoptotic proteins are neutralized to a certain degree, sufficient levels of Bax and Bak are activated and can trigger apoptosis. Support for the indirect model over the direct model comes from findings that Bak failed to interact with any BH3-only protein and that Bid/Bim double knockout cells that had Puma knockdown still underwent apoptosis (Willis et al., 2007). Furthermore, the BH3-only proteins that are classed as sensitizers (Noxa, Bad and Bik) were shown to be able to induce cytochrome c release (Uren et al., 2007) and apoptosis in the absence of the activators Bim and Bid (Willis et al., 2007) which would not be possible according to the direct activation model. While the indirect model does not provide a clear explanation as to how Bax and Bak become activated, it is proposed that in healthy cells or early apoptotic cells a proportion of Bax and Bak are in a primed conformation where the BH3 domain is accessible and bound by anti-apoptotic proteins (Adams and Cory, 2007). Therefore, once BH3-only proteins displace the antiapoptotic proteins, this releases 'activated' Bax and Bak which can oligomerize and induce MOMP.

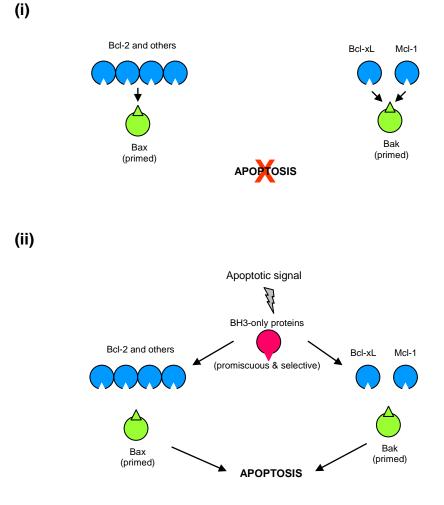
Activator proteins Bim / Bid Directly bind & activate Bax / Bak Anti-apoptotic proteins Bax / Bak Anti-apoptotic proteins

Direct Activation Model

В

Α

Indirect Activation Model



40

Figure 1.11. Direct and indirect models of Bax/Bak activation.

In the direct activation model (A), BH3-only proteins are divided into activator proteins (Bim and Bid) which directly bind and activate Bax/Bak, and sensitizer proteins (Bad and Noxa) which bind to anti-apoptotic proteins. The binding of sensitizer proteins to the anti-apoptotic proteins prevents the anti-apoptotic proteins from sequestering the activator proteins, thus allowing the free activator proteins to promote apoptosis. In the indirect activation model (B), anti-apoptotic proteins bind to Bax/Bak (which possibly exist in a primed conformation), therefore preventing apoptosis under normal conditions (i). Upon the induction of apoptotic signals, BH3-only proteins become activated and bind to anti-apoptotic proteins, thus releasing primed Bax/Bak which now can promote apoptosis (ii).

Since there is considerable evidence supporting both the direct activation (Kuwana *et al.*, 2005; Walensky *et al.*, 2006) and indirect activation (Uren *et al.*, 2007; Willis *et al.*, 2007) models, it is possible that both may occur under different circumstances or that certain aspects of both models are occurring (Adams and Cory, 2007; Basanez and Hardwick, 2008; Giam *et al.*, 2008). Whether Bcl-2 family members interact via the direct or indirect activation models or a combination of both, ultimately it is the balance of pro- and anti-apoptotic proteins within the cell that dictates if a cell will survive or undergo apoptosis. In cancer cells this balance is often shifted in favour of anti-apoptotic proteins, thereby allowing the cells to evade apoptosis.

1.12 INHIBITING ANTI-APOPTOTIC PROTEINS

Since many human cancers are characterized by the overexpression of anti-apoptotic proteins leading to tumour progression and chemoresistance, there has been considerable focus on targeting these proteins. A number of different compounds have been identified and designed that inhibit or reduce the levels of anti-apoptotic proteins and thus overcome the apoptotic block and restore sensitivity of cancer cells to chemotherapeutic agents. One strategy utilized antisense oligonucleotides to target mRNAs, thus reducing the *de novo* synthesis of antiapoptotic proteins. The antisense oligonucleotide, Oblimersen (G3139, Genasense) targets Bcl-2 mRNA (Klasa et al., 2002), but in clinical trials had limited success (Waters et al., 2000; Morris et al., 2002; O'Brien et al., 2005). The most successful strategy to target antiapoptotic proteins has been the design of small-molecule inhibitors which are able to mimic BH3-only proteins by binding to the hydrophobic grooves of anti-apoptotic proteins. Due to differences in the hydrophobic grooves, these small molecule inhibitors display varied affinities for the different anti-apoptotic proteins (the structures of some small-molecules inhibitors are displayed in Figure 3.1). Some of these inhibitors including BH3-Is, HA14-1, and Antimycin-A, bind to anti-apoptotic proteins at high concentrations (Zhang et al., 2007) and induce cell death in a Bax/Bak independent manner (van Delft et al., 2006). Therefore, these inhibitors have additional targets other than anti-apoptotic proteins and as such could lead to unpredicted toxicities. Gossypol and the 'pan-inhibitor' Obatoclax (GX015-070, Gemin X) bind to anti-apoptotic proteins at lower concentrations and have entered clinical trials, however, they have proved to be relatively unsuccessful (Heist *et al.*, 2010; Parikh *et al.*, 2010), and have also been shown to act in a Bax/Bak independent fashion (van Delft *et al.*, 2006; Konopleva *et al.*, 2008; Tse *et al.*, 2008).

1.12.1 ABT-737 / ABT-263

By far the most potent and well-studied small-molecule inhibitor of anti-apoptotic proteins is ABT-737 (see Figure 3.2A) developed by Abbott Laboratories. This compound binds to Bcl-2, Bcl-xL, and Bcl-w in the nanomolar range (Oltersdorf *et al.*, 2005) and is able to induce apoptosis in a Bax/Bak dependent fashion, indicating that it is a bona-fide BH3-mimetic (van Delft et al., 2006). In in vitro studies, ABT-737 displayed single agent activity against a number of lymphoid cancers and SCLC (Oltersdorf et al., 2005; Konopleva et al., 2006; Del Gaizo Moore et al., 2007; Del Gaizo Moore et al., 2008), and synergized with a range of chemotherapeutics (Oltersdorf et al., 2005). In mouse models, ABT-737 displayed promising results with limited side-effects (Oltersdorf et al., 2005; Konopleva et al., 2006). Due to the low affinity ABT-737 has for Mcl-1, the activity of the compound is limited to cancer types with low Mcl-1 expression (Konopleva et al., 2006; van Delft et al., 2006). Another limitation of ABT-737 is that it is not orally bioavailable and as such the compound ABT-263 was developed with similar binding activity but improved oral absorption and dosing flexibility, and as such has entered clinical trials (Park et al., 2008a; Tse et al., 2008). Greater detail on anti-apoptotic inhibitors including ABT-737 and ABT-263 is provided in Sections 3.1.2-3.1.5.

1.13 TUMOUR TARGETING

The basis of chemotherapy primarily involves the killing of proliferating cancer cells by targeting general cellular processes including DNA, RNA, and protein synthesis. However, there are many types of normal cells in the body that also rapidly divide and proliferate and are susceptible to the mechanisms of action of chemotherapeutics. For this reason, the

effectiveness of cancer therapy is often limited by unwanted side-effects of chemotherapeutic drugs, such as dose-dependent cardiotoxicity associated with doxorubicin, which subsequently restricts the dosage and duration of therapy. In order to circumvent such problems, there has been considerable interest in developing strategies to selectively deliver or target drugs to tumour cells. Therefore, high drug levels and drug activity may be confined to a localized tumour site with minimal action on normal tissues, consequently leading to reduced side effects and improved quality of life.

1.13.1 Drug Delivery

Targeted drug delivery involves the use of drug carrier vehicles to encapsulate and deliver the drug to the tumour site in order to achieve higher drug concentrations and activity. Delivery of the drug also minimizes the potential of the drug to interact with normal cells and lead to the induction of side-effects. Several types of drug carrier vehicles have been extensively studied including liposomes, micelles, and various other nanoparticles (reviewed by Lammers et al., 2008; Singh and Lillard, 2009). These delivery vehicles need to be nontoxic, non-immunogenic, biocompatible and biodegradable, have long circulation times, avoid clearance by the reticuloendothelial system, allow high levels of drug loading, and allow release of the drug once it has reached the tumour site (Singh and Lillard, 2009). The drug-loaded delivery vehicles are able to passively accumulate at the sites of solid tumours due to the enhanced penetration and retention (EPR) effect (Singh and Lillard, 2009). The EPR effect occurs due to the very high permeability of tumour blood vessels, allowing small carrier vehicles to selectively deliver drug and be retained in the tumour interstitial space (Maeda et al., 2000). Ligands may also be attached to the surface of the delivery vehicles, allowing for active targeting where the attached ligand specifically binds to a target receptor on tumour cells (Lammers et al., 2008).

Liposomal Doxorubicin

The use of liposomal formulations for doxorubicin delivery have been shown to target the drug to tumour sites while reducing drug levels in heart tissues, thus, reducing cardiac toxicity in comparison to free doxorubicin (Papahadjopoulos *et al.*, 1991; Working and

Dayan, 1996; Berry *et al.*, 1998). Pegylated liposomes are particularly effective for doxorubicin delivery since pegylation increases serum half-life and reduces opsonization (Gabizon *et al.*, 2003; Veronese and Pasut, 2005). In clinical trails, pegylated liposomal doxorubicin demonstrated reduced cardiotoxic effects without a reduction in anticancer efficacy (Johnston and Gore, 2001; O'Brien *et al.*, 2004; Rifkin *et al.*, 2006), and as such the pegylated liposomal doxorubicin formulation, Doxil (Caelyx), has been FDA approved for the treatment of recurrent ovarian cancer, multiple myeloma, and AIDS-related Kaposi's sarcoma (Lammers *et al.*, 2008).

1.13.2 Targeting Signalling Pathways

There are several processes implicated in tumourigenesis and cancer progression including angiogenesis, invasion and metastasis, and these processes are regulated via various receptors and signalling pathways (Hanahan and Weinberg, 2000). Another targeting strategy is to identify these receptors and signalling molecules that are exclusively expressed or overexpressed on/in cancer cells while having a limited expression profile in normal tissues. Therefore, such receptors and signalling molecules make ideal targets for either designing novel drugs or modifying existing ones, enabling them to interact specifically with cancer cells. For example, epidermal growth factor receptor (EGFR) is overexpressed in many types of cancers including colorectal, pancreatic, breast, and ovarian cancers, and its overexpression is associated with advanced disease and poor clinical prognosis in patients (DeVita *et al.*, 2005). The identification of EGFR as an oncogene makes it an ideal target for the development of anticancer agents. Such agents approved for clinical use include the monoclonal antibody inhibitor cetuximab and the EGFR tyrosine kinase inhibitor gefitinib (Iressa) (Lurje and Lenz, 2009).

Targeting Angiogenesis

In recent times, a focus has been placed on developing drugs that target angiogenesis since is appears that all solid tumours to some extent are dependent on angiogenesis for growth. The signal protein, vascular endothelial growth factor (VEGF), plays an important role in stimulating angiogenesis in tumours (DeVita *et al.*, 2005), and is the target of the monoclonal

antibody bevacizumab (Avastin) which is clinically approved to treat a range of metastatic cancers (Mukherji, 2010). Another candidate for anti-tumour targeting strategies is the $\alpha\nu\beta3$ integrin which has been shown to be heavily overexpressed on endothelial cancer cells involved in angiogenesis, while having a low expression level on most normal tissues (Brooks *et al.*, 1994b; Mulgrew *et al.*, 2006). Monoclonal antibodies (for example, Abergrin) and RGD-peptides (arginine-glycine-aspartic acid; for example, Cilengitide) have been used to target the $\alpha\nu\beta3$ integrin in an attempt to inhibit tumour growth and metastasis and have entered clinical trials (Cai and Chen, 2006). Endogenous extracellular matrix (ECM) ligands of the $\alpha\nu\beta3$ integrin contain an exposed RGD sequence which serves as the recognition site (Eliceiri and Cheresh, 1999), and many types of RGD antagonists have been synthesized to inhibit such interactions and prevent downstream signalling (Dunehoo *et al.*, 2006). Greater detail on $\alpha\nu\beta3$ integrins and targeting strategies is provided in Section 5.1.

1.14 RESEARCH OBJECTIVES

Over the last 20 years, research in the Cutts/Phillips laboratory has demonstrated that doxorubicin is able to form DNA adducts in the presence of formaldehyde (Zeman *et al.*, 1998; Cutts *et al.*, 2001). Furthermore, the combination of doxorubicin with formaldehyde-releasing prodrugs has been shown to be synergistic in a range of cancer cell lines (Cutts *et al.*, 2001; Cutts *et al.*, 2005; Swift *et al.*, 2006), and caused a reduction in tumour volume in a mouse model (Cutts *et al.*, unpublished data). Although anthracycline-DNA adduct forming treatments are still in the preclinical developmental stage, it is important to determine how the anticancer effects of this treatment can be enhanced in a clinical setting. Therefore, the overall aim of this project is to enhance the anticancer potential of anthracyclines-DNA adducts in clinically relevant situations. In particular, this project aims to look at ways of potentially overcoming the two major limitations of chemotherapeutics that are commonly encountered in the clinic – chemoresistance and side-effects.

Cancer cells are often associated with an increased expression of anti-apoptotic proteins, such as Bcl-2, allowing them to survive in the face of chemotherapeutic treatments, thus making them inherently resistant. Previous studies have demonstrated that overexpression of Bcl-2

confers resistance to doxorubicin-DNA adduct forming treatments (Swift *et al.*, 2006). The first part of this project will investigate the use of the Bcl-2 inhibitor ABT-737 to determine if the combination of this inhibitor with doxorubicin-DNA adduct forming treatments can overcome Bcl-2 mediated resistance.

The use of pre-activated anthracycline compounds that do not require formaldehyde for DNA adduct formation potentially possess even greater anticancer efficacy than the combination of doxorubicin with formaldehyde-releasing prodrugs. The second part of this project will involve the use of the pre-activated anthracycline doxazolidine and assess its ability to kill cancer cells, including Bcl-2 overexpressing cancer cells.

Side-effects are another major limitation of chemotherapy and in recent times a lot of focus has been placed on developing tumour targeting strategies to maximize drug action at the tumour site while minimizing the effects on normal cells, thus minimizing side-effects. Another part of this project will investigate the $\alpha\nu\beta3$ integrin as a cancer cell target for the development of targeting strategies to potentially localize anthracycline-DNA adduct formation specifically to tumour cells.

Chapter 2

MATERIALS & METHODS

2.1 CELL LINES

The HL-60 promyelocytic leukemic cell line (HL-60/WT; wild-type) and the mitoxantrone resistant variant cell line, HL-60/MX2, were obtained from the American Type Culture Collection (Virginia, USA). HL-60/MX2 cells exhibit reduced topoisomerase-II α expression and no detectable levels of topoisomerase-II β (Harker *et al.*, 1991; Harker *et al.*, 1995). HL-60 cells overexpressing Bcl-2 (HL-60/Bcl2) and the parental empty vector control cell line (HL-60/Puro) were obtained as a gift from Dr. Gino Vairo (CSL Limited, Melbourne, Australia). Both cell lines contain a plasmid expressing puromycin resistance (pEFPGK-puro), with the HL-60/Bcl2 cells containing the human bcl-2 gene under control of the EF1 α promoter (Vairo *et al.*, 1996). HL-60/Bcl2 and HL-60/Puro cells were maintained in the presence of 2 µg/mL puromycin (Sigma Aldrich).

U937 (human leukemic monocyte lymphoma) cells were obtained from Dr. Carleen Cullinane (Peter MacCallum Cancer Institute, Melbourne, Australia). HCT116 (human colorectal carcinoma) cells were supplied by Dr. M. Koi (Brunel University, Uxbridge, UK).

The mouse mammary epithelial cell lines; $66c14/\beta$ Babe, $66c14/\beta$ 3, 4T1.2/pRS, $4T1.2/sh\beta$ 3 and 4T1.2/neo, were kindly provided by Dr. Robin Anderson (Peter MacCallum Cancer Institute, Melbourne, Australia). 66c14 and 4T1 cells were derived from a spontaneous mammary carcinoma in a Balb/c/CH3 mouse (Aslakson and Miller, 1992), with the 4T1.2cell line being a variant cloned from 4T1 cells (Lelekakis *et al.*, 1999). The $66c14/\beta$ 3 cell line was created as outlined by Sloan and colleagues (2006). Briefly, the full-length mouse β 3 integrin subunit was subcloned into a pBabe-puro retroviral vector. Phoenix packaging cells were transiently transfected with the target β 3 cDNA and the culture supernatant was used to infect 66c14 cells. Subsequently a pool of 66c14 cells stably expressing high levels of the β 3 subunit was selected by puromycin resistance followed by fluorescence-activated cell sorting (FACS). An empty vector control cell line was also created and termed 66c14/pBabe.

To create the 4T1.2/shβ3 cell line, shRNA (5'-AAGGATGATCTGTCCACGATC-3'), was ligated into a pRetroSuper vector (pRS) which was subsequently transfected into PT67 packaging cells. The culture supernatant was used to infect 4T1.2 cells and selection was

performed via puromycin resistance. The bulk cell population was single cell cloned and five clones displaying knockdown of the β 3 integrin subunit were pooled to generate the 4T1.2/sh β 3 cell line. Similarly, a non-targeting hairpin sequence (5'-AGTACTGCTTACGATACGG-3') was used to generate the 4T1.2/pRS cell line via the same procedure. 4T1.2/neo cells were created by transfecting 4T1.2 cells with a vector containing a neomycin resistance gene, and these cells were used for implantation into Balb/c mice for mouse studies (see Section 2.15).

All HL-60 cell lines as well as U937 and HCT116 cells were routinely passaged in RPMI 1640 media (Gibco) supplemented with 10% fetal bovine serum (FBS; Thermo Electron, Melbourne, Australia). All mouse mammary epithelial cell lines (66cl4 and 4T1.2 cell lines) were routinely passaged in alpha minimal essential medium (α -MEM; Gibco) supplemented with 5% FBS, 1% penicillin-streptomycin (Gibco), and 1% GlutaMAX (Gibco). All cell lines were maintained at 37 °C, 5% CO₂. Suspension cells were treated approximately 30 min after seeding, while adherent cells were treated at least 12 hr after seeding.

Trypsin-ethylenediaminetetraacetic acid (EDTA; 0.05%; Gibco) was used to detach HCT116 cells while an Enzyme-Free Cell Dissociation Solution (Millipore) was used to detach all mouse mammary epithelial cell lines to better preserve the integrity of cell surface components including integrins.

2.2 DRUGS AND COMPOUNDS

2.2.1 Anthracyclines and Related Compounds

Doxorubicin was provided by Pfizer (New York, USA; formerly Farmitalia, Milan, Italy), and radiolabeled [¹⁴C]-doxorubicin (specific activity of 55 mCi/mmol) was obtained from GE Healthcare Biosciences (Little Chalfont, UK), and both were dissolved in Milli-Q water to a 1 mM stock solution and stored at -20 °C. MEN-10755 was a gift from Menarini Richerche SpA (Pomezia, Italy), and was also dissolved in Milli-Q water and stored at -20 °C. Barminomycin was isolated and characterized as previously described (Kimura *et al.*,

1987), and was provided as a gift from Prof. Ken-Ichi Kimura (Iwate University, Iwate, Japan). Barminomycin was dissolved in methanol and stored at -20 °C and diluted in phosphate buffered saline (PBS), pH 7.4, for further use. Doxazolidine was synthesized as described previously (Post *et al.*, 2005) and provided as a gift from Dr. Tad Koch (University of Colorado, Boulder, Colorado, USA) and was dissolved in anhydrous DMSO and used immediately. Concentrations of the above mentioned drugs were determined spectrophotometrically at 480 nm with a molar extinction coefficient of 11,500 M⁻¹ cm⁻¹.

2.2.2 Formaldehyde-Releasing Prodrugs

All formaldehyde-releasing prodrugs were provided by Prof. Abraham Nudelman. AN-9 (pivaloyloxymethyl butyrate; Nudelman *et al.*, 1992), AN-7 (butyroyloxymethyl-diethyl phosphate; Nudelman *et al.*, 2001), and AN-193 (Nudelman *et al.*, 2005), were synthesized as described previously. The prodrug, AN-158 which releases acetaldehyde, butyric acid, and pivalic acid upon esterase-mediated hydrolysis was synthesized as described previously (Cutts *et al.*, 2001). Prodrug stock solutions were kept in glass vials and stored under argon at 4 °C. Stock solutions were diluted in DMSO (typically to 50 mM sub-stock solutions), with the exception of AN-7 which was diluted in Milli-Q water, using glass syringes and glass vials before being diluted further in PBS if required.

2.2.3 Other Compounds

ABT-737 (A-779024; absolute configuration is "R") and its enantiomer (A-793844; absolute configuration is "S") were synthesized and kindly provided by Abbott Laboratories (Abbott Park, Illinois, USA). The compounds were dissolved in DMSO to produce a 5 mM stock solution and stored at -20 °C. Etoposide (Sigma Aldrich) was dissolved in DMSO to a 1 mM stock solution and stored at -20 °C. The peptides c(RGDfK) (cyclo(Arg-Gly-Asp-_D-Phe-Lys)) and c(RADfK) (cyclo(Arg-Ala-Asp-_D-Phe-Lys)) were obtained from Peptides International (Louisville, KY, USA) and were dissolved in Milli-Q water to a 7 mM and 10 mM stock solution respectively and stored at -20 °C. The pan-caspase inhibitor Z-VAD-fmk was obtained from Promega, and the necroptosis inhibitor necrostatin-1 was obtained from

Sigma Aldrich. A lysate of human Rad9 transfected 293T cells that was used as a Rad9 positive control for immunoblotting was obtained from Santa Cruz.

2.3 IMMUNOBLOTTING

2.3.1 Preparation of Whole Cell Lysates

Cells were treated for indicated times, harvested, and washed twice with ice-cold PBS containing 1 mM PMSF (phenylmethylsulphonyl fluoride). Cell pellets were resuspended in chilled lysis buffer (typically between 50-100 μ L; 50 mM Tris-HCl pH 7.5, 150 mM NaCl, 1% Nonidet P-40, 1 x protease inhibitor cocktail (Roche), 1 mM PMSF and 10 μ g/mL aprotinin, in Milli-Q water) and incubated on ice for 30 min. Lysates were centrifuged (12,000 rpm, 20 min at 4 °C) to remove cellular debris and the supernatant containing cellular proteins was either immediately subjected to SDS-PAGE or stored overnight at -20 °C.

2.3.2 Determination of Protein Concentration and SDS-PAGE

The protein concentration of each sample was determined using the Bio-Rad DC protein assay kit (Bio-Rad) according to the manufacturer's instructions. Typically 50 µg protein per sample was denatured via addition of 1 x SDS loading buffer (50 mM Tris-HCl pH 6.8, 2% SDS, 0.1% bromophenol blue, and 10% (v/v) glycerol) in the presence of 100 mM β -mercaptoethanol, boiled for 5 min, and loaded onto NuPAGE 10% Bis-Tris gels (Invitrogen). Samples were run in the presence of 1 x NuPAGE MES SDS running buffer (Invitrogen), typically at 100 V for approximately 90 min to separate proteins.

2.3.3 Western Transfer

Western transfer of proteins was carried out using a semi-dry blotting apparatus (Thermo Scientific) with 1 x Western transfer buffer (48 mM Tris-HCl pH 7.5, 38.5 mM glycine, 0.037% SDS and 20% (v/v) methanol). Three sheets of Whatman 3MM blotting paper cut to

the size of the gel were placed onto the apparatus after being pre-soaked in 1 x Western transfer buffer. The gel was placed on top of the blotting paper and a sheet of methanol-activated polyvinylidene fluoride (PVDF) membrane cut to the size of the gel was placed on top of the gel, followed by three more sheets of pre-soaked Whatman blotting paper. Transfer of proteins from the gel to the PVDF membrane was achieved by applying an electric field (2 mA/cm^2) for 90 min.

2.3.4 Immunoprobing

PVDF membranes were blocked in 10% (w/v) skim milk powder in PBS overnight at 4 °C under gentle rocking, washed three times for 5 min each with TBS-T (Tris-buffered saline containing 0.1% (v/v) Tween-20), before application of the primary antibody. Table 2.1 lists the primary antibodies and the typical dilutions used for immunoblotting. Membranes were probed with primary antibodies overnight at 4 °C under gentle rocking and washed three times for 5 min each with TBS-T. Secondary antibodies (Table 2.1) were applied for a minimum of 1 hr at room temperature under gentle rocking before being removed and the membrane washed three times for 5 min each with TBS-T. Membranes were exposed to Lumi-Light enhanced chemiluminescence (ECL) detection reagent (Roche) and the chemiluminescent signal detected using a gel documentation system. Membranes were then re-probed with primary (anti-actin or anti-GAPDH) and secondary antibodies and subjected to detection as listed above to determine if the protein loading across the lanes was equal.

2.4 GROWTH INHIBITION ASSAY

The measurement of growth inhibition enables the determination of the cytotoxicity of a particular drug or compound against a particular cell line or between different cell lines. The MTS assay is a colorimetric growth inhibition assay where the tetrazolium salt MTS (3-(4,5-dimethylthiazol-2-yl)-5-(3-carboxymethoxyphenyl)-2-(4-sulfophenyl)-2H-tetrazolium, inner salt) is bioreduced in metabolically active cells into a soluble formazan product that can

Table 2.1. Primary and secondary antibodies used for Western blotting analysis.

Antibodies	Source	Company	Dilution
Primary			
anti-Bcl2	Mouse (mono)	Calbiochem	1:500
anti-FLAG	Mouse (mono)	Sigma Aldrich	1:2000
anti-Mcl1	Rabbit (poly)	Santa Cruz	1:500
anti-actin	Rabbit (poly)	Sigma Aldrich	1:2000
anti-GAPDH	Mouse (mono)	Ambion	1:2000
anti-Rad9	Rabbit (poly)	Santa Cruz	1:250
Secondary			
anti-mouse	Rabbit	Sigma Aldrich	1:2000
anti-rabbit	Goat	Sigma Aldrich	1:2000

be measured spectrophotometrically. The IC_{50} (the half-maximal inhibitory concentration) of a particular drug can then be determined.

Cell Number Optimization

Cell number optimization experiments were performed to ensure that the cell density used in the assay was in the linear range of cell growth at the end of the assay. Serial dilutions of cells in RPMI 1640 media were performed and added (100 μ L) to 96-well plates in quadruplicate ranging from 0 - 1x10⁶ cells/mL. To each well, 100 μ L of RPMI 1640 media was added to simulate drug treatment and the cells were incubated for 48 hr at 37 °C, 5% CO₂. After 48 hr incubation, solutions of MTS (1.6 mg/mL in PBS, Promega) and the electron coupling reagent, PMS (1.6 mg/mL in PBS, phenazine methosulfate, Sigma Aldrich), were made and 50 μ L of a 90% MTS, 10% PMS solution was added to each well. Cells were incubated for a further 3 hr at 37 °C, 5% CO₂, and the absorbance at 490 nm in each well was recorded using a SpectraMax M2 plate reader (Molecular Devices, Sunnydale, CA, USA). The absorbance values of RMPI 1640 media alone control samples were subtracted from cell-containing samples. The optimal cell density for HL-60/Puro and HL-60/Bcl2 cells was determined to be 200,000 cells/mL, and this cell density was used for subsequent MTS assay experiments, as well as other cell viability assays involving HL-60 cell lines.

Drug Treatments

Cells ($2x10^5$ cells/mL for HL-60/Puro and HL-60/Bcl2 cells) were seeded into 96-well plates (100 µL per well) in quadruplicate. Cells were treated with a serial dilution of drug concentrations ranging over at least a 5-log scale (100 µL in RPMI 1640 media) and incubated for 48 hr at 37 °C, 5% CO₂. For experiments involving doxazolidine, the drug was serially diluted in DMSO to 100x concentrations before being diluted further in RPMI 1640 media to 10x concentrations, and finally added to 96-well plates to obtain the final concentrations. For all drug treatments, cells were incubated with a MTS/PMS solution and absorbance values recorded as described above. The results were plotted as A₄₉₀ versus log₁₀ drug concentration and the IC₅₀ value determined for the drug in question.

2.5 CELL VIABILITY ASSAYS

For all cell viability assays the following cell densities were used: for U937 and all HL-60 cell lines, $2x10^5$ cells/mL were used; for HCT116 cells, $8x10^4$ cells/mL were used; and for all 66cl4 and 4T1.2 mouse mammary epithelial cell lines, $4x10^4$ cells/mL were used.

2.5.1 Sub-G1 FACS Assay

Cells were treated in 6-well plates for indicated times, pelleted (1200 rpm for 5 min), and fixed by resuspension in 70% ethanol for at least 30 min at 4 °C (typically overnight). After fixation, cells were pelleted (2000 rpm for 5 min), washed in PBS, and centrifuged again (2000 rpm for 5 min). Cell pellets were resuspended in 250 μ L of staining solution (2.5 μ g/mL propidium iodide (PI) and 50 μ g/mL RNase A in PBS) and incubated for 30 min at 37 °C in the dark. Samples were transferred to FACS tubes, kept on ice, and analysed immediately.

Analysis was performed using a FACSCanto II flow cytometer (BD Biosciences, San Jose, CA, USA) employing FACSDiva software. Samples (10,000 events recorded) were gated to distinguish and omit small debris and doublets by employing a forward-scatter versus side-scatter dot plot and applying an appropriate exclusion gate. The gated events were plotted as a PI-histogram and a marker region was set up to distinguish cells with normal DNA content (G1-phase, S-phase and G2-phase of cell cycle) from cells with fragmented DNA represented in the sub-G1 region. Apoptotic cells that have undergone DNA fragmentation would have lost small fragments of DNA in the wash step during sample preparation and as such would contain less DNA than non-apoptotic cells. An example histogram plot showing the sub-G1 population of a sample is displayed in Figure 2.1. Quantitative data was obtained where the percentage of sub-G1 events was proportional to the percentage apoptosis for a given sample.

2.5.2 Caspase-3 Activation Assay

In this assay the caspase-3 substrate, Ac-DEVD-AFC (Calbiochem), was used. This substrate becomes cleaved in the presence of active caspase-3 to release the AFC (7-amino-4-

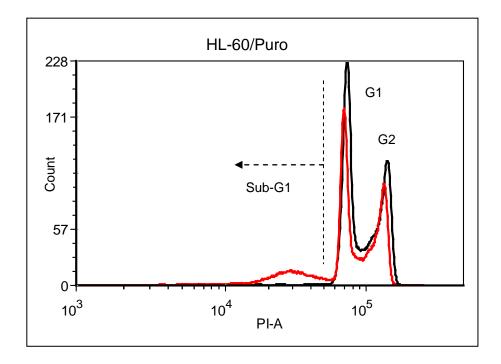


Figure 2.1 Example histogram plot obtained from sub-G1 FACS analysis.

Samples of untreated (black graph) and doxorubicin/AN-9 treated (red graph; 500 nM doxorubicin and 25 μ M AN-9 for 6 hr) HL-60/Puro cells subjected to sub-G1 FACS analysis. In addition to the G1 and G2 cell-cycle populations, the treated sample also consists of a sub-G1 population of cells which are scored as apoptotic.

trifluoromethylcoumarin) fluorophore, and the resulting fluorescence can be measured. Cells were treated in 6-well plates for indicated times, pelleted (1200 rpm for 5 min), and lysed in chilled lysis buffer (10 mM EDTA, 0.5% Triton-X 100, 10 mM Tris-HCl pH 8, in Milli-Q water) for 10 min at room temperature. DNA was sheared using a syringe and 23 gauge needle, and samples were centrifuged at 13,000 rpm for 15 min at 4 °C. The caspase-3 substrate, Ac-DEVD-AFC, was added to substrate buffer (0.1 M HEPES pH 7, 10% PEG-3350, 0.1% CHAPS, 10 mM DTT in Milli-Q water) to achieve a final concentration of 50 μ M. An aliquot of the cell lysate (20 μ L consisting of approximately 25 μ g protein) was added to 80 μ L substrate mix and the resulting solution was mixed and added to a 96-well black, clear bottom plate. Samples were incubated for 4 hr in the dark and the fluorescence intensity (excitation 400 nm, emission 505 nm) was recorded using a SpectraMax M2 plate reader (Molecular Devices, Sunnydale, CA, USA). The fluorescence intensity obtained from a lysis buffer control sample was subtracted from samples containing cell lysates.

2.5.3 Apoptotic Morphology Assay

This assay measures apoptosis by the visualization of nuclear morphology of treated cells. Cells undergoing apoptosis typically display nuclear fragmentation, chromatin condensation, and the formation of apoptotic bodies (Saraste and Pulkki, 2000; Ziegler and Groscurth, 2004), which can be detected in this assay by microscopic analysis.

Polylysine-coated coverslips were prepared one day prior to the experiment. Coverslips were sonicated for 15 min in acetone and washed three times with distilled water and allowed to dry. Poly-L-Lysine (500 μ L, 0.1% (w/v); Sigma Aldrich) was added onto the coverslips and incubated for 1 hr at room temperature. Coverslips were rinsed gently with distilled water and allowed to "slant-dry" overnight.

Cells were treated in 6-well plates for indicated times, pelleted (1200 rpm for 5 min), and washed in PBS. Cell were fixed by resuspension in 3.7% paraformaldehyde in PBS and incubated for 15 min at room temperature. Cells were centrifuged (2000 rpm for 5 min), and cell pellets were washed once with PBS and resuspended in 30 μ L PBS before being added onto the polylysine-coated coverslips. Coverslips were incubated for 30 min at room

temperature to allow the cells to adhere and washed twice gently with PBS. Cells were permeabilized by the addition of 0.5% (v/v) Triton-X 100 in Milli-Q water and incubated for 5 min at room temperature. Coverslips were washed three times gently with PBS before incubation with Hoechst 33258 (1 μ g/mL in Milli-Q water) for 30 min at 37 °C in the dark. Coverslips were washed twice gently with PBS and mounted onto microscope slides and incubated at 4 °C in the dark until analysis. Cells were visualized using an Olympus IX81 inverted microscope using a UV filter under 40x magnification. The nuclear morphology of 200 cells per sample was examined and cells with round, intact nuclei, were scored as non-apoptotic, while cells displaying clear nuclear fragmentation and/or condensation were scored as apoptotic.

2.5.3.1 Mitotic Catastrophe

To determine if cells were undergoing mitotic catastrophe, the same procedure was used as described above for the morphology assay. The presence of large cells with multiple nuclei is indicative of mitotic catastrophe (Castedo *et al.*, 2004), and as such, cells displaying these characteristics under microscopic visualization were scored as undergoing mitotic catastrophe. An example of HeLa cells undergoing mitotic catastrophe is shown in Figure 2.2.

2.5.4 Propidium Iodide Uptake Assay

The propidium iodide uptake assay was used to measure cell viability, where healthy cells with an intact cell membrane exclude propidium iodide, while cells with a compromised cell membrane display an increase in propidium iodide fluorescence. This increase in fluorescence can be recorded by FACS analysis.

Cells were treated for indicated times, pelleted (1200 rpm for 5 min), washed in 2 mL PBS, and resuspended in 250 μ L of propidium iodide staining solution (5 μ g/mL propidium iodide and 0.3% (v/v) FBS in PBS). Samples were transferred to FACS tubes, kept on ice, and analyzed immediately.

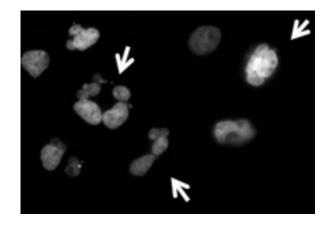


Figure 2.2. Example of cancer cells undergoing mitotic catastrophe.

HeLa cells with an abrogated G2/M cell cycle checkpoint (via ATR knockdown) displayed characteristic features of mitotic catastrophe in response to treatment with doxorubicin/AN-9. The arrows point out large, multinucleated cells, undergoing mitotic catastrophe (Forrest *et al.*, 2012).

As with the sub-G1 apoptosis assay described above, analysis was performed using a FACSCanto II flow cytometer employing FACSDiva software. Samples (10,000 events recorded) were gated to distinguish and omit small debris and doublets by employing a forward-scatter versus side-scatter dot plot and applying an appropriate exclusion gate. The gated events were plotted as propidium iodide fluorescence versus cell counts and an appropriate marker region was set up based on a vehicle treated control sample to distinguish healthy PI-negative cells from PI-positive cells. Quantitative data was obtained where the PI-positive cells were scored as non-viable and the final data was expressed as percentage cell death.

2.6 ALKALINE COMET ASSAY (single cell gel electrophoresis)

The alkaline Comet assay was used to detect single and double-stranded DNA breaks resulting from the mechanism of drug action, and was performed essentially as described previously (Salti *et al.*, 2000). Cells (4 mL at $2x10^5$ cells/mL for all HL-60 cell types) were treated for indicated times and 200 µL aliquots of the cell suspensions were used for the Comet assay, while the remaining portion was used for sub-G1 FACS analysis to ensure that DNA damage was due to drug action and not due to the downstream effects of apoptosis.

The 200 μ L cell suspension aliquots were added to individual wells of a 24-well plate and 1 mL of 1% (w/v) Type-VII low gelling temperature agarose (Sigma Aldrich) in PBS that was melted and kept at 40 °C was added to each well. Immediately, 1 ml of the agarose cell suspension was pipetted onto glass microscope slides that had been pre-coated overnight with 1% (w/v) Type-1A agarose (Sigma Aldrich) in Milli-Q water. A 40 x 22 mm coverslip was then placed on top of the agarose cell suspension and once the agarose had set (2-3 minutes) the coverslip was removed.

Slides were then positioned in containers on ice and submerged in ice-cold alkaline lysis buffer (100 mM Na₂EDTA, 2.5 M NaCl, 10 mM Tris-HCl, pH adjusted to 10.5 with 5 M NaOH, and 1% (v/v) Triton-X 100 in Milli-Q water) and incubated on ice for 1 hr in the

dark. Slides were rinsed twice with ice-cold Milli-Q water and washed four times for 15 min each with ice-cold Milli-Q water in the dark. Slides were transferred to a Horizon horizontal electrophoresis apparatus and covered with alkaline electrophoresis buffer (300 mM NaOH, 1 mM EDTA in Milli-Q water) so the buffer level was just above the slides. Slides were incubated with the alkaline electrophoresis buffer for 1 hr in the dark at 4 °C and subjected to electrophoresis for 30 min at 30 V at 4 °C. Slides were removed from the apparatus and immediately placed in containers and washed with neutralization buffer (0.5 M Tris-HCl, pH 7.5 in Milli-Q water) for 10 min. Slides were then washed twice with PBS for 10 min and rinsed with Milli-Q water or left overnight and re-hydrated with Milli-Q water before staining with 2.5 µg/mL propidium iodide in Milli-Q water for 7 min. Stain solution was rinsed off with Milli-Q water over 5-10 min before analysis.

Slides were viewed using an Olympus BX40 fluorescence microscope with a 20x objective lens and images captured with a CoolSNAP-Pro monochrome CCD camera (Media Cybernetics, Bethesda, Maryland, USA). Analysis was performed using Komet 5.5 software (Andor Technology, Belfast, UK) and the Olive Tail Moment (OTM) values of 50 cells per slide were measured and averaged (Olive, 1989). The OTM takes into account the length and the intensity of the produced comet, with higher OTM values signifying a greater degree of DNA strand breaks.

2.7 NASH ASSAY

The Nash assay is a colorimetric assay for measuring formaldehyde levels (Nash, 1953). In this project the Nash assay was used to detect and quantitate formaldehyde levels released from the prodrugs AN-9, AN-7, AN-193, and AN-158 upon esterase-mediated hydrolysis. Following initial dilution in DMSO, or Milli-Q water in the case of AN-7, prodrugs were diluted in PBS to final concentrations of 50 or 100 μ M. Prodrugs were incubated in the presence of porcine liver carboxyl esterase (Sigma Aldrich), at a final concentration of 10 ng/µL, to catalyse hydrolysis and formaldehyde release. Control samples were also set up where prodrugs were incubated with Milli-Q water instead of esterase. Formaldehyde (Merck) standards (0-200 μ M diluted in PBS) were also prepared and assayed simultaneously. All samples (final volume of 100 μ L) were incubated for 1 hr at 37 °C. Nash reagent (2 M ammonium acetate, 50 mM acetic acid, and 50 mM acetylacetone in Milli-Q water) was added to samples in a 1:1 volume ratio (100 μ L Nash reagent added to 100 μ L samples) and the resulting solutions were incubated for 30 min at 50 °C. In the presence of formaldehyde, a yellow-coloured lutidine compound (diacetyl-dihydrolutidine) is produced which can be detected spectrophotometrically. Samples were transferred to 96 well plates and the absorbance was recorded at 412 nm using a SpectraMax M2 plate reader (Molecular Devices, Sunnydale, CA, USA). Formaldehyde levels were quantitated by subtracting control readings (PBS alone) and comparing absorbance values to the formaldehyde standards.

2.8 [¹⁴C]-DOXORUBICIN DNA ADDUCT LEVELS

Cells were treated with $[^{14}C]$ -doxorubicin alone or in combination with formaldehydereleasing prodrugs (or the acetaldehyde-releasing prodrug, AN-158, as a control) for indicated times, harvested, and resuspended in 200 µL PBS.

Genomic DNA Isolation

Genomic DNA from samples was isolated using a QIAmp Blood Mini Kit (Qiagen) with the following protocol alterations to minimize the loss of doxorubicin-DNA adducts: (1) 10 mg/mL RNase A (40 μ L) was added to the lysis reaction; (2) the lysis incubation was carried out at 50 °C for 30 min instead of 56 °C for 10 min; (3) Buffer AW2 was used instead of Buffer AW1; and (4) Milli-Q water was used to elute DNA from the spin columns. Samples were then subjected to two phenol extractions and one chloroform extraction to remove non-covalently bound drug and the DNA was ethanol precipitated (13,000 rpm for 20 min at 4 °C) in the presence of glycogen and sodium acetate, and washed in 70% ethanol. The DNA pellet was allowed to dry before being resuspended in 100 μ L TE (tris-EDTA) buffer and the concentration of DNA was determined spectrophotometrically at 260 nm.

Scintillation Counting

Aliquots (90 μ L) of resuspended DNA were added to 1 mL of ReadySafe Scintillation Cocktail (Beckman Coulter, Fullerton, California, USA). Samples were mixed by vortexing and the level of [¹⁴C]-doxorubicin incorporated into DNA was monitored using a Wallac 1410 Liquid Scintiallation Counter. The [¹⁴C] counts per minute for each sample were recorded and final results were expressed as doxorubicin-DNA adducts per 10 kbp DNA.

2.9 siRNA KNOCKDOWN OF MCL-1

Silencer[®] Select siRNA duplex sequences targeting the Mcl-1 gene were purchased from Ambion (Austin, Texas, USA) with the sense and antisense sequences for the two siRNA duplexes used presented in Table 2.2. The siRNA duplexes were dissolved in nuclease/ribonuclease free water to a concentration of 5 μ M and aliquots stored in RNase-free tubes at -80 °C. To ensure siRNA integrity, RNase-free tubes and filter tips were used for the transfection process and all materials were sprayed with RNase Away solution.

Table 2.2. Silencer[®] Select siRNA duplex sequences used.

Target	siRNA ID	Sense sequence (5' $ ightarrow$ 3')	Antisense sequence (5' $ ightarrow$ 3')
Mcl-1	s8585	CAACUUCCGUAAUUAGGAAtt	UUCCUAAUUACGGAAGUUca
Mcl-1	s8583 (validated)	CCAGUAUACUUCUUAGAAAtt	UUUCUAAGAAGUAUACUGGga

Note: GAPDH (positive) and scrambled (negative) control sequences were not disclosed by the manufacturer.

Western Analysis of siRNA Knockdown

LipofectamineTM 2000 transfection reagent (Invitrogen) was added to 250 μ L Opti-MEM (Invitrogen) at the indicated volumes (either 4 or 6 μ L were used since optimization experiments showed that using higher volumes resulted in considerable cell kill levels after transfection) and incubated for 5 min at room temperature. The siRNA duplexes (scrambled and both Mcl-1 duplexes) were added to 250 μ L Opti-MEM to give final concentrations of 10 nM and incubated for 5 min at room temperature. The two Opti-MEM mixtures containing transfection reagent and siRNA duplexes were combined and incubated for 20 min at room temperature to allow formation of transfection complexes. The transfection complex mixtures were added to 6-well plates. Subsequently, HCT116 cells (2x10⁵ cells) were added to the transfection complexes and the plates gently rocked prior to incubation. Plates were incubated for 6 hr at 37 °C, 5% CO₂, after which the media was removed and replaced with fresh 2.5 mL RPMI 1640 media. Plates were incubated for a total of 72 hr and cells were harvested and prepared for Western analysis as described in Section 2.3 to determine if Mcl-1 protein levels had been knocked-down.

Sub-G1 FACS Analysis After Transfection

Transfections were set up as mentioned above, although the lower volume of 4 μ L LipofectamineTM 2000 was used to minimize cell kill induced by the transfection reagent. Both positive (GAPDH siRNA) and negative (scrambled siRNA) controls were set up alongside the Mcl-1 siRNA samples and concentrations of all siRNA duplexes used were 10 nM. After 48 hr incubation of cells with transfection complexes, the media was removed and cells were detached and re-seeded into 6-well plates (1.6x10⁵ cells). Cells were incubated for a further 24 hr in a 37 °C, 5% CO₂ incubator before drug treatment. Following drug treatment (24 hr with ABT-737), cells were harvested and the level of apoptosis induced measured via sub-G1 FACS analysis as described in Section 2.5.1.

2.10 ANTI-FLAG CO-IMMUNOPRECIPITATION

Co-immunoprecipitation (co-IP) studies were performed to identify proteins interacting with FLAG-tagged (eight amino acid long peptide tag) Bcl-2 expressed by HL-60/Bcl2 cells in response to drug treatment.

Preparation of Whole Cell Lysates

HL-60/Bcl2 cells (approximately 5×10^6 in total) were treated for indicated times and whole cell lysates were prepared as described in Section 2.3.1, with the exception that between 300-500 µL of chilled lysis buffer was used. Lysates were either assayed immediately and the protein concentration of each sample was determined using the Bio-Rad DC protein assay kit (Bio-Rad) according to the manufacturer's instructions. An equal amount of protein from each sample, typically 1-2 mg was used for the co-IP. An aliquot of each sample was used as the 'total input' sample for SDS-PAGE analysis.

Pre-Clearing Lysates

Cell lysates were subjected to pre-clearing using sepharose 4B beads (Sigma Aldrich). The beads, 100 μ L per sample (total volume depending on number of samples), were centrifuged at 4000 rpm for 1 min at 4 °C, the supernatant discarded, and the same volume of co-IP lysis buffer (1% (v/v) Triton-X-100, 10% (v/v) glycerol, 150 mM NaCl, 20 mM Tris-HCl pH 7.5, 2 mM EDTA, in Milli-Q water) was added to the beads. The bead pellet was washed with co-IP lysis buffer another three times. The bead pellet was resuspended in co-IP lysis buffer (using half the original volume of beads used), and 50-100 μ L of the resuspended beads were added to each cell lysate. Samples were incubated for 1 hr at 4 °C under constant rotation.

Adding Lysates to Anti-FLAG M2 Affinity Gel Beads

Anti-FLAG M2 affinity gel beads (Sigma Aldrich), 100 μ L per sample (total volume depending on number of samples), were centrifuged at 4000 rpm for 1 min at 4 °C, the supernatant discarded, and the same volume of co-IP lysis buffer was added to the bead

pellet. The pellet was washed another two times with co-IP lysis buffer, once with 100 mM glycine (pH 3.5), and twice more with co-IP lysis buffer.

The pre-cleared lysates were centrifuged at 4000 rpm for 10 min at 4 °C, and 50-100 μ L of the anti-FLAG M2 affinity gel preparation was added to each pre-cleared lysate sample. Samples were incubated for 1 hr at 4 °C under constant rotation to allow the FLAG-tagged Bcl-2 protein to bind to the anti-FLAG M2 affinity gel beads. Samples were centrifuged at 4000 rpm for 3 min at 4 °C and an aliquot of the supernatant was used as the 'unbound fraction' for SDS-PAGE analysis. Samples were washed five times in co-IP lysis buffer and the supernatant from the first wash was used as the 'wash fraction' for SDS-PAGE analysis.

Elution and Analysis

Freshly prepared FLAG-elution buffer (50 μ L; 2x protease inhibitor cocktail (Roche), 300 μ g/mL of FLAG peptide (Sigma Aldrich), 10 mM HEPES pH 7.9, 300 mM KCl, 1.5 mM MgCl2, 0.05% (v/v) Nonidet-P40, in Milli-Q water) was added to each bead pellet and samples were incubated for 30 min at 4 °C under constant rotation. Samples were centrifuged at 4000 rpm for 5 min and an aliquot of the supernatant was used as the 'bound (eluted) fraction' for SDS-PAGE analysis. The bead pellet was washed three times in co-IP lysis buffer, boiled for 5 min, centrifuged at 4000 rpm for 5 min, and an aliquot of the supernatant was used as the 'bead fraction' for SDS-PAGE analysis. Samples corresponding to the total input, unbound fraction, wash fraction, bound fraction, and bead fraction were subjected to SDS-PAGE, Western transfer, and immunoprobing as described in Sections 2.3.2-2.3.4.

2.11 MASS SPECTROMETRY

Mass spectrometry was performed to identify proteins interacting with Bcl-2 following treatment with doxazolidine in HL-60/Bcl2 cells.

Sample Preparation

Samples were subjected to anti-FLAG co-IP as described in Section 2.10, except the supernatant elutes (bound fractions) from the co-IP were not assayed by SDS-PAGE, Western transfer, and immunoprobing, but instead were vacuum dried and resuspended in 100 μ L of 8 M urea, 10 mM DTT, 100 mM Tris-HCL pH 8.3, and incubated for 5 hr at room temperature. Samples were alkylated in the dark for 1 hr by the addition of 4 μ l of 1 M iodoacetamide, and the reaction stopped by addition of 4 μ l of 1 M DTT for 1 hr in the dark. The urea was then diluted by the addition of 1 mL distilled water and samples were digested with 1 μ g trypsin overnight at 37 °C. The volume of the sample was then reduced to 150 μ L in a vacuum centrifuge. Peptides were purified/concentrated by C₁₈ Zip-Tip (Millipore) according to the manufacturer's protocol and resuspended in 10 μ L of 2% acetonitrile, 0.1 % trifluoroacetic acid.

Liquid Chromatography-MALDI-MS

Peptides were separated on an UltiMate nano-LC system (Dionex) equipped with a Dionex Pepmap C₁₈ trapping column (5 μ M, 100 Å, 300 μ m x 1 mm), and a Vydac Everest (Grace, Deerfield, IL, USA) C₁₈ analytical column (5 μ M, 300 Å, 150 μ m x 15 cm). The column effluent was directed to a MALDI-plate spotter (Proteineer fc; Bruker Daltronics, Billerica, MA, USA) where fractions were collected every 10 sec on a 384 position AnchorChip plate with 800 μ m anchorsize. For each fraction, 2.4 μ L of the matrix solution (4 mg/mL α -cyano-4-hydroxycinnamic acid dissolved in 90% acetonitrile containing 0.1% trifluoroacetic acid and 10 mM ammonium dihydrogenphosphate) was added to the column eluant. The target plate was analysed with an Ultraflex III MALDI TOF/TOF (Bruker Daltronics). Calibration of the instrument was performed externally using a peptide standard mixture (Bruker Daltonics). All spectra acquisition was performed automatically with FlexControl version 3.3 and WARP-LC version 1.2 software. Mass spectrometry peak lists were generated by FlexAnalysis version 3.3 and the peak list was filtered to remove common contaminants (matrix and keratin peaks).

MS/MS Database Search

All MS data were exported to mzML format prior to MS/MS Database searching. The conversion was performed with CompassExport version 3.0.1 (Bruker Daltonics), which preserves peak list information generated by FlexAnalysis. MS/MS database search and statistical validation was performed using the Trans Proteomic Pipeline software (Institute for Systems Biology). This software was used to combine search results from the following search engines: Mascot version 2.3.01, OMSSA version 2.1.9 and X!Tandem version 2010.10.01.1.

Our analysis workflow started by searching each file (corresponding to a single instrument run) using the three search engines. The three search results were then subjected to statistical analysis using the program PeptideProphet (Keller *et al.*, 2002). Results from PeptideProphet were then analysed using iProphet, which combines evidence from multiple identifications of the same peptide across multiple search engines and spectra (Shteynberg *et al.*, 2011). Finally, protein level statistical analysis was performed using ProteinProphet (Nesvizhskii *et al.*, 2003) with default parameters. All database searches were performed against a custom database with all human entries from the Uniprot Swissprot database. The final list of proteins identified in each sample was restricted to only include proteins having a probability match between 1-0.6.

2.12 DETECTION OF THE β 3 INTEGRIN SUBUNIT BY FLOW CYTOMETRY

Cell surface expression of the β 3 integrin subunit on 66cl4 and 4T1.2 cell lines was determined by flow cytometry as described previously (Sloan *et al.*, 2006). Cells (1x10⁶) were pelleted (1200 rpm for 5 min) and resuspended in 500 µL of blocking buffer (incomplete α -MEM supplemented with 2% FBS and 2% BSA) for 30 min on ice. Cells were centrifuged (1200 rpm for 5 min) and incubated with 2 µg/mL hamster anti-mouse- β 3 (CD61) antibody (BD Biosciences, San Jose, CA, USA) diluted in 500 µL labeling medium (incomplete α -MEM supplemented with 2% FBS) for 1 hr on ice. Cells were washed twice with wash buffer (PBS supplemented with 2% FBS) to remove unbound antibody and the cell pellets were resuspended and incubated with 2 μ g/mL FITC-conjugated mouse anti-Armenian and Syrian hamster antibody cocktail (BD Biosciences) diluted in 500 μ L labeling medium for 45 min on ice. Cells were then washed twice in wash buffer, resuspended in PBS, kept on ice and analysed by flow cytometry immediately. Control samples were included where the cells were only incubated in the presence of the anti-hamster secondary antibody (labeling medium was used instead of primary antibody) to determine background levels of FITC fluorescence.

Analysis was performed using a FACSCanto II flow cytometer (BD Biosciences) employing FACSDiva software. Samples (10,000 events recorded) were gated to distinguish and omit small debris and doublets by employing a forward-scatter versus side-scatter dot plot and applying an appropriate exclusion gate. The gated events were plotted as counts versus FITC fluorescence and compared to the control samples incubated only with secondary antibody.

2.13 VITRONECTIN ADHESION ASSAY

Cell culture plates (96-well) were coated in duplicate with 5 µg/mL vitronectin from human plasma (Sigma Aldrich), and 2% (w/v) BSA in PBS at a volume of 100 µL/well and incubated overnight at 4 °C. The wells were rinsed gently with PBS and blocked with 1% (w/v) BSA in PBS for 1 hr at 37 °C and rinsed twice with PBS before the addition of cells. Cell pellets (200,000 cells) were resuspended in serum-free α -MEM supplemented with 0.2% (w/v) BSA and labelled with 10 µg/mL calcein (Invitrogen) for 45 min at 37 °C. Calcein is a cell-permeable dye that becomes fluorescent upon esterase-mediated hydroysis in live cells. Cells were washed twice and resuspended in serum-free α -MEM supplemented with 0.2% (w/v) BSA before being added to the coated wells (100 µL of 20,000 cells/well). After the addition of cells, the 96-well plate was spun (250 g for 5 min) and the cells were allowed to adhere to the coated wells for 45 min at 37 °C. Non-adherent cells were removed by gentle rinsing in PBS (average of 4 washes). The adherent cells were lysed with 1% (v/v) Triton-X 100 and incubated for 30 min before the calcein fluorescence intensity was recorded

(excitation 485 nm, emission 530 nm) using a SpectraMax M2 plate reader (Molecular Devices, Sunnydale, CA, USA).

Calcein-labeled standards were also set up simultaneously. Following the calcein incubation for 45 min at 37 °C and the rinse steps, an aliquot of cells was lysed with 1% (v/v) Triton-X 100 and dilutions (0-100 μ L) were added to wells of a 96-well plate where the 100 μ L dilution contained the same number of cells as added to the coated wells (i.e. 20,000 cells). The calcein fluorescence intensity was recorded and a standard curve was constructed allowing the percentage of adherent cells on the vitronectin and BSA coated wells to be determined.

Experiments were also set up to determine whether the c(RGDfK) and c(RADfK) peptides affected cell adhesion to vitronectin. Following the incubation with calcein and the two washes, 250 μ L cell suspensions were incubated either with c(RGDfK) or c(RADfK) peptides or Milli-Q water as a vehicle control. Cells were incubated for 45 min at 37 °C to allow for peptide binding before being added to the 96-well plate (100 μ L of 20,000 cells/well) and the protocol continued as described above.

2.14 MATRIGEL INVASION ASSAY

Invasion assays were performed in 8 μ m pore size Transwell permeable support chambers (Corning Inc, Corning, NY, USA) inserted into 24-well plates. Matrigel (BD Biosciences, Bedford, MA, USA) was thawed overnight on ice at 4 °C, diluted in PBS to 3 mg/mL, and 100 μ L aliquots were added to the upper chamber of the Transwell. The Matrigel-coated Transwell chambers were allowed to set for 4 hr at 37 °C before the addition of cells. Cells (1x10⁵ cells in 100 μ L serum-free α -MEM) were gently added to the Matrigel-coated upper chambers. The upper chambers were then lowered into the 24-well plate which contained 600 μ L of α -MEM supplemented with 10% FBS that acted as a chemoattractant for the invading cells. Negative controls were also set up in which 24-well plate lower chambers contained α -

MEM without any FBS. The Transwell chambers were incubated for 24 hr at 37 °C, 5% CO_2 to allow cells to invade to the underside of the Transwell membrane.

Following the incubation, the contents from the upper chamber including Matrigel and noninvaded cells was removed gently using a cotton swab. The upper chamber was then washed in PBS and placed into a 24-well plate containing 3.7% paraformaldehyde in PBS and incubated for 15 min at room temperature. Chambers were then rinsed in PBS and placed in wells containing 0.5% (v/v) Triton-X 100 in Milli-Q water and incubated for 5 min at room temperature to lyse the invaded cells. Chambers were washed three times gently with PBS before incubation in wells containing Hoechst 33258 (1 μ g/mL in Milli-Q water) for 30 min at 37 °C in the dark. Chambers were then washed three times in PBS and the Transwell membrane was gently removed from the chamber using a scalpel and placed onto a microscope slide. Cells were visualized using an Olympus IX81 inverted microscope using a UV filter under 40x magnification. Stained cells were counted as invaded cells from at least 6 fields of view from duplicate samples.

2.15 MOUSE STUDIES

Female Balb/c mice (6-8 weeks old; Animal Resources Centre, Perth, WA) were used for all mouse studies. Mice were anaesthetized by isofluorane inhalation and 4T1.2/neo cancer cells (10 μ L of 1x10⁵ cells, suspended in saline) were injected into the fourth mammary fat pad using a 26 gauge needle. Once the tumours were palpable, the mice were randomized into treatment groups with five mice per group. Doxorubicin (2 mg/kg, 200 μ L in saline) was administered by intravenous tail vein injection using a 27 gauge needle; AN-7 (100 mg/kg, 200 μ L in water) was administered by an oral gavage needle; and AN-9 (100 mg/kg, 20 μ L in DMSO) was administered by intratumoural injection using a 27 gauge needle once mice were anaesthetized via isofluorane inhalation. Mice were treated twice weekly for three weeks and on each dosing day, mice were weighed and the percentage weight change was recorded. If >10% weight loss was recorded the mice were culled. Mice were also monitored closely for any signs of distress that may have indicated the presence of metastatic disease (e.g. ruffled

fur, lethargy, hunched back, restricted movement or laboured breathing). Tumour volume was recorded using electronic calipers (volume = $(\text{length x width}^2)/2$). Mice were culled by anesthetic overdose once the tumour size reached approximately 15 mm in diameter or until tumour ulceration was evident. Post-mortem analysis was performed whereby the primary tumour, spleen, and lungs were removed and weighed, and any visible metastatic growth was noted.

Chapter 3

ABT-737 OVERCOMES BCL-2 MEDIATED RESISTANCE TO DOXORUBICIN-DNA ADDUCTS

3.1 INTRODUCTION

3.1.1 Bcl-2

Bcl-2 was the first anti-apoptotic protein to be discovered and was identified due to a characteristic chromosomal translocation, t(14:18), found in the majority of follicular lymphoma cases (Tsujimoto et al., 1984; Bakhshi et al., 1985; Tsujimoto et al., 1985). The Bcl-2 gene normally resides on chromosome 18, but becomes translocated to chromosome 14 under control of the immunoglobulin chain heavy intron enhancer, resulting in transcriptional upregulation and overexpression of Bcl-2 protein in B-cells (Tsujimoto et al., 1984; Bakhshi et al., 1985; Tsujimoto et al., 1985). It was later discovered that Bcl-2 functions by promoting cell survival (Vaux et al., 1988). Bcl-2 is localized to the outer mitochondrial membrane where is acts to prevent Bax/Bak induced MOMP and is also located on the nuclear envelope and endoplasmic reticulum membrane (Hacki et al., 2000; Kirkin et al., 2004). Bcl-2 has been shown to be highly expressed in pro-B cells, mature B-cells and mature T-cells, and plays a vital role in the survival of mature lymphocytes (Merino et al., 1994; Cory, 1995). Bcl-2 knockout mice survive to birth but about half die by six weeks and are characterized by a range of abnormalities including growth retardation, kidney disease, distortion of the small intestines, and loss of lymphocytes via apoptosis resulting in failure of immune function (Nakayama et al., 1993; Nakayama et al., 1994; Kamada et al., 1995).

Bcl-2 has been shown to be overexpressed in a wide range of human cancers, including follicular lymphoma (FL) and diffuse-large B-cell lymphomas which commonly result from the t(14:18) chromosomal Bcl-2 translocation (Papajik *et al.*, 2001). Overexpression of Bcl-2 is also common in acute and chronic leukemia, non-Hodgkin's lymphoma, myeloma, as well as prostate, colorectal, renal, and SCLC (Kirkin *et al.*, 2004). High Bcl-2 levels in cancer are often associated with disease progression and chemoresistance to a wide range of agents in a wide range of tumours (Pepper *et al.*, 1998; Schmitt *et al.*, 2000). Furthermore, Bcl-2 mediated chemoresistance has been demonstrated against doxorubicin treatment as single agent *in vitro* (Panaretakis *et al.*, 2002), and *in vivo* (Schmitt *et al.*, 2000), and against

doxorubicin-DNA adduct forming treatments (doxorubicin in combination with AN-9; Swift *et al.*, 2006).

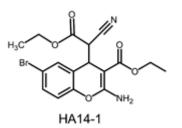
3.1.2 Targeting Anti-Apoptotic Proteins

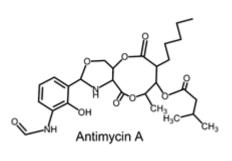
3.1.2.1 Antisense-Based Strategies

Antisense oligonucleotides (short oligodeoxynucleotides) function by hybridizing with complimentary mRNAs leading to their degradation, thus reducing *de novo* synthesis of the target protein. Oblimersen (G3139, Genasense) is an 18 base pair antisense oligonucleotide that targets the first six codons of Bcl-2 mRNA (Klasa et al., 2002). Oblimersen was able to reduce Bcl-2 protein levels in preclinical studies (Kitada et al., 1993). For example, in human breast cancer cells, Oblimersen reduced Bcl-2 protein by more than 80% resulting in high levels of apoptosis (Chi et al., 2000). Furthermore, in mouse xenograft models, antisense oligonucleotide treatment reduced tumour growth of transplanted human tumours (Cotter et al., 1994; Schlagbauer-Wadl et al., 2000). Oblimersen entered numerous clinical trials and was generally well tolerated, however, as a single agent Oblimersen achieved only modest clinical benefits in patients (Waters et al., 2000; Morris et al., 2002; O'Brien et al., 2005). This is believed to be attributed to a lack of efficient intracellular delivery, low stability, and minor Bcl-2 reductions in patients (Waters et al., 2000; Kim et al., 2007). However, in combination with standard chemotherapeutics for various types of cancer, Oblimersen proved to be more effective (Rudin et al., 2004; Tolcher et al., 2005; Bedikian et al., 2006; O'Brien et al., 2007).

3.1.2.2 BH3 Mimetics / Small Molecule Inhibitors

Since apoptosis relies on interactions between Bcl-2 family members, a promising strategy to promote apoptosis in chemoresistant cells is to use compounds that interfere and disrupt anti-apoptotic protein interactions. Several small molecule inhibitors (Figure 3.1) have been identified and designed which are able to mimic BH3-only proteins and bind to the hydrophobic grooves of anti-apoptotic proteins, thus preventing them from blocking apoptotic progression.





D

В

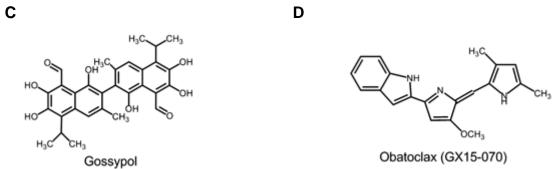


Figure 3.1. Structures of the small molecule Bcl-2 inhibitors (A) HA14-1, (B) Antimycin A, (C) gossypol, and (D) Obatoclax (Vogler et al., 2009).

BH3-Peptides

Short peptides have been synthesized containing the BH3 domain sequence from BH3-only proteins. These BH3-peptides have been shown to disrupt complexes formed between proand anti-apoptotic proteins and induce cytochrome c release (Letai *et al.*, 2002; Kuwana *et al.*, 2005). Despite proof of principle studies, using peptides as therapeutics is limited by their poor pharmacological properties such as low cellular permeability, and poor metabolic stability *in vivo* (Denicourt and Dowdy, 2004). Modification of the BH3 peptides by hydrocarbon stapling (using non-natural amino acids) to create 'stabilized alpha-helix of Bcl-2 domains' (SAHBs) makes the alpha-helix more stable and the peptide more resistant to protease degradation (Walensky *et al.*, 2004). A SAHB of the Bid-BH3 peptide was shown to induce apoptosis in leukemic cells and inhibited the growth of human leukemia xenografts *in vivo* (Walensky *et al.*, 2004).

Non-Peptide Inhibitors

Several non-peptide inhibitors have been tested for their ability to inhibit anti-apoptotic Bcl-2 family members. The hydrophobic grooves of anti-apoptotic proteins differ slightly and as such the different inhibitors display varied affinities for the different proteins. A number of different inhibitors have been identified including HA14-1 (Figure 3.1A; Wang *et al.*, 2000), BH3-Is (Degterev *et al.*, 2001), and Antimycin-A (Figure 3.1B; Tzung *et al.*, 2001), which have been shown to interact with anti-apoptotic proteins and induce apoptosis, however, do so at high (micromolar) concentrations which limits their application in a clinical setting (Zhang *et al.*, 2007). Another major disadvantage with these inhibitors is that they all induce apoptosis in a Bax/Bak independent manner (van Delft *et al.*, 2006), highlighting that these molecules may have a variety of other targets apart from anti-apoptotic proteins which could lead to unpredictable effects and toxicities.

Of the small molecule inhibitors that have been discovered, three have been tested in clinical trials, namely gossypol (Figure 3.1C), Obatoclax (Figure 3.1D), and ABT-263. Gossypol is a natural polyphenol compound found in seeds and roots of the cotton plant and has been shown to bind and antagonize anti-apoptotic proteins (Kitada *et al.*, 2003). Gossypol is able to bind to Bcl-2, Bcl-xL, Bcl-w, and Mcl-1 at sub-micromolar to micromolar concentrations (Zhai *et al.*, 2006), induce apoptosis (Mohammad *et al.*, 2005), and display anticancer

activity against a range of cancer types (as reviewed by Zhang *et al.*, 2007). However, in clinical trials, gossypol was shown to induce gastrointestinal toxicities (Liu *et al.*, 2009), and did not show improved efficacy when combined with topotecan in a SCLC trial (Heist *et al.*, 2010). Furthermore, gossypol was also shown to kill cells in a Bax/Bak independent manner possibly causing non-mechanism based toxicities (Lei *et al.*, 2006; van Delft *et al.*, 2006; Tse *et al.*, 2008). Derivatives of gossypol (apogossypolone, apogossypol, and TW-37) have been designed to improve the pharmacological properties and reduce the systemic toxicities associated with gossypol and have shown promising anticancer properties in preclinical testing (as reviewed by Zhang *et al.*, 2007; Azmi and Mohammad, 2009).

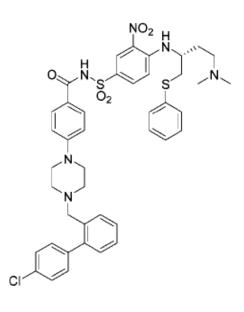
Obatoclax (GX-015-070) is an indole-derivative developed by Gemin X that acts as a broadspectrum inhibitor of Bcl-2, Bcl-xL, Bcl-w, and Mcl-1 with low micromolar affinity (Zhai *et al.*, 2006). The compound displaces Bak from Mcl-1 and Bcl-xL, upregulates Bim, and induces caspase-mediated apoptosis (Perez-Galan *et al.*, 2007; Trudel *et al.*, 2007a; Li *et al.*, 2008). Obatoclax showed single agent activity and enhanced *in vitro* cytotoxicity of the proteosome inhibitor bortezomib (Perez-Galan *et al.*, 2007; Trudel *et al.*, 2007a) and several other anticancer agents (Lessene *et al.*, 2008). Some clinical trials showed that Obatoclax was well tolerated (Haura *et al.*, 2008; Schimmer *et al.*, 2008), while another trial showed that Obatoclax treatment resulted in significant neuropsychiatric dose-limiting toxicities even at low doses in solid tumours and lymphoma (Hwang *et al.*, 2010). Furthermore, Obatoclax did not display any clinical activity in patients with myelofibrosis (Parikh *et al.*, 2010), although trials on different cancers are ongoing. Studies have also revealed that Obatoclax can induce apoptosis in the absence of Bax/Bak, indicating that the compound may have additional targets that contribute to its cytotoxicity (Konopleva *et al.*, 2008; Mott *et al.*, 2008; Tse *et al.*, 2008).

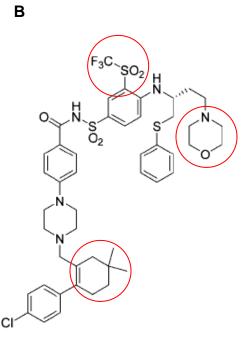
3.1.3 ABT-737

3.1.3.1 Discovery and Mechanism

The most studied and most potent small molecule inhibitor of anti-apoptotic proteins is the compound ABT-737 (Figure. 3.2A) developed by Abbott Laboratories (Oltersdorf *et al.*,

Α









С

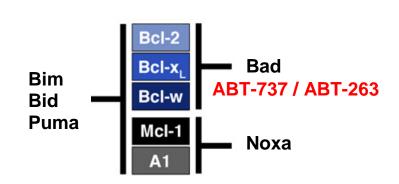


Figure 3.2. Structures and interactions of the Bcl-2 inhibitors developed by Abbott Laboratories.

Structures of (A) ABT-737 (Oltersdorf *et al.*, 2005) and (B) the second generation inhibitor, ABT-263 (Tse *et al.*, 2008). The three sites that were modified from ABT-737 to produce ABT-263 are circled in red. Both ABT-737 and ABT-263 display a similar binding profile for anti-apoptotic proteins as the BH3-only protein Bad (C). They possess a high affinity for Bcl-2, Bcl-xL, and Bcl-w, but not for Mcl-1 and A1 (adapted from van Delft *et al.*, 2006).

2005). The method 'SAR by NMR' (structure-activity relationships by nuclear magnetic resonance) (Shuker *et al.*, 1996) was used to screen a chemical library to identify molecules that interact with the Bcl-xL hydrophobic groove (Oltersdorf *et al.*, 2005). This led to the design of a compound that bound to Bcl-xL with high affinity but also bound to human serum albumin (HSA). The compound was modified to reduce HSA binding and also to increase affinity to Bcl-2. The resultant cell permeable compound, ABT-737, binds with high affinity in the subnanomolar range (Ki ≤ 1 nM) to Bcl-xL, Bcl-2, and Bcl-w, but has low affinity for Mcl-1 and A1 (Ki > 1 μ M) (Oltersdorf *et al.*, 2005). ABT-737 is much more potent than previously discovered inhibitors and has a binding affinity profile for anti-apoptotic proteins similar to the BH3-only protein Bad (Figure 3.2C), and as such is often described as a Bad-mimetic.

ABT-737 functions by its expected mechanism of action of competing for the hydrophobic grooves and sequestering specific anti-apoptotic proteins, and has been shown to disrupt Bcl-2/Bax heterodimers (Konopleva *et al.*, 2006; Touzeau *et al.*, 2011), Bcl-xL/Bak heterodimers (Huang and Sinicrope, 2008), and interactions between Bim and anti-apoptotic proteins (Del Gaizo Moore *et al.*, 2007; Huang and Sinicrope, 2008). By disrupting these Bcl-2 family interactions, ABT-737 rapidly induces classical hallmarks of apoptosis, including oligomerization of Bax/Bak, cytochrome c release and caspase activation (Vogler *et al.*, 2008), and compared to other small molecule inhibitors ABT-737 does not kill cells lacking both Bax and Bak, indicating that it is a bona-fide BH3 mimetic (van Delft *et al.*, 2006).

3.1.3.2 Anticancer Activity

Studies have demonstrated that ABT-737 is effective *in vitro* as a single agent in many lymphoid cancers, including FL (Oltersdorf *et al.*, 2005), chronic lymphocytic leukemia (CLL) (Oltersdorf *et al.*, 2005; Del Gaizo Moore *et al.*, 2007; Vogler *et al.*, 2008), acute myeloid leukemia (AML) (Konopleva *et al.*, 2006), acute lymphoblastic leukemia (ALL) (Del Gaizo Moore *et al.*, 2008), mantle cell lymphoma (Touzeau *et al.*, 2011), and multiple myeloma (Kline *et al.*, 2007). ABT-737 displays weak cytotoxic activity against most solid tumours although SCLC cells are relatively sensitive (Oltersdorf *et al.*, 2005; Tahir *et al.*, 2007). Due to the specific binding profile of ABT-737 for anti-apoptotic proteins it is expected that cells with high levels of Bcl-2, Bcl-xL and Bcl-w, and low Mcl-1 will be most

sensitive to ABT-737. Indeed this was shown to be the case with SCLC cells (Tahir *et al.*, 2007) and mantle cell lymphoma cells (Touzeau *et al.*, 2011), with cell lines possessing high Bcl-2 and low Mcl-1 levels being more sensitive to ABT-737 treatment. ABT-737 is not only cytotoxic to established cell lines but also primary patient derived cells (Oltersdorf *et al.*, 2005; Konopleva *et al.*, 2006; Del Gaizo Moore *et al.*, 2007; Del Gaizo Moore *et al.*, 2008). Studies have also shown that ABT-737 displays selective toxicity. For example, ABT-737 was cytotoxic to primary patient derived AML progenitor, blast and stem cells, as well as primary CLL cells, but not to non-malignant peripheral blood mononuclear cells (PBMCs) (Konopleva *et al.*, 2006; Del Gaizo Moore *et al.*, 2007).

In many cell types, the single agent activity of ABT-737 is low but the inhibitor has also been shown to act synergistically with many chemotherapeutic agents to overcome chemoresistance. ABT-737 synergistically enhanced the anticancer activity of doxorubicin, etoposide, paclitaxel, cisplatin, and cytosine arabinoside in a range of cancer cell lines (Oltersdorf *et al.*, 2005; Konopleva *et al.*, 2006; van Delft *et al.*, 2006). ABT-737 has been shown to overcome imatinib resistance caused by Bcl-2 overexpression or loss of Bim/Bad in Bcr/Abl+ leukemic cells (Kuroda *et al.*, 2006), and reversed paclitaxel resistance in Bcl-2 overexpressing breast cancer cell lines (Kutuk and Letai, 2008).

3.1.3.3 In vivo Studies

The efficacy of ABT-737 has been characterized in several mouse models. ABT-737 treatment improved survival in a FL mouse model (Oltersdorf *et al.*, 2005), and suppressed leukemia burden and extended survival in an AML severe combined immunodeficiency (SCID) model (Konopleva *et al.*, 2006). The inhibitor caused regression of established SCLC xenografts by causing apoptotic cell death as indicated by caspase activity found in tumour sections (Oltersdorf *et al.*, 2005). In a xenograft mouse myleloma model, ABT-737 induced complete regression when administered as a daily treatment (Trudel *et al.*, 2007b). Furthermore, ABT-737 combined with standard vincristine, dexamethasone, and L-asparaginase (VXL) treatment in an ALL xenograft model enhanced event-free survival compared to ABT-737 or VXL alone (Kang *et al.*, 2007). In these *in vivo* studies, ABT-737 was generally well tolerated with minimal effects on normal tissues. The only commonly

encountered toxicities were temporary lymphopenia and thrombocytopenia that can be easily managed in a clinical setting (Oltersdorf *et al.*, 2005; Konopleva *et al.*, 2006).

Although studies have demonstrated that ABT-737 is effective *in vivo* both as a single agent and in combination with various chemotherapeutics, the potential use of ABT-737 in the clinic is limited by its poor physiochemical and pharmaceutical properties. ABT-737 is not orally bioavailable and has low aqueous solubility, making intravenous delivery difficult and as such the compound is administered intraperitoneally in mouse studies, which is not ideal for clinical use. For these reasons, Abbott laboratories synthesized a new derivative of ABT-737 called ABT-263 (Navitoclax) (Park *et al.*, 2008a; Tse *et al.*, 2008).

3.1.4 ABT-263

ABT-263 (Figure 3.2B) is a second generation BH3 mimetic modified from ABT-737 at three key structural sites to maximize oral absorption and provide greater dosing flexibility and easier administration for patients (Park et al., 2008a; Tse et al., 2008). Despite these structural modifications, ABT-263 displays similar binding affinities as ABT-737 for Bcl-2, Bcl-xL and Bcl-w (Ki \leq 1 nM), but also has a poor affinity for Mcl-1 and A1 (Figure 3.2C; Tse et al., 2008). Therefore, ABT-263 functions via the same mechanism as ABT-737 and showed single agent activity in numerous cancer cell lines derived from lymphoid malignancies (Lock et al., 2008; Tse et al., 2008), and SCLC (Shoemaker et al., 2008; Tse et al., 2008). In vivo, oral administration of ABT-263 resulted in complete regression of ALL (Lock et al., 2008; Tse et al., 2008) and SCLC (Shoemaker et al., 2008; Tse et al., 2008) xenograft mouse models, and enhanced the activity of several chemotherapeutic agents in hematologic tumours (Ackler et al., 2008; Tse et al., 2008; Ackler et al., 2010). Using a SCLC xenograft model, ABT-263 administered orally at the same dose and schedule as ABT-737 administered intraperitoneally, achieved similar efficacy (Park et al., 2008a). Daily dosing of ABT-263 in mouse models was well tolerated with minimal toxicity except for thrombocytopenia, as observed with ABT-737, which can be managed in the clinic (Tse et al., 2008). Phase I clinical trials have also been completed with ABT-263 in patients with various lymphoid malignancies (Wilson et al., 2010), and SCLC (Gandhi et al., 2011). The

inhibitor was well tolerated with common side-effects including diarrhea, nausea, fatigue, as well as dose-related thrombocytopenia, lymphopenia and neutropenia (Wilson *et al.*, 2010; Gandhi *et al.*, 2011). ABT-263 was most effective against CLL and FL with partial responses (more than 50% tumour reduction) being observed in patients (Wilson *et al.*, 2010).

3.1.5 Mcl-1 Mediated Resistance to ABT-737 and ABT-263

Mcl-1

Knockout studies have demonstrated that Mcl-1 is essential for embryogenesis as Mcl-1 deficient mice display peri-implantation lethality of embryos (Rinkenberger et al., 2000). Mcl-1 is also required for the function of the immune system as induced deletion results in a loss of bone marrow, hematopoietic stem cells (Opferman et al., 2005), and B and T lymphocytes (Opferman et al., 2003). Mcl-1, like Bcl-2, is primarily located on the outer mitochondrial membrane where it acts to prevent cytochrome c release and apoptosis (Yang et al., 1995), however, it is unique among the anti-apoptotic proteins in terms of its short half-life and its complex regulation (Warr and Shore, 2008). The half-life of Mcl-1 in various cell types is in the range of a few hours (Michels *et al.*, 2005). This rapid turn over is due to ubiquitin-dependent degradation by the 26S proteosome following polyubiquitination of Mcl-1 by the E3 ligase Mule/LASU1 (Zhong et al., 2005). Mcl-1 is also regulated at the transcriptional level as various signalling pathways including the MAPK/ERK pathway are able to stimulate Mcl-1 expression (Warr and Shore, 2008). Furthermore, Mcl-1 can become phosphorylated at a number of sites within PEST domains (rich in proline, glutamic acid, serine, and threonine) in the N-terminus which can either prolong or shorten its half-life (Domina et al., 2004; Kobayashi et al., 2007; Warr and Shore, 2008). As depicted in Figure 1.11B, Mcl-1 (along with Bcl-xL) has been demonstrated to bind to Bak at mitochondria, thus preventing Bak-mediated MOMP and apoptosis (Willis et al., 2005).

Resistance

Both ABT-737 and ABT-263 display low binding affinity to the anti-apoptotic proteins Mcl-1 and A1 (Oltersdorf *et al.*, 2005; Tse *et al.*, 2008). While A1 is not commonly expressed in cancers, Mcl-1 on the other hand is overexpressed in a range of hematopoietic and lymphoid cancers, including CLL, CML, multiple myeloma, and B-cell lymphoma, as well as a number of solid tumours (Warr and Shore, 2008). Studies have demonstrated that cancer cells expressing high levels of Mcl-1 are more resistant to ABT-737 treatment (Konopleva *et al.*, 2006; van Delft *et al.*, 2006; Tahir *et al.*, 2007; Touzeau *et al.*, 2011), and results of an RNAi based screen demonstrated that Mcl-1 is the major resistance factor to ABT-737 treatment in insensitive SCLC cell lines (Lin *et al.*, 2007). For this reason, the effectiveness of ABT-737 will be greatest in tumours that express high levels of Bcl-2, but also express low levels of Mcl-1. Due to its short half-life and various points of regulation, Mcl-1 can be targeted by a number of different strategies to reduce its levels and overcome ABT-737 resistance. Indeed, studies have shown that downregulation of Mcl-1 via various methods including siRNA has resulted in an increase in ABT-737 sensitivity in numerous cancer cell lines (Konopleva *et al.*, 2006; Chen *et al.*, 2007; Lin *et al.*, 2007; Tahir *et al.*, 2007; Touzeau *et al.*, 2011).

3.1.6 Project Objectives

As shown by Swift and colleagues (2006), Bcl-2 overexpression confers resistance to doxorubicin/AN-9 DNA adduct-forming treatments, which may limit the clinical potential of this drug combination. While various strategies and compounds have been used to inhibit Bcl-2 in cancer cells, ABT-737 has been shown to be the most potent inhibitor developed to date. The major objective of this project was to use the small-molecule Bcl-2 (Bcl-xL and Bcl-w) inhibitor ABT-737, to determine if Bcl-2 mediated chemoresistance to doxorubicin/AN-9 can be overcome. This 'triple treatment' of doxorubicin, AN-9, and ABT-737 was investigated in a Bcl-2 overexpressing HL-60 cell model (HL-60/Bcl2) together with the empty vector control cell line (HL-60/Puro) using three independent apoptosis assays.

Once it was ascertained that ABT-737 could overcome Bcl-2 mediated resistance, the next objective was to use various control compounds to determine the molecular mechanisms involved in the synergistic cell death response to the triple treatment. In particular, the dependence on DNA adduct formation to induce cell death in the triple treatment was

examined. Other cancer cell lines were also used to establish that the effectiveness of the triple treatment was not just limited to HL-60 cells.

Finally, considering that Mcl-1 has been recognized as a major resistance factor to ABT-737, shRNA was used to knockdown Mcl-1 levels to determine if sensitivity to ABT-737 could be increased.

3.2 **RESULTS**

3.2.1 Bcl-2 overexpressing HL-60 cell model

To ascertain whether ABT-737 can overcome Bcl-2 mediated resistance to doxorubicin/AN-9 adduct forming treatments, HL-60 promyelocytic leukemic cells which constitutively overexpress Bcl-2 (HL-60/Bcl2) were used. HL-60 cells were chosen as they have been previously shown to be sensitive to doxorubicin/AN-9 treatments (Swift et al., 2006). Figure 3.3A shows that the Bcl-2 protein levels were much greater in HL-60/Bcl2 cells compared to the empty vector control cell line (HL-60/Puro), and the wild-type cell line (HL-60/WT). In comparison, U937 (human leukemic monocyte lymphoma) cells express lower levels of endogenous Bcl-2 relative to the three HL-60 cell lines. The overexpressed Bcl-2 in the HL-60/Bcl2 cells appears as a higher molecular weight band in comparison to endogenous Bcl-2 (26 kDa band) which is present in all three cell lines at similar levels. This increase in size of the overexpressed Bcl-2 is due to the presence of an additional FLAG-tag (eight amino acid long peptide tag) on the plasmid Bcl-2 protein (Figure 3.3B). It has been previously demonstrated that the presence of the FLAG-tag does not affect Bcl-2 function (Vairo et al., 1996). Endogenous Mcl-1 levels were also determined due to the importance of Mcl-1 in conferring resistance to ABT-737 (see Section 3.1.5). Figure 3.3C shows that the HL-60 cell lines express much lower Mcl-1 levels relative to U937 cells (this will be addressed in more detail in Section 3.2.10).

3.2.2 ABT-737 is cytotoxic as a single agent in HL-60 cells

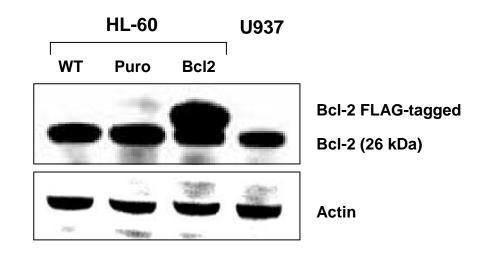
The effect of ABT-737 as a single agent was investigated in HL-60/Puro and HL-60/Bcl2 cells via growth inhibition and apoptosis assays. Preliminary experiments performed with the MTS assay showed that the optimum cell density to use in growth inhibition assays was 200,000 cells/mL as both cell lines displayed log phase growth at this density. This cell density was also used for all subsequent apoptosis assays using HL-60 cells. As indicated in Table 3.1, a 48 hr MTS growth inhibition assay revealed that the IC₅₀ value for ABT-737 in

HL-60/Bcl2 cells was approximately 10-fold higher compared to HL-60/Puro cells (748 nM vs. 74 nM; a representative IC₅₀ graph is shown in Figure 3.4). The sub-G1 FACS assay was used as a measure of apoptosis where the HL-60 cell lines were treated with increasing concentrations of ABT-737 for 24 hr. In all three HL-60 cells lines tested, apoptosis gradually increased in a dose-dependent manner. In HL-60/WT (Figure 3.5A) and HL-60/Puro (Figure 3.5B) cells, 40-50% apoptosis was achieved with approximately 100 nM ABT-737, while in HL-60/Bcl2 cells (Figure 3.5C) in order to achieve the same level of cell kill, about a 10-fold higher concentration (1000-2000 nM) of ABT-737 was required. It should also be noted that the enantiomer (with the opposite configuration of the dimethylaminoethyl group) which binds with very low affinity to Bcl-2 and as such is used as a negative control (Oltersdorf *et al.*, 2005), only induced low levels of apoptosis in HL-60/Puro and HL-60/Bcl2 cells.

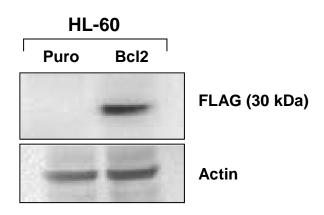
Time course experiments were conducted to determine how quickly ABT-737 is able to induce apoptosis in Bcl-2 overexpressing HL-60 cells. HL-60/Bcl2 cells were treated with 500 nM ABT-737 and as seen in Figure 3.6, cell kill was rapidly induced with the majority of cell death occurring within the first 2 hr of treatment, after which a plateau was reached. The ability of ABT-737 to induce apoptosis so rapidly can be expected since the compound directly targets the apoptotic machinery.

These results demonstrate that nanomolar levels of ABT-737 are able to effectively inhibit the growth of and kill HL-60 cells, highlighting its potential as an effective single agent in this cancer cell line. ABT-737 was also able to kill HL-60 cells overexpressing Bcl-2, although a higher concentration was required to neutralize Bcl-2 and allow the apoptotic cascade to proceed. Approximately 10-fold higher concentrations of ABT-737 were required in HL-60/Bcl2 cells to achieve similar levels of growth inhibition and apoptosis to non-Bcl-2 overexpressing cells. Therefore, even in the presence of high Bcl-2 levels, ABT-737 as a single agent was able to rapidly kill these cancer cells.

Α



В



С

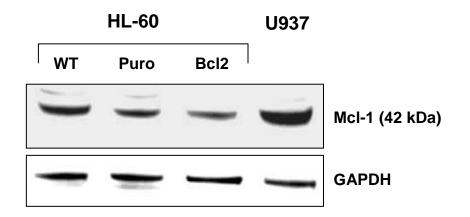


Figure 3.3. Bcl-2 and Mcl-1 protein levels in HL-60 and U937 leukemic cell lines.

Western analysis was performed to determine the level of (A) Bcl-2 and (C) Mcl-1 protein in HL-60/WT, HL-60/Puro, HL-60/Bcl2, and U937 cells. These blots are representative of three independent experiments yielding similar results. Western analysis was also used to (B) confirm that the higher molecular weight Bcl-2 protein band represents FLAG-tagged Bcl-2 by using an anti-FLAG antibody. For all three blots, untreated cells were harvested and protein extracts (50 μ g) were subjected to SDS-PAGE and Western transfer. Actin was used as a loading control for (A) and (B) and GAPDH was used as a loading control for (C).

Table 3.1. Growth inhibition data for HL-60/Puro and HL-60/Bcl2 cells treated with ABT-737.

Cell line	ABT-737 IC ₅₀ (nM)
HL-60/Puro	74 ± 16
HL-60/Bcl2	748 + 109

Error represents the standard error of the mean from three independent experiments.

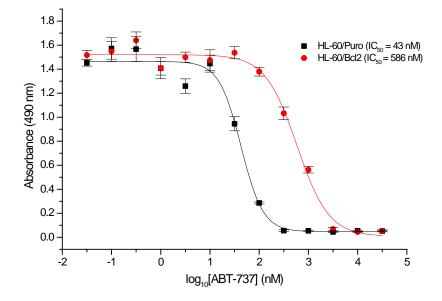
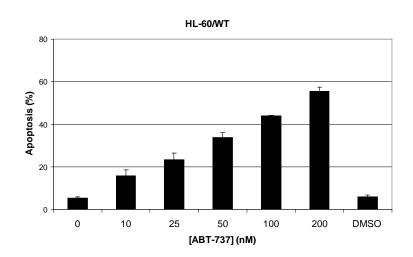


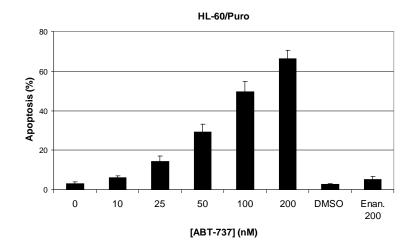
Figure 3.4. Representative IC₅₀ graph for HL-60/Puro and HL-60/Bcl2 cells treated with ABT-737.

HL-60/Puro and HL-60/Bcl2 cells were treated with various concentrations of ABT-737 for 48 hr and IC_{50} values determined via the MTS growth inhibition assay. Error bars represent standard error of the mean of quadruplicate samples. This graph is representative of three independent experiments.

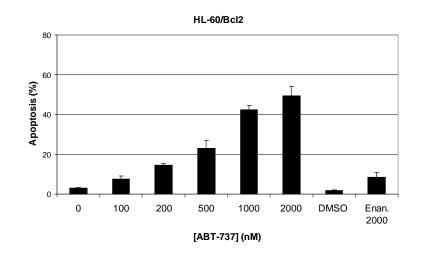


В

Α



С



94

Figure 3.5. ABT-737 induces cell kill as a single agent in HL-60 cells in a dosedependent manner.

HL-60 cells were treated with increasing concentrations of ABT-737 from 10-200 nM in (A) HL-60/WT, and (B) HL-60/Puro cells, and from 100-2000 nM in (C) HL-60/Bcl2 cells. Cells were treated for 24 hr after which flow cytometry was conducted to determine the percentage of apoptotic (sub-G1) cells. DMSO was used as a vehicle control (equivalent to the DMSO level at highest ABT-737 concentration), and the ABT-737 enantiomer (enan.) was used as a negative control. Error bars represent the standard error of the mean from three independent experiments.

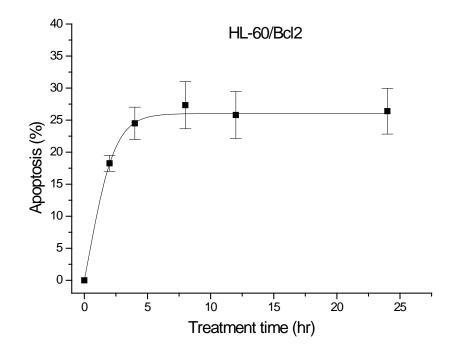


Figure 3.6. ABT-737 induces cell kill rapidly in HL-60/Bcl2 cells.

HL-60/Bcl2 cells were treated with 500 nM ABT-737 for 2-24 hr and subsequently subjected to FACS analysis to determine the level of sub-G1 apoptotic cells. Error bars represent the standard error of the mean from three independent experiments.

3.2.3 Overexpression of Bcl-2 confers resistance to doxorubicin/AN-9 DNAadduct forming treatments

It is now well documented that the combination of doxorubicin with formaldehyde-releasing prodrugs results in DNA adduct formation and a synergistic apoptotic response within a few hours (Cutts et al., 2001; Cutts et al., 2005; Swift et al., 2006). In previous studies, ratios of around 1:50 of doxorubicin to AN-9 have typically been used to obtain these synergistic results (Cutts et al., 2001; Cutts et al., 2005; Swift et al., 2006). Various concentrations of doxorubicin and AN-9 were tested to determine which combinations resulted in cell kill in HL-60 cells. As shown in Figure 3.7, after 6 hr treatment, the combinations of 500 nM doxorubicin with 25 µM AN-9 (1:50) and 500 nM doxorubicin with 50 µM AN-9 (1:100) in HL-60/Puro cells resulted in much higher levels of apoptosis compared to HL-60/Bcl2 cells. However, the level of cell kill for the 500 nM doxorubicin / 50 μ M AN-9 combination was at the detectable limit for the sub-G1 assay (approximately 70% apoptosis), and for this reason the combination of 500 nM doxorubicin with 25 µM AN-9 was used for subsequent experiments. A time course study was performed using single agent controls to demonstrate that this combination of doxorubicin/AN-9 was synergistic. In both HL-60/Puro (Figure 3.8A) and HL-60/Blc2 (Figure 3.8B) cell lines, doxorubicin (500 nM) and AN-9 (25 μ M) alone did not induce cell kill above background levels, therefore, under these treatment conditions, the impairment of topoisomerase-II by doxorubicin does not contribute to cell kill. In HL-60/Puro cells the combination of doxorubicin/AN-9 resulted in a synergistic induction of apoptosis after 6 and 8 hr treatments, while in HL-60/Bcl2 cells the combination treatment did not induce cell kill above background levels, even after 8 hr. The 6 hr treatment time point was chosen for future experiments. This result demonstrates that overexpression of Bcl-2 confers resistance to doxorubicin/AN-9 DNA adduct forming treatments in HL-60 cells by causing a block in the apoptotic pathway, thus preventing cell kill.

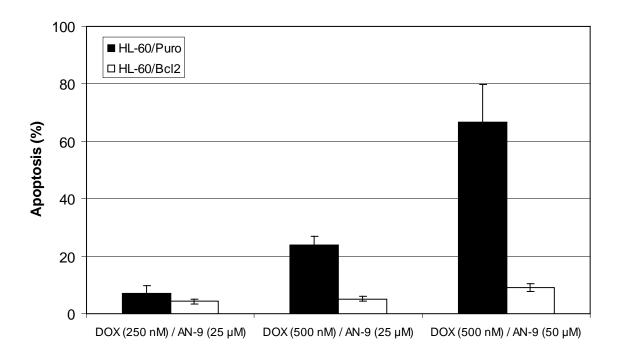
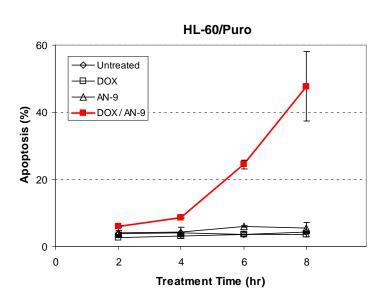


Figure 3.7. Doxorubicin/AN-9 treatment induces apoptosis in HL-60/Puro but not in HL-60/Bcl2 cells.

HL-60/Puro and HL-60/Bcl2 cells were treated for 6 hr with the combination of doxorubicin (either 250 or 500 nM) and AN-9 (either 25 or 50 μ M). Apoptosis levels were determined by subjecting the cells to sub-G1 FACS analysis. Error bars represent the standard deviation from two independent experiments.



В

Α

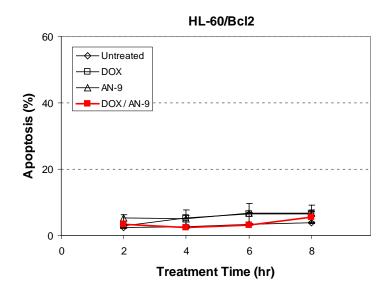


Figure 3.8. Bcl-2 overexpression confers resistance to doxorubicin/AN-9 treatment in HL-60 cells.

HL-60/Puro (A) and HL-60/Bcl2 (B) cells were treated with doxorubicin (500 nM), AN-9 (25 μ M), and the combination of both drugs for 2-8 hr, after which flow cytometry was performed to determine the percentage of apoptosis (sub-G1 cells). Error bars represent the standard deviation from two independent experiments.

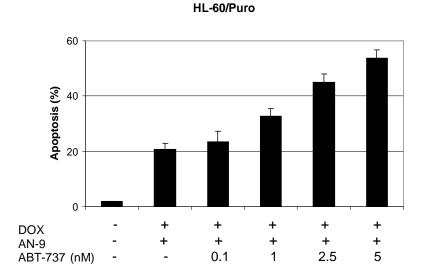
3.2.4 Nanomolar levels of ABT-737 overcomes Bcl-2 mediated resistance to doxorubicin/AN-9 treatment

To establish whether the resistance observed in the Bcl-2 overexpressing HL-60 cells could be overcome by inhibiting Bcl-2, ABT-737 was used in combination with doxorubicin and AN-9 to form a 'triple treatment'. As shown in Figure 3.7 and Figure 3.8, the combination of doxorubicin (500 nM) and AN-9 (25μ M) resulted in approximately 20-25% apoptosis after 6 hr treatment in HL-60/Puro cells, while only background levels of apoptosis were detected in HL-60/Bcl2 cells. In HL-60/Puro cells the simultaneous addition of ABT-737 (0.1-5 nM) to the doxorubicin/AN-9 combination resulted in a gradual dose-dependent increase in apoptosis (Figure 3.9A). The ability of ABT-737 to increase cell kill in response to this DNA adduct forming treatment was even further pronounced in HL-60/Bcl2 cells (Figure 3.9B). These cells were completely resistant to doxorubicin/AN-9 treatment, however, the addition of 10 or 25 nM ABT-737 resulted in a synergistic increase in apoptosis, thus reflecting that the anti-apoptotic function of Bcl-2 can be effectively inhibited by ABT-737. It is important to note that the concentrations of ABT-737 that were able to enhance apoptosis levels were much lower than the corresponding IC₅₀ values (see Table 3.1) and did not induce apoptosis as a single agent (data not shown).

3.2.5 The triple treatment is synergistic in three independent apoptosis assays

Sub-G1 Assay

To validate the observation that low nanomolar levels of ABT-737 can overcome the inherent resistance caused by Bcl-2 overexpression to DNA adduct forming treatments, HL-60/Puro and HL-60/Bcl2 cells were treated with 2.5 nM and 25 nM ABT-737 respectively, and the level of apoptosis (sub-G1 assay) induced by the triple treatment, as well as all single and double agent control treatments was measured. Using the same treatment conditions as described above (500 nM doxorubicin, 25 μ M AN-9, 6 hr treatment), in both cell lines the three single agents failed to induce apoptosis above background levels (Figure 3.10A). The combination of doxorubicin/AN-9 was synergistic in HL-60/Puro cells with the addition of



В

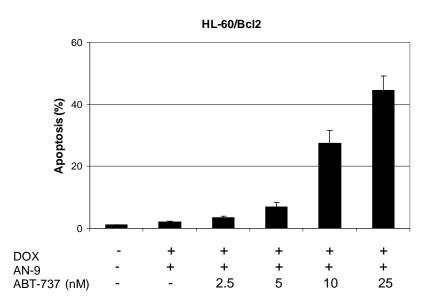
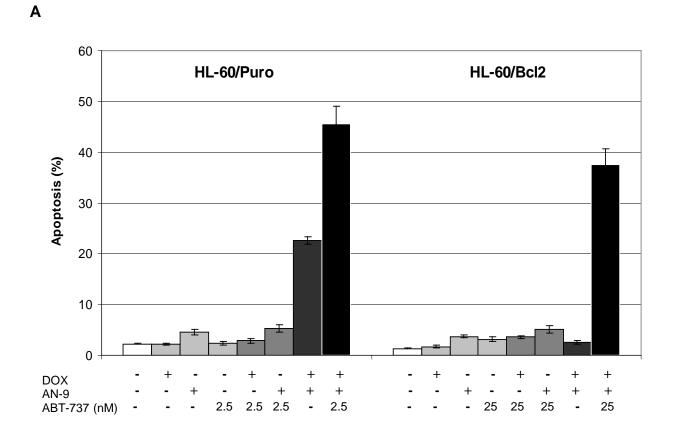


Figure 3.9. Bcl-2 mediated resistance to doxorubicin/AN-9 is overcome by ABT-737.

HL-60/Puro (A) and HL-60/Bcl2 (B) cells were treated simultaneously with doxorubicin (500 nM), AN-9 (25 μ M), and increasing concentrations of ABT-737 for 6 hr. The percentage of apoptotic cells was determined by sub-G1 FACS analysis. The data represents the average from four (A) and three (B) independent experiments. In both graphs the error bars represent the standard error of the mean.

Α





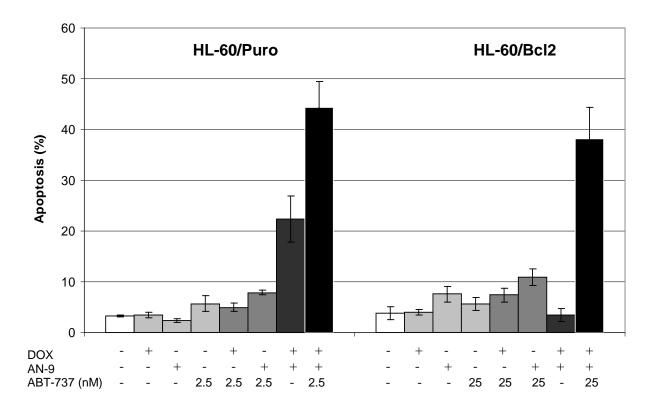


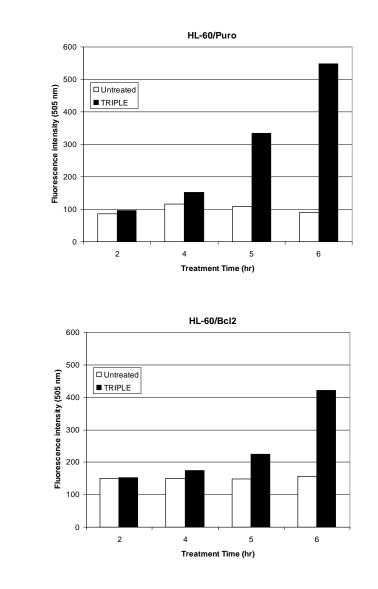
Figure 3.10. ABT-737 synergistically potentiates apoptosis induced by doxorubicin/AN-9 treatments.

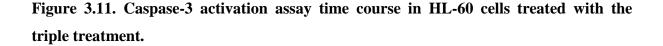
HL-60/Puro and HL-60/Bcl2 cells were treated for (A) 6 hr with doxorubicin (500 nM), AN-9 (25 μ M), and ABT-737 (2.5 nM in HL-60/Puro cells and 25 nM in HL-60/Bcl2 cells), and for (B) 4 hr with doxorubicin (1 μ M), AN-9 (50 μ M), and ABT-737 (2.5 nM in HL-60/Puro cells and 25 nM in HL-60/Bcl2 cells) as single agents and in the combinations listed above. All single and double agent controls are included. The percentage of apoptotic cells was determined by sub-G1 FACS analysis. Error bars represent the standard error of the mean from three independent experiments. 2.5 nM ABT-737 resulting in a further increase in apoptosis, whereas in HL-60/Bcl2 cells, apoptosis above background was only induced when ABT-737 was added to the doxorubicin/AN-9 combination. Similar findings were obtained when a shorter treatment time of 4 hr was used (Figure 3.10B), although higher concentrations of doxorubicin (1 μ M) and AN-9 (50 μ M) were used in order to achieve synergy in HL-60/Puro cells for the combination treatment. Even at this shorter treatment time of 4 hr, ABT-737 was able to overcome resistance to doxorubicin/AN-9 in HL-60/Bcl2 cells, further highlighting the rapid mechanism of action of ABT-737.

Caspase-3 Activation Assay

The second apoptosis assay performed was a caspase-3 activation assay. Caspase-3 is an effector caspase and therefore activation of this caspase demonstrates that the caspase cascade has been initiated and that the cell is committed to death (Degterev *et al.*, 2003). Since caspase activation precedes DNA fragmentation (detected by the sub-G1 assay), it may be anticipated that an earlier time point than 6 hr may be optimal for this assay, therefore, a preliminary time course was performed to determine the optimal treatment time. As seen in Figure 3.11, in both cell lines, the triple treatment resulted in an increase in fluorescence above background after 5 hr which is indicative of caspase-3 activation. However, this increase was much greater after 6 hr and as such a 6 hr treatment time was chosen for subsequent analysis with this assay.

Using the same drug concentrations as used in the sub-G1 assay, the single agent and double agent control samples did not increase caspase activity above background levels in both cell lines (Figure 3.12). In HL-60/Puro cells, the DNA adduct forming combination of doxorubicin/AN-9 caused an increase in caspase-3 activity which was further increased by the addition of ABT-737. In HL-60/Bcl2 cells, caspase-3 activity above background was only evident when 25 nM ABT-737 was added to the doxorubicin/AN-9 combination, reflecting that inhibition of Bcl-2 is required to overcome resistance in this cell line. The use of 2.5 nM ABT-737 did not increase caspase-3 activity since a higher level of ABT-737 is required to overcome resistance in HL-60/Bcl2 cells.





HL-60/Puro (A) and HL-60/Bcl2 (B) cells were treated with the triple treatment (500 nM doxorubicin, 25 μ M AN-9, and either 2.5 nM ABT-737 in HL-60/Puro cells or 25 nM ABT-737 in HL-60/Bcl2 cells) for 2-6 hr, and at each time point cells were harvested and analysed by the caspase-3 activation assay. Samples were not standardized based on protein levels since the cell number and therefore protein content in each sample was not expected to change after 6 hr. Approximately 25 μ g protein from each sample was used for the fluorescence measurements.

В

Α

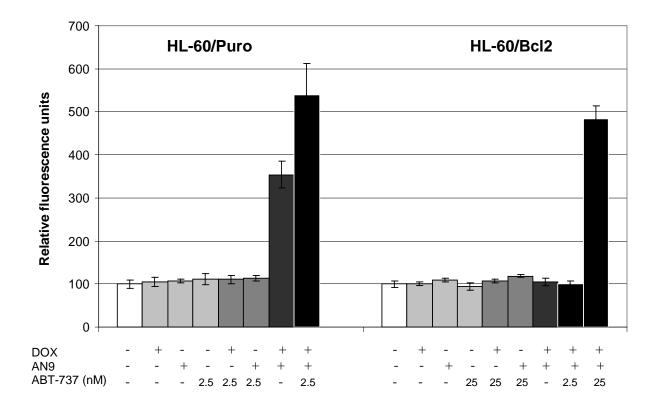


Figure 3.12. Caspase-3 activation induced by doxorubicin/AN-9 treatment is greatly enhanced in the presence of ABT-737.

HL-60/Puro and HL-60/Bcl2 cells were treated with doxorubicin (500 nM), AN-9 (25 μ M), and either 2.5 or 25 nM ABT-737 for 6 hr as single agents and in the combinations listed above. Cells were lysed and approximately 25 μ g protein was used for the determination of fluorescence intensity in the caspase-3 activation assay. Fluorescence intensity for each sample was recorded at 505 nM and standardized to the untreated control sample which was given a value of 100 fluorescence units. Error bars represent the standard error of the mean from three independent experiments.

Morphology Assay

Another characteristic hallmark of apoptosis is chromatin condensation and nuclear fragmentation which can be detected visually under a fluorescence microscope using the Hoechst nuclear stain. This morphology assay was used as the third independent apoptosis assay to demonstrate that the triple treatment was synergistic in Bcl-2 overexpressing HL-60 cells. Since chromatin condensation and nuclear fragmentation occur after caspase activation and DNA fragmentation, a preliminary time course was performed to identify the optimum treatment time for the morphology assay. The same concentrations of the three agents were used in this assay as for the two other assays. Figure 3.13A shows typical images obtained for HL-60/Puro and HL-60/Bcl2 cells after 4-12 hr treatment with the triple treatment (doxorubicin, AN-9 and ABT-737). The number of cells displaying chromatin condensation and/or nuclear fragmentation were counted and presented as the percentage of apoptotic cells in Figure 3.13B. It is clear that for both cell lines the number of apoptotic cells increases with time, however, at the 8 and 12 hr time points there were so many cells displaying apoptotic morphology that it became difficult to accurately delineate how many cells a local area of fragmentation was attributable to. For this reason, a 6 hr treatment time was chosen for this assay (the same treatment time as the two other apoptosis assays). Doxorubicin/AN-9 treatment resulted in chromatin condensation and nuclear fragmentation in a fraction of HL-60/Puro cells (Figure 3.14A – middle panel), in contrast, the nuclei of HL-60/Bcl2 cells treated with doxorubicin/AN-9 appear round and comparable to untreated samples (Figure 3.14A – top panel), indicating that this treatment was not inducing apoptosis in these cells. The addition of ABT-737 to form the triple treatment increased the proportion of cells displaying apoptotic morphology (Figure 3.14A – bottom panel). The number of apoptotic cells counted from the images was quantitated and shown in Figure 3.14B.

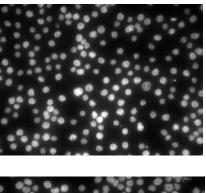
In summary, the overexpression of Bcl-2 conferred resistance to doxorubicin/AN-9 DNA adduct forming treatments as evidenced by the lack of apoptosis seen in HL-60/Bcl2 cells in all three apoptotic assays utilized. The Bcl-2 inhibitor ABT-737 was able to rapidly overcome this resistance and resulted in characteristic hallmarks of apoptosis in the Bcl-2 overexpressing cells.

Α

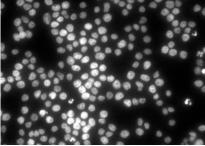
4 hr

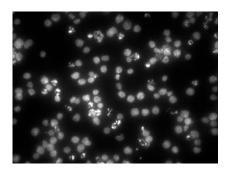
6 hr

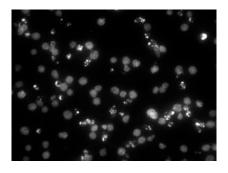
8 hr

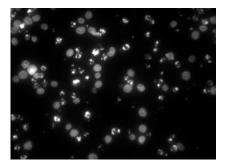


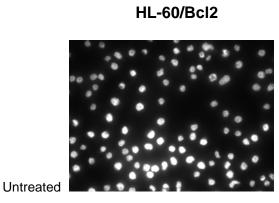
HL-60/Puro

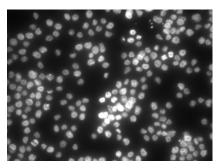


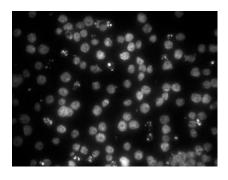


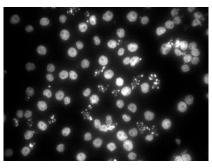


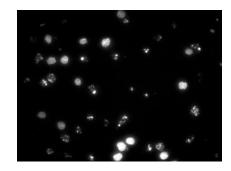












12 hr

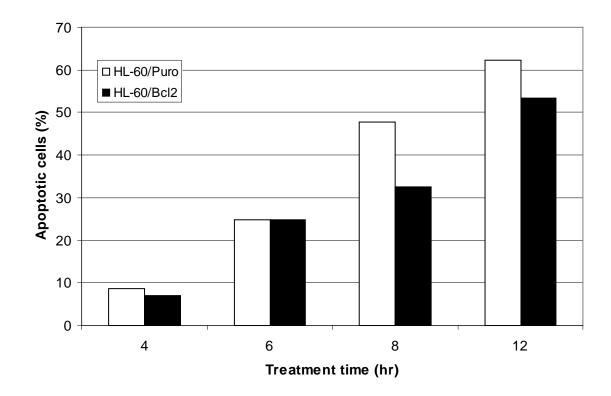


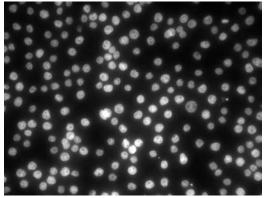
Figure 3.13. The number of morphologically apoptotic HL-60 cells increases with treatment time following administration of the triple treatment.

HL-60/Puro and HL-60/Bcl2 cells were treated with the triple treatment (500 nM doxorubicin, 25 μ M AN-9, and either 2.5 nM ABT-737 in HL-60/Puro cells or 25 nM ABT-737 in HL-60/Bcl2 cells) up to 12 hr. Cells were subjected to the apoptosis morphology assay where they were stained with Hoechst and analysed by fluorescence microscopy. Several images of each sample were taken and (A) representative images of HL-60/Puro (left-side) and HL-60/Bcl2 (right-side) cells are shown for each time point. Cells displaying clear chromatin condensation and/or nuclear fragmentation were (B) counted as apoptotic and the percentage of apoptotic cells was determined.

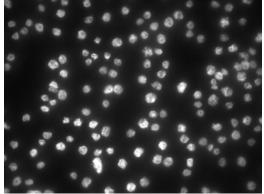
В

Α

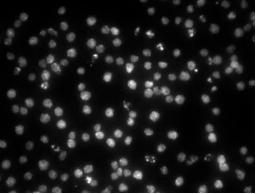
HL-60/Puro

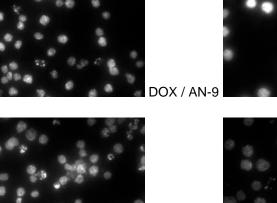


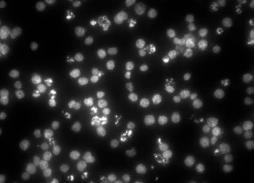
HL-60/Bcl2

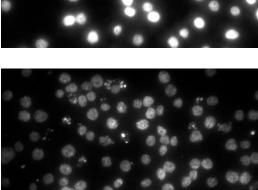


Untreated

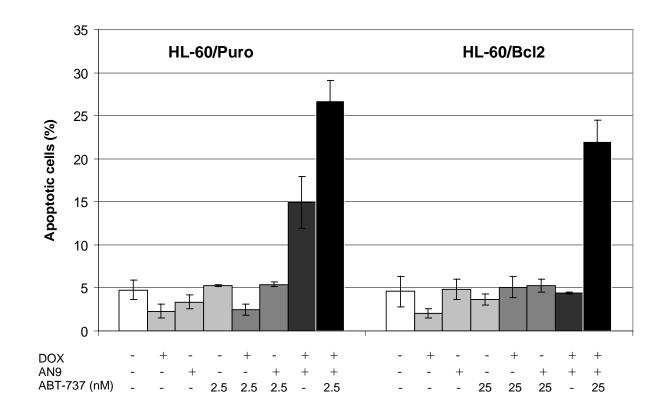








TRIPLE



В

Figure 3.14. ABT-737 potentiates the level of morphologically apoptotic cells induced by doxorubicin/AN-9 treatments in Bcl-2 overexpressing HL-60 cells.

HL-60/Puro and HL-60/Bcl2 cells were treated with doxorubicin (500 nM), AN-9 (25 μ M), and ABT-737 (either 2.5 nM in HL-60/Puro cells or 25 nM in HL-60/Bcl2 cells) for 6 hr as single agents and in the combinations listed above. Cells were stained with Hoechst and analysed by fluorescence microscopy. Florescence microscopy images (A) of untreated HL-60/Puro and HL-60/Bcl2 cells after Hoechst staining reveal round nuclei (top panels). Treatment with single agents and combinations of doxorubicin/ABT-737 and AN-9/ABT-737 produced similar images to untreated cells. Middle panels show images obtained following doxorubicin/AN-9 treatment, while bottom panels show images obtained following triple treatment. Images are representative of three independent experiments. Cells displaying clear chromatin condensation and/or nuclear fragmentation were counted as apoptotic and (B) the percentage of apoptotic cells was determined. Error bars represent the standard error of the mean from three independent experiments.

3.2.6 Cell kill induced by the triple treatment is dependent on caspasemediated apoptosis

As shown by the three apoptosis assays discussed above, a high level of cell kill was induced when ABT-737 was added to doxorubicin/AN-9 treatments. While the cell kill measured by these assays measures hallmarks of apoptosis this does not discount the possibility that other forms of caspase-independent cell death contributed to the overall cell kill. The sub-G1 assay is not entirely specific for apoptosis since necrotic cells may also undergo DNA fragmentation (Fairbairn and O'Neill, 1995; Didenko *et al.*, 2003). To determine if the cell kill measured was completely apoptotic, the pan-caspase inhibitor Z-VAD-fmk was employed in the sub-G1 assay. HL-60/Puro and HL-60/Bcl2 cells were pre-treated with 30 μ M Z-VAD-fmk for 1 hr before being treated with the triple treatment for 6 hr. At the concentration used, Z-VAD-fmk alone did not induce cell kill. As shown in Figure 3.15, the addition of Z-VAD-fmk to the triple treatment reduced the levels of cell kill to background levels in both cell lines. Therefore, the cell kill induced by the triple treatment is completely caspase-dependent and as such it can be assumed that apoptosis is the predominant mechanism of cell kill.

3.2.7 Identifying the molecular mechanisms responsible for the synergy induced by the triple treatment

3.2.7.1 The triple treatment does not affect Bcl-2 protein levels

The overexpression of Bcl-2 conferred resistance to DNA adduct-forming doxorubicin/AN-9 treatments. Overcoming this resistance can be achieved by inhibiting Bcl-2 as is expected to be the case with ABT-737, however, a reduction in Bcl-2 protein levels may also contribute to an increase in sensitivity. Western analysis was performed to determine if the combination of doxorubicin and AN-9, or the triple treatment, affected Bcl-2 protein levels. As demonstrated in Figure 3.16, in both HL-60/Puro and HL-60/Bcl2 cells the level of Bcl-2 protein was unaffected by either of the treatments.

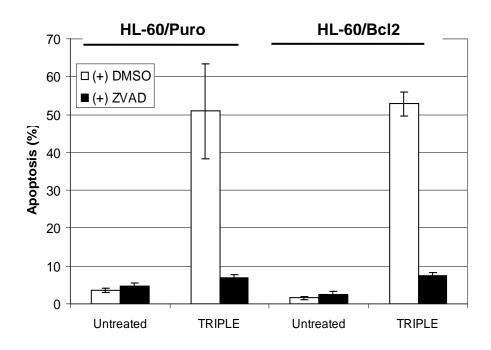


Figure 3.15. Cell kill induced by the triple treatment is caspase-dependent.

HL-60 cells were pre-treated with 30 μ M Z-VAD-fmk pan-caspase inhibitor for 1 hr before applying the triple treatment (500 nM doxorubicin, 25 μ M AN-9, and either 2.5 nM ABT-737 in HL-60/Puro cells or 25 nM ABT-737 in HL-60/Bcl2 cells) for 6 hr, after which the percentage of sub-G1 cells was determined by FACS analysis. Error bars represent the standard deviation from two independent experiments.

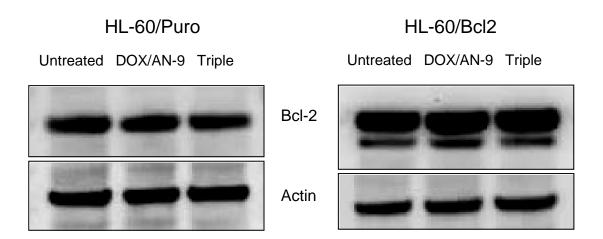


Figure 3.16. Bcl-2 protein levels are unaffected by the doxorubicin/AN-9 combination or the triple treatment.

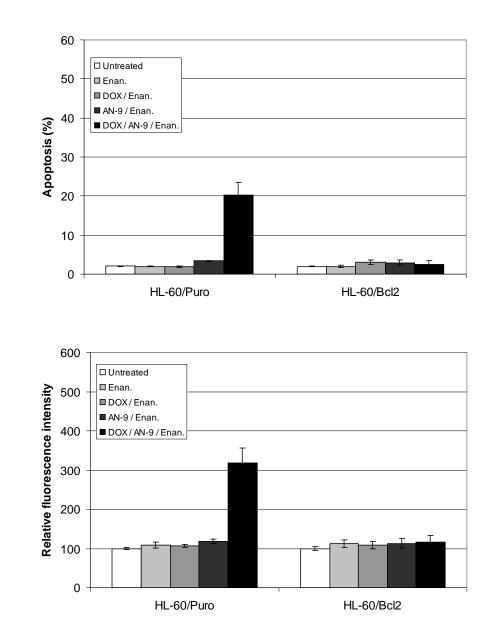
HL-60/Puro and HL-60/Bcl2 cells were treated with the doxorubicin/AN-9 combination (500 nM doxorubicin, 25 μ M AN-9) and the triple treatment (addition of 2.5 nM ABT-737 in HL-60/Puro and 25 nM ABT-737 in HL-60/Bcl2 cells) for 5 hr 30 min. Cells were harvested, lysed, and protein extracts (25 μ g) subjected to SDS-PAGE and Western transfer before being probed for Bcl-2 (26 kDa). Actin was used as a loading control. This blot is representative of two independent experiments showing similar results.

3.2.7.2 Control compounds demonstrate that cell death induced by the triple treatment is dependent on doxorubicin-DNA adduct formation

To identify and confirm the molecular mechanism and interactions responsible for the cell kill induced by the triple treatment, various control compounds were utilized. These compounds included the ABT-737 enantiomer which binds with a much lower affinity to Bcl-2, Bcl-xL and Bcl-w (Oltersdorf *et al.*, 2005); MEN-10755 (see Figure 3.18A), a disaccharide analogue of doxorubicin where the additional sugar group imparts steric constraints, preventing the compound from forming DNA adducts in the presence of formaldehyde (Messori *et al.*, 2001); and barminomycin (see Figure 4.1A) which is a pre-activated anthracycline that is able to form DNA adducts without the requirement for formaldehyde (Perrin *et al.*, 1999; Moufarij *et al.*, 2001).

The addition of the ABT-737 enantiomer to doxorubicin/AN-9 did not increase the level of apoptosis (Figure 3.17A), or caspase-3 activity (Figure 3.17B), in either cell line relative to the doxorubicin/AN-9 combination (shown in Figures 3.10A and 3.12). This is especially evident in HL-60/Bcl2 cells where use of the enantiomer had no effect in terms of overcoming resistance to doxorubicin/AN-9 treatment. This confirms that the correct configuration of the compound is required to enable high affinity binding and inhibition of Bcl-2 in order to overcome the block in apoptosis.

The compound MEN-10755 was able to induce cell kill as a single agent as effectively as doxorubicin after 24 hr treatment by inhibiting topoisomerase-II (Figure 3.18B). However, unlike doxorubicin, MEN-10755 did not induce apoptosis (Figure 3.18C), or increase caspase-3 activity (Figure 3.18D) in HL-60/Puro cells when combined with AN-9 in a 6 hr treatment, since the compound is unable to form DNA adducts in the presence of formaldehyde. For this reason, no synergy was observed in either cell line when MEN-10755 was used in combination with AN-9 and ABT-737, thus providing evidence that the main mechanism of cell kill induced by the triple treatment (doxorubicin/AN-9/ABT-737) is DNA adduct formation.

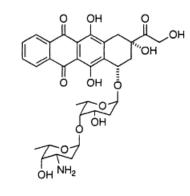


Α

В

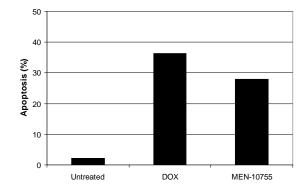
Figure 3.17. The ABT-737 enantiomer does not contribute to cell kill.

HL-60/Puro and HL-60/Bcl2 cells were treated with the ABT-737 enantiomer (2.5 nM in HL-60/Puro and 25 nM in HL-60/Bcl2 cells) for 6 hr as a single agent and in the combinations listed (500 nM doxorubicin, 25 μ M AN-9). (A) The percentage of apoptotic cells was determined via sub-G1 FACS analysis, and (B) the fluorescence intensity for each sample was recorded at 505 nM in the capsase-3 activation assay and standardized to the cell control sample, which was given a value of 100 fluorescence units. Error bars represent the standard error of the mean from three independent experiments.

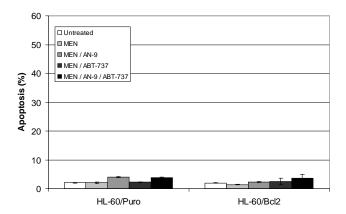




Α



С



D

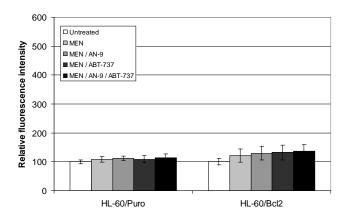
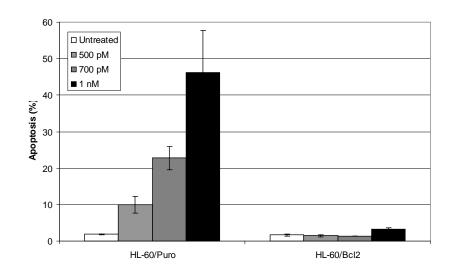


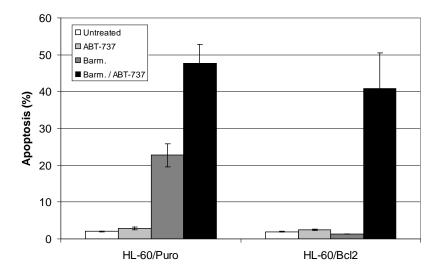
Figure 3.18. The non-DNA adduct forming compound MEN-10755 does not contribute to cell kill.

MEN-10755 (A) is an analogue of doxorubicin containing an additional sugar group. (B) HL-60/Puro cells were treated with 500 nM MEN-10755 or doxorubicin for 24 hr and the cells subjected to sub-G1 FACS apoptosis analysis (n=1). (C & D) HL-60/Puro and HL-60/Bcl2 cells were treated with MEN-10755 (500 nM) for 6 hr as a single agent and in the combinations listed (25 μ M AN-9 and 2.5 nM ABT-737 in HL-60/Puro or 25 nM ABT-737 in HL-60/Bcl2 cells). In (C) the percentage of apoptotic cells was determined via sub-G1 FACS analysis, and in (D) the fluorescence intensity for each sample was recorded at 505 nM in the caspase-3 activation assay and standardized to the cell control sample which was given a value of 100 fluorescence units. To ensure sensitivity of the cells, samples that were known to induce cell kill were also analyzed and displayed expected levels of apoptosis and caspase-3 activity (data not shown). Error bars represent the standard error of the mean from three independent experiments.



В

Α



С

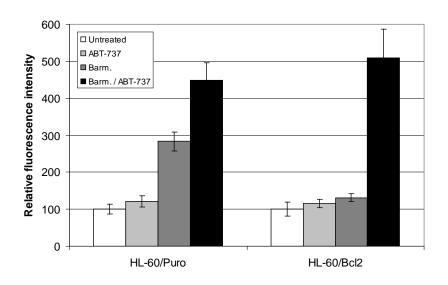


Figure 3.19. ABT-737 overcomes resistance to the pre-activated anthracycline barminomycin.

(A) HL-60/Puro and HL-60/Bcl2 cells were treated with increasing concentrations of barminomycin (0.5-1 nM) for 6 hr and the level of apoptosis determined by sub-G1 FACS analysis. (B & C) HL-60/Puro and HL-60/Bcl2 cells were treated with barminomycin (700 pM) for 6 hr and in combination with ABT-737 (2.5 nM in HL-60/Puro or 25 nM in HL-60/Bcl2 cells). The level of apoptosis was determined via (B) sub-G1 FACS analysis, and (C) the caspase-3 activation assay where the fluorescence intensity for each sample was recorded at 505 nM and standardized to the cell control sample which was given a value of 100 fluorescence units. Error bars represent the standard error of the mean from three independent experiments.

The pre-activated anthracycline barminomycin is highly cytotoxic and was shown to induce apoptosis after 6 hr as a single agent at sub-nanomolar levels in HL-60/Puro cells (Figure 3.19A). This is due to its ability to form DNA adducts in the absence of additional formaldehyde or prodrugs. As observed with the DNA adduct forming combination of doxorubicin/AN-9, barminomycin was unable to induce cell kill in the Bcl-2 overexpressing cells. However, once Bcl-2 is neutralized by the addition of ABT-737 the resistance to barminomycin was overcome, resulting in synergistic cell kill (Figure 3.19B). The addition of ABT-737 also increased cell kill induced by barminomycin in HL-60/Puro cells. Similar findings were observed in the caspase-3 activation assay where the addition of ABT-737 to barminomycin resulted in an increase in caspase-3 activity (Figure 3.19C). These results with barminomycin provide further evidence that once Bcl-2 is prevented from blocking apoptosis, cell kill is dependent on DNA adduct formation.

3.2.7.3 Cell kill induced by the triple treatment is independent of topoisomerase-II poisoning

To demonstrate if the main mechanism of doxorubicin action as a single agent (topoisomerase-II poisoning) contributed to cell kill induced by the triple treatment (doxorubicin, AN-9 and ABT-737), the topoisomerase-II reduced HL-60/MX2 cell line was used. Using the same treatment conditions as for HL-60/Puro and HL-60/Bcl2 cells, the HL-60/MX2 cells were shown to be sensitive to both the doxorubicin/AN-9 combination and the triple treatment (Figure 3.20). The HL-60/MX2 cells were just as sensitive to the doxorubicin/AN-9 combination as HL-60/Puro cells (Figure 3.10A), highlighting that in the presence of formaldehyde-releasing prodrugs the mechanism of doxorubicin action is switched to DNA adduct formation. However, the triple treatment induced less cell kill in HL-60/MX2 cells (~34% apoptosis) compared to HL-60/Puro cells (40-50% cell kill, Figure 3.10A). This may be explained by the possibility that HL-60/MX2 cells are slightly less sensitive to ABT-737 and as such a higher concentration than 2.5 nM ABT-737 may be required to induce the same level of cell kill as seen in HL-60/Puro cells for the triple treatment. Nevertheless, this result with HL-60/MX2 cells suggests that the mechanism of cell kill activated by the triple treatment is independent of topoisomerase-II.

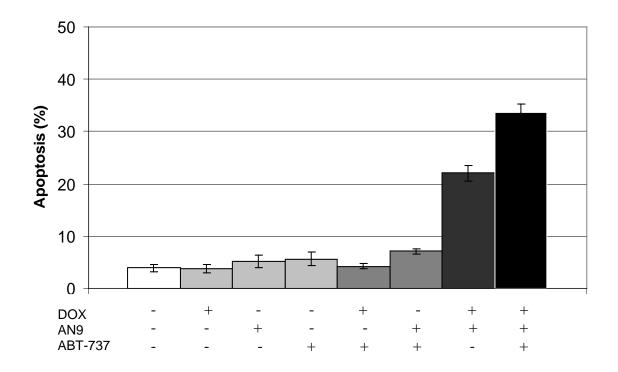


Figure 3.20. The triple treatment is synergistic in topoisomerase-II reduced cells.

HL-60/MX2 cells were treated with doxorubicin (500 nM), AN-9 (25 μ M), and ABT-737 (2.5 nM) as single agents and the combinations listed above for 6 hr. Cells were subjected to sub-G1 FACS analysis to determine the percentage of apoptotic cells. Error bars represent the standard error of the mean from three independent experiments.

To further establish if topoisomerase-II mediated DNA breaks play any major role in the mechanism of action induced by the triple treatment, the Comet assay was employed which measures the extent of single and double-strand DNA breaks. The Comet assay provides olive tail moment (OTM) values for each sample, where the higher the OTM value the greater the degree of DNA strand breaks. In this assay, the same concentrations of doxorubicin (500 nM), AN-9 (25 µM), and ABT-737 (2.5 nM in HL-60/Puro and HL-60/MX2 cells and 25 nM in HL-60/Bcl2 cells) were used as for the apoptosis assays, however, a shorter treatment time of 4 hr was used in order to minimize DNA fragmentation caused by apoptosis, which if detected in the Comet assay would give artificially high OTM recordings. A preliminary sub-G1 apoptosis experiment (Figure 3.21A) showed that after 4 hr treatment, the level of apoptosis induced by all treatments in all cell lines was minimal, thus, the OTM measurements in the Comet assay should be due primarily to drug action. As illustrated in Figure 3.21B, the highest OTM values and thus the greatest level of DNA strand breaks were seen following treatment with doxorubicin and doxorubicin/ABT-737 in HL-60/Puro and HL-60/Bcl2 cells. In these samples doxorubicin would be expected to act as a topoisomerase-II poison and cause double-strand DNA breaks. The OTM values were similar in both HL-60/Puro and HL-60/Bcl2 cells indicating that although Bcl-2 overexpression is blocking apoptosis, DNA breaks are still occurring. Sample images obtained from the Comet assay are shown in Figure 3.21C where a greater Comet tail is clearly visible following doxorubicin treatment in HL-60/Bcl2 cells relative to untreated cells. In doxorubicin/AN-9 and triple treatment samples, although doxorubicin was used, the OTM was lower, indicating that less DNA breaks were formed due to the preferential formation of DNA adducts in the presence of the formaldehyde-releasing prodrug AN-9 (these findings are consistent with the Comet assay results of Swift et al, 2006). Treatment with AN-9 or ABT-737 or the combination of both these drugs resulted in only background OTM values, indicating that these compounds do not induce single or double-strand DNA breaks. The OTM values induced by doxorubicin/AN-9 and triple treatment samples were above background levels and this may be caused by free doxorubicin that has not reacted with formaldehyde to form DNA adducts. Even if this is the case, the portion of free doxorubicin that has not reacted with formaldehyde would not be expected to contribute to apoptosis since doxorubicin as a single agent under the treatment conditions used to measure apoptosis (500 nM, 6 hr treatment) does not induce cell kill. In the topoisomerase-II reduced HL-60/MX2 cells, the OTM values for all samples were at background levels, thus confirming that in the other two

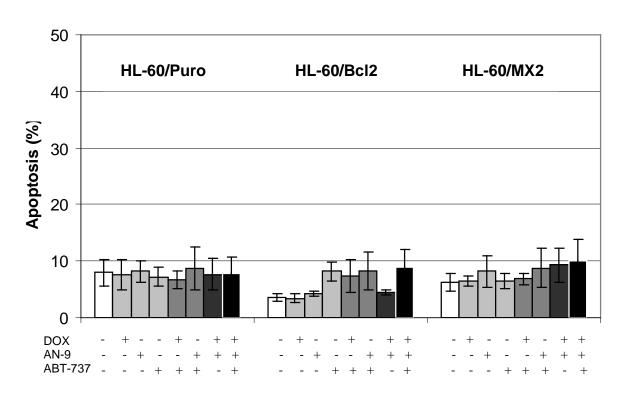
cell lines the high OTM values were due to topoisomerase-II dependent double-strand DNA breaks.

3.2.7.4 Increasing formaldehyde levels increases DNA adduct formation and apoptosis

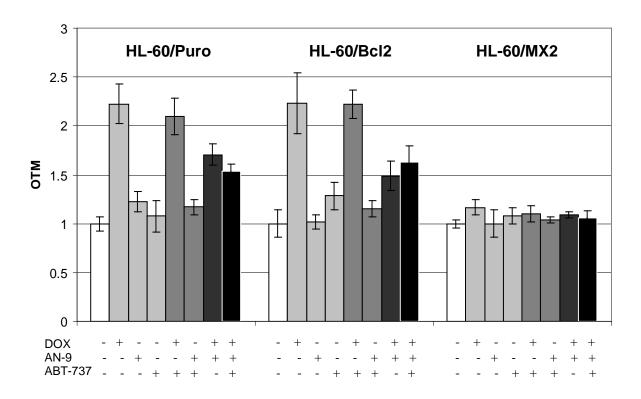
The formaldehyde-releasing prodrugs AN-9, AN-7, and AN-193 (structures shown in Figure 1.5), as well as the acetaldehyde-releasing prodrug AN-158 (Cutts *et al.*, 2001), were subjected to the colorimetric Nash assay to measure the level of formaldehyde released from the prodrugs in the presence of esterase. There is a linear relationship between the absorbance produced via the Nash assay and the amount of formaldehyde present in the samples, as illustrated in Figure 3.22A, allowing quantitation of formaldehyde levels by comparison to standards. Figure 3.22B shows that in the presence of esterase, the prodrugs AN-9 and AN-7 release the equivalent of 1 molecule of formaldehyde (50 μ M), while AN-193 releases the equivalent of 2 molecules of formaldehyde (100 μ M). Therefore, twice as much AN-9 is required to produce the same level of formaldehyde as released from AN-193. The prodrug AN-158 on the other hand does not release formaldehyde and therefore is used as a control compound.

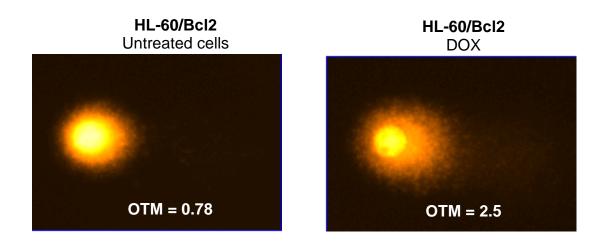
To further characterize the mechanism of cell kill in response to the triple treatment, HL-60/Puro and HL-60/Bcl2 cells were treated with the combination of [¹⁴C]-doxorubicin and prodrugs that release differing amounts of formaldehyde. To ensure a high enough sensitivity for scintillation counting, a higher concentration of 1 μ M [¹⁴C]-doxorubicin was used in comparison to the apoptosis assays where 500 nM doxorubicin was used. The resulting levels of doxorubicin-DNA adducts after 4 hr treatment were quantitated and the results presented in Figure 3.23. In both cell lines, only very low levels of DNA adducts were detected in response to doxorubicin alone and in combination with the prodrug AN-158, which as shown via the Nash assay does not release any formaldehyde. The combination of doxorubicin with the prodrug AN-193 which releases two molecules of formaldehyde upon esterase hydrolysis, resulted in approximately double the level of DNA adducts per 10 kbp when compared to AN-9 at the same concentration (50 μ M). Using half the concentration of AN-193 (25 μ M) resulted in similar DNA adduct levels to 50 μ M AN-9 in both cell lines. The







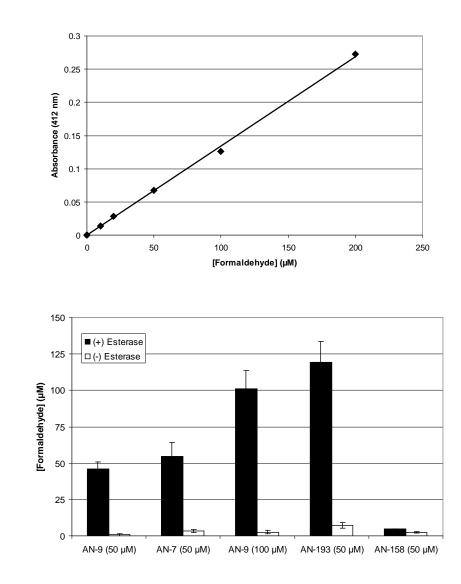


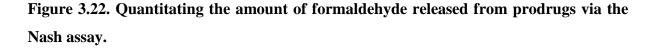


С

Figure 3.21. DNA strand breaks are reduced in the presence of formaldehyde-releasing prodrugs.

HL-60 cells were treated with doxorubicin (500 nM), AN-9 (25 μ M), and ABT-737 (2.5 nM in HL-60/Puro and HL-60/MX2 cells or 25 nM in HL-60/Bcl2 cells) as single agents and the combinations listed above for 4 hr. Cells were subjected to (A) sub-G1 FACS analysis to determine the percentage of apoptotic cells (error bars represent the standard deviation from two independent experiments), or (B) the Comet assay where the OTM of 50 cells per sample was recorded as an indication of the degree of DNA strand breaks. The OTM values were standardized to the cell control which was given an OTM value of 1 (error bars represent the standard error of the mean from four independent experiments). Sample images of untreated and doxorubicin treated HL-60/Bcl2 cells showing Comet tails and OTM values are shown in (C).





In the Nash assay, (A) formaldehyde standards (0-200 μ M) and (B) prodrug samples (50 or 100 μ M) were prepared and assayed simultaneously. The prodrug samples were incubated in the presence and absence of esterase, before being incubated with the Nash reagent, along with the formaldehyde standards. The absorbance of all samples was recorded at 412 nm and the amount of formaldehyde released from the prodrugs was quantitated (B) by comparison to the formaldehyde standards (an example of a formaldehyde standard curve is shown in A). Error bars represent the standard error of the mean from three independent experiments.

В

Α

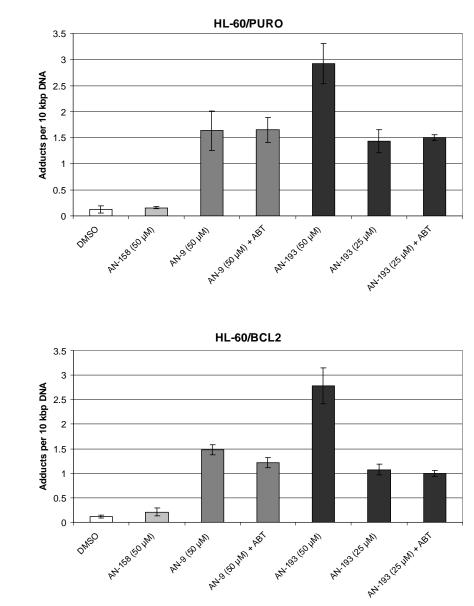


Figure 3.23. Increasing the amount of formaldehyde available increases doxorubicin-DNA adduct levels.

HL-60/Puro (A) and HL-60/Bcl2 (B) cells (4 mL at 300,000 cells/mL) were treated with 1 μ M [¹⁴C]-doxorubicin in combination with AN-158 (50 μ M), AN-9 (50 μ M), or AN-193 (25 or 50 μ M), in the presence or absence of ABT-737 (2.5 nM in HL-60/Puro or 25 nM in HL-60/Bcl2 cells) for 4 hr. After treatment, DNA was extracted, scintillation counting performed, and the level of doxorubicin-DNA adducts quantitated. Error bars represent the standard error of the mean from three independent experiments.

Α

В

presence of ABT-737 did not alter the DNA adduct levels, indicating that the compound does not interfere with the process of DNA adduct formation in cells.

The level of apoptosis (Figure 3.24) and caspase-3 activation (Figure 3.25) induced by the combination of doxorubicin with the different prodrugs and ABT-737 after 6 hr treatment was determined. Due to the lack of formaldehyde release and resulting lack of DNA adduct formation, the combination of AN-158 with doxorubicin and in the triple treatment (AN-158, doxorubicin, ABT-737) did not induce apoptosis and caspase-3 activity above background levels. The use of AN-193 (12.5 μ M) in combination with doxorubicin and the triple treatment resulted in comparable levels of apoptosis and caspase-3 activity to samples where 25 μ M AN-9 was used. At the same concentration (12.5 μ M), the use of AN-9 did not induce cell kill or caspase-3 activation, suggesting that the amount of released formaldehyde was not high enough to result in sufficient DNA adduct formation and thus the threshold for apoptosis induction was not reached.

In summary, cell kill induced by the triple treatment was dependent on formaldehyde and the greater the amount of formaldehyde available, the greater the level of DNA adduct formation and apoptosis induced.

3.2.8 ABT-737 is synergistic with doxorubicin as a single agent

Studies have reported that ABT-737 is synergistic with a range of clinically used chemotherapeutics with different mechanisms of action (Oltersdorf *et al.*, 2005). The results in this present study have demonstrated that ABT-737 is synergistic with the DNA adduct forming treatments of doxorubicin/AN-9 and barminomycin, even when Bcl-2 is overexpressed. To determine if synergy also occurs when doxorubicin acts as a topoisomerase-II poison, doxorubicin was used as a single agent in HL-60 cells. Longer treatment times of 24 hr were employed since DNA damage and apoptosis arising from topoisomerase-II poisoning does not occur as rapidly as induced by DNA adduct formation. Figure 3.26 shows that the combination of doxorubicin (300 nM) and ABT-737 (10 nM) in HL-60/WT cells resulted in a greater than additive response using the sub-G1 apoptosis

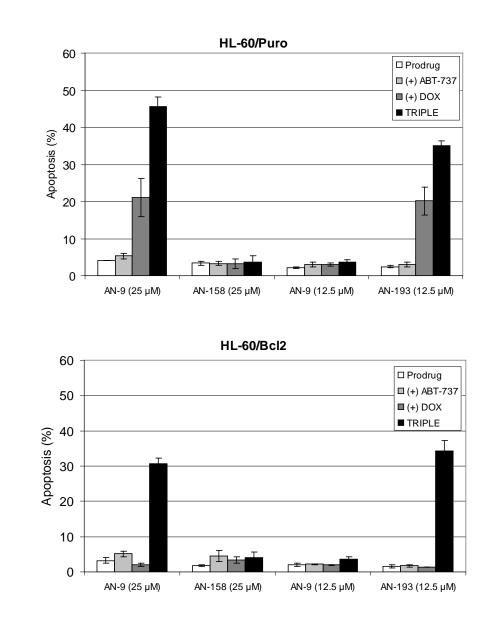


Figure 3.24. Increasing the amount of formaldehyde available increases apoptosis levels.

HL-60/Puro (A) and HL-60/Bcl2 (B) cells were treated with the prodrugs AN-158 (25 μ M), AN-9 (12.5 or 25 μ M), or AN-193 (12.5 μ M) as single agents and in combination with ABT-737 (2.5 nM in HL-60/Puro or 25 nM in HL-60/Bcl2 cells), doxorubicin (500 nM), or in a triple treatment for 6 hr. The percentage of apoptotic cells was determined by sub-G1 FACS analysis. It should be noted that doxorubicin, ABT-737, and the combination of doxorubicin/ABT-737 controls were not shown in this figure since they have been shown previously in Figure 3.10A. Error bars represent the standard error of the mean from three independent experiments.

Α

В

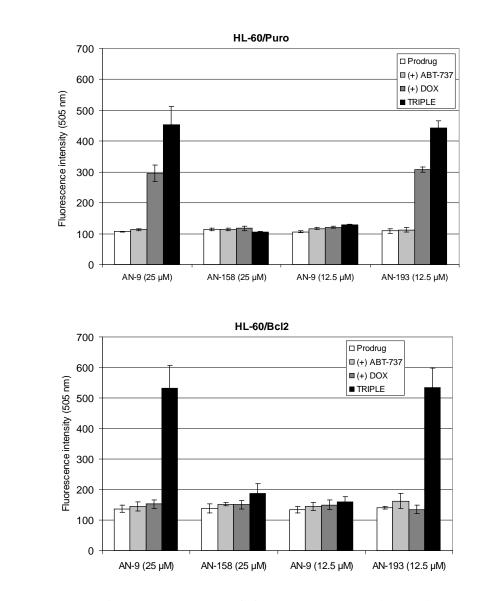


Figure 3.25. Increasing the amount of formaldehyde available increases caspase-3 activity.

HL-60/Puro (A) and HL-60/Bcl2 (B) cells were treated with the prodrugs AN-158 (25 μ M), AN-9 (12.5 or 25 μ M), or AN-193 (12.5 μ M) as single agents and in combination with ABT-737 (2.5 nM in HL-60/Puro or 25 nM in HL-60/Bcl2 cells), doxorubicin (500 nM), or in a triple treatment for 6 hr. Cells lysates were subjected to the caspase-3 activation assay and fluorescence intensity for each sample was recorded at 505 nm. It should be noted that doxorubicin, ABT-737, and the combination of doxorubicin/ABT-737 controls were not shown in this figure since they have been shown previously in Figure 3.12. Error bars represent the standard error of the mean from three independent experiments.

В

Α

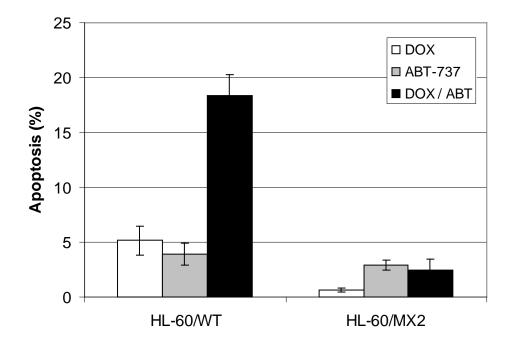


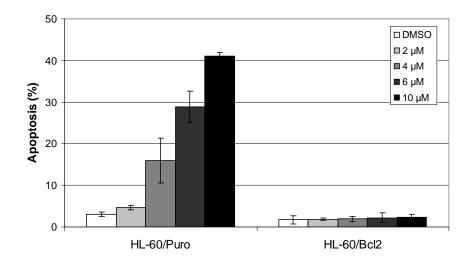
Figure 3.26. ABT-737 is synergistic with doxorubicin in HL-60 cells but not in the topoisomerase-II reduced HL-60/MX2 cells.

Cells were treated with doxorubicin (300 nM) and ABT-737 (10 nM) for 24 hr after which flow cytometry was conducted to determine the percentage of sub-G1 apoptotic cells. The apoptosis levels from untreated control samples were subtracted from all treated samples. Error bars represent the standard error of the mean from three independent experiments.

assay. Preliminary experiments indicated that a 24 hr treatment time was optimal for the induction of a synergistic response. HL-60/WT cells were compared to the topoisomerase-II reduced HL-60/MX2 cell line and as shown in Figure 3.26, no increase in cell kill was observed with the combination treatment in these cells. This highlights that the synergy seen in HL-60/WT cells is entirely due to the ability of doxorubicin to act as a topoisomerase-II poison.

3.2.9 ABT-737 overcomes Bcl-2 mediated resistance to etoposide

ABT-737 was shown to overcome Bcl-2 mediated resistance to the DNA adduct forming treatments of doxorubicin and formaldehyde-releasing prodrugs (AN-9 and AN-193), and barminomycin. To determine if this can be extended to clinically used chemotherapeutics with an alternative mechanism of action, the topoisomerase-II poison etoposide was used. As displayed in Figure 3.27A, etoposide induced apoptosis in a dose-dependent manner in HL-60/Puro cells after 6 hr treatment, however, Bcl-2 overexpression conferred resistance to the drug as no cell kill was induced in HL-60/Bcl2 cells. In HL-60/Puro cells, the addition of ABT-737 to etoposide resulted in a slight increase in apoptosis (Figure 3.27B), although a higher concentration of ABT-737 (10 nM) was required compared to doxorubicin/AN-9 treatments. In the Bcl-2 overexpressing cells, the addition of low nanomolar ABT-737 (25 nM) to etoposide resulted in a highly synergistic response with high levels of apoptosis induced (Figure 3.27B). No apoptosis was observed in the topoisomerase-II reduced HL-60/MX2 cells, indicating that cell kill mediated by etoposide alone in HL-60/Puro cells, or the synergy observed between ABT-737 and etoposide in HL-60/Bcl2 cells was dependent on topoisomerase-II. These results demonstrate that in addition to DNA adduct forming treatments, ABT-737 is also able to overcome Bcl-2 mediated resistance to the topoisomerase-II poison etoposide.



В

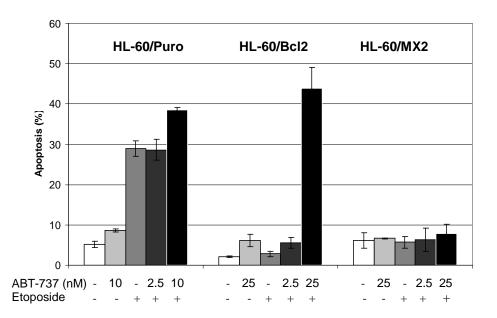


Figure 3.27. ABT-737 overcomes Bcl-2 mediated resistance to etoposide.

HL-60/Puro and HL-60/Bcl2 cells were (A) treated with increasing concentrations of etoposide (2-10 μ M) for 6 hr. HL-60/Puro, HL-60/Bcl2, and HL-60/MX2 cells were (B) treated with 6 μ M etoposide and ABT-737 for 6 hr. In both (A) and (B) the percentage of apoptotic cells was determined by sub-G1 FACS analysis. Error bars represent the standard error of the mean from three independent experiments.

Α

3.2.10 The triple treatment is synergistic in other cancer cell lines

All of the experimental data presented so far has involved the use of HL-60 cells to demonstrate that Bcl-2 mediated resistance to DNA adduct forming treatments can be overcome with the use of ABT-737. To determine if this triple treatment is beneficial against other cancer cells lines, U937 (human leukemic monocyte lymphoma) and HCT116 (human colorectal carcinoma) cell lines were used.

U937 leukemic cells

In comparison to HL-60 cells, U937 cells express lower levels of endogenous Bcl-2 protein (Figure 3.3A), and higher levels of Mcl-1 protein (Figure 3.3C), which is not a favourable expression profile for ABT-737 sensitivity. As shown in Figure 3.28A, a dose-dependent increase in apoptosis was observed in U937 cells following ABT-737 treatment, however, micromolar not nanomolar (compared to Figure 3.5A) concentrations were required to achieve appreciable levels of cell kill. The combination of doxorubicin and AN-9 (at the same concentrations and treatment time as used for HL-60 cells) was shown to be synergistic in U937 cells (Figure 3.28B). The addition of ABT-737 to form a triple treatment resulted in a synergistic increase in apoptosis (Figure 3.28C), however, a higher concentration of 10 nM was required to achieve this synergy (compared to 2.5 nM for HL-60/Puro cells). This is consistent with the observation that U937 cells are less sensitive to ABT-737 which is most likely due to the higher Mcl-1 expression level.

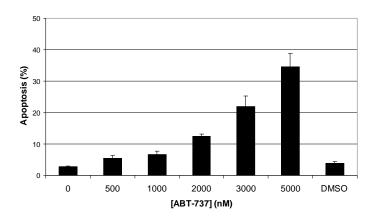
HCT116 colon cancer cells

Western analysis revealed that HCT116 cells express extremely low levels of endogenous Bcl-2 in comparison to HL-60 and U937 cells (Figure 3.29A). Mcl-1 protein expression levels (Figure 3.29B) on the other hand are comparable to HL-60/WT cells. This indicates that HCT116 cells are more reliant on Mcl-1 (and possibly Bcl-xL or Bcl-w) to prevent apoptosis instead of Bcl-2. Despite the extremely low level of Bcl-2 protein, HCT116 cells were shown to undergo apoptosis in response to micromolar concentrations of ABT-737 (Figure 3.30A). Although the expression levels of other anti-apoptotic proteins were not

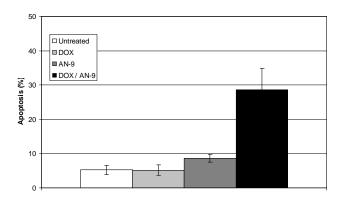
determined in this study, the sensitivity of HCT116 cells to ABT-737 is likely due to the ability of ABT-737 to also inhibit Bcl-xL and Bcl-w, which may also be imparting resistance. The DNA adduct forming treatment of doxorubicin (250 nM) and AN-9 (50 μ M) was synergistic in HCT116 cells following a 24 hr treatment (Figure 3.30B), and the addition of 100 nM ABT-737 resulted in a further synergistic increase in cell kill (Figure 3.30C). Similar to U937 cells, higher concentrations of ABT-737 were required to increase cell kill compared to HL-60/Puro cells, and this most likely correlates with the greater reliance on Mcl-1 to block apoptosis.

3.2.11 Mcl-1 knockdown increases ABT-737 sensitivity in HCT116 cells

Since Mcl-1 is the main form of resistance to ABT-737 (Lin et al., 2007), HCT116 cells (which express very low Bcl-2 and relatively high Mcl-1 protein) were used to determine if knockdown of Mcl-1 via siRNA increases sensitivity to the inhibitor. Using Lipofectamine[™] 2000 (4 or 6 μ L) as the transfection reagent, Figure 3.31A shows that the two siRNA sequences used (s8583 (validated) and s8585) resulted in considerable knockdown of Mcl-1 protein levels after 72 hr in HCT116 cells. Sub-G1 FACS analysis showed that transfection with 6 µL LipofectamineTM 2000 caused a slight increase in apoptosis above background (data not shown), and for this reason 4 µL LipofectamineTM 2000 was used for subsequent analysis. To determine if this knockdown of Mcl-1 subsequently resulted in an increase in ABT-737 sensitivity, transfected cells were treated with the inhibitor for 24 hr and the level of apoptosis induced measured by sub-G1 FACS analysis. As shown in Figure 3.31B, the use of a non-targeting scrambled siRNA sequence and a GAPDH siRNA sequence as negative and positive controls respectively, did not increase the level of cell kill induced by ABT-737 above that observed for untreated cells. Use of both Mcl-1 siRNA's resulted in much greater apoptosis levels following ABT-737 treatment, in particular, the s8583 sequence resulted in approximately a 5-fold increase in cell kill in response to 1 µM ABT-737. These results demonstrate that when Mcl-1 levels are knocked down, ABT-737 is more effective in inducing apoptosis as a single agent.



В



С

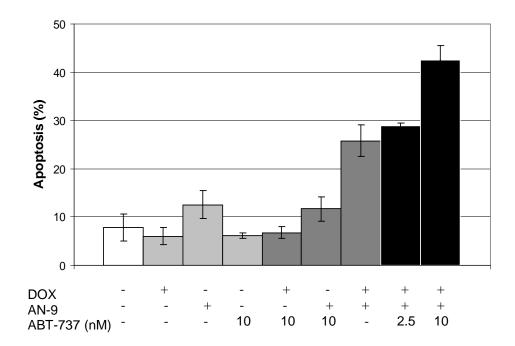


Figure 3.28. U937 cells are sensitive to ABT-737 and the triple treatment.

U937 cells (2 mL at 200,000 cells/mL) were treated with (A) increasing concentrations of ABT-737 from 500-5000 nM for 24 hr, (DMSO was used as a vehicle control equivalent to the DMSO level at highest ABT-737 concentration), (B) with doxorubicin (500 nM), AN-9 (25 μ M), and the combination of both drugs for 6 hr, and (C) with the triple treatment (500 nM doxorubicin, 25 μ M AN-9, and either 2.5 or 10 nM ABT-737) for 6 hr. Cells were subjected to sub-G1 FACS analysis to determine the percentage of apoptotic cells. Error bars represent the standard error of the mean from three independent experiments.

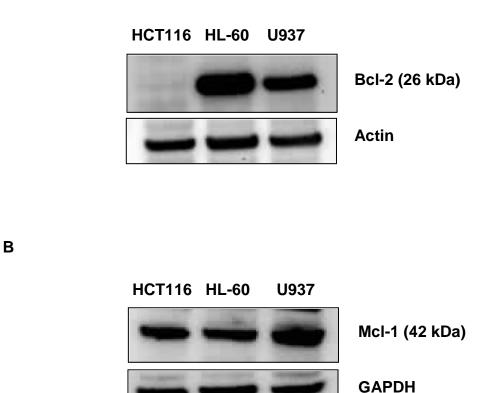
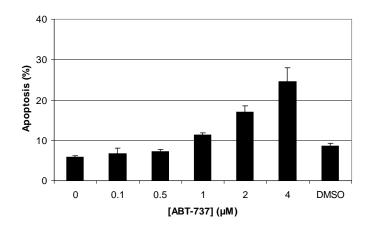


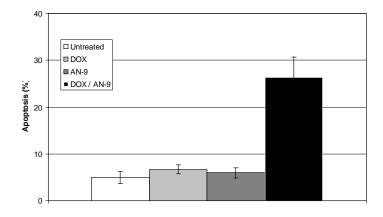
Figure 3.29. Bcl-2 and Mcl-1 protein levels in HCT116 cells.

Western analysis was performed to determine the level of (A) Bcl-2 protein and (B) Mcl-1 protein in HCT116 cells in comparison to HL-60/WT and U937 cells. For both blots, untreated cells were harvested and protein extracts ($50 \mu g$) were subjected to SDS-PAGE and Western transfer. Blots are representative of two independent experiments yielding similar results. Actin and GAPDH were used as loading controls.



В

Α



С

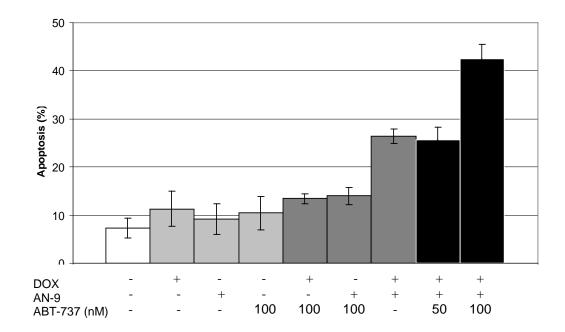


Figure 3.30. HCT116 cells are sensitive to ABT-737 and the triple treatment.

HCT116 cells $(1.6x10^5 \text{ cells})$ were treated with (A) increasing concentrations of ABT-737 from 0.1-4 μ M for 24 hr, (DMSO was used as a vehicle control equivalent to the DMSO level at highest ABT-737 concentration), (B) with doxorubicin (250 nM), AN-9 (50 μ M), and the combination of both drugs for 24 hr, and (C) with the triple treatment (250 nM doxorubicin, 50 μ M AN-9, and either 50 or 100 nM ABT-737) for 24 hr. Cells were subjected to sub-G1 FACS analysis to determine the percentage of apoptotic cells. Error bars represent the standard error of the mean from three independent experiments.

1 2 3 4 5 6 7 McI-1 (42 kDa)

> 1 = Untreated cells 2 = Lipofectamine[™] 2000 (6 μL) 3 = Scrambled siRNA 4 = Mcl-1 siRNA s8583 (4 μl LF) 5 = Mcl-1 siRNA s8583 (6 μL LF) 6 = Mcl-1 siRNA s8585 (4 μL LF) 7 = Mcl-1 siRNA s8585 (6 μL LF)

В

Α

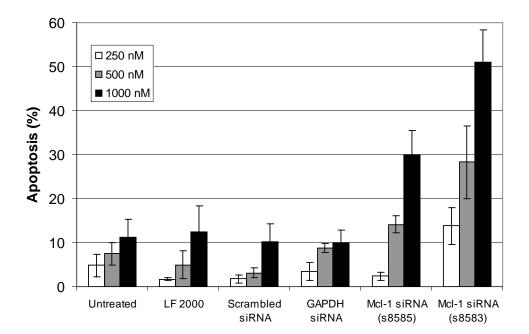


Figure 3.31. Mcl-1 knockdown increases ABT-737 sensitivity in HCT116 cells.

HCT116 cells $(2x10^5$ cells) were (A) transfected with siRNA targeting Mcl-1 (10 nM) using LipofectamineTM 2000 (4 µL or 6 µL) for 6 hr. After 72 hr, cells were harvested and protein extracts (30 µg) were subjected to SDS-PAGE and Western transfer. This blot is representative of two independent experiments yielding similar results. GAPDH was used as a loading control. Using 10 nM siRNA and 4 µL LipofectamineTM 2000, HCT116 cells were (B) transfected with Mcl-1 siRNA (a scrambled siRNA sequence was used as a negative control and GAPDH siRNA was used as a positive control) for 48 hr before the cells were harvested, re-plated (2 mL at 80,000 cells / mL), incubated for a further 24 hr and treated with ABT-737 for 24 hr. Sub-G1 FACS analysis was performed and the background apoptosis level from untreated cells was subtracted from ABT-737 treated samples. Error bars represent the standard error of the mean from three independent experiments. LF is used as abbreviation for LipofectamineTM 2000.

3.3 DISCUSSION

3.3.1 Overexpression of Bcl-2 confers chemoresistance

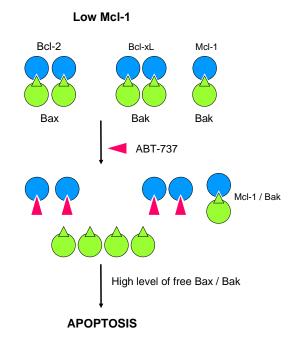
The overexpression of anti-apoptotic proteins is a major factor in the inherent resistance of cancer cells to various cytotoxic agents. It is generally considered that the ratio of pro- and anti-apoptotic proteins dictates whether cells undergo apoptosis or not, and the overexpression of anti-apoptotic proteins in cancer cells leads to a shift in the balance of this ratio in favour of cell survival. Considering that the main mechanism by which standard chemotherapeutic drugs kill cancer cells is via inducing apoptosis, any block to the apoptotic pathway that prevents cancer cell death will impact on the clinical efficacy of the drug. The overexpression of Bcl-2 and other anti-apoptotic proteins is believed to block apoptosis by sequestering pro-apoptotic Bax/Bak (according to the more favoured indirect activation of Bax/Bak model – see Figure 1.11) to such an extent that even in the presence of pro-apoptotic cascade is inhibited (Uren *et al.*, 2007; Willis *et al.*, 2007). Due to the fact that a number of different types of human cancers are commonly associated with Bcl-2 overexpression and chemoresistance, this has prompted the development of strategies to target and inhibit anti-apoptotic proteins to overcome the block in apoptosis.

While the combination of doxorubicin with AN-9 (and other formaldehyde-releasing prodrugs) has been shown to kill a variety of cancer cells in a synergistic manner (Cutts *et al.*, 2001; Cutts *et al.*, 2005; Engel *et al.*, 2006; Swift *et al.*, 2006), Swift and colleagues (2006) demonstrated in HL-60 cells that overexpression of Bcl-2 confers resistance (as determined by a lack of DNA fragmentation and apoptosis), thus limiting the clinical potential of this DNA adduct inducing drug combination. This Bcl-2 mediated resistance to the doxorubicin/AN-9 combination was also demonstrated in this study (see Figure 3.8). In order to overcome this resistance, the BH3 mimetic small molecule inhibitor ABT-737, which displays subnanomolar affinity for Bcl-2, Bcl-xL and Bcl-w (Oltersdorf *et al.*, 2005), was examined initially as a single agent and in combination with doxorubicin/AN-9 treatment to determine if Bcl-2 mediated resistance can be overcome.

3.3.2 ABT-737 as a single agent

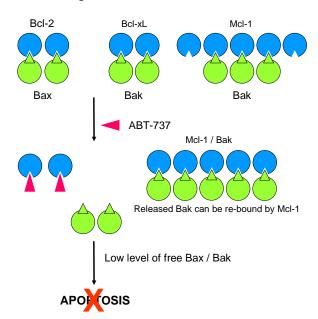
ABT-737 displayed single agent activity in a dose-dependent manner in HL-60/WT and HL-60/Puro cells (Figures 3.5A-B) in the low nanomolar range. The sensitivity of cancer cells to ABT-737 is primarily attributed to a favorable expression profile of anti-apoptotic proteins. In other words, due to the low affinity that the inhibitor has for Mcl-1, a low expression of Mcl-1 and a high dependence on Bcl-2 (or Bcl-xL and Bcl-w) to prevent apoptosis is required for ABT-737 to have maximal effect (Touzeau et al., 2011). HL-60 cells have been shown to express relatively low levels of Mcl-1 in comparison to other leukemic cell lines (Dai and Grant, 2007), with no detectable interaction between Bak and Mcl-1 (Konopleva et al., 2006). This suggests that in HL-60 cells, Bak is primarily held in check by Bcl-xL which can be inhibited by ABT-737, thus freeing Bak to induce MOMP together with free Bax. Cells with higher Mcl-1 levels on the other hand displayed Bak/Mcl-1 interaction and as such were more resistant to ABT-737 treatment due to the inability of the compound to inhibit Mcl-1 and free Bak (Konopleva et al., 2006). Figure 3.32 illustrates how Mcl-1 levels may affect the release of pro-apoptotic Bak and subsequent apoptosis in cancer cells. Furthermore, in HL-60 cells an abundant amount of endogenous Bcl-2 was shown to interact with Bax, reflecting that these cells are highly dependent on Bcl-2 for keeping Bax in check, and subsequent treatment with ABT-737 reduced this heterodimerization (Konopleva et al., 2006).

Even when Bcl-2 was overexpressed in HL-60/Bcl2 cells, ABT-737 still displayed single agent activity in both growth inhibition (Table 3.1) and apoptosis (Figure 3.5C) assays at approximately a 10-fold higher concentration than HL-60/WT cells, but still at submicromolar levels. The inhibitor was able to induce apoptosis in the Bcl-2 overexpressing HL-60 cells within a few hours (Figure 3.6), indicating that by directly targeting the apoptotic machinery a rapid cell death response can be achieved. Previous studies have also demonstrated that ABT-737 displays cytotoxicity even when Bcl-2 is overexpressed *in vitro*, and ABT-737 treatment also prolonged survival in a Bcl-2 overexpressing lymphoma mouse model (van Delft *et al.*, 2006). These findings highlight that even in tumours that heavily overexpress Bcl-2, ABT-737 can still display clinical potential (as long as Mcl-1 expression levels are low). Therefore, the ability of ABT-737 as a single agent to potently induce



В

High Mcl-1



Α

Figure 3.32. Sensitivity of cells to ABT-737 is dependent on Mcl-1 levels.

Cancer cells expressing (A) low levels of Mcl-1 are typically highly sensitive to ABT-737 since the inhibitor is able to free high levels of 'primed' Bax and Bak from the anti-apoptotic proteins Bcl-2 and Bcl-xL. Released Bax and Bak are able to induce MOMP and trigger apoptosis. Cancer cells expressing (B) high levels of Mcl-1 are typically more resistant to ABT-737 since in these cells it would be expected that a high proportion of Bak would be held in check by Mcl-1, and due to the low affinity that ABT-737 has for Mcl-1, the inhibitor would not able to disrupt Bak/Mcl-1 complexes. Furthermore, any Bak released from Bak/Bcl-xL complexes may then be re-bound by Mcl-1 resulting in low levels of free Bak. As such, the total level of free Bax and Bak may not reach the threshold required to promote MOMP and apoptosis.

apoptosis (as observed in Figures 3.5A-B for HL-60 cells) is highly dependent on the relative expression levels of anti-apoptotic proteins and their ability to prevent Bax/Bak from initiating the apoptotic cascade.

3.3.3 ABT-737 overcomes Bcl-2 mediated chemoresistance to doxorubicin-DNA adduct forming treatments

The addition of low nanomolar concentrations of ABT-737 to doxorubicin/AN-9 treatments increased cell kill in HL-60/Puro cells (Figure 3.9A) and overcame resistance in the Bcl-2 overexpressing HL-60 cells (Figure 3.9B). The addition of ABT-737 to form this 'triple treatment' (doxorubicin/AN-9/ABT-737) resulted in high levels of cell kill as monitored by DNA fragmentation (sub-G1 assay, Figure 3.10), caspase-3 activation (Figure 3.12), and chromatin condensation (morphology assay, Figure 3.14), all of which are classical hallmarks of apoptosis. Due to the rapid action of ABT-737, resistance to doxorubicin/AN-9 treatment was able to be overcome after just 4 hr treatment (Figure 3.10B). The use of the caspase inhibitor Z-VAD-fmk reduced the levels of cell kill in response to the triple treatment to background levels (Figure 3.15), further supporting caspase-dependent apoptosis as the cell death mechanism. In all three assays, the triple treatment was shown to be synergistic, with higher levels of ABT-737 (25 nM in HL-60/Bcl2 cells versus 2.5 nM in HL-60/Puro) required to achieve synergy in HL-60/Bcl2 cells due to the greater presence of Bcl-2 'targets' in these cells. The ability of ABT-737 (in the triple treatment) to increase cell kill in HL-60/Puro cells indicates that while the levels of Bcl-2 are not high enough to cause resistance to doxorubicin/AN-9 treatment in these cells, there is still some level of constraint caused by Bcl-2 that is overcome by inhibition with ABT-737. The synergy was more pronounced in HL-60/Bcl2 cells where the addition of ABT-737 completely overcame resistance to doxorubicin/AN-9 treatment as demonstrated in the three independent apoptosis assays. These findings are very promising since if in the future doxorubicin-DNA adduct forming treatments become clinically applicable, ABT-737 can potentially be used to increase sensitivity in Bcl-2 overexpressing cancer types that would otherwise be resistant.

3.3.4. Identifying the molecular mechanisms responsible for the synergy induced by the triple treatment

When the mechanism of cell kill in response to the triple treatment was investigated, it was found that the presence of ABT-737 did not change Bcl-2 expression levels (Figure 3.16). Therefore, the increase in sensitivity seen with the triple treatment, especially in HL-60/Bcl2 cells, is due to inhibition, not reduction or degradation of Bcl-2 by ABT-737. Furthermore, it was shown that the enantiomer (with the opposite configuration of the dimethylaminoethyl group) which displays low affinity for Bcl-2 (Oltersdorf *et al.*, 2005) did not increase cell kill or caspase-3 activity (Figure 3.17), indicating that the correct configuration of the compound is required to bind and inhibit Bcl-2. Control compounds that do not result in DNA adduct formation (i.e. MEN-10755; Figure 3.18) and AN-158; Figures 3.24-25), did not induce cell kill or caspase-3 activation when combined in a triple treatment with ABT-737. Barminomycin on the other hand which forms DNA adducts as a single agent was synergistic with ABT-737 (Figure 3.19). Therefore, the use of these control compounds confirms the absolute requirement and role of DNA adduct formation in the cell kill mechanism induced by the triple treatment.

Cell kill in response to the triple treatment was also shown to occur independently of topoisomerase-II, confirming that the topoisomerase-II poisoning function of doxorubicin and the resulting DNA strand breaks do not play a major role in the observed cell kill mechanism. This was demonstrated by the findings that the triple treatment was still able to induce cell kill in a topoisomerase-II reduced (HL-60/MX2) cell line (Figure 3.20), and in the Comet assay where less DNA breaks were induced by the triple treatment even though this treatment induced high levels of cell kill (Figure 3.21). Topoisomerase-II mediated double-strand breaks induced by doxorubicin as a single agent occur on different sequences of DNA (Capranico *et al.*, 1990; Cullinane and Phillips, 1990), and induce apoptosis at later time points (Swift *et al.*, 2006) relative to DNA adduct formation, reflecting that these lesions are independent. The results of this study validate that that in the presence of formaldehyde-releasing prodrugs, the mechanism of doxorubicin is switched from topoisomerase-II poisoning to DNA adduct formation, and it is the DNA adduct formation that induces cell kill in the triple treatment.

When the level of DNA adducts was measured directly using a $[^{14}C]$ -doxorubicin assay, it was shown that in HL-60/Bcl2 cells, doxorubicin-DNA adducts formed to the same extent as in HL-60/Puro cells (Figure 3.23). Therefore, it is expected that the same DNA adduct response pathways would be activated in both cell lines. The cellular processing of anthracycline-DNA adducts is only just beginning to be understood (see Figure 1.8 for a proposed model of DNA adduct processing) and appears to involve the stalling of DNA or RNA polymerases and the induction of double-stranded DNA breaks. These adduct mediated double-stranded DNA breaks occur in topoisomerase-II defective cells and as such differ from topoisomerase-II mediated breaks (Bilardi, 2010). Subsequently, ATM and ATR mediated signalling pathways become activated to trigger DNA repair and cell survival, or cell death (Forrest, 2010). In response to DNA damage, ATM and ATR can activate downstream p53-mediated upregulation of the pro-apoptotic BH3-only proteins Noxa and Puma (Oda et al., 2000; Nakano and Vousden, 2001; Roos and Kaina, 2006), which in turn can bind to anti-apoptotic proteins, causing a release of free Bax/Bak which triggers the apoptotic cascade. It has been demonstrated that in response to doxorubicin-DNA adducts, p53 appears to be involved in mediating early cytotoxic responses (Forrest, 2010), however, HL-60 cells are p53 null (Wolf and Rotter, 1985). In the absence of p53, related proteins including p63 and p73 can become upregulated (Roos and Kaina, 2006) which also can induce transcription of Noxa (Martin et al., 2009) and Puma (Melino et al., 2004) to promote apoptosis. Indeed, HL-60 cells have been shown to augment p73 in response to DNA damage, indicating that p53-independent mechanisms may still be inducing Noxa and Puma upregulation (Chakraborty et al., 2010).

Although DNA adducts were formed in both HL-60/Puro and HL-60/Bcl2 cells, apoptosis was not induced in response to doxorubicin/prodrug treatments in HL-60/Bcl2 cells, indicating that the overexpression of Bcl-2 completely blocks the apoptotic cascade from proceeding. While BH3-only proteins like Noxa and Puma may be upregulated via p53-independent mechanisms, the level of Bcl-2 may be so high that not enough Bax/Bak are released to trigger MOMP and apoptosis. Indeed it has been demonstrated that in Bcl-2 overexpressing HeLa cells, Bax oligomerization at the outer mitochondrial membrane does not occur (Antonsson *et al.*, 2001). It appears that the Bcl-2 overexpressing HL-60 cells are able to tolerate the presence of doxorubicin-DNA adducts (at least in the short term of 8 hr), and the resulting DNA damage may be repaired with time, although the exact repair

mechanisms are only beginning to be elucidated (Spencer *et al.*, 2008; Bilardi, 2010). Only when ABT-737 is added, resulting in the inhibition of Bcl-2 (Bcl-xL and Bcl-w), is there presumably sufficiently high enough levels of free Bax/Bak to trigger MOMP and apoptosis. Furthermore, the addition of ABT-737 to doxorubicin/AN-9 treatments did not affect DNA adduct levels (Figure 3.23), reflecting that the actions of the inhibitor do not interfere with DNA adduct formation.

The ability of ABT-737 to synergize with and overcome Bcl-2 mediated resistance is not limited only to DNA adduct inducing treatments such as doxorubicin/AN-9 and barminomycin. ABT-737 was also shown to synergize with doxorubicin as a single agent (over longer treatment times) in HL-60/WT cells, but not HL-60/MX2 cells (Figure 3.26), indicating that this synergy is dependent on the ability of doxorubicin to impair topoisomerase-II function. Another topoisomerase-II poison, etoposide, was also used to demonstrate that ABT-737 can overcome Bcl-2 mediated resistance to the drug in Bcl-2 overexpressing HL-60 cells (Figure 3.27). The ability of ABT-737 to overcome Bcl-2 mediated resistance to a range of different DNA damaging drugs, as seen in this study and others (Oltersdorf et al., 2005; Konopleva et al., 2006; van Delft et al., 2006) highlights the exceedingly important clinical potential of this inhibitor when combined with standard chemotherapeutics. The main reason behind this synergy is that DNA damaging drugs can alter the balance of pro and anti-apoptotic proteins to favour the induction of apoptosis when combined with ABT-737. In particular, it has been demonstrated that Noxa, which can be upregulated (by p53-dependent or -independent mechanisms) in response to DNA damaging agents, promotes Mcl-1 proteosomal degradation (Willis et al., 2005; Czabotar et al., 2007). The expression of Noxa in mouse embryonic fibroblasts resulted in reduced Mcl-1 levels and this coincided with increased sensitivity to ABT-737 treatment (van Delft et al., 2006). Other studies have demonstrated that DNA damaging agents such as etoposide, cytosine arabinoside (van Delft et al., 2006), and the combination of carboplatin/etoposide (Tahir et al., 2007), resulted in an increase in Noxa and/or decrease in Mcl-1 levels, and as such were synergistic with ABT-737. Therefore, this Noxa-mediated reduction of Mcl-1 levels may also be contributing to the high levels of synergy seen in Bcl-2 overexpressing HL-60 cells in response to the triple treatment.

The upregulation of Puma (via p53-dependent or independent mechanisms) in response to DNA damage (Nakano and Vousden, 2001; Melino et al., 2004) may also be contributing to the synergy observed between ABT-737 and DNA adduct forming treatments. The BH3 domain of Puma is able to interact with all anti-apoptotic proteins (Chen et al., 2005; Certo et al., 2006) (see Figure 3.2C), and together with ABT-737 inhibition, can lead to a high level of Bax/Bak release to trigger apoptosis. Another possible avenue that may be contributing to synergy is the observation that upon DNA damage a portion of p53 translocates to the outer mitochondrial membrane and interacts with Bcl-2 within a regulatory domain (Mihara et al., 2003; Deng et al., 2006). This p53/Bcl-2 interaction leads to a release of Bax and promotes apoptosis (Deng et al., 2006), which can be augmented in the presence of ABT-737, leading to a synergistic response. Similar effects have been shown via a p73-dependent process involving p73 upregulation of GRAMD4 and subsequent GRAMD4/Bcl-2 interaction (John et al., 2011). Furthermore, pro-apoptotic Bax can become upregulated via p53 (Miyashita and Reed, 1995), or p73 (Melino et al., 2004; Zhang et al., 2011), providing another means for favouring an apoptotic response and leading to synergy between ABT-737 and DNA damaging agents.

3.3.5 Mcl-1 mediated resistance to ABT-737

While ABT-737 is highly potent in HL-60 cells, both as a single agent and in inducing a synergistic response with doxorubicin/AN-9 in a triple treatment, it is still effective in other cancer cell lines with a less favourable anti-apoptotic expression profile. ABT-737 was shown to induce apoptosis as a single agent in U937 leukemic cells (Figure 3.28A), and HCT116 colorectal carcinoma cells (Figure 3.30A), albeit at higher micromolar levels. Both of these cell lines were shown to be sensitive to DNA adduct inducing doxorubicin/AN-9 treatments with synergy displayed (Figures 3.28B and 3.30B), and the addition of ABT-737 to form a triple treatment further potentiated the level of cell kill (Figures 3.28C and 3.30C). However, in order to induce synergy in the triple treatment, higher concentrations of ABT-737 were required compared to HL-60 cells (2.5 nM in HL-60/Puro cells versus 10 nM in U937 and 100 nM in HCT116 cells). The reason for the requirement of higher ABT-737 concentrations most likely stems from the lower Bcl-2 and higher Mcl-1 expression in U937

cells (see Figure 3.3), and the greater reliance on Mcl-1 to prevent apoptosis in HCT116 cells due to the virtual absence of Bcl-2 (Figure 3.29). Since Mcl-1 has been shown to be the major resistance factor to ABT-737 (Lin *et al.*, 2007), cells that express high Mcl-1 levels and/or are more reliant on Mcl-1 to block apoptosis are going to be more resistant to the inhibitor (as depicted in Figure 3.32; Konopleva *et al.*, 2006; van Delft *et al.*, 2006; Tahir *at al.*, 2007). However, the ability of ABT-737 to effectively inhibit Bcl-2, Bcl-xL, and Bcl-w, even if they are present at relatively low levels can still be advantageous, especially when used in combination with DNA damaging agents that can induce Noxa-mediated degradation of Mcl-1 to free as much Bax/Bak as possible over the threshold required to trigger apoptosis.

Many strategies have been investigated to knockdown or inhibit Mcl-1 in cells to increase sensitivity to ABT-737. Such strategies have included the use of shRNA (Konopleva et al., 2006; van Delft et al., 2006; Chen et al., 2007), the cyclin-dependent kinase inhibitor roscovitine (van Delft et al., 2006; Chen et al., 2007; Lin et al., 2007), and the MAPK pathway inhibitors sorafenib and PD98059 (Konopleva et al., 2006; Lin et al., 2007), all of which increased the lethality of ABT-737 in various cancer cell lines. In this study, shRNA targeting Mcl-1 was used to knockdown Mcl-1 levels in HCT116 cells (Figure 3.31A). It should be noted that while complete Mcl-1 knockdown was not achieved in HCT116 cells, this may actually be favourable in a clinical setting. Due to the importance of Mcl-1 in the development and maintenance of the immune system (Opferman et al., 2003; Opferman et al., 2005), complete knockdown may have severe effects on normal immune cells. Therefore, in a therapeutic sense, a threshold level of Mcl-1 knockdown needs to be reached where its levels are low enough to release Bak but high enough to not compromise immune function. Following Mcl-1 knockdown with shRNA, the sensitivity of ABT-737 in HCT116 cells was greatly increased (Figure 3.31B). Hence, it may be feasible in the future to combine the triple treatment with compounds/strategies that reduce Mcl-1 levels, thus broadening the potential use of the triple treatment to cancer cells which express high levels of both Bcl-2 and Mcl-1.

3.3.6 Clinical implications of ABT-737 and the triple treatment

Although the effectiveness of ABT-737 is limited due to its low affinity for Mcl-1, the use of broad-spectrum inhibitors (i.e. compounds that display high affinity for all anti-apoptotic proteins, such as Obatoclax) may cause greater clinical problems. For example, if a particular cancer only overexpresses Bcl-xL then a broad-spectrum inhibitor is more likely to induce systemic toxicities to normal cells, especially by inhibiting Mcl-1 given its important role in maintaining immune function. The development of specific inhibitors with high affinities for each of the anti-apoptotic proteins would be ideal as then a particular set of inhibitors could be used depending on which anti-apoptotic proteins are overexpressed in that cancer cell type. For example, the compound A-385358 displays selective inhibition for Bcl-xL over other anti-apoptotic proteins (Shoemaker *at al.*, 2006).

The technique of BH3 profiling has been developed to predict the dependence of cancer cells on anti-apoptotic proteins (Certo *et al.*, 2006). The principle of this technique is to isolate mitochondria from cancer cells and incubate them with a panel of BH3 peptides (peptides derived from the BH3 domains of BH3-only pro-apoptotic proteins) and determine the extent of cytochrome c release. Since different BH3-only proteins have different affinities for antiapoptotic proteins, it is therefore possible to determine which anti-apoptotic proteins the cancer cells depend on to prevent apoptosis. The use of such techniques could enable clinicians to determine if broad-spectrum or specific inhibitors would be more suitable against particular cancer types, thus leading to a more personalized approach to treatment.

As with any treatment, the effects on normal cells and potential side-effects need to be considered before clinical use. Since the expression of anti-apoptotic proteins is not limited to cancer cells, the inhibition of these proteins may be expected to trigger unwanted apoptosis in normal cells. However, it has been demonstrated by a number of groups that ABT-737 has limited effects on normal/non-malignant cells (Konopleva *et al.*, 2006; Del Gaizo Moore *et al.*, 2007), and *in vivo* both ABT-737 and the orally bioavailable derivative ABT-263 were well tolerated with lymphopenia and particularly thrombocytopenia being the most common side-effects (Oltersdorf *et al.*, 2005; Konopleva *et al.*, 2006; Wilson *et al.*, 2010; Gandhi *et al.*, 2011). Platelets primarily rely on a Bcl-xL/Bak switch for survival (Mason *et al.*, 2007),

and have a short life-span since over time Bcl-xL becomes degraded (Bertino *et al.*, 2003), freeing pro-apoptotic Bak to trigger apoptosis. Therefore, the inhibition of Bcl-xL via ABT-737 or ABT-263 reduces the level of Bcl-xL/Bak complexes resulting in an even more rapid clearance of old circulating platelets (Mason *et al.*, 2007). Since younger platelets have greater Bcl-xL levels, they are less susceptible to ABT-737/ABT-263 mediated killing and as such platelet numbers recover and stabilize over time (Tse *et al.*, 2008), thus allowing the thrombocytopenia to be easily managed in a clinical setting.

It is speculated that cancer cells exist in a 'primed for death' state where BH3-only proteins are constantly activated due to the numerous physiological aberrancies, including oncogene activation and cell cycle checkpoint violation associated with cancer cells (Certo *et al.*, 2006; Del Gaizo Moore et al., 2007). As such, cancer cells overexpress anti-apoptotic proteins to evade cell death via these multiple stress signals and BH3-only protein activation. Evidence supporting the primed for death model comes from the findings that in CLL (Del Gaizo Moore et al., 2007) and ALL cells (Del Gaizo Moore et al., 2008), a large extent of Bim is complexed with Bcl-2. Non-malignant cells on the other hand undergo normal physiological functions and Bim is kept in an inactive state bound to dynein light chains (Puthalakath et al., 1999). Therefore, the tonic apoptotic stimuli present in these cancer cells makes them highly sensitive to ABT-737 treatment since the inhibition of Bcl-2 would not only free Bax from Bcl-2/Bax complexes, but also free activated Bim from Bcl-2/Bim complexes, allowing Bim to bind to more Bcl-2 thus freeing even more Bax. Indeed, it was demonstrated that cell lines with the greatest level of Bim/Bcl-2 complexes were most sensitive to ABT-737 treatment (Del Gaizo Moore *et al.*, 2008). These findings are clinically relevant as it may create a therapeutic window where primed cancer cells are much more sensitive to anti-apoptotic inhibitors compared to normal (non-primed) cells, thus leading to fewer side-effects.

Due to the synergy observed in the triple treatment, the concentrations of ABT-737 used in the triple treatment are much lower than if ABT-737 was used as a single agent. This would be expected to minimize any ABT-737 related side-effects *in vivo*. Furthermore, the use of doxorubicin in combination with formaldehyde-releasing prodrugs to form DNA adducts also allows lower concentrations of doxorubicin to be used, thus potentially reducing serious cardiotoxic side-effects. For these reasons, it would be anticipated that the triple treatment would be well-tolerated *in vivo*. The main clinical disadvantages of ABT-737 are its low

aqueous solubility and lack of oral bioavailabilily, which have lead to the development of the second generation BH3 mimetic, ABT-263 (Navitoclax) (Park *et al.*, 2008a; Tse *et al.*, 2008). Considering that ABT-263 displays similar binding affinities to anti-apoptotic proteins as ABT-737 (Tse *et al.*, 2008), it would be expected that the combination of ABT-263 with doxorubicin/AN-9 treatments would be as effective as the ABT-737 triple treatment used in this study, but with the added advantage of being more flexible to dosing regimens *in vivo*.

3.3.7 Conclusions

This study described the combination of the DNA adduct forming treatment of doxorubicin/AN-9 with the Bcl-2 inhibitor ABT-737 to overcome Bcl-2 mediated chemoresistance. The combination of doxorubicin/AN-9 resulted in synergistic cell kill in HL-60 leukemic cells, however, Bcl-2 overexpression (HL-60/Bcl-2 cells) conferred resistance to this combination, which may limit the therapeutic potential of this treatment. ABT-737 was shown to induce cell kill as a single agent, even in Bcl-2 overexpressing cells, reflecting that this inhibitor is highly potent in cancer cells with high Bcl-2 levels. Cancer cells expressing lower levels of Bcl-2 and higher levels of Mcl-1 (e.g. U937 leukemic cells and HCT116 colon carcinoma cells) were more resistant to ABT-737, however, the use of strategies to knockdown or inhibit Mcl-1 may be used to increase sensitivity to ABT-737. The addition of low nanomolar levels of ABT-737 to doxorubicin/AN-9, forming a triple treatment, was able to overcome Bcl-2 mediated resistance in HL-60 cells, leading to high levels of synergistic cell kill, thereby making previously resistant cancer cells susceptible to doxorubicin-DNA adduct forming treatments. Considering that a wide range of cancer cell types overexpress Bcl-2, Mcl-1, and other anti-apoptotic proteins, this study shows that the use of small-molecule anti-apoptotic protein inhibitors like ABT-737 can broaden the potential clinical use of doxorubicin/AN-9 and related DNA adduct-forming treatments.

Chapter 4

USING DOXAZOLIDINE TO DEMONSTRATE THAT BCL-2 OVEREXPRESSION PROVIDES ONLY SHORT-TERM RESISTANCE TO DOXORUBICIN-DNA ADDUCTS IN HL-60 CELLS

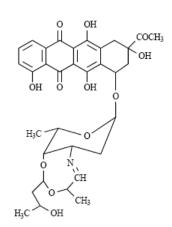
4.1 INTRODUCTION

While it has been demonstrated that doxorubicin-DNA adduct formation does occur to some extent in cancer cells when doxorubicin is used as a single agent, by utilizing formaldehyde from endogenous sources (Coldwell *et al.*, 2008) or from doxorubicin redox cycling (Taatjes *et al.*, 1997b; Kato *et al.*, 2000), the use of formaldehyde-releasing prodrugs in combination with doxorubicin results in much greater levels of cytotoxicity against a range of cancer cells (Kasukabe *et al.*, 1997; Niitsu *et al.*, 2000; Cutts *et al.*, 2001; Cutts *et al.*, 2005; Engel *et al.*, 2006; Swift *et al.*, 2006). The formation of doxorubicin-DNA adducts in the presence of formaldehyde-releasing prodrugs is a multi-step process, and as such compounds that are able to form DNA adducts as single agents would be expected to act more effectively since less steps would be required for DNA adduct formation. The compounds barminomycin and doxoform/doxazolidine possess the ability to form DNA adducts in the absence of endogenous or exogenous formaldehyde and are discussed below.

4.1.1 Pre-Activated Anthracyclines

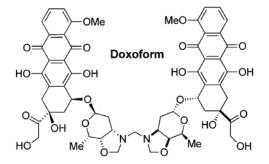
4.1.1.1 Barminomycin

Barminomycin is a natural anthracycline derivative isolated from a strain of the soil bacterium *Actinomadura roseoviolacea* (Kikuchi *et al.*, 1985; Uchida *et al.*, 1988). The structure of barminomycin (Figure 4.1A) is atypical of anthracyclines as it contains an eightmembered interconvertible imine-containing ring system attached to the sugar group (Uchida *et al.*, 1988). Barminomycin is able to form DNA adducts spontaneously in the absence of formaldehyde (Perrin *et al.*, 1999; Moufarij *et al.*, 2001) at a much faster rate (few minutes), and at much lower concentrations (low nanomolar) as a single agent compared to doxorubicin (Moufarij *et al.*, 2001). As with doxorubicin-DNA adducts, barminomycin adducts occur preferentially at 5'-GC-3' sequences following initial intercalation (Kimura *et al.*, 1989; Perrin *et al.*, 1999; Cutts *et al.*, 2000), and covalent attachment occurs with only one strand of DNA (Moufarij *et al.*, 2001). Although barminomycin-DNA adducts are similar to doxorubicin-DNA adducts, they are essentially irreversible, persisting for up to 5 days at





Α



С

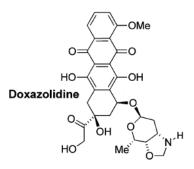


Figure 4.1. Structures of doxorubicin-formaldehyde conjugates.

Barminomycin (A) contains an eight-membered ring system attached to the daunosamine sugar group (Kimura *et al.*, 2010). Doxoform (B) consists of two doxorubicin molecules bound via their daunosamine sugar groups by a methylene bridge. Doxoform is unstable and hydrolyses to doxazolidine (C) which is able to form DNA adducts. (Me = methyl group) (Post *et al.*, 2005).

37 °C (Moufarij *et al.*, 2001), and are also much more heat stable (Perrin *et al.*, 1999; Moufarij *et al.*, 2001). This enhanced stability of the barminomycin-DNA adduct appears to be due to greater shielding of the aminal linkage from hydrolysis (Kimura *et al.*, 2010). Barminomycin possesses considerable cytotoxic activity against HeLa human cervical cancer cells (Kimura *et al.*, 1988), and P388 leukemia cells (Uchida *et al.*, 1988) when compared to doxorubicin, showing up to 1000-fold greater activity (Uchida *et al.*, 1988). Despite such potency, further *in vivo* analysis has not been pursued since barminomycin has been deemed unsuitable for clinical use due to its extremely high toxicity, lack of cancer cell selectivity, and lack of bio-availability (Kimura *et al.*, 2010).

4.1.1.2 Doxoform and Doxazolidine

The absolute requirement of formaldehyde for anthracycline-DNA adduct formation prompted Koch and colleagues (University of Colorado, Boulder, CO) to synthesize anthracycline derivatives conjugated to formaldehyde. Conjugates of doxorubicin, daunorubicin and epirubicin, termed doxoform, daunoform and epidoxoform respectively, consist of two anthracycline molecules bound together by their daunosamine sugars via a methylene bridge (Fenick et al., 1997; Taatjes et al., 1998). The structure of doxoform is shown in Figure 4.1B. Doxoform is extremely unstable and hydrolyses under physiological conditions to release two molecules of the activated drug doxazolidine (Figure 4.1C), which further hydrolyses to yield doxorubicin and formaldehyde (Fenick et al., 1997). Cellular localization studies showed that the primary cellular target for the conjugates is the nucleus (Taatjes et al., 1999a; Taatjes et al., 1999b). Doxazolidine is the active compound that directly forms adducts with DNA (Post et al., 2005), and these adducts are identical to those formed with doxorubicin and formaldehyde, but occur at a much faster rate (Fenick et al., 1997). While both doxorubicin and doxazolidine are able to induce apoptosis of cancer cells, topoisomerase-II deficient cells are resistant to doxorubicin but not doxazolidine, highlighting that doxazolidine as a single agent induces apoptosis not via topoisomerase-II poisoning but rather by DNA adduct formation (Kalet et al., 2007). Further evidence that doxazolidine functions via a topoisomerase-II independent mechanism comes from the finding that G2/M cell cycle arrest which is typical of topoisomerase-II inhibitors (including doxorubicin) is not observed with doxazolidine treatment (Kalet et al., 2007). Both doxoform and doxazolidine display a half-life in aqueous media in physiological conditions of 1-3

minutes (Post *et al.*, 2005), but despite this instability these conjugates possess remarkable anticancer activity (Fenick *et al.*, 1997; Post *et al.*, 2005).

The conjugates, doxoform, daunoform and epidoxoform, showed enhanced toxicity against MCF-7 breast cancer cells (doxoform was 150-fold more toxic compared to doxorubicin) (Fenick *et al.*, 1997; Taatjes *et al.*, 1998), and were 3 to 80-fold more toxic against three types of metastatic prostate cancer cell lines compared to their parent drugs (Taatjes *et al.*, 1999a). Furthermore, the conjugates are massively more cytotoxic against P-gp overexpressing MCF-7/ADR resistant cells relative to their parent drugs, with doxoform being some 10,000-fold more toxic compared to doxorubicin (Fenick *et al.*, 1997; Taatjes *et al.*, 1998). In fact, the conjugates completely overcame resistance in MCF7/ADR cells, displaying similar IC₅₀ values to the sensitive cells (Fenick *et al.*, 1997; Taatjes *et al.*, 1998). Similarly to doxoform, doxazolidine was also shown to be much more effective than doxorubicin at inhibiting the growth of a range of cancer cell lines, including prostate, small-cell lung, liver, and doxorubicin sensitive and resistant breast cancer cells (Post *et al.*, 2005; Kalet *et al.*, 2007), but not cardiomyocytes, suggesting no further increase in cardiotoxicity compared to doxorubicin (Kalet *et al.*, 2007).

The greater anticancer activity of doxoform and doxazolidine relative to doxorubicin may be explained by the observations that the conjugates are taken up more rapidly and more abundantly, and are retained much longer in both doxorubicin-sensitive and resistant cancer cells compared to their parent drugs (Taatjes *et al.*, 1999b; Post *et al.*, 2005). The greater uptake and retention of doxoform and doxazolidine and their ability to overcome P-gp resistance is most likely attributed to the fact that they are more lipophilic and uncharged at physiological pH relative to doxorubicin. Substrates for P-gp commonly contain positive charges and hydrophobic regions (Lampidis *et al.*, 1997) which is characteristic of doxorubicin, suggesting that it is subjected to continuous efflux from P-gp overexpressing cells. On the other hand, the characteristics of the conjugates make them poor substrates for efflux pumps. The ability of doxoform and doxazolidine to rapidly form covalent DNA adducts also renders the conjugates less available for drug efflux. Further development of doxoform and doxazolidine for clinical use is hindered by their hydrolytic instability, limited solubility, and non-specific toxicity, which, due to their potency may lead to serious side-

effects. Therefore, it is necessary to increase the stability of these compounds and develop targeting strategies to maximize their potential as chemotherapeutics.

4.1.2 Project Objectives

While the combination of doxorubicin with formaldehyde-releasing prodrugs has been shown to induce high levels of cancer cell death via DNA adduct formation, the use of doxorubicin-formaldehyde conjugates promises to be an even more effective way of inducing DNA adduct formation. The first aim of this project was to use the doxorubicin-formaldehyde conjugate, doxazolidine, which is able to form DNA adducts in the absence of formaldehyde, and assess its ability to induce cytotoxicity as a single agent in cancer cells in comparison to doxorubicin and doxorubicin/AN-9 treatments. Furthermore, by using HL-60/Bcl2 cells, the effect of Bcl-2 overexpression on doxazolidine efficacy was analyzed.

Based on results in HL-60/Bcl2 cells it was discovered that Bcl-2 mediated resistance to doxazolidine was only short-lived, with the cells becoming increasingly sensitive to the drug over time, and as such another major aim of this project was to investigate this phenomenon. To gain a better understanding as to what type of changes are occurring in HL-60/Bcl2 cells in response to doxazolidine treatment over time, the mechanism of cell death was examined. Possible explanations as to why Bcl-2 mediated resistance is overcome over time were also investigated, including the involvement of Bcl-2 family proteins. Long-term treatments of HL-60/Bcl2 cells with other drugs including the combination of doxorubicin/AN-9, and doxorubicin as a single agent, were also undertaken to determine if the ability to overcome Bcl-2 mediated resistance (at least in HL-60 cells) is a wider-occurring event.

4.2 **RESULTS**

4.2.1 Doxazolidine displays much greater cytotoxicity than doxorubicin and the combination of doxorubicin with AN-9 in cancer cells

Doxazolidine has been identified as the active metabolite of doxorubicin that is able to form DNA adducts as a single agent (Post et al., 2005), and due to its ability to form covalent adducts with DNA directly, studies have shown that doxazolidine is much more cytotoxic to cancer cells than doxorubicin (Post et al., 2005; Kalet et al., 2007). The ability of doxazolidine to induce apoptosis was compared to doxorubicin and the combination of doxorubicin/AN-9 in HL-60 and U937 leukemic cancer cells, as well as HCT116 colon cancer cells. Figure 4.2 shows that in HL-60/WT and U937 cells, 50 nM doxazolidine was able to induce much higher levels of apoptosis after 4 hr treatment compared to doxorubicin (at the same concentration) and the combination of doxorubicin/AN-9 (1:1000). In the topoisomerase-II reduced HL-60/MX2 cells, doxazolidine was as cytotoxic as observed in the HL-60/WT cells, indicating that its mechanism of action is not dependent on the activity of topoisomerase-II. The superior cytotoxicity of doxazolidine over doxorubicin and the combination of doxorubicin/AN-9 was also observed in HCT116 cells after 24 hr treatment, indicating that these findings are not just limited to leukemic cell lines. These results demonstrate that although doxazolidine has a very short half-life and in just a few minutes becomes hydrolyzed to yield doxorubicin and formaldehyde (Post et al., 2005), it is still able to induce high levels of cell kill via DNA adduct formation.

4.2.2 Overexpression of Bcl-2 confers resistance to short-term doxazolidine treatments in HL-60 cells which can be overcome by ABT-737

Bcl-2 is overexpressed in many cancer types and is one of the major causes of inherent chemoresistance to a range of drugs including anthracycline-DNA adduct forming treatments. In the previous chapter, a HL-60 cell model (Figure 3.3A) was used to demonstrate that Bcl-2 overexpression confers resistance to doxorubicin/formaldehyde-

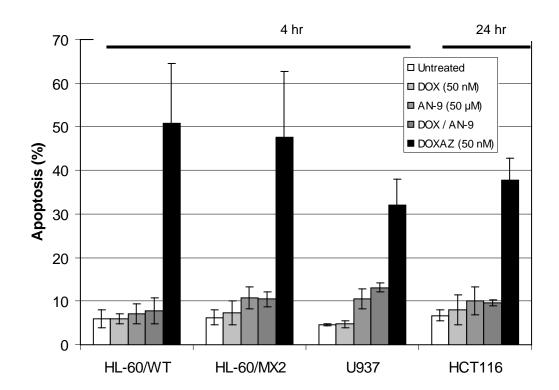


Figure 4.2. Doxazolidine is more cytotoxic than doxorubicin and the combination of doxorubicin/AN-9 in leukemic and colon cancer cells.

HL-60/WT, HL-60/MX2, and U937 leukemic cells were treated with doxazolidine (50 nM), doxorubicin (50 nM), and the combination of doxorubicin (50 nM) with AN-9 (50 μ M) for 4 hr, while HCT116 colon cancer cells were treated for 24 hr. Following treatment, the percentage of apoptotic cells was determined by sub-G1 FACS analysis. Error bars represent the standard error of the mean from three independent experiments.

releasing prodrug combinations, as well as barminomycin treatment (see Figures 3.8 and 3.19A). The same cell model was used to determine if Bcl-2 overexpression also confers resistance to doxazolidine. Doxazolidine induces a dose-dependent increase in apoptosis in HL-60/Puro control cells with high levels of DNA fragmentation (sub-G1 assay; Figure 4.3A) and caspase-3 activation (Figure 4.3B) evident after 4 hr treatment with 50 nM doxazolidine. In Bcl-2 overexpressing HL-60 cells on the other hand, no major increase in either sub-G1 apoptosis (Figure 4.3A) or caspase-3 activation (Figure 4.3B) was observed, even with a 10-fold higher concentration of doxazolidine (500 nM). These results highlight that high levels of Bcl-2 inhibit the induction of apoptosis, thus rendering HL-60 cells resistant to doxazolidine treatment, at least in the short term of 4 hr.

The use of the Bcl-2 inhibitor ABT-737 was shown in the previous chapter to overcome resistance to doxorubicin/formaldehyde-releasing prodrug combinations as well as barminomycin, resulting in high levels of apoptosis (see Figures 3.10 and 3.19B). As shown in Figure 4.4, the addition of 2.5 nM ABT-737, but not the enantiomer, synergistically increased the level of cell kill induced by doxazolidine (20 nM) in HL-60/Puro cells. This indicates that endogenous levels of Bcl-2 in HL-60/Puro cells imparted some degree of apoptosis inhibition which was overcome in the presence of ABT-737. The synergy of ABT-737 with doxazolidine is much more pronounced in HL-60/Bcl2 cells where the cells were completely resistant to doxazolidine, and the addition of ABT-737 (but not the enantiomer) overcame this resistance, inducing high levels of apoptosis (> 50%). A 10-fold higher concentration of ABT-737 (25 nM) was used to achieve this synergistic cell kill in HL-60/Bcl2 cells due to the greater number of Bcl-2 targets in these cells relative to the control HL-60/Puro cells. These results indicate that as seen with doxorubicin/formaldehydereleasing prodrug combinations in the previous chapter, low nanomolar concentrations of ABT-737 can effectively enhance the efficacy of doxazolidine in Bcl-2 overexpressing cancer cells.

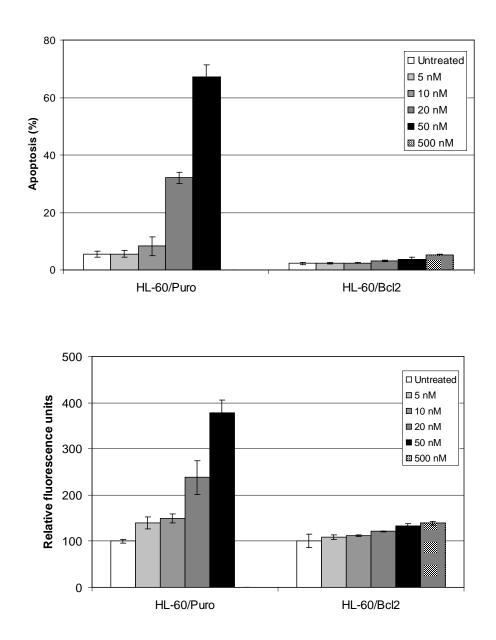


Figure 4.3. Bcl-2 overexpression confers resistance to 4 hr doxazolidine treatment in HL-60 cells.

HL-60/Puro and HL-60/Bcl2 cells were treated with doxazolidine (5-500 nM) for 4 hr before being subjected to the sub-G1 DNA fragmentation assay (A), or the caspase-3 activation assay (B). For the caspase-3 activation assay the fluorescence intensity for each sample was recorded and standardized to the cell control sample which was given a value of 100 fluorescence units. Error bars represent the standard error of the mean from three independent experiments.

Α

В

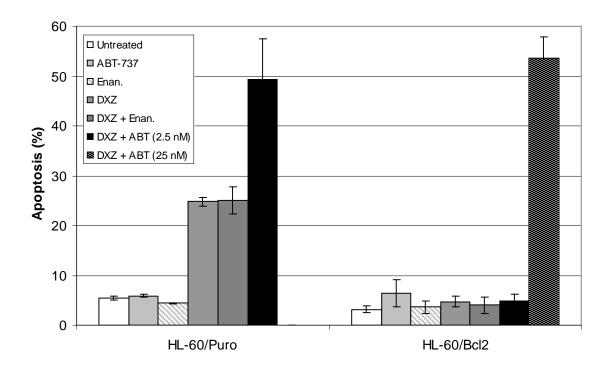


Figure 4.4. ABT-737 is synergistic with doxazolidine and overcomes Bcl-2 mediated resistance in HL-60 cells.

HL-60/Puro and HL-60/Bcl2 cells were treated with ABT-737, the ABT-737 enantiomer (2.5 nM in HL-60/Puro cells and either 2.5 or 25 nM in HL-60/Bcl2 cells), doxoazolidine (20 nM), and the combinations listed for 4 hr. The percentage of apoptotic cells was determined by sub-G1 FACS analysis. Error bars represent the standard error of the mean from three independent experiments.

4.2.3 Bcl-2 overexpressing HL-60 cells become sensitive to doxazolidine treatment over time

Based on the results shown in Figure 4.2 and from previous studies (Post *et al.*, 2005; Kalet *et al.*, 2007), it is evident that doxazolidine is able to induce apoptosis much more effectively and more rapidly than doxorubicin and the combination of doxorubicin with formaldehydereleasing prodrugs such as AN-9. To determine if doxazolidine displayed greater effectiveness over longer term treatments, a 48 hr growth inhibition assay was employed. When the IC₅₀ values were compared in HL-60/Puro control cells (Table 4.1), it was observed that doxazolidine was more effective than doxorubicin/AN-9, which in turn was more effective than doxorubicin as a single agent. The data shows that doxazolidine was approximately 10-fold more effective in inhibiting the growth of HL-60/Puro cells than doxorubicin/AN-9, and approximately 14-fold more effective than doxorubicin. These results are not surprising considering that doxazolidine is able to form DNA adducts more efficiently than the combination of doxorubicin/AN-9 which requires more steps for DNA adduct formation to occur. Furthermore, the main mechanism of action of doxorubicin as a single agent is the formation of less cytotoxic topoisomerase-II mediated DNA breaks, and as such the IC₅₀ value of doxorubicin was much greater than that observed for doxazolidine.

The growth inhibition experiments were also performed in HL-60/Bcl2 cells (Table 4.1). As may be expected, Bcl-2 overexpression resulted in higher IC₅₀ values for both doxorubicin (greater than 2-fold; representative dose-dependence graphs shown in Figure 4.5A), and to a lesser extent, doxorubicin/AN-9 treatments, compared to the control cell line. However, the IC₅₀ value obtained in HL-60/Bcl2 cells for doxazolidine did not differ from that observed in HL-60/Puro control cells (representative dose-dependence graphs shown in Figure 4.5B), indicating that Bcl-2 overexpression did not affect the sensitivity of HL-60 cells to the growth inhibitory effects induced by doxazolidine in this 48 hr assay. In HL-60/Bcl2 cells, doxazolidine was approximately 18-fold and 41-fold more effective in growth inhibition compared to doxorubicin/AN-9 and doxorubicin respectively.

Following the findings of the growth inhibition assay, the sub-G1 apoptosis assay was used to determine if the Bcl-2 overexpressing HL-60 cells became increasingly sensitive to

	IC ₅₀ (nM)		
Cell line	Doxazolidine	DOX / AN-9 (1:50)	Doxorubicin
HL-60/Puro	6.9 ± 0.6	74 ± 7	100 ± 6
HL-60/Bcl2	5.6 ± 0.7	109 ± 7	247 ± 21

Table 4.1. Growth inhibition data for HL-60/Puro and HL-60/Bcl2 cells treated with doxazolidine, doxorubicin, and the combination of doxorubicin and AN-9.

Error represents the standard error of the mean from three independent experiments.

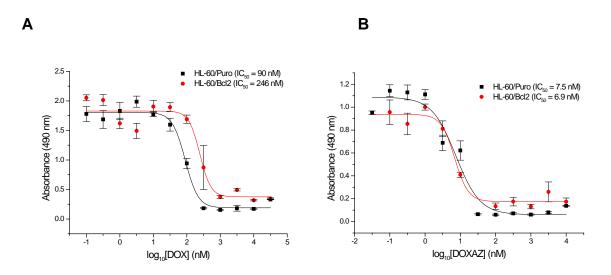


Figure 4.5. Representative dose-dependence graphs for HL-60/Puro and HL-60/Bcl2 cells treated with doxazolidine and doxorubicin.

HL-60/Puro and HL-60/Bcl2 cells were treated with various concentrations of (A) doxorubicin and (B) doxazolidine for 48 hr, and IC_{50} values determined via the MTS growth inhibition assay. Error bars represent the standard error of the mean of quadruplicate samples. These graphs are representative of three independent experiments.

doxazolidine over longer treatment times. As illustrated in Figure 4.6, the resistance of HL-60/Bcl2 cells to doxazolidine, which was evident after 4 hr treatment (see Figure 4.3), was gradually overcome, with approximately 40% apoptosis observed after 36 hr treatment with 20 nM doxazolidine. Doxorubicin, at the same concentration did not induce apoptosis over time, indicating that the contribution of topoisomerase-II mediated poisoning effects are negligible in the mechanism of action of doxazolidine at the time points tested. These results indicate that with longer treatment times of 18 hr or more, Bcl-2 overexpression is no longer a major resistance factor to doxazolidine treatment in HL-60 cells. To determine if Bcl-2 (or Bcl-w or Bcl-xL) still imparts any resistance to doxazolidine after 24 hr treatment, the Bcl-2 inhibitor ABT-737 was used in combination with doxazolidine. The concentration of ABT-737 used (25 nM) was the same as that used for the short-term 4 hr treatments where the inhibitor greatly increased doxazolidine-induced apoptosis in Bcl-2 overexpressing HL-60 cells (see Figure 4.4). After 24 hr treatment, doxazolidine induced approximately 20% apoptosis in HL-60/Bcl2 cells, however, in the presence of ABT-737, the level of apoptosis induced was increased (Figure 4.7). This suggests that while Bcl-2 no longer imparts complete resistance to doxazolidine over longer treatment times (≥ 18 hr), anti-apoptotic proteins still impose some degree of apoptotic resistance which is overcome by ABT-737.

4.2.4 The increase in sensitivity of Bcl-2 overexpressing HL-60 cells to doxazolidine appears to be mediated by apoptosis and not other forms of cell death

The increase in the population of sub-G1 cells and hence DNA fragmentation over time in response to doxazolidine treatment suggests that cell kill is mediated by classical apoptosis, however, the contribution of other forms of cell death cannot be ruled out. Since necrotic cells may also undergo DNA fragmentation (Fairbairn and O'Neill, 1995; Didenko *et al.*, 2003), the sub-G1 assay is not entirely specific for apoptosis, and as such the pan-caspase inhibitor Z-VAD-fmk was used to determine if doxazolidine mediated cell death in HL-60/Bcl2 cells is due to caspase-dependent apoptosis. HL-60/Puro and HL-60/Bcl2 cells were pre-treated with 30 μ M Z-VAD-fmk for 1 hr before being treated with doxazolidine (20 nM) for 4 hr and 24 hr respectively (Figure 4.8). In both cell lines at the concentration and

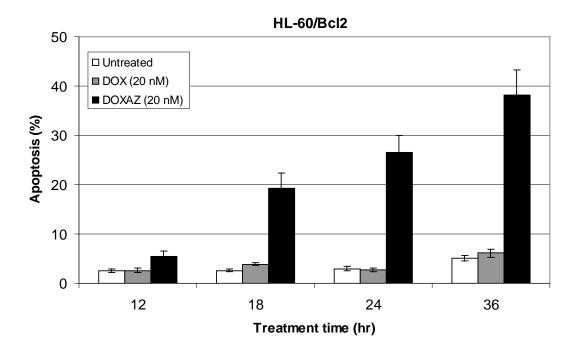


Figure 4.6. Bcl-2 overexpressing HL-60 cells become increasingly sensitive to doxazolidine over time.

HL-60/Bcl2 cells were treated with doxorubicin and doxazolidine (20 nM) for 12-36 hr, and the percentage of apoptotic cells following each treatment was determined by sub-G1 FACS analysis. Error bars represent the standard error of the mean from three independent experiments.

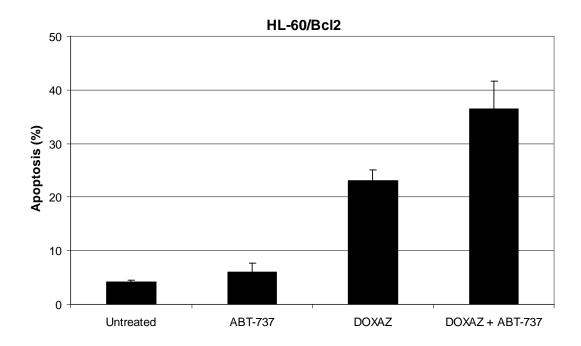


Figure 4.7. ABT-737 increases doxazolidine-induced apoptosis in HL-60/Bcl2 cells after 24 hr treatment.

HL-60/Bcl2 cells were treated with ABT-737 (25 nM), doxazolidine (20 nM), or the combination of both agents for 24 hr. The percentage of apoptotic cells was determined by sub-G1 FACS analysis. Error bars represent the standard error of the mean from three independent experiments.

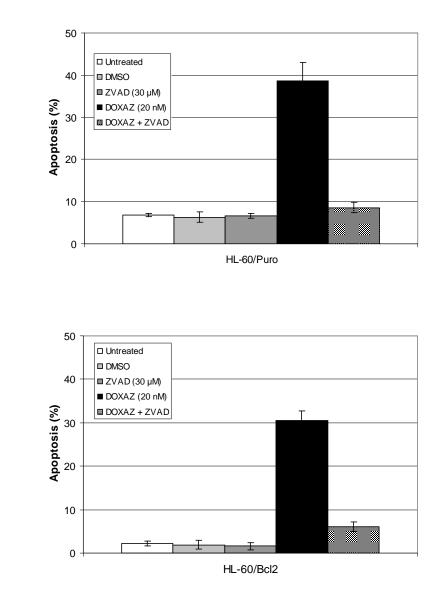


Figure 4.8. Cell death induced by doxazolidine in HL-60 cells is caspase-dependent.

HL-60/Puro (A) and HL-60/Bcl2 (B) cells were pre-treated with 30 μ M Z-VAD-fmk pancaspase inhibitor for 1 hr before being treated with doxazolidine (20 nM) for 4 hr and 24 hr respectively. The percentage of sub-G1 apoptotic cells was determined by FACS analysis. Error bars represent the standard error of the mean from three independent experiments.

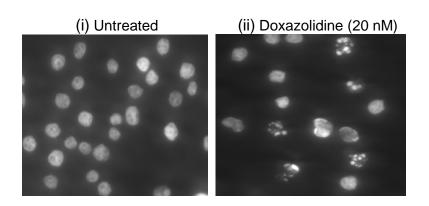
В

Α

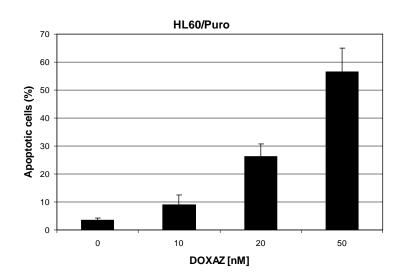
treatment times used, Z-VAD-fmk alone did not induce cell kill, however, the addition of Z-VAD-fmk reduced the levels of cell kill induced by doxazolidine to background levels in both cell lines. This indicates that both short-term (HL-60/Puro) and longer-term (HL-60/Bcl2) doxazolidine-induced cell death appears to be mediated by caspase-dependent apoptosis.

Next, the nuclear morphology of HL-60 cells treated with doxazolidine was examined via microscopic analysis to determine if the cells were displaying characteristics typical of classical apoptosis, or other forms of cell death such as mitotic catastrophe. In the case of classical apoptosis, cells display chromatin condensation, nuclear fragmentation, and the formation of apoptotic bodies (Saraste and Pulkki, 2000; Ziegler and Groscurth, 2004), while mitotic catastrophe which is described as a form of cell death caused by aberrant mitosis, typically results in large cells with multiple nuclei (Castedo *et al.*, 2004; Vakifahmetoglu *et al.*, 2008). Mitotic catastrophe can result in cell death by both caspase-dependent and independent mechanisms (Mansilla *et al.*, 2006), and is viewed as a precursor stage to eventual cell death by either apoptosis or necrosis (Vakifahmetoglu *et al.*, 2008). Mitotic catastrophe has been observed in cancer cells in response to DNA damaging agents including doxorubicin/AN-9 when the G_2/M cell cycle checkpoint was abrogated (see Figure 2.2 for a visual example of cancer cells undergoing mitotic catastrophe; Forrest *et al.*, 2012).

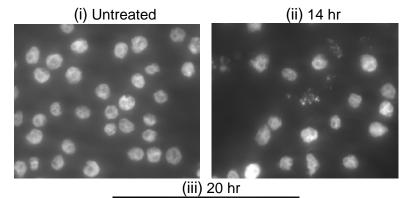
When the nuclear morphology of HL-60/Puro cells was analyzed in response to short-term 4 hr doxazolidine treatments, as seen in Figure 4.9A, the treated cells displayed chromatin condensation and nuclear fragmentation typical of apoptosis. As seen in Figure 4.9B a dose-dependent increase in the number of apoptotic cells (cells displaying chromatin condensation and/or nuclear fragmentation) was observed which is consistent with the results of both sub-G1 (see Figure 4.3A) and caspase-3 activation (see Figure 4.3B) assays. No visual evidence of mitotic catastrophe was observed for any of the concentrations of doxazolidine tested in HL-60/Puro cells. For HL-60/Bcl2 cells a time course was performed to observe the nuclear morphology of the cells at different doxazolidine treatment times. As shown in the sample images (Figure 4.9C) at both 14 hr and 20 hr treatment times, cells were displaying chromatin condensation and nuclear fragmentation typical of apoptosis, and the percentage of these apoptotic cells increased with time (Figure 4.9D). As seen with the short-term

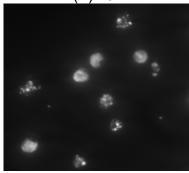


Α



С





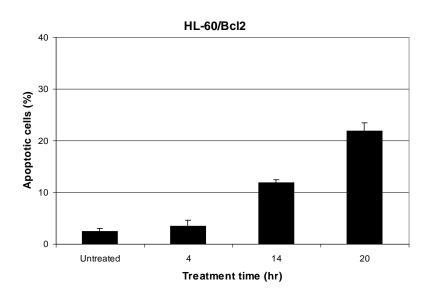


Figure 4.9. HL-60 cells display apoptotic morphology in response to short-term and long-term doxazolidine treatment.

HL-60/Puro cells were treated with doxazolidine (10-50 nM) for 4 hr (A-B), and HL-60/Bcl2 cells were treated with 20 nM doxazolidine for 14 and 20 hr (C-D). Following treatment, cells were stained with Hoechst nuclear stain and analysed by fluorescence microscopy. Several images of each sample were taken and representative images of HL-60/Puro and HL-60/Bcl2 cells are shown in (A) and (C) respectively. Cells displaying clear chromatin condensation and/or nuclear fragmentation were counted as apoptotic and the percentage of apoptotic cells was determined for HL-60/Puro (B) and HL-60/Bcl2 (D) cells. Error bars represent the standard error of the mean from three independent experiments.

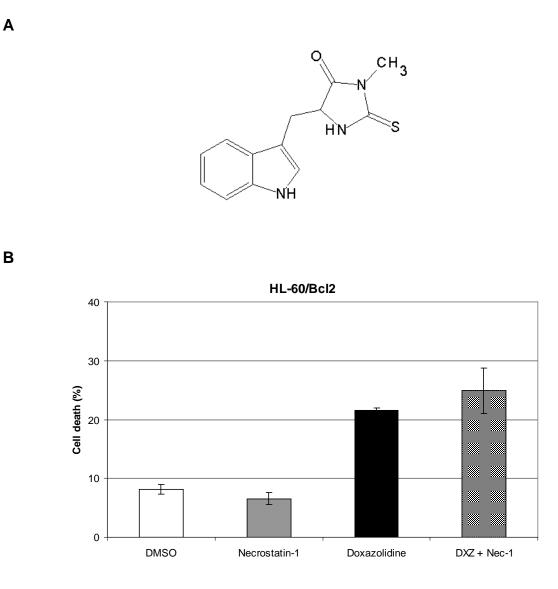
D

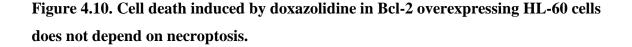
treatments in HL-60/Puro cells, no evidence of mitotic catastrophe was apparent, indicating that even at longer treatment times where HL-60/Bcl2 cells become sensitive to doxazolidine, there appears to be no contribution of mitotic catastrophe to eventual cell death.

Another form of cell death termed necroptosis was investigated as a possible mechanism contributing to doxazolidine induced cell kill in Bcl-2 overexpressing HL-60 cells. Necroptosis is considered to be a caspase-independent, programmed form of necrosis that depends on the serine/threonine kinase activity of RIP1 (receptor-interacting protein 1) (Galluzzi and Kroemer, 2008; Rosenbaum et al., 2010), and results in cell morphology similar to that of necrosis (Degterev et al., 2005). Necroptosis has been shown to occur in response to DNA damaging agents (Cabon et al., 2012), and has been observed in HL-60 cells previously (Han et al., 2009). The propidium iodide cell viability assay was used to demonstrate if necrostatin-1 (Figure 4.10A), which inhibits the RIP1 kinase and subsequent necroptosis (Degterev et al., 2005; Han et al., 2009), has any affect on cell death induced by doxazolidine in HL-60/Bcl2 cells. As demonstrated in Figure 4.10B, doxazolidine induced approximately 20% cell death in HL-60/Bcl2 cells after 24 hr treatment, and this cell death was not reduced by pre-treatment with an inhibitory concentration of necrostatin-1 (which was non-cytotoxic as a single agent at the concentration used) (Degterev et al., 2005). This suggests that necroptosis, as with mitotic catastrophe, does not contribute to cell death induced by doxazolidine in Bcl-2 overexpressing HL-60 cells over longer treatment times (24 hr).

4.2.5 Bcl-2 mediated resistance is also overcome in response to longer-term doxorubicin and doxorubicin/AN-9 treatments

The results from this study have demonstrated that Bcl-2 mediated resistance to doxazolidine in HL-60 cells is short-lived, with the cells becoming increasingly sensitive over longer treatment times. Based on these findings, the question was asked, is this effect of overcoming Bcl-2 mediated resistance specific to doxazolidine treatment or is this a more general effect observed in response to DNA adduct forming treatments or DNA damaging agents? The DNA adduct forming combination treatment of doxorubicin/AN-9 (1:50) was used to





HL-60/Bcl2 cells were pre-treated with 50 μ M necrostatin-1 (structure shown in A) for 1 hr before being treated with doxazolidine (20 nM) for 24 hr (B). Cell viability was assessed by propidium iodine staining where the percentage of dead cells was determined after setting up appropriate gates during FACS analysis. Error bars represent the standard error of the mean from three independent experiments.

181

determine if a similar short-lived Bcl-2 resistance effect was seen. The results presented previously (Chapter 3, Figure 3.8) showed that HL-60/Bcl2 cells were completely resistant to the combination treatment of doxorubicin/AN-9 up to 8 hr treatment time, while control HL-60/Puro cells were highly sensitive at this time point. Longer treatment times were not investigated in the previous chapter due to the ability of the Bcl-2 inhibitor, ABT-737, to effectively overcome this resistance after just 6 hr treatment. The results shown in Figure 4.11 indicate that after 12 hr treatment with doxorubicin/AN-9, the Bcl-2 overexpressing HL-60 cells were still heavily resistant to the treatment, with less than 10% cell kill observed. However, after 18 hr treatment a higher level of synergistic cell kill was observed in the HL-60/Bcl2 cells in response to doxorubicin/AN-9 treatment. This increase in cell kill over time suggests that as with doxazolidine, Bcl-2 overexpression provides only short-term resistance to DNA adduct forming treatments.

To determine if this short-lived resistance to Bcl-2 is a phenomenon specific to anthracycline-DNA adduct forming treatments, doxorubicin as a single agent was used. In the absence of exogenous formaldehyde, doxorubicin functions mainly as a topoisomerase-II poison, leading to double-stranded DNA breaks (Tewey et al., 1984), therefore inducing DNA damage by another mechanism. As shown in Figure 4.12A, in HL-60/Puro control cells, doxorubicin (500 nM) as a single agent induced approximately 20% apoptosis after 18 hr treatment with greater levels of apoptosis observed after 24 hr. At the same time point of 18 hr, HL-60/Bcl2 cells were completely resistant to doxorubicin treatment (Figure 4.12B). However, at later time points of 24 and 36 hr, doxorubicin induced apoptosis in HL-60/Bcl2 cells, indicating that the Bcl-2 mediated resistance was short-lived. This delay in sensitivity to doxorubicin in HL-60/Bcl2 cells relative to HL-60/Puro cells is illustrated in Figure 4.12C. To determine if this increase in cell kill in HL-60/Bcl2 cells over time is caspase-dependent, the pan-caspase inhibitor Z-VAD-fmk was used. As shown in Figure 4.12D, pre-treatment of the cells with the caspase inhibitor reduced the level of sub-G1 apoptosis to near background levels, indicating that the ability of doxorubicin, as with doxazolidine, to overcome Bcl-2 mediated resistance is caspase-dependent. Considering that doxorubicin as a single agent functions via a different mechanism than doxazolidine and doxorubicin/AN-9, these results suggest that short-lived Bcl-2 mediated resistance in HL-60 cells may be observed in response to various DNA damaging agents.

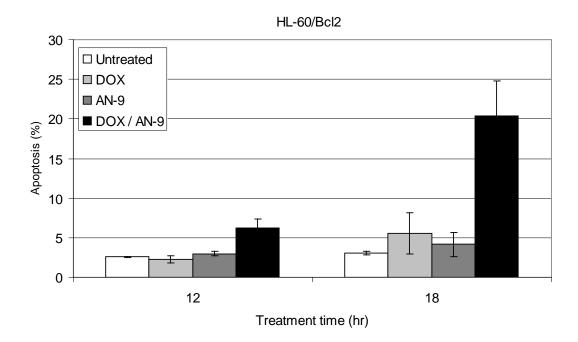
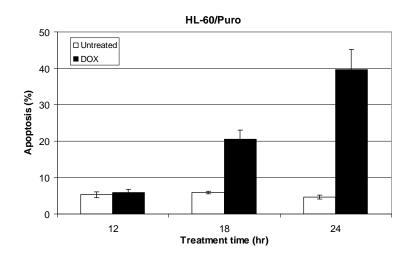
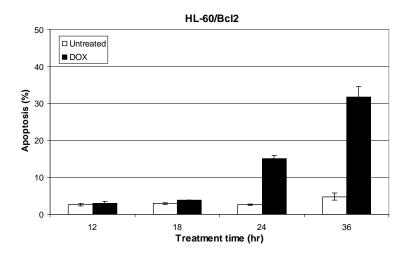


Figure 4.11. Bcl-2 mediated resistance to doxorubicin/AN-9 is overcome over longer treatment time.

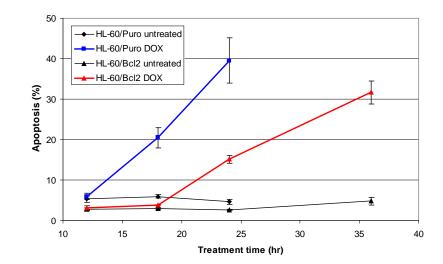
HL-60/Bcl2 cells were treated with doxorubicin (500 nM), AN-9 (25 μ M), or the combination of both drugs for 12 and 18 hr. Following treatment, cells were subjected to sub-G1 FACS analysis to determine the percentage of apoptosis. Error bars represent the standard error of the mean from three independent experiments.



В



С



Α

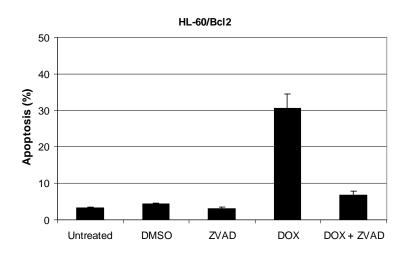


Figure 4.12. Bcl-2 overexpression delays doxorubicin-mediated cell kill in HL-60 cells.

HL-60/Puro (A) and HL-60/Bcl2 cells (B) were treated with doxorubicin (500 nM) for 12-24 and 12-36 hr respectively. Following treatment, cells were subjected to sub-G1 FACS analysis to determine the percentage of apoptosis. The results from (A) and (B) are presented as a line graph in (C). To determine if the cell kill induced by doxorubicin at 36 hr is caspase-dependent, (D) HL-60/Bcl2 cells were pre-treated with 30 μ M of the Z-VAD-fmk pancaspase inhibitor for 1 hr before being treated with doxorubicin (500 nM) for 36 hr, and the percentage of apoptosis determined by sub-G1 FACS analysis. Error bars for (A-C) represent the standard error of the mean from three independent experiments, and the error bars for (D) represent the standard deviation from two independent experiments.

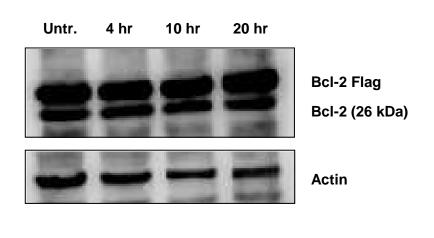
D

4.2.6 Investigating the mechanism/s responsible for overcoming Bcl-2 mediated resistance in HL-60 cells

The evidence presented in this study demonstrates that apoptosis is the main form of cell death involved in overcoming Bcl-2 mediated resistance to doxazolidine in HL-60 cells. Therefore, it is presumed that the mechanism responsible for overcoming this resistance leads to the induction of apoptosis over time, and most likely involves the Bcl-2 protein family members. One possible explanation may be that the levels of anti-apoptotic proteins are decreasing over time in response to doxazolidine treatment, thus reducing interactions with pro-apoptotic Bax and Bak. This in turn would trigger the release of Bax and Bak allowing apoptosis to proceed. However, as illustrated via immunoblotting in Figure 4.13A, Bcl-2 protein levels did not change over time in HL-60/Bcl2 cells treated with doxazolidine. The levels of Mcl-1, another anti-apoptotic protein known to have a short half-life (Warr and Shore, 2008), also did not change over time (Figure 4.13B). Although the levels of all anti-apoptotic proteins were not investigated, these immunoblotting results suggest that in HL-60 cells, levels of Bcl-2 and Mcl-1 remain relatively constant over time following doxazolidine treatment.

4.2.6.1 Is apoptosis induced by Rad9/Bcl-2 interactions?

The next potential mechanism in overcoming Bcl-2 mediated resistance that was investigated was the involvement of the protein Rad9. Rad9 is a cell cycle checkpoint control protein which regulates multiple cellular processes that influence genomic integrity in response to DNA damage (Lieberman, 2006; Lieberman *et al.*, 2011). These processes include cell cycle arrest, DNA repair, and apoptosis. Many of the functions of Rad9 are carried out as part of a heterotrimeric complex called the 9-1-1 complex (see Figure 4.16; Hang and Lieberman, 2000; Parrilla-Castellar *et al.*, 2004). However, in response to DNA damage, Rad9 also has been shown to translocate to the cytosol and interact with Bcl-2 and Bcl-xL via a BH3-like domain, thus triggering the release of Bax and Bak and the apoptotic cascade (Komatsu *et al.*, 2000) (see Figure 4.17). It has been shown previously that DNA damage caused by doxorubicin-DNA adduct formation leads to the recruitment of ATR (Forrest, 2010; Forrest



В

Α

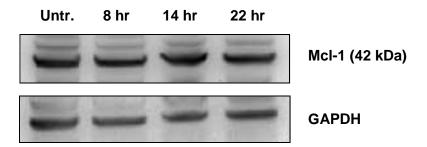


Figure 4.13. Expression levels of the anti-apoptotic proteins Bcl-2 and Mcl-1 remain constant in response to doxazolidine treatment.

HL-60/Bcl2 cells were treated with doxazolidine (20 nM) for the indicated times and immunoblotting was performed to determine the expression levels of (A) Bcl-2 and (B) Mcl-1 protein at each time point relative to untreated cells. Actin was used as a loading control for (A) and GAPDH was used as a loading control for (B). These blots are representative of three independent experiments yielding similar results.

et al., 2012), and another study has shown that the activation of ATR can lead to apoptosis induction by Rad9 (Ishii *et al.*, 2005). Therefore, it was reasoned that in response to DNA damage (and ATR recruitment) induced by doxazolidine treatment, Rad9 may be playing a role in inducing apoptosis over time in HL-60 cells.

We first investigated expression levels of Rad9. Since overexpression of Rad9 has been previously shown to induce apoptosis (Komatsu *et al.*, 2000), an increase in Rad9 protein levels over time in response to doxazolidine treatment may potentially be promoting apoptosis. However, as shown in Figure 4.14A, Rad9 levels remained relatively constant over time, indicating that doxazolidine treatment did not cause an increase in Rad9 expression.

If Rad9 does indeed play a role in inducing apoptosis it would be expected to interact with Bcl-2, as has been shown in previous studies (Komatsu et al., 2000; Ishii et al., 2005). Coimmunoprecipitation experiments were performed using anti-FLAG affinity gel beads (anti-FLAG antibody attached to agarose) which would be expected to bind to FLAG-tagged Bcl-2 protein expressed by the plasmid present in HL-60/Bcl2 cells. Therefore, if Rad9 was interacting with Bcl-2 it would be expected to be detected in the eluted (bound) fraction by Western blot analysis using an anti-Rad9 antibody. HL-60/Bcl2 cells were treated with doxazolidine (20 nM) for 12 and 24 hr and subjected to co-IP analysis. As shown in Figure 4.14B, following co-IP in both treated and untreated samples, the majority of Rad9 protein was detected in the unbound fractions, with a smaller amount remaining in the wash fractions. No bands were detected in the bound (eluted) fractions (despite the fact that the bound fractions had protein levels six times more concentrated than in the unbound fractions), indicating that Rad9 did not interact with the anti-FLAG affinity gel, and thus did not interact with Bcl-2. To confirm that the anti-FLAG affinity gel was able to bind to FLAG-tagged Bcl-2 protein, the PVDF membrane was also probed with anti-FLAG antibody. It can be seen that a band corresponding to the size of FLAG-tagged Bcl-2 (approximately 30 kDa) was detected in the bound fractions (with a smaller amount remaining in the bead fractions), but not in the unbound fractions of both untreated and treated samples. These co-IP results demonstrate that while FLAG-tagged Bcl-2 protein was able to interact with the anti-FLAG affinity gel as expected, Rad9 did not interact with Bcl-2. Therefore, the proposed mechanism that doxazolidine treatment overcomes Bcl-2 mediated

resistance in HL-60 cells over time via Rad9 induced apoptosis was not supported by the co-IP experiments.

4.2.6.2 Using mass spectrometry to identify Bcl-2 binding partners

Since the co-IP data failed to provide evidence for Rad9/Bcl2 interactions in response to doxazolidine treatment, mass spectrometry was used as a more sensitive means for identifying Bcl-2 binding partners that may be responsible for inducing apoptosis over time. The anti-FLAG co-IP experiments were repeated, except instead of detecting proteins by immunoprobing, the bound (eluted) fractions were subjected to mass spectrometry (see Section 2.11). The analysis was performed on both untreated and doxazolidine treated (20 nM, 24 hr; these treatment conditions were shown previously in Figure 4.6 to overcome resistance) HL-60/Bcl2 cell samples, and only the proteins that were identified exclusively in the treated samples, on both occasions the analysis was performed, with a probability match greater than 0.6 were listed in Table 4.2. A number of proteins (not listed) were detected in both untreated and treated samples, however, these proteins were excluded as they would not be expected to be implicated in overcoming Bcl-2 mediated resistance. Bcl-2 itself was detected in both untreated and treated samples, which is expected since the elution process of the anti-FLAG co-IP would release any FLAG-tagged proteins that have bound to the anti-FLAG affinity gel beads, including the FLAG-tagged Bcl-2 overexpressed in HL-60/Bcl2 cells. The mass spectrometry results revealed that five proteins were present in the bound fractions in response to doxazolidine treatment, and as such could be potential binding partners for Bcl-2 and play a role in overcoming resistance.

Of the five identified proteins, only Bim (Bcl2-like protein 11) is a Bcl-2 family member that has been characterized as a pro-apoptotic protein. Bim interacts with anti-apoptotic proteins including Bcl-2, thus releasing Bax and Bak from anti-apoptotic proteins, allowing Bax and Bak to trigger the apoptotic cascade (Puthalakath *et al.*, 1999; Chen *et al.*, 2005; Certo *et al.*, 2006). The only other protein identified by mass spectrometry that is able to interact with Bcl-2 family members (i.e. Bax) is nucleophosmin (Kerr *et al.*, 2007; Thompson *et al.*, 2008). The functions of the identified proteins and any potential roles that they may have in apoptosis will be discussed in Section 4.3.5.

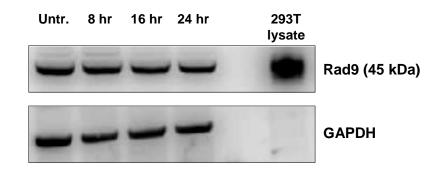
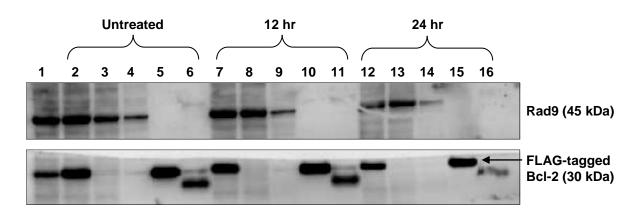


Figure 4.14. Rad9 expression does not increase nor does Rad9 interact with Bcl-2 in response to doxazolidine treatment in HL-60/Bcl2 cells.

HL-60/Bcl2 cells were treated with doxazolidine (20 nM) for the indicated times and subjected to either:

(A) Western analysis to determine the expression levels of Rad9. A lysate of human Rad9 transfected 293T cells was used as a positive control where Rad9 was detected at approximately 45 kDa. GAPDH was used as the loading control. This blot is representative of three independent experiments yielding similar results.



1 = HL-60/Bcl2 whole cell lysate 2/7/12 = Total input 3/8/13 = Unbound fraction 4/9/14 = Wash fraction 5/10/15 = Bound (eluted) fraction (6 x conc.) 6/11/16 = Bead fraction (6 x conc.)

Figure 4.14 (continued).

В

(B) Anti-FLAG co-IP analysis to determine if Rad9 is interacting with Bcl-2 in response to treatment over time. A lysate of untreated HL-60/Bcl2 cells was used as a positive control for both Rad9 and FLAG-tagged Bcl-2 proteins. Aliquots of samples corresponding to the total input, unbound fractions, wash fractions, bound (eluted) fractions, and bead fractions, were subjected to SDS-PAGE and Western transfer before the PVDF membrane was cut and probed with either anti-RAD9 or anti-FLAG antibodies. Two bands were observed after probing with anti-FLAG, the upper band corresponding to FLAG-tagged Bcl-2 (30 kDa), and the lower band only seen in the bead fractions almost certainly corresponding to the antibody light chains (25 kDa). Note that the aliquots used for SDS-PAGE corresponding to the unbound fractions and wash fractions were taken from volumes equivalent to that used for the total input (i.e. $300 \,\mu$ L), while the aliquots corresponding to the bound fractions and bead fractions are expected to be 6-fold more concentrated than in the other fractions. This blot is representative of three independent experiments yielding similar results.

Proteins Identified	Function	Interactions with Bcl-2 family members
Bcl2-like protein 11 (BIM)	Apoptosis induction	Bcl-2 and other anti-apoptotic proteins (Chen <i>et al.</i> , 2005; Certo <i>et a</i> l., 2006)
Nucleophosmin (B23 / numatrin)	Ribosome biogenesis Protein chaperoning Histone assembly Cell proliferation Apoptosis (pro and anti)	Bax (Kerr <i>et al</i> ., 2007; Thompson <i>et al</i> ., 2008)
Hornerin	Cornification	_
Thyroid hormone receptor- associated protein 3 (THRAP3 / TRAP150)	RNA processing and regulating RNA stability	_
U4/U6 small nuclear ribonucleoprotein Prp31 (PRPF31)	Pre-mRNA splicing	_

 Table 4.2. Potential Bcl-2 binding partners identified by mass spectrometry following doxazolidine treatment of HL-60/Bcl2 cells.

HL-60/Bcl2 cells were treated with doxazolidine (20 nM) for 24 hr and both treated and untreated samples were subjected to anti-FLAG co-IP as outlined in Section 2.10. The eluted (bound fractions) from the co-IP were used for mass spectrometry analysis as described in Section 2.11. The list of proteins identified in the samples was restricted to those having a probability match of greater than 0.6 and any obvious contaminating proteins such as keratins were excluded. This mass spectrometry analysis was performed on two independent experiments and only those proteins that were identified in both experiments were short-listed. Finally, any proteins that appeared in both untreated and treated samples were excluded so that only proteins identified exclusively in the treated samples were considered to be potential Bcl-2 binding partners in response to doxazolidine treatment. Note that Bcl-2 was identified in the bound fractions in both untreated and treated samples, which is expected since the elution process would release FLAG-tagged Bcl-2 (along with any binding partners) from the anti-FLAG affinity gel beads.

4.3 **DISCUSSION**

4.3.1 Doxazolidine induces rapid cell kill without the requirement of formaldehyde

Since it was discovered that doxorubicin is able to form cytotoxic DNA adducts in the presence of formaldehyde, there has been great interest in exploiting this mechanism of action by the addition of exogenous formaldehyde. While the use of formaldehyde-releasing prodrugs such as AN-9 have proven to be effective in increasing doxorubicin-DNA adduct formation and cytotoxicity in cancer cells, the development of doxorubicin conjugates that do not require exogenous formaldehyde to induce DNA adduct formation may prove to be even more efficacious as an anticancer treatment strategy. In this study, the doxorubicin-formaldehyde conjugate doxazolidine, which is the active metabolite of doxorubicin that is able to form DNA adducts, was investigated as a single agent.

Comparison of doxazolidine with doxorubicin/AN-9 and doxorubicin, revealed that low nanomolar levels of doxazolidine (50 nM) induced cell kill in leukemic and colon cancer cell lines, while the other drug treatments did not (Figure 4.2). High levels of cell kill were also observed in the topoisomerase-II reduced HL-60/MX2 cell line, which is consistent with previous findings and confirms that unlike doxorubicin, the mechanism of action of doxazolidine is primarily topoisomerase-II independent (Kalet *et al.*, 2007). Therefore, doxazolidine is able to form cytotoxic DNA adducts as a single agent and as such does not need the presence of formaldehyde-releasing prodrugs to switch its mechanism of action to DNA adduct formation.

The greater efficacy of doxazolidine compared to the doxorubicin/AN-9 combination was further supported by the IC₅₀ values in HL-60/Puro cells (Table 4.1), which demonstrate that doxazolidine is approximately 10-fold more effective in growth inhibition. Although both doxazolidine and the combination of doxorubicin/AN-9 both induce DNA adduct formation, the superiority of doxazolidine can be explained by the fact that it is able to perform this function more efficiently. In the case of doxorubicin combined with formaldehyde-releasing

prodrugs, DNA adduct formation is a multi-step process requiring the following steps to occur; 1) the interacalation of doxorubicin into DNA, 2) esterase-mediated hydrolysis of the prodrug to release formaldehyde, 3) the reaction of formaldehyde with doxorubicin to form a reactive Schiff base, and 4) the formation of a covalent aminal linkage with guanine to produce a drug-DNA monoadduct. Doxazolidine, on the other hand does not require additional formaldehyde to form DNA adducts, and as such, upon intercalation fewer steps are required for DNA adduct formation, making the whole process more efficient. For this reason, doxazolidine is able to form DNA adducts at a lower concentration and more rapidly than the combination of doxorubicin and AN-9, which are favourable attributes in a clinical setting.

Despite displaying greater *in vitro* efficacy against cancer cells compared to doxorubicin and doxorubicin/AN-9, the clinical potential of doxazolidine is limited by its hydrolytic instability, short half-life, and non-specific toxicity which would lead to side-effects. As such, targeting methods need to be developed to make doxazolidine (and other doxorubicin-formaldehyde conjugates) more stable and more amenable to clinical use.

4.3.2 Targeting doxorubicin-formaldehyde conjugates

In order to overcome the limitations associated with doxazolidine, there has been an effort to design more stable DNA adduct forming conjugates, and prodrugs that release active doxazolidine specifically at tumour sites.

The conjugate doxsaliform was developed from the condensation of doxorubicin, formaldehyde and salicylamide, which hydrolyses to yield an active doxorubicinformaldehyde Schiff base (Cogan *et al.*, 2004). Doxsaliform was shown to be more hydrolytically stable than doxazolidine with a half-life of 57 minutes under physiological conditions (Burke and Koch, 2004; Cogan *et al.*, 2004), although the drug was less potent at inhibiting cancer cell growth compared to doxazolidine (Post *et al.*, 2005). The salicylamide fragment has been modified to permit the attachment of tumour targeting moieties, including tamoxifen (TAM) which is able to bind to the estrogen receptor commonly overexpressed on breast cancer cells. The lead compound DOXSAL-TEG-TAM (TEG; triethylene glycol) was shown to be more cytotoxic to estrogen receptor positive breast cancer cells compared to both doxorubicin and untargeted doxsaliform (Burke and Koch, 2004; Burkhart *et al.*, 2004).

In the search for even more stable and tumour targetable prodrugs of doxazolidine, Burkhart and colleagues (2006) synthesized doxazolidine carbamate prodrugs that are hydrolysed by carboxylesterases. The lead compound Pentyl-PABC-DOXAZ (Figure 4.15A; PPD; where PABC is a self-eliminating spacer used to reduce steric hinderance) was shown to be stable for up to 24 hr under various conditions including in human plasma (Barthel *et al.*, 2009), and displayed similar or better growth inhibition against cancer cells compared to doxorubicin (Burkhart et al., 2006). PPD also showed higher uptake and retention in doxorubicin-resistant breast cancer cells and displayed lower toxicity in rat cardiomyocytes compared to doxorubicin (Burkhart et al., 2006). In mouse models, PPD was shown to effectively inhibit the growth of hepatocellular carcinoma and NSCLC xenografts relative to untreated control mice (Barthel et al., 2009). In these mouse studies, while doxorubicin was shown to display a greater antitumour effect compared to PPD, there was much less evidence of cardiotoxicity and nephrotoxicity associated with PPD treatment. The carboxylesterase 2 enzyme (CES2) was identified to be the main enzyme responsible for cleavage and activation of PPD (Barthel *et al.*, 2008), and although CES2 is expressed in cancer types including liver, pancreatic, colon, kidney, and thyroid cancers (Xu et al., 2002), with low expression in cardiomyocytes (Barthel et al., 2008), the enzyme is not considered to be a reliable marker for tumour tissue (Barthel *et al.*, 2012). Therefore, it is anticipated that PPD would only have a limited spectrum for therapy and as such second generation doxazolidine prodrugs were developed.

Recently, Barthel and colleagues (2012) developed stable doxazolidine prodrugs that become hydrolysed by proteases linked with cancer progression, triggering the release of active doxazolidine (Figure 4.15B). The lead compound GaFK-DOXAZ (containing N-acetyl glycine followed by the plasmin recognition sequence of D-alanine-L-phenylalanine-L-lysine) was shown to be cleaved by plasmin, as well as trypsin and cathepsin B. High levels of proteolytic activity are strongly correlated with tumour progression, especially in angiogenic and invasive tumour environments, with low levels observed in normal, static tissues (Koblinski *et al.*, 2000; Choong and Nadesapillai, 2003). In particular, high levels of

Α

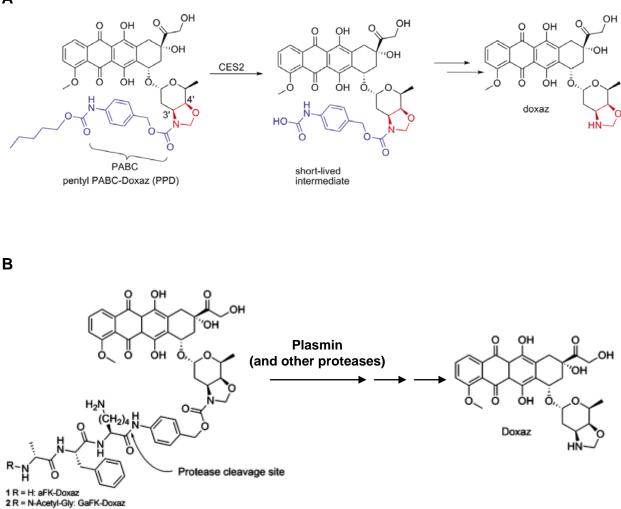


Figure 4.15. Tumour-targetable doxazolidine prodrugs.

Pentyl-PABC-DOXAZ (A) is activated primarily by the carboxyesterase 2 enzyme CES2 to yield a short-lived intermediate which rapidly releases active doxazolidine (Barthel *et al.*, 2009). Second generation prodrugs of doxazolidine were developed which can be activated by plasmin and other proteases including cathepsin B (B). The proteases cleave the prodrug to release an intermediate which spontaneously liberates active doxazolidine. Therefore, doxazolidine release is limited to regions of high proteolytic activity such as the microenvironments of angiogenic and invasive tumours (Barthel *et al.*, 2012).

plasmin pathway components are associated with poor cancer prognosis (Ulisse *et al.*, 2009). Therefore, it is expected that activation of GaFK-DOXAZ would occur preferentially in the tumour microenvironment. GaFK-DOXAZ was shown to be stable in human plasma and displayed poor membrane permeability, therefore limiting the uptake and likelihood of doxazolidine release within normal cells and consequently minimizing side-effects. GaFK-DOXAZ was shown to release doxazolidine and inhibit the growth of numerous cancer cell types when co-treated with proteases, thus providing promising data for further testing of this compound, or the development of other protease-activated prodrugs of doxazolidine.

Due to the low stability and high potency of doxazolidine in killing cancer cells, the further development of stable, targeted conjugates which can deliver doxazolidine specifically to tumours, such as PPD and GaFK-DOXAZ, is imperative to enhance the potential of doxazolidine to be considered for clinical use in the future.

4.3.3 Bcl-2 mediated resistance to doxazolidine treatment is short-lived

In the previous chapter, it was demonstrated that overexpression of Bcl-2 (HL-60/Bcl2 cells) conferred resistance to the DNA adduct forming treatments of doxorubicin/AN-9 and barminomycin, and that the Bcl-2 (Bcl-w and Bcl-xL) inhibitor ABT-737 overcame this resistance, resulting in high levels of cell kill. Likewise in this chapter, the overexpression of Bcl-2 rendered HL-60 cells completely resistant to doxazolidine treatment after 4 hr (Figure 4.3), which may affect the efficacy of this drug in cancer types associated with high levels of Bcl-2. However, the addition of the inhibitor ABT-737 resulted in high levels of synergistic cell kill in HL-60/Bcl2 cells (Figure 4.4), suggesting that in a clinical setting the use of ABT-737 (or ABT-263) may increase the therapeutic potential of not only doxorubicin/AN-9 but also doxazolidine treatments.

When longer treatment times were used it was discovered that the HL-60/Bcl2 cells became increasingly sensitive to doxazolidine treatment over time. Apoptosis data showed that in HL-60/Bcl2 cells, between 12-36 hr the levels of cell kill increased, indicating that the resistance mediated by Bcl-2 was gradually overcome (Figure 4.6). It may be suggested that

since doxazolidine has such a short-half live and hydrolyses to doxorubicin in minutes, that the cell kill may be attributed to doxorubicin-mediated topoisomerase-II poisoning to some extent. However, when HL-60/Bcl2 cells were treated with the same concentration of doxorubicin as doxazolidine, no increase in cell kill over time was observed, reflecting that the cell kill is exclusively due to DNA adduct formation. At the 24 hr treatment time point, ABT-737 was able to increase doxazolidine induced cell kill (Figure 4.7), reflecting that there is still some sort of constraint on cell death caused by Bcl-2 (or Bcl-w or Bcl-xL). The phenomenon of overcoming Bcl-2 resistance is most evident in the growth inhibition assay, where after 48 hr the Bcl-2 overexpressing and control HL-60 cells displayed the same IC₅₀ value (Table 4.1), indicating that unlike at the 24 hr time point, Bcl-2 is no longer imparting any resistance at this 48 hr treatment time point. When cells are faced with DNA damage, such as that induced by doxazolidine treatment, the DNA damage response pathways become activated. In this case it is presumed that the degree of DNA damage is too severe to trigger DNA repair, and as such the cell is forced to activate a cell death response.

Evidence indicated that the increase in sensitivity of HL-60/Bcl2 cells to doxazolidine treatment over time is attributed to the induction of classical apoptosis, rather than other forms of cell death. The pan-caspase inhibitor Z-VAD-fmk reduced the level of cells undergoing DNA fragmentation (in the sub-G1 assay) in response to long-term (24 hr) doxazolidine treatment in HL-60/Bcl2 cells to background levels (Figure 4.8B). This suggests that the DNA fragmentation induced in these cells is an effect of caspase-mediated apoptosis and not necrosis. The nuclear morphology of HL-60/Bcl2 cells in response to doxazolidine treatment also displayed clear nuclear condensation and fragmentation over time, typical to cells undergoing apoptosis (Figure 4.9). Also, no evidence of mitotic catastrophe was detected in the nuclear morphology assay, thus ruling out the possibility that mitotic catastrophe may be occurring as a precursor to apoptosis. Also, the inability of nectrostatin-1 to reduce doxazolidine-induced cell death in HL-60/Bcl2 cells suggests that necroptosis was not a contributing factor to overall cell death induction (Figure 4.10). Based on these results it is predicted that over time there is some sort of biochemical change occurring in the HL-60/Bcl2 cells which alleviates the block in cell death. Furthermore, it is likely that any change in HL-60/Bcl2 cells that is contributing to the increased sensitivity to doxazolidine over time, involves components of the apoptotic machinery, and not some other

form of cell death mechanism (the potential mechanisms involved in overcoming resistance are discussed in Section 4.3.5).

4.3.4 Short-lived Bcl-2 mediated resistance is not just limited to doxazolidine treatment

In addition to doxazolidine, HL-60/Bcl2 cells were also treated with the combination of doxorubicin/AN-9, and doxorubicin as a single agent, to determine if these treatments could also overcome Bcl-2 mediated resistance over time. As observed with doxazolidine treatment, the HL-60/Bcl2 cells were resistant to both doxorubicin/AN-9 (Figure 4.11) and doxorubicin treatment (Figure 4.12C) to a certain time point, after which the level of cell kill increased. In the case of doxorubicin, this increase in cell kill appeared to be mediated by caspase-dependent apoptosis, as pre-treatment with the caspase-inhibitor Z-VAD-fmk reduced sub-G1 DNA fragmentation to near background levels (Figure 4.12D). These findings indicate that overcoming Bcl-2 mediated resistance in HL-60/Bcl2 cells is not specific to just doxazolidine, but also occurs in response to other DNA adduct forming treatments like doxorubicin/AN-9, and other forms of DNA damage such as topoisomerase-II poisoning as induced by doxorubicin.

Comparison of the IC₅₀ values obtained from the 48 hr growth inhibition assay (Table 4.1) reveals that while for doxazolidine the IC₅₀ values are the same in both control and Bcl-2 overexpressing cells, indicating that Bcl-2 resistance is completely overcome, the IC₅₀ values for both doxorubicin/AN-9 and doxorubicin are both higher in HL-60/Bcl2 cells. This may be a reflection of the fact that doxazolidine is more potent that the other treatments (as seen in Figure 4.2), and therefore the mechanism/s responsible for overcoming Bcl-2 mediated resistance may be operating much earlier or to a greater extent in response to doxazolidine treatment. It is possible that over longer treatment times in the growth inhibition assay, or the use of more long-term assays such as colony-formation assays, Bcl-2 resistance may also be completely overcome in response to doxorubicin/AN-9 and doxorubicin treatments. Nevertheless, with all three drug treatments it appears that Bcl-2 is able to block apoptotic

cell death to a certain extent before the level of DNA damage becomes too great and the ultimate fate of the cell is switched to cell death.

This phenomenon of short-term Bcl-2 mediated resistance has also been previously reported in numerous studies in many cancer cell types using different drugs. Hoetelmans and colleagues (2003) showed that Bcl-2 overexpressing rat CC531 colon carcinoma cells treated with doxorubicin had a higher IC_{50} value after 24 hr, however, after a 5 day treatment there was no difference in the IC_{50} values in both Bcl-2 overexpressing and parental cell lines. Similarly, in MTLn3 rat mammary adenocarcinoma cells, Bcl-2 overexpression was unable to prevent the inhibition of colony formation in soft-agar following treatment with both doxorubicin and etoposide (Huigsloot et al., 2003). This delay in drug susceptibility in Bcl-2 overexpressing cancer cells was also seen HL-60 cells (Allouche et al., 1997; Liang et al., 2010). Bcl-2 overexpression in HL-60 cells was shown to provide resistance to short-term treatments with the anthracycline daunorubicin (Allouche et al., 1997), and the topoisomerase-II inhibitor B1 (Liang et al., 2010), but not to longer-term treatments. B1 was also shown to overcome Bcl-2 mediated resistance in other leukemic cell lines, U937 and K562 (Allouche et al., 1997). In these studies, the mechanism of cell death induced over time showed all the hallmarks of being classical apoptosis (Allouche et al., 1997; Liang et al., 2010). This is consistent with the findings from the present study which showed that longerterm treatment with doxazolidine induced hallmarks of classical apoptosis, with no evidence of other forms of cell death like necrosis, mitotic catastrophe or necroptosis being observed.

Short-term delays in the onset of cell death have also been observed in cancer cells overexpressing Bcl-xL, another anti-apoptotic protein. Neuroblastoma cells overexpressing Bcl-xL protein were shown to only provide short-term resistance to etoposide treatment but not longer-term protection (Dole *et al.*, 1995). The same study also demonstrated that Bcl-xL overexpression in neuroblastoma cells did provide a long-term survival advantage (up to 8 days) in response to treatment with the alkylating agents cisplatin and 4-hydroperoxy-cyclophosphamide (Dole *et al.*, 1995). Furthermore, Bcl-2 overexpression in HeLa cervical cancer cells did not protect against long-term clonogenic survival to doxorubicin or etoposide, but did protect against treatment with the antimetabolite 5-fluoro-2'-deoxyuridine (Elliott *et al.*, 1998). These studies indicate that whether anti-apoptotic proteins are able to protect cancer cells from apoptosis in the long-term depends on the type of damage induced

by the drug in question. It appears that anthracycline-DNA adduct forming treatments and topoisomerase-II poisons are able to overcome anti-apoptotic resistance, but other types of DNA damaging agents such as classical alkylating agents and antimetabolites may not. With so many Bcl-2 protein family members and possible interactions, it is likely that the mechanisms involved in overcoming anti-apoptotic resistance may vary depending on the particular drug and damage induced.

4.3.5 What is the mechanism responsible for overcoming Bcl-2 mediated resistance?

Based on the findings from the present study and previous studies (Allouche et al., 1997; Liang *et al.*, 2010), it is highly likely that any changes that occur over time to promote cell death and overcome Bcl-2 mediated resistance will involve the intrinsic apoptotic pathway and the Bcl-2 family of proteins. In the study by Liang and colleagues (2010) where the topoisomerase-II inhibitor B1 overcame resistance to Bcl-2 over time in HL-60/Bcl2 cells, it was shown that B1 treatment caused a down-regulation of the protein $14-3-3\sigma$ via MBD2 (a methyl-CpG-binding protein) mediated transcriptional silencing. The 14-3-3 σ protein interacts with Bad, keeping it in an inactive state, therefore a reduction of 14-3-3 σ levels would reduce these interactions with Bad, allowing Bad to dimerize with Bcl-2 and promote Bax release and apoptosis (Masters et al., 2001; Subramanian et al., 2001; Certo et al., 2006). The expression levels of 14-3-3 σ were not investigated in the present study, but the downregulation of this protein in response to doxazolidine treatment may need to be considered as a potential mechanism for promoting apoptosis in HL-60/Bcl2 cells. B1 treatment also caused a downregulation in Bcl-2 and an increase in Bax, thus increasing Bax:Bcl-2 ratios and favoring apoptosis induction (Liang et al., 2010). In the present study, the expression levels of the anti-apoptotic proteins Bcl-2 and Mcl-1 remained relatively constant in response to doxazolidine treatment (Figure 4.13). Although it is evident that the cells are dying via apoptosis over time, the increase in cell kill can not be attributed to a reduction in these anti-apoptotic proteins.

One potential mechanism for overcoming Bcl-2 mediated resistance that was investigated was the interaction between Rad9 and Bcl-2. While many of the functions of Rad9 are carried out as part of the heterotrimeric 9-1-1 complex (Figure 4.16), Rad9 has also been shown to translocate out of the nucleus and promote apoptosis in response to DNA damage (Komatsu *et al.*, 2000). Rad9 is able to interact with the anti-apoptotic proteins Bcl-2 and Bcl-xL via its BH3-like domain (Komatsu *et al.*, 2000; Ishii *et al.*, 2005), leading to the release of Bax and Bak and apoptosis induction. Rad9 overexpression has been demonstrated to induce cell kill (Komatsu *et al.*, 2000), however, in response to doxazolidine, Rad9 levels remained constant (Figure 4.14A).

Previous studies have proposed models of how Rad9 is able to function as a mediator of apoptosis (see Figure 4.17), including caspase-3 cleavage of Rad9 (Lee *et al.*, 2003), and ATR mediated downregulation of Frag1 protein (Ishii *et al.*, 2005). The ATR/Frag1 model was reasoned to potentially occur in response to doxazolidine treatment on the basis that it has been previously demonstrated that DNA damage caused by doxorubicin-DNA adduct formation leads to the activation of ATR (Forrest, 2010; Forrest *et al.*, 2012). However, co-IP analysis revealed that Rad9 was not interacting with Bcl-2 in response to doxazolidine treatment (Figure 4.14B). Furthermore, it should be noted that Rad9 was not detected by mass spectrometry as a potential Bcl-2 binding partner, thus ruling out the possibility that immunoblotting was not sensitive enough to detect any interaction between Rad9 and Bcl-2 in the anti-FLAG co-IP assay. Therefore, both co-IP and mass spectrometry failed to provide evidence for a Rad9/Bcl-2 interaction, thus negating the proposition that in response to doxazolidine treatment Rad9 may be playing a role in inducing apoptosis over time in HL-60 cells.

The involvement of Rad9 may depend on the type of DNA damage induced. Previous studies have shown that Rad9 was required for S-phase cell cycle activation in response to cytarabine and UV radiation, but was not required in response to ionizing radiation or the topoisomerase poisons etoposide and camptothecin (Roos-Mattjus *et al.*, 2003; Loegering *et al.*, 2004). A similar drug-specific involvement of Rad9 may be occurring in relation to its apoptotic role, and as such Rad9 may not be promoting apoptosis in response to DNA adduct forming treatments.

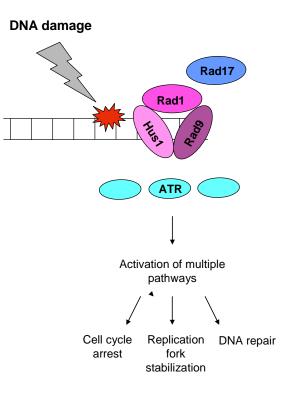


Figure 4.16. The 9-1-1 complex regulates multiple cellular pathways in response to DNA damage.

The 9-1-1 complex is a heterotrimeric complex composed of the cell cycle checkpoint control proteins Rad9, Rad1, and Hus1 (Hang and Lieberman, 2000; Parrilla-Castellar *et al.*, 2004). Another cell cycle checkpoint protein called Rad17, together with subunits of the replication factor C complex, are responsible for recruiting and loading the 9-1-1 complex onto chromatin (Bermudez *et al.*, 2003; Parrilla-Castellar *et al.*, 2004). Loading of the 9-1-1 complex occurs in response to various types of DNA damage caused by many different genotoxic stresses, including alkylating agents, ultraviolet and ionizing radiation (Parrilla-Castellar *et al.*, 2004). At the sites of DNA damage, the 9-1-1 complex is able to tether and activate a multitude of different proteins, including ATR, which subsequently can activate other proteins (such as Ckh1) and signaling pathways, leading to replication fork stabilization and cell cycle arrest (Zou *et al.*, 2002; Parrilla-Castellar *et al.*, 2004). In addition to activating DNA damage response pathways, the 9-1-1 complex also plays a direct role in DNA repair, including base-excision repair, HR, and mismatch repair (Parrilla-Castellar *et al.*, 2004; Helt *et al.*, 2005; Pandita *et al.*, 2006; Lieberman *et al.*, 2011).

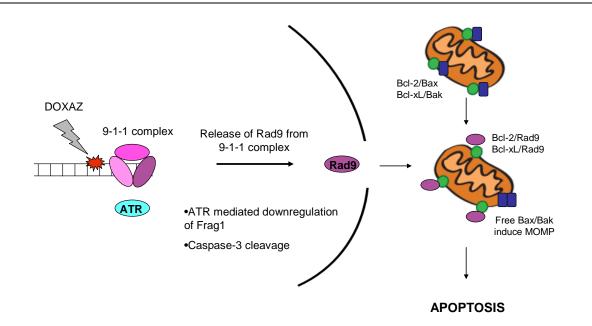


Figure 4.17. Model of Rad9-mediated apoptosis induction in response to doxazolidineinduced DNA damage.

As part of the 9-1-1 complex, Rad9 is able to perform multiple functions including cell cycle arrest and DNA repair, however, Rad9 is also able to promote apoptosis independently of the 9-1-1 complex. Rad9 is able to translocate to the mitochondrial membrane and promote apoptosis by disrupting the interactions between the anti-apoptotic proteins Bcl-2 and Bcl-xL with Bax and Bak. The released Bax and Bak are subsequently able to induce MOMP and trigger the apoptotic cascade. A couple of models have been proposed to explain how Rad9 is able to function as a mediator of apoptosis independently of the 9-1-1 complex. Rad9 has been shown to be cleaved by caspase-3 following the induction of DNA damage, causing the N-terminal portion of Rad9 containing the BH3-like domain to translocate to the cytosol and bind to Bcl-xL, triggering apoptosis (Lee et al., 2003). Another study identified the FRAG1 gene which codes for a protein involved in Rad9-related damage checkpoint control, possibly by interacting with and loading Rad9 onto damaged chromatin (Ishii et al., 2005). In response to replicative stress and the activation of ATR, it was shown that ATR causes the downregulation of Frag1 protein, leading to the release of Rad9 from the 9-1-1 complex. The released Rad9 then translocates into the cytosol where it interacts with Bcl-2, thus freeing Bax and triggering apoptosis (Ishii *et al.*, 2005). The ATR/Frag1 model is most likely to occur in response to doxazolidine treatment due to the documented involvement of ATR in the DNA damage response to DNA adducts (Forrest, 2010; Forrest et al., 2012).

The more sensitive technique of mass spectrometry was used to identify potential Bcl-2 binding partners in response to doxazolidine treatment that may be involved in promoting apoptosis and overcoming Bcl-2 mediated resistance. Five potential proteins were identified as listed in Table 4.2, and their functions are described below, along with any involvement in apoptotic responses.

The protein hornerin is expressed by epidermal cells in both regenerating and psoriatic skin, as well as healthy skin, and possibly plays a role in the process of cornification and contributes to the barrier function of healthy skin (Takaishi *et al.*, 2005; Wu *et al.*, 2009). There is no evidence that hornerin plays any role in apoptosis and it is almost certain that this protein is a contaminant from skin that coincidently was only detected in the doxazolidine treated samples.

The U4/U6 small nuclear ribonucleoprotein Prp31 (PRPF31) is a component of the spliceosome which processes pre-mRNA. Mutations in PRPF31 cause inefficient mRNA splicing and induce apoptosis in retinal cells, leading to the disease retinitis pigmentosa (Yuan *et al.*, 2005; Tanackovic *et al.*, 2011; Yin *et al.*, 2011). However the mechanism of apoptosis induction was not elucidated, and no previous evidence of any interaction with Bcl-2 or other anti-apoptotic members has been recorded.

Thyroid hormone receptor-associated protein 3 (THRAP3) plays a role in RNA splicing and degradation, therefore affecting RNA stability (Bracken *et al.*, 2008; Lee *et al.*, 2010). Recently, THRAP3 was shown to be phosphorylated in response to DNA damage, primarily by ATR, and is excluded from DNA damage sites (Beli *et al.*, 2012). THRAP3 shows high sequence similarity to BCLAF1 (Bcl-2 associated factor 1) which has a similar function to THRAP3 in RNA processing and they both form part of a complex called SNIP1 (Bracken *et al.*, 2008). Interestingly, BCLAF1 has been shown to interact with Bcl-2 and Bcl-xL and promote apoptosis *in vitro* (Kasof *et al.*, 1999), but not *in vivo* (McPherson *et al.*, 2009). The fact that THRAP3 shares sequence similarity with a known Bcl-2 interacting protein (BCLAF1), and the finding that THRAP3 may be involved in the DNA damage response, raises questions that THRAP3 may in some way be implicated in the apoptotic response to doxazolidine treatment over time, and that further experimental work is needed to provide an answer.

Nucleophosmin is a multi-functional protein involved in numerous cellular activities including ribosome biogenesis, chaperoning of proteins including histories, DNA repair processes, and cell proliferation (see reviews Ye, 2005; Grisendi et al., 2006). Its primary location is in the nucleolus, but it is able to shuttle to and from the cytoplasm where it interacts with a range of proteins. Nucleophosmin is frequently overexpressed in many solid cancers, but the gene coding for nucleophosmin is also frequently mutated, translocated, and deleted in various cancer types, indicating that nucleophosmin possesses both oncogenic and tumour-suppressing properties (Grisendi et al., 2006). Studies have also shown that nucleophosmin is implicated in apoptosis, both in inhibiting and promoting cell death. Nucleophosmin can prevent apoptosis indirectly a number of possible ways such as by increasing DNA repair (Wu et al., 2002), or by interacting with p53 and inhibiting its transcriptional activity (Maiguel et al., 2004). Studies have also shown that overexpression of nucleophosmin reduces apoptosis (Wu et al., 1999; Hsu and Yung, 2000), while downregulation induces apoptosis (Wu et al., 1999), suggesting that nucleophosmin acts in an antiapoptotic fashion. However, nucleophosmin has also been shown to directly associate with activated Bax, leading to its translocation to the mitochondria, suggesting a pro-apoptotic role for nucleophosmin (Kerr et al., 2007; Thompson et al., 2008). Nucleophosmin knockdown using shRNA was shown to reduce the levels of apoptosis induced by staurosporine in SH-SY5Y neuroblastoma cells (Kerr et al., 2007). Furthermore, the compound 2-(5-methyl-2-phenyl-1,3-thiazol-4-yl)ethanohydrazide was able to inhibit Bax/nucleophosmin interactions and subsequent apoptosis induction by UV treatment in HEK293 cells (Thompson et al., 2008). Bcl-2 was shown to disrupt the Bax/nucleophosmin interaction (Thompson et al., 2008), although no previous evidence has been shown that nucleophosmin interacts directly with Bcl-2. With its numerous functions and interactions it is possible that nucleophosmin may play roles in both promoting and inhibiting apoptosis depending on the treatment and the type of damage induced, and further studies are required to investigate the potential involvement of nucleophosmin in promoting apoptosis and overcoming Bcl-2 mediated resistance in response to doxazolidine treatment.

Of the five proteins identified by mass spectrometry, only Bim is confirmed as a proapoptotic protein, and possesses a BH3 domain capable of interacting with Bcl-2 (Puthalakath *et al.*, 1999; Chen *et al.*, 2005; Certo *et al.*, 2006). Upon apoptotic stimuli (in this case doxazolidine induced DNA adduct formation), Bim becomes activated and can potentially interact with all five major anti-apoptotic proteins, including Bcl-2 (see Figure 1.10B). Under normal (non-apoptotic) circumstances, the anti-apoptotic proteins interact with Bax and Bak and prevent these proteins from inducing MOMP and triggering the apoptotic cascade (see Figure 1.11B). The formation of Bim/Bcl-2 complexes (and other Bim/anti-apoptotic protein complexes), releases Bax and Bak and promotes apoptosis. Therefore, it is probable that in response to doxazolidine treatment, greater levels of Bim become activated over time, resulting in an increase in Bim/Bcl2 interactions until a certain threshold is reached where sufficient levels of Bax and Bak are released and are able to promote apoptosis, thus overcoming resistance to doxazolidine.

In order to confirm that increased Bim/Bcl-2 interactions are occurring in response to doxazolidine treatment over time, co-IP analysis needs to be performed. Likewise, further analysis needs to be performed to determine if the other proteins identified by mass spectrometry reflect a 'real' interaction with Bcl-2 or just some form of contamination or non-specific interaction. It should be noted that the mass spectrometry was performed at the very end of experimental work for this thesis and as such there was insufficient time to perform further analysis.

There is no doubt that the Bcl-2 family proteins are a complex family and there are so many interactions between different family members that could affect apoptosis induction or prevention. With so many interactions, one would need to investigate and explore all possible events to completely understand the entire mechanism occurring in response to drug treatment. Furthermore, the interactions between Bcl-2 family members are dynamic in that over time slight shifts in expression levels or changes in the ratios of one protein to another could lead to the threshold for triggering apoptosis. In this study, only preliminary experiments have been performed to determine the mechanism responsible for overcoming Bcl-2 mediated resistance in HL-60 cells, but with different drugs inducing different types of DNA damage, the mechanisms involved in overcoming anti-apoptotic resistance may vary depending on the particular drug and damage induced, as well as the cancer cell line used.

4.3.6 Conclusions

The doxorubicin-formaldehyde conjugate doxazolidine is able to form DNA adducts as a single agent and was much more effective at killing cancer cells compared to the combination of doxorubicin/AN-9 and doxorubicin. However, due to its short-half life and high cytotoxicity, stable, tumour-targeted prodrugs of doxazolidine have been developed in order for doxazolidine to be potentially suitable for clinical use. Treatment of Bcl-2 overexpressing HL-60 cells with doxazolidine revealed that the cells are resistant to a certain time, after which (\geq 18 hr) the resistance is overcome and the cells die via classical apoptosis. Short-lived Bcl-2 mediated resistance was also observed in response to doxorubicin/AN-9 and doxorubicin treatment, indicating that this may be a widespread phenomenon. When the mechanism responsible for overcoming Bcl-2 mediated resistance in response to doxazolidine treatment was investigated, there was no evidence of a decrease in Bcl-2 or Mcl-1 expression, or of Rad9/Bcl-2 interactions that may be promoting apoptosis. Mass spectrometry revealed Bim as a potential Bcl-2 binding partner that may play a role in overcoming Bcl-2 mediated resistance. These results suggest that some drugs such as doxazolidine may induce so much DNA damage that even high levels of Bcl-2 are not capable of preventing cancer cell death, which is a major clinical advantage for anti-cancer therapies, provided that they are sufficiently tumour-specific.

Chapter 5

ASSESSMENT OF THE αvβ3 INTEGRIN AS A METHOD OF TARGETING DOXORUBICIN-DNA ADDUCTS TO TUMOURS

5.1 INTRODUCTION

5.1.1 Targeting Angiogenesis and Metastasis

Angiogenesis, the growth of new blood vessels from pre-existing ones, is an essential process for supplying cells with oxygen and nutrients required for cellular function and survival, as well as removing carbon dioxide and metabolic waste products (Hanahan and Weinberg, 2011). Angiogenesis is vital during embryogenesis, tissue repair, and wound healing, but is also implicated in tumour growth. Tumours rely on angiogenesis to expand to a larger size enabling continual proliferation of tumour cells, and to facilitate metastasis to distant sites in the body (Hanahan and Folkman, 1996). Angiogenesis is regulated by pro-angiogenic (e.g. VEGF) and anti-angiogenic (e.g. thrombospondin-1) factors which can promote or block angiogenesis for normal physiological processes (Hanahan and Weinberg, 2011). In tumours, this balance is shifted to promote angiogenesis (Hanahan and Folkman, 1996), enabling activated endothelial cells to undergo adhesion (with the ECM and other cells), migration, and invasion through the tumour microenvironment. Once the new tumour vasculature is formed, these processes (adhesion, migration, and invasion) also enable tumour cells to metastasize from the primary site and start a secondary tumour cell population.

The processes of angiogenesis and metastasis are both considered to be hallmarks of cancer (Hanahan and Weinberg, 2000), and due to their importance in cancer progression, the identification of the various signalling pathways and molecules involved in their regulation is essential. In particular, the receptors and signalling molecules implicated in adhesion, migration, and invasion, make ideal candidates for targeting strategies since they typically have higher expression profiles in/on tumour cells relative to normal cells. For example, the signal protein VEGF plays an important role in promoting angiogenesis (Ferrara, 1999) and is overexpressed in a number of malignant cancers, leading to a poor clinical outcome (Jenab-Wolcott and Giantonio, 2009). Therefore, VEGF has emerged as a key target to inhibit angiogenesis of tumours and the humanized monoclonal anti-VEGF antibody bevacizumab (Avastin) has been clinically approved to treat a wide range of malignant cancer types (Iwamoto and Fine, 2010; McDermott and George, 2010; Planchard, 2011). The

integrin family has also been identified to play important roles in various stages of angiogenesis by promoting adhesion with the ECM and by facilitating metastasis (Desgrosellier and Cheresh, 2010), and as such have also been considered as potential targets for cancer therapy. This chapter focuses on the $\alpha\nu\beta3$ integrin as a candidate for targeting doxorubicin-DNA adducts to tumour cells.

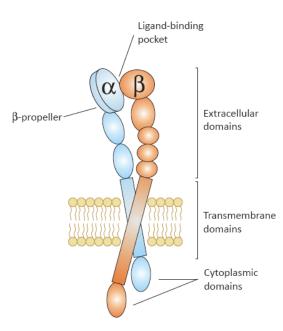
5.1.2 Integrins

5.1.2.1 Integrin Structure

The integrins are a family of transmembrane glycoproteins expressed on cell surfaces that act as adhesion receptors for various ECM components (Desgrosellier and Cheresh, 2010). As shown in Figure 5.1A, integrins are heterodimers comprised of α and β subunits that contain a large extracellular head domain, a single transmembrane domain, and a short cytoplasmic tail domain (Campbell and Humphries, 2011; Niland and Eble, 2011). There have been 18 α and 8 β subunits identified that assemble into 24 different integrins with different tissue distributions and different binding properties (Campbell and Humphries, 2011). The subunits associate non-covalently and form a ligand binding region at their interface on the extracellular face of cells, allowing the integrins to interact with different types of ECM molecules (Xiong *et al.*, 2002; Campbell and Humphries, 2011).

5.1.2.2 Ligand Binding

Most integrins are able to bind to a variety of ECM ligands, and conversely many ECM molecules are able to interact with multiple integrins (Plow *et al.*, 2000; Takada *et al.*, 2007). For example, laminin, a component of the basement membrane, interacts with the integrins $\alpha 3\beta 1$, $\alpha 6\beta 1$, $\alpha 6\beta 4$, and $\alpha 7\beta 1$ (Niland and Eble, 2011). Integrins bind to ligands at specific recognition sequences within the ligand peptides. Within this sequence, ligands contain an acidic residue used for initial recognition, while the specificity for particular ligands is based on additional contacts made with the integrin-binding site (Xiong *et al.*, 2002). The first binding site to be defined was the RGD (Arg-Gly-Asp) sequence present in many ECM molecules including vitronectin and fibronectin (Hynes, 1992). The αv -family, $\alpha 5\beta 1$, $\alpha 8\beta 1$,



Α

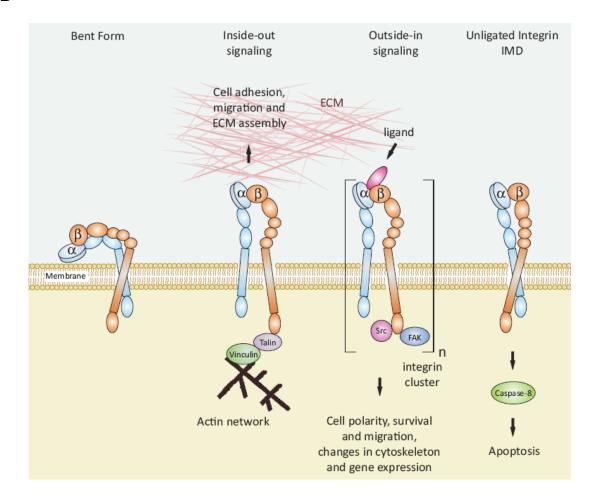


Figure 5.1. Integrin structure and signalling mechanisms.

A schematic representation of integrin structure is depicted in (A) where the α and β subunits come together to form the extracellular ligand binding domain. Integrins can exist in various activation states and can mediate a range of signalling events (B). Integrins can adopt a 'bent' conformation where the head domains are positioned towards the cell surface and have a low affinity for ligands. Integrin activation to an 'extended' conformation arises when the cytoplasmic domains interact with cytoskeletal proteins, and this mediates "inside-out" signalling to promote adhesion and migration. In response to ligand binding, integrins can cluster together to form signalling hubs, and this "outside-in" signalling can facilitate a range of responses including migration, invasion, and proliferation. Unligated ligands on the other hand can activate caspase-8 leading to integrin-mediated death (adapted from Mas-Moruno *et al.*, 2010).

and α IIb β 3 integrins all recognize ligands with an RGD sequence (Campbell and Humphries, 2011). Other integrins recognize different sequences on ligands including the LDV (Leu-Asp-Val) sequence which is recognized by the α 4 β 1, α 4 β 7, and α 9 β 1 integrins (Takada *et al.*, 2007; Campbell and Humphries, 2011).

Ligand binding is dependent on divalent metal cations, in particular, Ca^{2+} , Mg^{2+} , and Mn^{2+} ions (Campbell and Humphries, 2011). At the ligand-binding region, integrin subunits contain metal-ion dependent adhesion sites (Lee *et al.*, 1995) to which metal cations bind and stabilize interactions between the integrin subunits and the ligand (Bergelson and Hemler, 1995; Craig *et al.*, 2004). Once a ligand has bound to an integrin, this triggers structural changes in the integrin that are needed for cell signalling ("outside-in" signalling; see Section 5.1.2.4). For a more detailed description of subunit structure and ligand binding interactions see Campbell and Humphries (2011).

5.1.2.3 Integrin Activation (Inside-Out Signalling)

The binding of ligands to integrins is typically not constitutive as this would lead to inappropriate adhesion, but instead is regulated in response to activation signals. This regulation is mediated by inside-out signalling which involves the alteration of the conformation and ligand affinity of the integrin receptors from within the cell. Integrins exist in at least two distinct conformations - a 'bent' conformation where the extracellular domains are bent towards the plasma membrane, and an 'extended' conformation where the extracellular domains remain upright (Figure 5.1B; Campbell and Humphries, 2011). Most current models suggest that in the 'bent' conformation integrins adopt an unbound (low-affinity) state and activation to the 'extended' conformation is required for high-affinity ligand binding (Beglova *et al.*, 2002; Banno and Ginsberg, 2008; Campbell and Humphries, 2011; Niland and Eble, 2011). However, studies have also shown ligands binding to integrins in a 'bent' conformation (Adair *et al.*, 2005), thus indicating the possibility of multiple conformations with differing ligand affinities.

The activation of integrins to a high-affinity state is regulated by interactions between the integrin cytoplasmic tails with cytoskeletal proteins (Hughes *et al.*, 1996; Calderwood *et al.*, 1999; Liddington and Ginsberg, 2002). The α and β cytoplasmic tails are clasped together,

stabilizing the integrin in the low-affinity state (Hughes *et al.*, 1996; Banno and Ginsberg, 2008). In response to certain adhesion cues in the form of growth factors or cytokines, cytoskeletal proteins such as talin can interact with the subunit tails, consequently disrupting α and β cytoplasmic tail interactions and leading to the high-affinity 'extended' extracellular conformation (Calderwood *et al.*, 1999; Banno and Ginsberg, 2008). Once activated, integrins are able to bind to various ECM components promoting cell adhesion and motility, and relay signals back into cells via outside-in signaling (Figure 5.1B).

5.1.2.4 Integrin Function (Outside-In Signalling)

Integrins play major roles in cell-cell and cell-matrix interactions during embryogenesis, wound healing, immune reactions, and angiogenesis (Hynes, 1992; Takada *et al.*, 2007). These interactions not only promote cell adhesion but also regulate cell migration, invasion, proliferation, and survival. Since integrins lack any enzymatic activity, they mediate signalling events through the formation of signalling complexes within the cell (Campbell and Humphries, 2011). This outside-in signalling which occurs in response to ligand binding, triggers structural rearrangements in integrins that subsequently promotes various intracellular signalling pathways (Figure 5.1B).

The formation of integrin-mediated signalling complexes called focal adhesions is instigated by two events - conformational changes in the integrin cytoplasmic tails in response to ligand binding (Luo *et al.*, 2007), and integrin receptor clustering in the plane of the plasma membrane (Buensuceso *et al.*, 2003). These conformational changes unclasp the α and β cytoplasmic tails, exposing binding sites for a variety of effector molecules which are able to trigger downstream signalling pathways, and by clustering together this creates large signalling 'hubs' from which integrins are able to ultimately regulate events including cell migration and invasion (Campbell and Humphries, 2011).

The formation of focal adhesions triggers the recruitment of a multitude of proteins including tensin, talin, α -actinin, and vinculin, all of which are able to interact directly or indirectly with actin, therefore forming a physical link between the ECM and the cytoskeleton (as summarized in Desgrosellier and Cheresh, 2010; Niland and Eble, 2011). By mediating such linkages, integrins are able to provide traction required for cell motility, which is essential for

processes such as cell migration and invasion. Upon ligation, integrins are also able to recruit and activate several kinases including focal adhesion kinases, Src-family kinases, and integrin-linked kinase, as well as scaffolding molecules such as p130(Cas) (Vuori *et al.*, 1996; Defilippi *et al.*, 2006; Desgrosellier and Cheresh, 2010), and adapter proteins such as paxillin (Liu and Ginsberg, 2000; Brown *et al.*, 2005) and Grb2 (Schlaepfer *et al.*, 1998), which can recruit additional signalling molecules. Thus, through the creation of focal adhesions, integrins are able to relay their signals through a number of different pathways, including the MAPK/ERK pathway to ultimately promote cell motility, migration and invasion (Cary *et al.*, 1996). In fact, it is estimated that focal adhesions can involve over 150 different molecules including various kinases, phosphatases, and adapter proteins (Zaidel-Bar *et al.*, 2007).

Upon ligation, integrins also play roles in regulating cell proliferation (Schwartz and Assoian, 2001; Cruet-Hennequart *et al.*, 2003), and promoting cell survival (Scatena *et al.*, 1998; Matter and Ruoslahti, 2001; Bao and Stromblad, 2004). Unligated integrins on the other hand recruit and activate caspase-8 in a death-receptor independent process to trigger integrin-mediated death (IMD) (Stupack *et al.*, 2001). This form of cell death (IMD) is distinct from anoikis which is apoptosis induced in response to cellular detachment (loss of adhesion) from the ECM (Frisch and Francis, 1994; Frisch and Screaton, 2001). Integrin receptor clustering can also induce cross-talk with various growth factor receptors including the pro-angiogenic VEGF and fibroblast growth factor (FGF) receptors (Yamada and Even-Ram, 2002). Generally, integrins act as positive regulators to activate these receptors leads to induction of angiogenesis (Ivaska and Heino, 2010). Some integrins can even directly bind to pro-angiogenic factors such as VEGF and angiopoietins to promote angiogenesis (Carlson *et al.*, 2001; Vlahakis *et al.*, 2007). Ultimately, the overall cellular response depends on the identity of the integrin that binds to the ECM.

5.1.2.5 Integrins and Cancer

Due to the importance of integrins in facilitating cell contacts with the ECM, many integrins are expressed on a wide variety of cells and most cells express several integrin types (Hynes, 1992). While such integrin-mediated interactions are essential during embryogenesis, wound

healing, and immune reactions, the ability of integrins to promote cell survival, proliferation, migration, and invasion, all of which are considered to be key processes implicated in tumour growth, tumour angiogenesis, and metastasis, it is therefore not surprising that many integrins contribute to cancer progression. The expression of some integrins can vary considerably between normal and tumour tissue with many integrins being overexpressed on tumour or tumour-associated cells. In particular, tumour expression of the integrins $\alpha\nu\beta3$, $\alpha\nu\beta5$, $\alpha\nu\beta6$, $\alpha4\beta1$, $\alpha5\beta1$, and $\alpha6\beta4$, has been correlated with disease progression in a number of malignant cancer types (Desgrosellier and Cheresh, 2010). For this reason, many integrins have become candidates for tumour targeting strategies, especially the $\alpha\nu\beta3$ integrin which is discussed in more detail below.

5.1.3 The αvβ3 Integrin

The $\alpha v\beta 3$ integrin interacts with numerous ECM ligands containing the tripeptide RGD sequence, including vitronectin (the $\alpha v\beta 3$ integrin is often referred to as the vitronectin receptor), fibronectin, fibrinogen, osteopontin, thrombospondin, and von Willebrand factor (Takada *et al.*, 2007). It has a limited expression profile in humans, with minimal expression on epithelial or quiescent endothelial cells, including intestinal, vascular, and smooth muscle cells (Eliceiri and Cheresh, 1999; Wilder, 2002). High expression levels are limited to activated macrophages and osteoclasts where the $\alpha v\beta 3$ integrin appears to contribute to immune function and bone resorption respectively, as well as activated endothelial cells implicated in angiogenesis (Eliceiri and Cheresh, 1999; Wilder, 2002). Since angiogenesis is a vital process for tumour growth and metastasis, several invasive tumour types including breast (Sloan et al., 2006), ovarian (Cannistra et al., 1995), glioma (Gingras et al., 1995), prostate (Zheng et al., 1999), and melanoma (Albelda et al., 1990), have been shown to characteristically express high levels of the $\alpha\nu\beta3$ integrin. Upregulation of the $\alpha\nu\beta3$ integrin (and other integrins) occurs in response to low oxygen tension, such as the hypoxic conditions encountered in the tumour microenvironment, and this upregulation is mediated by the transcription factor HIF-1 (Cowden Dahl et al., 2005). Moreover, pro-angiogenic cytokines including bFGF have been shown to induce avß3 integrin cell surface expression (Swerlick et al., 1992; Brooks et al., 1994b; Li et al., 2010).

As mentioned above, angiogenic cues trigger $\alpha\nu\beta3$ integrin upregulation, and upon ligation, the $\alpha\nu\beta3$ integrin induces signalling events via focal adhesions (as described in Section 5.1.2.4) to promote angiogenesis and metastasis. Studies have shown that $\alpha\nu\beta3$ integrin activation can increase cell surface expression of the pro-angiogenic receptors for VEGF and FGF, and that inhibition of $\alpha\nu\beta3$ integrin with blocking antibodies decreases the presence of these receptors (Tsou and Isik, 2001). The $\alpha\nu\beta3$ integrin has also been shown to interact directly with VEGF receptors leading to their activation (Soldi *et al.*, 1999). Further evidence supporting the role of $\alpha\nu\beta3$ integrin in mediating angiogenesis comes from the finding that the use of $\alpha\nu\beta3$ antagonists (antibodies and peptides) inhibited angiogenesis on chick chorioallantoic membranes without affecting pre-existing vessels (Brooks *et al.*, 1994a; Brooks *et al.*, 1994b).

The expression level of the $\alpha\nu\beta3$ integrin appears to be directly related to the metastatic potential of the cancer, with studies showing that highly invasive and metastatic breast (Wong *et al.*, 1998) and prostate (Zheng *et al.*, 1999) cancer cells express much higher levels of $\alpha\nu\beta3$ integrin compared to cells with low metastatic potential. Moreover, exogenous overexpression of the $\alpha\nu\beta3$ integrin in non-metastatic mouse mammary epithelial cells has been shown to increase adhesion, migration, and invasion *in vitro* and promote spontaneous metastasis to lung and bone in mouse models, without affecting primary tumour growth and weight (Sloan *et al.*, 2006). Similarly, overexpression of constitutively active $\alpha\nu\beta3$ integrin in human breast cancer cells enhanced lung metastases in a mouse model (Felding-Habermann *et al.*, 2001), thus further highlighting the importance of the $\alpha\nu\beta3$ integrin in tumour progression. Furthermore, it has been shown that approximately 100,000-300,000 $\alpha\nu\beta3$ integrin molecules are present per cell on invasive breast, melanoma, and prostate cancer cell lines, thus providing an extensive number of targets for $\alpha\nu\beta3$ antagonists and targeting strategies (Mulgrew *et al.*, 2006).

5.1.4 Targeting the αvβ3 Integrin

Due to the involvement of the $\alpha\nu\beta3$ integrin in tumour angiogenesis and its limited expression on normal cells, the selective inhibition of this integrin may be used as a potential anti-cancer targeting strategy with minimal side-effects. Antagonists of the $\alpha\nu\beta3$ integrin have disrupted neovascularization in several tissues including the chick chorioallantoic membrane (Brooks et al., 1994b), quail embryo (Drake et al., 1995), and mouse retina (Hammes et al., 1996), and have blocked avß3 integrin mediated adhesion, migration and invasion in vitro (Mi et al., 2006; Sloan et al., 2006; Chen et al., 2008; Park et al., 2008b). In tumour models, the use of $\alpha\nu\beta\beta$ antagonists have been shown to not only block tumourassociated angiogenesis but also cause tumour regression without affecting pre-existing vessels (Brooks *et al.*, 1994a). The use of such $\alpha\nu\beta3$ antagonists alone results in apoptosis since the integrin is prevented from interacting with its endogenous ligands, and this loss of anchorage triggers cell death (anoikis) (Brooks et al., 1994a). Furthermore, integrins undergo endocytosis and as such are able to internalize targeted compounds allowing for effective drug delivery (Bretscher, 1989; Cressman et al., 2009a; Cressman et al., 2009b; Ivaska and Heino, 2010). There are two major classes of antagonists that have been used to target the $\alpha v\beta 3$ integrin – monoclonal antibodies and RGD peptides.

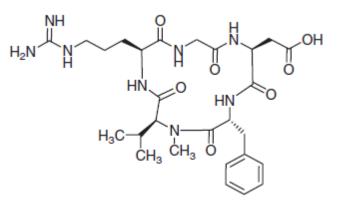
5.1.4.1 Antibodies

Function-blocking monoclonal antibodies were among the first $\alpha\nu\beta3$ integrin antagonists developed. The murine LM609 antibody showed considerable anti-angiogenic activity and reduced tumour growth in a preclinical breast cancer mouse model (Brooks *et al.*, 1995). In response to promising studies with LM609, humanized versions of the antibody including VitaxinTM (MEDI-523) and AbegrinTM (etaracizumab, MEDI-522) were developed and entered clinical trails (Desgrosellier and Cheresh, 2010). Abegrin was shown to reduce tumour growth *in vivo* using cancers that express high levels of $\alpha\nu\beta3$ integrin (Mulgrew *et al.*, 2006). In Phase I trials, both Vitaxin and Abegrin displayed a favourable safety profile and were well tolerated in patients with various solid tumours (Gutheil *et al.*, 2000; McNeel *et al.*, 2005; Delbaldo *et al.*, 2008), however, in a Phase II trial the antitumour activity of Abegrin appeared to be minimal (Hersey *et al.*, 2010). Another monoclonal antibody, the

fully humanized CNTO-95, targets both $\alpha\nu\beta3$ and $\alpha\nu\beta5$ integrins and displayed antitumour activity both *in vitro* and *in vivo* (Trikha *et al.*, 2004; Chen *et al.*, 2008), and was well tolerated in a Phase I clinical trial (Mullamitha *et al.*, 2007).

5.1.4.2 RGD Peptides

Short synthetic peptides containing the RGD recognition sequence have also been used to target the $\alpha v\beta 3$ integrin. A wide variety of linear and cyclic RGD peptides have been produced, and by modifying the conformation of the RGD sequence as well as the flanking residues, peptides have been developed with a very high affinity and selectivity for the $\alpha\nu\beta3$ integrin (Marinelli et al., 2003; Dunehoo et al., 2006). In general, cyclic peptides display greater stability (Bogdanowich-Knipp et al., 1999), have a longer circulation time in the bloodstream (Burkhart et al., 2004), and display greater selectivity and binding activity (Mas-Moruno et al., 2010) in comparison to linear peptides. Cyclic peptides have been shown to accumulate in tumours relative to other tissues in a human tumour xenograft model (Janssen et al., 2002). The structures of the commonly used RGD peptides cilengitide and RGD-4C are shown in Figure 5.2. The cyclic peptide c(RGDf(NMe)V (cilengitide) is an inhibitor of both $\alpha\nu\beta3$ and $\alpha\nu\beta5$ integrins and has been shown to inhibit the growth and metastasis of invasive melanoma (Buerkle et al., 2002), as well as glioblastoma and medulloblastoma brain tumours in animal models (MacDonald et al., 2001). Cilengitide has also been combined with radio-immuno therapy in a breast cancer mouse model resulting in increased efficacy (Burke *et al.*, 2002). Cilengitide has entered clinical trials where it has been shown to display antitumour activity as a single agent in patients with recurrent glioblastoma with minimal toxicity (Nabors et al., 2007; Reardon et al., 2008), however, in other trials cilengitide has offered little clinical benefit (Friess et al., 2006). Currently, cilengitide has entered a Phase III trial in combination with temozolomide and radiotherapy in glioblastoma patients, as well as several Phase II trials against other invasive cancer types (Mas-Moruno et al., 2010).



Α

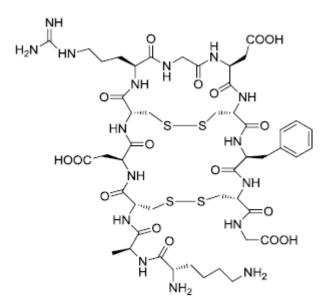


Figure 5.2. Structures of the commonly used RGD peptides (A) cilengitide, and (B) RGD-4C.

5.1.5 Project Objectives

The major aim of this part of the project was to determine if the $\alpha\nu\beta3$ integrin is a suitable candidate for targeting doxorubicin-DNA adducts to integrin-expressing tumours. Two sets of mouse mammary cancer cell lines (derived from 66cl4 and 4T1.2 cells) with either high or low expression of $\alpha\nu\beta3$ integrin were used for this project. To determine if the $\alpha\nu\beta3$ integrin affects processes implicated in cancer progression, adhesion and invasion assays were employed in high and low $\alpha\nu\beta3$ integrin expressing 66cl4 and 4T1.2 cancer cells. These cell lines were also used to determine if $\alpha\nu\beta3$ integrin levels affect the sensitivity of cancer cells to doxorubicin-DNA adduct-forming treatments.

Another objective was to use an RGD peptide in $\alpha\nu\beta3$ integrin expressing cells to determine if the peptide affects the ability of the $\alpha\nu\beta3$ integrin to promote cancer progression, or affect the sensitivity of cells to doxorubicin-DNA adduct forming treatments.

Mouse studies were also performed to determine the tolerability and efficacy of doxorubicin-DNA adduct forming treatments in mice with highly invasive, $\alpha v\beta 3$ integrin expressing tumours. A Balb/c mouse model of spontaneous breast cancer metastasis was used, and the mice were treated with doxorubicin in combination with formaldehyde-releasing prodrugs to ascertain if doxorubicin-DNA adduct-forming treatments have an anti-cancer advantage over doxorubicin alone.

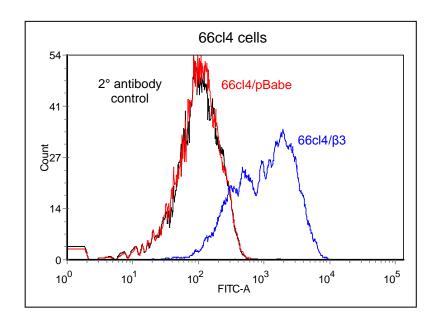
Based on both the *in vitro* cellular and *in vivo* mouse studies, it should then be possible to make a conclusion on the future potential effectiveness of targeting doxorubicin-DNA adduct formation to $\alpha\nu\beta3$ integrin expressing tumours using RGD peptide-based strategies.

5.2 **RESULTS**

5.2.1 avβ3 integrin expressing cell models

For this project, two sets of cell lines (66cl4 and 4T1.2) were used to ascertain the effectiveness of doxorubicin/AN-9 DNA adduct-forming treatments against highly invasive (high $\alpha\nu\beta3$ integrin expressing) and weakly invasive (low $\alpha\nu\beta3$ integrin expressing) cancer cells. Both 66cl4 and 4T1 cell lines (the 4T1.2 cell line is a variant cell line cloned from 4T1 cells) were derived from the same source – a spontaneous mammary carcinoma in a Balb/c/CH3 mouse (Aslakson and Miller, 1992). In a syngeneic orthotopic Balb/c mouse model where spontaneous tumours arise following implantation of cells in the mammary fat pad, it has been demonstrated that 4T1.2 cells are highly metastatic to lymph nodes, lung and bone, while 66cl4 cells are only weakly metastatic to lung (Eckhardt *et al.*, 2005). The expression level of the $\alpha\nu\beta3$ integrin was identified as a key factor influencing the degree of metastasis, with 4T1.2 cells expressing high levels of $\alpha\nu\beta3$ integrin and 66cl4 cells expressing high levels of $\alpha\nu\beta3$ integrin and 66cl4 cells integrin in 66cl4 cells (66cl4/ $\beta3$ cells) was sufficient to increase metastatic burden to bone (Sloan *et al.*, 2006), highlighting the importance of this integrin in promoting metastasis.

In the two sets of cell lines used in this project: 1) $66c14/\beta3$ (exogenous expression of mouse $\beta3$ integrin subunit) and $66c14/\betaBabe$ (control cell line) cells; and 2) 4T1.2/pRS (control cell line) and $4T1.2/sh\beta3$ (shRNA $\beta3$ integrin subunit knockdown) cells, FACS was used to determine the levels of $\beta3$ integrin subunit using an anti- $\beta3$ antibody. Figure 5.3A demonstrates that the 66c14 cells transfected with mouse $\beta3$ cDNA ($66c14/\beta3$ cells) display much higher $\beta3$ subunit levels compared with the $66c14/\betaBabe$ control cell line which has only background levels of $\beta3$ subunit, consistent with that shown by Sloan and colleagues (2006). As depicted in Figure 5.3B, control 4T1.2 cells (4T1.2/pRS) express high levels of $\beta3$ subunit which correlates with their high metastatic potential (Eckhardt *et al.*, 2005). The $4T1.2/sh\beta3$ cells display reduced levels of cell surface $\beta3$ subunit indicating that the knockdown of the $\beta3$ subunit via shRNA was successful. These results were repeated in cells that had remained in culture over three weeks and similar findings were observed, indicating



Α

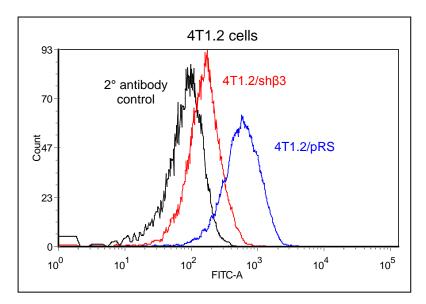


Figure 5.3. Levels of surface β3 integrin subunit in mouse mammary tumour cell lines.

Cell surface expression of the β 3 integrin subunit was determined in (A) 66cl4 cell lines and (B) 4T1.2 cell lines. Cells were incubated with an anti- β 3 primary antibody followed by a FITC-labelled secondary antibody, and the fluorescence levels detected by flow cytometry. Cells were also incubated only in the presence of secondary antibody to indicate levels of background fluorescence (black graphs). Levels of the β 3 integrin subunit did not change over a three week culture period. These results are representative of three independent experiments.

that the β 3 subunit levels did not change over time and therefore are stable in cell culture conditions. Although αv subunit levels were not determined in this study, Sloan and colleagues (2006) showed that $66cl4/\beta$ 3 cells which overexpress the β 3 subunit had a corresponding increase in αv subunit levels at the cell surface. Similar findings were observed in MCF7 cells (Pereira *et al.*, 2004; Liu *et al.*, 2012), and it was postulated that in response to exogenous expression of the β 3 subunit, there may be enhanced transcription of the αv subunit or a redistribution of an intracellular pool of the αv subunit to the cell surface to form complete $\alpha v\beta$ 3 integrin heterodimers (Sloan *et al.*, 2006; Liu *et al.*, 2012).

5.2.2 The αvβ3 integrin does not affect doxorubicin-DNA adduct formation

The ultimate aim of this project was to determine if doxorubicin-DNA adduct-forming treatments could be selectively targeted to $\alpha\nu\beta3$ integrin expressing cancer cells. For such a targeting strategy to be successful, the $\alpha\nu\beta3$ integrin expressing cancer cells need to be susceptible to the effects of DNA adduct forming treatments. To determine whether $\alpha\nu\beta\beta$ integrin levels affect doxorubicin-DNA adduct formation, [¹⁴C]-doxorubicin was used in combination with AN-9 in both sets of 66cl4 and 4T1.2 cells and the DNA adduct levels were quantitated. Figure 5.4A shows that the $\alpha\nu\beta3$ integrin overexpressing 66cl4/ $\beta3$ cells had similar DNA adduct levels measured to the control 66cl4/pBabe cells following treatment with doxorubicin/AN-9. Likewise, the $4T1.2/sh\beta3$ knockdown cells had similar DNA adduct levels detected to the high $\alpha\nu\beta\beta$ integrin expressing 4T1.2/pRS cells (Figure 5.4B). These results demonstrate that the levels of $\alpha\nu\beta3$ integrin do not affect the ability of doxorubicin and AN-9 to enter cancer cells and react to form DNA adducts. The DNA adduct levels recorded in both sets of cells are completely dependent on formaldehyde, since the use of AN-158 which does not release formaldehyde upon esterase-mediated hydrolysis, resulted in only background levels of DNA adducts when combined with doxorubicin. Furthermore, in both 66cl4 and 4T1.2 cell lines it can be seen that when a higher concentration of AN-9 was used (200 μ M versus 100 μ M), higher levels of DNA adducts were observed, indicating that when more formaldehyde is available the levels of doxorubicin-DNA adducts can be increased.

66cl4 cells



Α

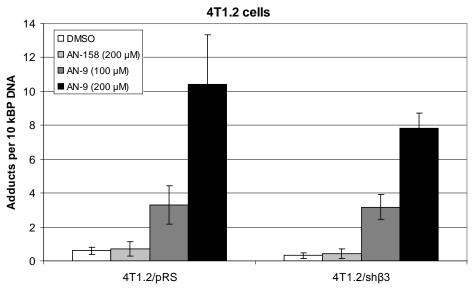


Figure 5.4. Levels of αvβ3 integrin do not affect doxorubicin-DNA adduct formation.

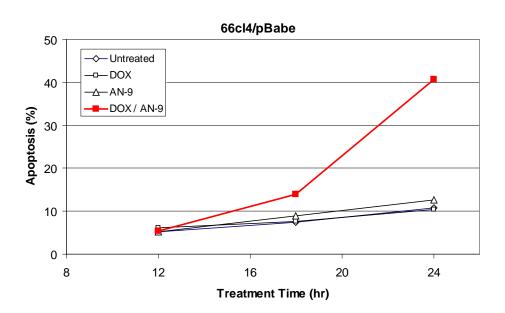
66cl4 (A) and 4T1.2 (B) cells $(2x10^5 \text{ cells})$ were treated with 1 μ M [¹⁴C]-doxorubicin in combination with DMSO (vehicle control), AN-158 (200 μ M), or AN-9 (100 or 200 μ M) for 6 hr. After treatment, DNA was extracted, scintillation counting performed, and the level of doxorubicin-DNA adducts quantitated. Error bars represent the standard error of the mean from three independent experiments.

5.2.3 Doxorubicin-DNA adduct-forming treatments cause synergistic cell death in highly invasive, $\alpha\nu\beta3$ integrin expressing cancer cells

Apoptosis assays were used to determine if the presence of high $\alpha\nu\beta3$ integrin levels affect the induction of cell death from doxorubicin-DNA adduct-forming treatments. Preliminary experiments were conducted in 66cl4/pBabe and 4T1.2/pRS control cell lines using a range of doxorubicin and AN-9 concentrations to determine the optimum concentrations of these drugs in inducing apoptosis in these cells. Ultimately, treatment with 500 nM doxorubicin and 50 μ M AN-9 for 24 hr in 66cl4/pBabe cells (Figure 5.5A), and treatment with 250 nM doxorubicin and 50 μ M AN-9 for 36 hr in 4T1.2/pRS cells (Figure 5.5B), induced low levels of cell kill with either agent alone and synergistic cell death when the drugs were used in combination. These drug concentrations and treatment times were subsequently used for further analysis (for all apoptosis assays, 8x10⁴ cells were used).

Treatment of $66cl4/\beta3$ cells with the doxorubicin/AN-9 combination resulted in synergistic cell kill, comparable to that seen with the treatment of the 66cl4/pBabe control cell line (Figure 5.6A). This indicates that exogenous expression of high levels of the $\alpha\nu\beta3$ integrin does not affect the sensitivity of these cells to the doxorubicin/AN-9 DNA adduct forming treatment. Likewise, doxorubicin/AN-9 treatment resulted in synergistic cell kill in both the high $\alpha\nu\beta3$ integrin expressing 4T1.2/pRS cells, and reduced $\alpha\nu\beta3$ integrin expressing 4T1.2/sh\beta3 cell line (Figure 5.6B), highlighting that these cancer cells are sensitive to the treatments irrespective of $\alpha\nu\beta3$ integrin levels.

To confirm that the cell death synergy observed in response to doxorubicin/AN-9 treatment was due to the formation of DNA adducts, control compounds which do not result in DNA adduct formation were used. The doxorubicin analogue MEN-10755 (see Figure 3.18A) is unable to form DNA adducts in the presence of formaldehyde due to steric hindrance from an additional sugar group (Messori et al., 2001), and as such did not induce apoptosis above background when combined with AN-9 in both 66cl4 and 4T1.2 cell lines (Figure 5.7). Furthermore, the prodrug AN-158 which does not release formaldehyde (see Figure 3.22B) also did not induce cell kill above background when combined with doxorubicin in both 66cl4 4T1.2 cell lines (Figure 5.7). The and use of these two control



Α

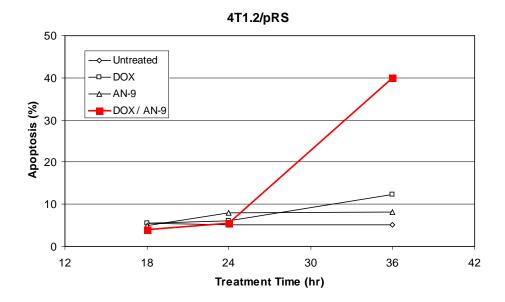
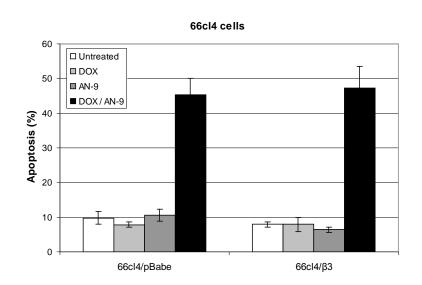
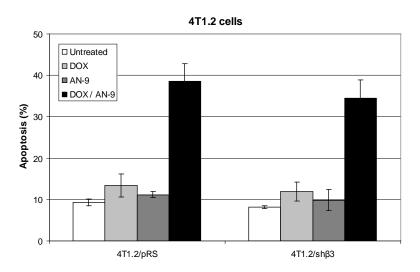


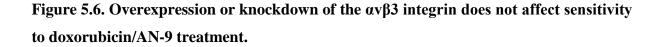
Figure 5.5. Doxorubicin/AN-9 treatment induces synergistic cell death over time in 66cl4/pBabe and 4T1.2/pRS control cell lines.

66cl4/pBabe cells (A) were treated with doxorubicin (500 nM), AN-9 (50 μ M), or the combination of both drugs for 12-24 hr, and 4T1.2/pRS cells (B) were treated with doxorubicin (250 nM), AN-9 (50 μ M), or the combination of both drugs for 18-36 hr. Cell numbers used in this assay and all apoptosis assays were 8x10⁴ cells. Flow cytometry was performed to determine the percentage of sub-G1 apoptotic cells (n=1).

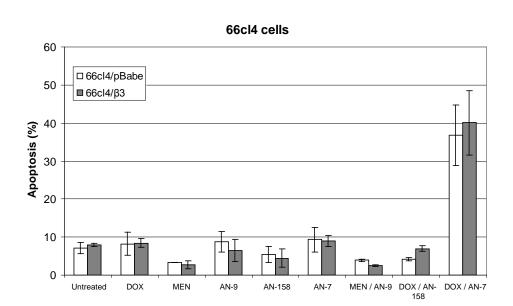


Α





66cl4 cell lines (A) were treated with doxorubicin (500 nM), AN-9 (50 μ M), and the combination of both drugs for 24 hr, and 4T1.2 cell lines (B) were treated with doxorubicin (250 nM), AN-9 (50 μ M), and the combination of both drugs for 36 hr. The percentage of apoptotic cells was determined by sub-G1 FACS analysis. The data represents the average from three (A) and four (B) independent experiments. In both graphs the error bars represent the standard error of the mean.



Α

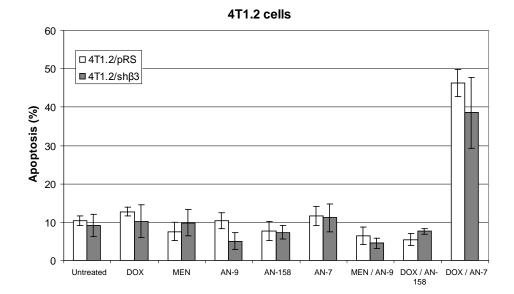


Figure 5.7. Non-DNA adduct forming treatments do not induce synergistic cell kill in $\alpha\nu\beta3$ integrin expressing cancer cells.

66cl4 cell lines (A) and 4T1.2 cell lines (B) were treated with doxorubicin, MEN-10755 (both at 500 nM in 66cl4 cells and 250 nM in 4T1.2 cells), AN-9, AN-158, and AN-7 (all at 50 μ M), as single agents and in the combinations listed. 66cl4 cells were treated for 24 hr while 4T1.2 cells were treated for 36 hr before cells were analysed by FACS to determine the percentage of sub-G1 apoptotic cells. Error bars represent the standard error of the mean from three independent experiments.

231

compounds (MEN-10755 and AN-158) highlights that the synergy observed between doxorubicin/AN-9 in $\alpha\nu\beta3$ integrin expressing tumour cell lines is completely dependent on formaldehyde-mediated DNA adduct formation. In addition to AN-9, another formaldehyde-releasing prodrug, AN-7 (see Figure 1.5B), also resulted in synergistic cell death in combination with doxorubicin, and as seen with doxorubicin/AN-9 treatments, the levels of cell death are comparable between high and low $\alpha\nu\beta3$ integrin expressing tumour cell lines (Figure 5.7).

In addition to the sub-G1 apoptosis assay, the caspase-3 activation assay was also performed (Figure 5.8). Much higher levels of caspase-3 activation were recorded in response to treatment with doxorubicin in combination with the formaldehyde-releasing prodrugs AN-9 and AN-7 in both 66cl4 and 4T1.2 cell lines, relative to the single agent treatments. This reflects that only when DNA adduct formation occurs is there an increase in capsase-3 activation and thus apoptosis. Furthermore, the level of caspase-3 activation did not differ between high and low $\alpha\nu\beta3$ integrin expressing cell lines.

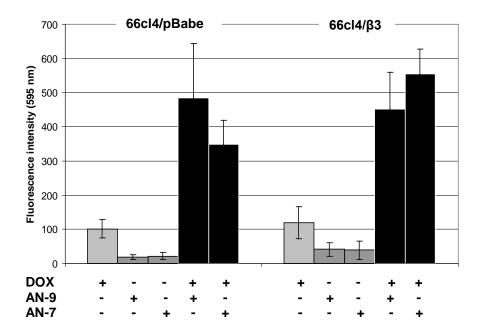
These apoptosis results highlight that both 66cl4 and 4T1.2 cancer cells are sensitive to DNA adduct forming treatments irrespective of $\alpha\nu\beta3$ integrin levels. This re-enforces the point that the strategy to target doxorubicin-DNA adduct formation to $\alpha\nu\beta3$ integrin overexpressing cancer cells is viable, once the cells are exposed to the drugs used for treatment.

5.2.4 The $\alpha\nu\beta$ 3 integrin promotes adhesion and invasion of 66cl4 and 4T1.2 cancer cells

Cancer progression is a complex, multi-step process which ultimately requires cancer cells to be able to adhere to the ECM, migrate, and invade through the basement membrane to distant sites of the body (Hanahan and Weinberg, 2011). Research has demonstrated that integrins, in particular the $\alpha\nu\beta3$ integrin, play pivotal roles in adhesion, migration, and invasion (Wong *et al.*, 1998; Sloan *et al.*, 2006), thus promoting angiogenesis and metastasis (Elicieri and Cheresh, 1999; Wilder, 2002; Desgrosellier and Cheresh, 2010). The ability of the $\alpha\nu\beta3$ integrin to stimulate tumour cell adhesion to the ECM and invasion through the basement membrane was investigated *in vitro* using the 66cl4 and 4T1.2 cell models.

The ECM protein vitronectin, an endogenous ligand for the $\alpha\nu\beta3$ integrin containing an RGD binding motif, was used to determine if the $\alpha\nu\beta3$ integrin promotes adhesion. In the adhesion assay, the cell permeable dye calcein (which fluoresces in live cells) was used to measure the proportion of cells adhering to vitronectin. Figure 5.9 demonstrates that in both sets of cell lines, the calcein fluorescence signal is proportional to the number of live cells, and as such is a suitable method for measuring the percentage of adhering cells in this assay. As depicted in Figure 5.10A, the 66cl4/pBabe control cell line only weakly adhered to both BSA control and vitronectin coated wells, while the $\alpha\nu\beta3$ integrin overexpressing 66cl4/β3 cells displayed a marked increase in adhesion (approximately 4-fold) to vitronectin versus BSA. Similarly, the $\alpha\nu\beta3$ integrin expressing 4T1.2/pRS cell line displayed a higher level of adhesion to vitronectin compared to the 4T1.2/sh $\beta3$ knockdown cell line (Figure 5.10B). These results demonstrate that the $\alpha\nu\beta3$ integrin (highly expressed on 66cl4/ $\beta3$ and 4T1.2/pRS cells) promotes adhesion to the ECM protein vitronectin, which is consistent with previous studies (Eckhardt *et al.*, 2005; Sloan *et al.*, 2006; Chia *et al.*, 2007).

The invasion of tumour cells was investigated using a Matrigel based assay in Transwell chambers, as described in Section 2.14. The sample images illustrate that in the absence of cells a faint autofluorescence is detected from the Transwell membrane pores (Figure 5.11A), however, when cells have invaded to the underside of the membrane a much brighter fluorescence from the invading cells is observed (Figure 5.11B-C). As illustrated by the sample images in Figure 5.11 and the quantitative data in Figure 5.12 the $\alpha\nu\beta3$ integrin overexpressing 66cl4/ $\beta3$ cells displayed a greater level of invasion through Matrigel towards the chemoattractant compared with 66cl4/pBabe cells, which is consistent with findings by Sloan and colleagues (2006). Due to the high cost per sample of the assay as well as extensive troubleshooting issues, the invasion assay was only performed in 66cl4 cell lines and not 4T1.2 cells. However, Eckhardt and colleagues (2005) showed that high $\alpha\nu\beta3$ integrin expressing 4T1.2 cells displayed a higher level of invasion relative to low $\alpha\nu\beta3$ integrin expressing tumour cells.



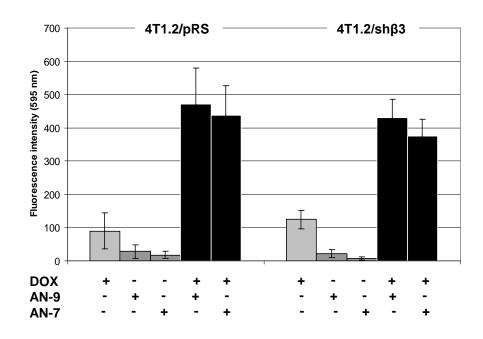
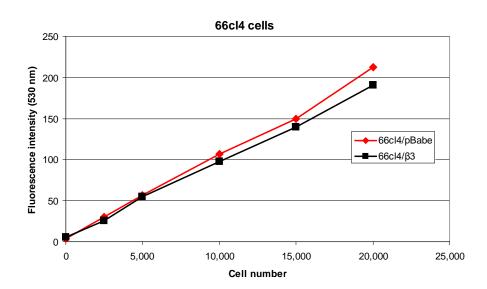


Figure 5.8. Caspase-3 activation levels are comparable between high and low $\alpha\nu\beta$ 3 integrin expressing cancer cells.

66cl4 cell lines (A) and 4T1.2 cell lines (B) were treated with doxorubicin (500 nM in 66cl4 cells and 250 nM in 4T1.2 cells), AN-9, and AN-7 (50 μ M) as single agents and in the combinations listed. 66cl4 cells were treated for 24 hr while 4T1.2 cells were treated for 36 hr before cells were lysed and 25 μ g protein was used for determination of fluorescence intensity in the caspase-3 activation assay. Fluorescence intensity for each sample was recorded at 505 nM and the fluorescence intensity value for untreated samples was subtracted from all treated samples. Error bars represent the standard error of the mean from four independent experiments.



Α

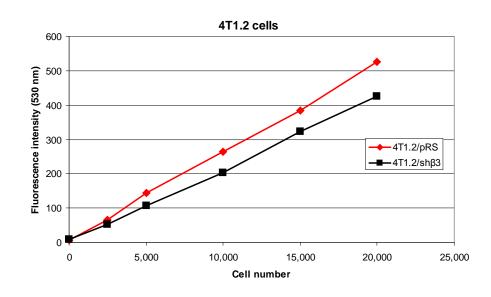


Figure 5.9. Linear relationship between calcein fluorescence and cell number.

66cl4 (A) and 4T1.2 (B) cells (20,000 cells) were incubated with calcein (10 μ g/mL) for 45 min (37 °C, 5% CO₂), washed, and resuspended in 1% (v/v) Triton-X 100. The fluorescence intensity of dilutions of the cell suspensions were recorded (excitation of 485 nm and emission of 530 nm). These results are representative of several independent experiments showing similar findings.

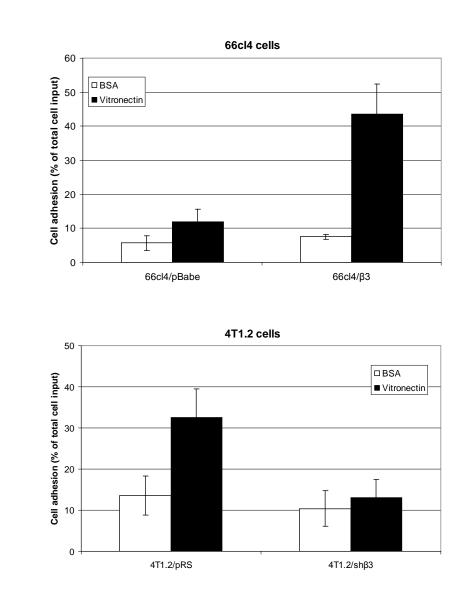
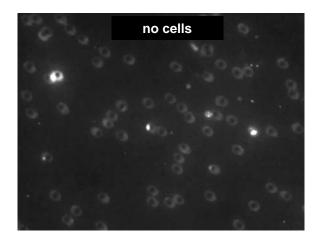


Figure 5.10. The $\alpha\nu\beta$ 3 integrin mediates adhesion of mouse mammary tumour cells to vitronectin.

66cl4 (A) and 4T1.2 (B) cells (200,000 cells) were incubated with calcein (10 μ g/mL) for 45 min, washed, and added to culture plates coated with BSA (2% (w/v)) or vitronectin from human plasma (5 μ g/mL). Cells (20,000 cells/well) were allowed to adhere for 45 min and once non-adherent cells were removed by washing in PBS, cells were resuspended in 1% (v/v) Triton-X 100, calcein fluorescence intensity recorded, and the percentage of cells adhering relative to total cell input was determined. Error bars represent the standard error of the mean from (A) three and (B) four independent experiments.

В

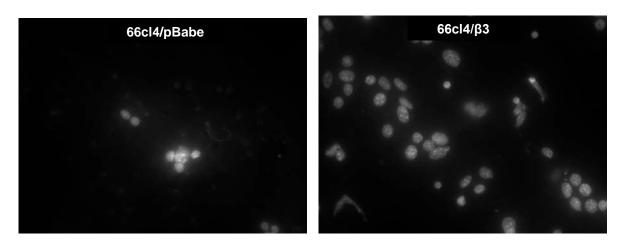
Α

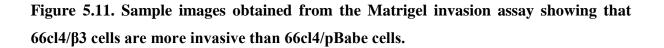


В

Α

С





66cl4 cells (100,000 cells / 100 μL) were added to Matrigel (3 mg/mL) coated Transwell chambers and allowed to invade for 24 hr at 37 °C. The membrane was removed from the transwell, stained with Hoechst 33258 and analysed by fluorescence microscopy (40x magnification). In the absence of cells, weak autofluorescence was seen from the membrane pores (A). In the presence of 66cl4/pBabe (B) and 66cl4/β3 cells (C), the nuclei of invaded cells are visible. These images were taken from one field of view and are representative of several fields analysed from duplicate samples and from independent experiments.

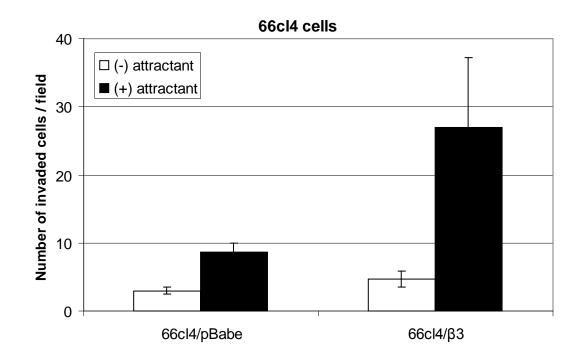


Figure 5.12. The αvβ3 integrin promotes tumour cell invasion in 66cl4 cells.

66cl4 cells were added to the upper chamber of 8 μ m pore Transwells which were coated with Matrigel (3 mg/mL). Transwells were incubated for 24 hr at 37 °C to allow the cells to invade through the Matrigel towards 10% FBS which was used as the chemoattractant in the lower chamber. Once non-invaded cells were removed, the Transwell membrane was stained with Hoechst 33258 and analysed by fluorescence microscopy (40x magnification). The number of invaded cells were counted in at least 6 fields and averaged from duplicate samples. Error bars represent the standard error of the mean from three independent experiments.

The results of both adhesion and invasion assays highlight that the $\alpha\nu\beta3$ integrin plays a pivotal role in promoting these processes, and as such is a key mediator of metastasis.

5.2.5 The c(RGDfK) peptide inhibits the ability of the $\alpha\nu\beta$ 3 integrin to promote adhesion

Since the $\alpha\nu\beta3$ integrin interacts with ECM ligands via an RGD sequence, RGD peptides have been used to target the $\alpha\nu\beta3$ integrin to inhibit its function (Marinelli *et al.*, 2003; Dunehoo et al., 2006). In this study the commercially available peptide c(RGDfK) which is commonly used for the delivery of therapeutic agents (Chen and Chen, 2011), and a control peptide c(RADfK) where the glycine residue is replaced with an alanine residue, were used to assess if RGD peptides can inhibit the ability of $\alpha v\beta 3$ expressing cancer cells to promote adhesion. It was noticed that when 66cl4/pBabe cells were grown in the presence of low micromolar levels of c(RGDfK) but not c(RADfK), the cells lost the ability to adhere to the culture plates after an overnight incubation. Although 66cl4/pBabe cells have been shown to express only very low levels of the $\alpha\nu\beta3$ integrin (Sloan *et al.*, 2006), other integrins also recognize RGD sequences (Campbell and Humphries, 2011), and therefore the RGD peptide may be binding to other integrins expressed by these cells which also promote cell adherence. As shown in Figure 5.13, when 66cl4/pBabe cells were incubated in the presence of 50 μ M or 500 μ M c(RGDfK), the percentage of adhering cells was greatly reduced. The c(RADfK) peptide on the other hand, did not reduce cell adherence to any great degree relative to the vehicle control sample, thus, it can be concluded that the inhibition of cell adherence to the culture plates is an RGD sequence specific effect. For the avß3 overexpressing 66cl4/ß3 cells, the presence of 50 μ M c(RGDfK) did not affect cell adherence, which is probably attributed to the peptide concentration not being high enough to bind to the greater number of $\alpha v\beta 3$ integrin targets, hence the threshold to affect overall cell adherence had not been reached. However, at a 10-fold higher concentration (500 μ M), the c(RGDfK) but not c(RADfK) peptide was able to reduce cell adherence by approximately 70%. It should be noted that although the cells were detached from the culture plates, they were trypan blue negative, reflecting that they were still viable.

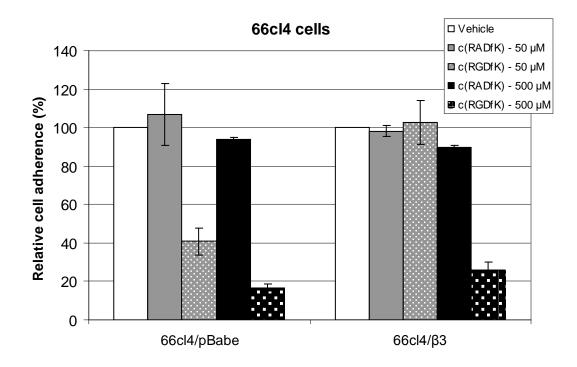


Figure 5.13. The c(RGDfK) peptide affects the adherence of $\alpha\nu\beta3$ integrin overexpressing 66cl4 cells to culture plates.

66cl4 cell lines (30,000 cells) were incubated with c(RGDfK) or c(RADfK) peptides (either 50 or 500 μ M) for 1 hr at 37 °C before being seeded into 24 well plates. Cells were incubated for 24 hr at 37 °C, 5% CO₂, and the number of adhering cells for each sample was counted on a haemocytometer in the presence of trypan blue. The percentage of adhering cells was determined relative to the vehicle control sample (Milli-Q water) which was given a value of 100% adherence. Error bars represent the standard error of the mean from three independent experiments.

Following the observation that RGD peptides can affect the overall adherence of 66cl4 cells, the vitronectin adhesion assay was used to assess if the c(RGDfK) peptide can inhibit the $\alpha\nu\beta3$ integrin specific property of adhesion to its endogenous ligand vitronectin. As previously shown in Figure 5.10, cells expressing high levels of $\alpha\nu\beta3$ integrin display greater adhesion to vitronectin, and since RGD peptides bind to $\alpha\nu\beta3$ integrins it is expected that RGD peptides will inhibit vitronectin adhesion. Indeed, Figure 5.14A shows that the c(RGDfK) peptide (500 μ M was used as this concentration affected cell adherence to culture plates) reduces the ability of 66cl4/ $\beta3$ cells to adhere to vitronectin. The c(RADfK) peptide however, did not affect vitronectin adhesion relative to the vehicle control sample, highlighting that the reduction in adhesion is almost certainly due to the RGD peptide binding to the $\alpha\nu\beta3$ integrin and inhibiting its ability to bind to vitronectin. When the percentage cell adhesion was standardized relative to the vehicle control sample, it can be concluded that the c(RGDfK) peptide inhibited cell adhesion to vitronectin by approximately 75% (Figure 5.14B). Note that this assay was not performed in 4T1.2/pRS cells since the difference between BSA and vitronectin adhesion was not as great as in 66cl4/ $\beta3$ cells.

5.2.6 The c(RGDfK) peptide does not interfere with doxorubicin/AN-9 mediated cell kill

If an RGD peptide-based tumour targeting strategy is to be successful, then the RGD peptides themselves should not interfere with the drug mechanism or react with the drugs, thus affecting treatment efficacy. To ensure that cell kill induced by DNA adduct forming treatments is not affected by RGD peptides, 66cl4 cells were treated with the doxorubicin/AN-9 combination in the presence of the c(RGDfK) peptide. The same concentrations of c(RGDfK) were used that caused a reduction in cell adherence shown in Figure 5.13 (50 μ M in 66cl4/pBabe cells and 500 μ M in 66cl4 β 3 cells). As illustrated in Figure 5.15, the c(RGDfK) peptides alone did not induce cell kill above background, but did cause the cells to detach from the culture plates (data not shown). Furthermore, the presence of the c(RGDfK) peptide did not affect the cell kill induced by the combination of doxorubicin/AN-9 in both 66cl4 cell lines. Therefore, at the concentration and treatment time

used, the c(RGDfK) peptide, while affecting cell adherence, does not interfere with the ability of doxorubicin/AN-9 to kill 66cl4 cells.

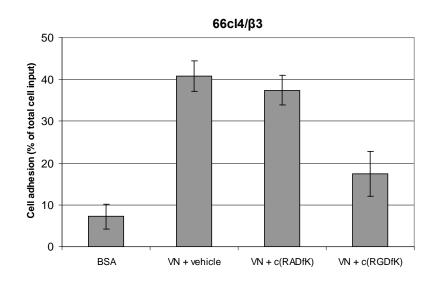
5.2.7 Mouse studies highlight the potential of targeting doxorubicin-DNA adducts to $\alpha v\beta 3$ integrin expressing tumours

Using the 66cl4 and 4T1.2 cell models, *in vitro* data from this study showed that doxorubicin-DNA adduct forming treatments are cytotoxic to cells expressing high levels of the $\alpha\nu\beta3$ integrin. Based on these findings, a Balb/c mouse model of spontaneous breast cancer metastasis was used to determine if doxorubicin-DNA adduct forming treatments could reduce $\alpha\nu\beta3$ integrin expressing 4T1.2 primary breast tumour growth, as well as the degree of metastasis *in vivo*. The major aims of the mouse studies were to assess the tolerability of doxorubicin-DNA adduct forming treatments and to determine if the treatments had any impact on reducing primary tumour growth or metastases. These preliminary studies could then be used to assess if RGD peptide-based $\alpha\nu\beta3$ integrin targeting strategies could be employed in this metastatic mouse model to enhance the efficacy of doxorubicin-DNA adduct-forming treatments in the future.

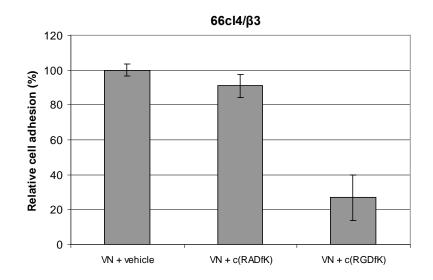
The cells used in this mouse model were 4T1.2/neo cells (transfected with a vector containing a neomycin resistance gene) which were injected into the fourth mammary fat pad of Balb/c mice. The 4T1.2/neo cells have been used previously in the same Balb/c mouse model and have been shown to express high levels of $\alpha\nu\beta3$ integrin and be highly metastatic to lymph nodes, lung, and bone (Eckhardt *et al.*, 2005). As anticipated, Figure 5.16 shows that *in vitro* the 4T1.2/neo cells (used subsequently in the mouse model) are sensitive to doxorubicin/AN-9 and doxorubicin/AN-7 treatments, with synergistic levels of cell death recorded (4T1.2/neo and 4T1.2/pRS cell lines are expected to behave identically).

Doxorubicin + orally administered AN-7

Initially, the formaldehyde-releasing prodrug AN-7 was chosen for the mouse model treatments with doxorubicin as it has high aqueous solubility and can be administered orally



В



Α

Figure 5.14. The c(RGDfK) peptide inhibits the ability of $\alpha\nu\beta3$ integrin overexpressing 66cl4 cells to adhere to vitronectin.

66cl4/β3 cells were incubated with calcein (10 µg/mL) for 45 min, washed, and incubated in the presence of either 500 µM c(RGDfK) or c(RADfK) peptides for 1 hr at 37 °C (Milli-Q water was used as the vehicle control). Cells were then added to culture plates coated with BSA (2% (w/v)) or vitronectin (VN) from human plasma (5µg/mL). Cells (20,000 cells/well) were allowed to adhere for 45 min and once non-adherent cells were removed by washing in PBS, cells were resuspended in 1% (v/v) Triton-X 100, calcein fluorescence intensity recorded, and the percentage of cells adhering relative to total cell input was determined. The raw percentage adhesion values are presented in (A), while in (B) the background adherence to BSA was subtracted from each sample and the percentage cell adhesion was standardized to the vehicle control sample which was given a value of 100% adhesion. Error bars represent the standard error of the mean from three independent experiments.

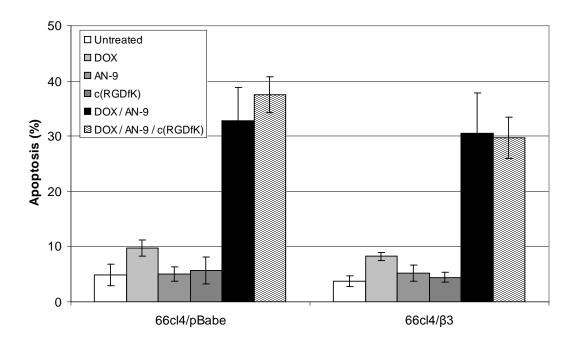


Figure 5.15. The c(RGDfK) peptide does not affect doxorubicin/AN-9 induced apoptosis.

66cl4 cells were treated with doxorubicin (500 nM), AN-9 (50 μ M), c(RGDfK) (50 μ M in 66cl4/pBabe cells and 500 μ M in 66cl4/ β 3 cells), and the combinations listed for 24 hr. The percentage of apoptotic cells was determined by sub-G1 FACS analysis. Error bars represent the standard error of the mean from three independent experiments.

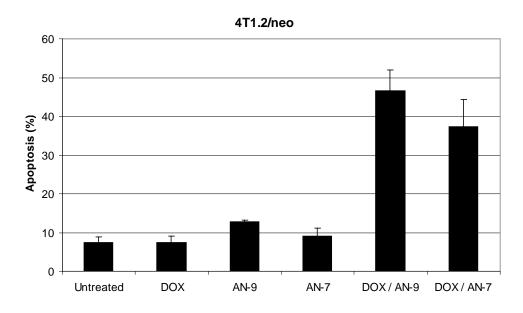


Figure 5.16. Doxorubicin-DNA adduct forming treatments are synergistic in 4T1.2/neo cells.

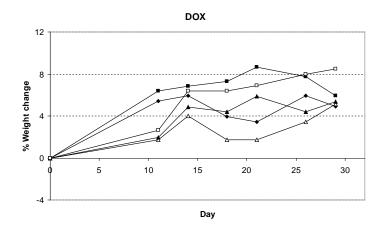
4T1.2/neo cells were treated with doxorubicin (250 nM), the formaldehyde-releasing prodrugs AN-9 and AN-7 (50 μ M), and the combination of doxorubicin with prodrugs for 36 hr. The percentage of apoptotic cells was determined by sub-G1 FACS analysis. Error bars represent the standard error of the mean from three independent experiments.

and as such the mice would be exposed to fewer injections. Furthermore, previous studies have used orally-administered AN-7 in combination with doxorubicin, resulting in enhanced anticancer activity in vivo relative to single agent treatments (Tarasenko et al., 2010; Tarasenko et al., 2012). In the first experiment (Figure 5.17), mice were treated with 2 mg/kg doxorubicin (intravenous tail vein) and the combination of doxorubicin with 100 mg/kg AN-7 (oral gavage), twice weekly for three weeks. Groups of untreated vehicle control mice or AN-7 treated mice were not included since these tolerability and efficacy studies were mainly focusing on benefits from doxorubicin/prodrug treatments over doxorubicin as a single agent. The mice in both groups did not display >10% weight loss (Figure 5.17A-B) or show signs of distress from the drug treatments over the three weeks, and as such the treatments were considered to be well-tolerated. Once the mice were culled, the primary tumour, spleen, and lungs were weighed to assess if the combination treatment had any anti-tumour or antimetastatic advantage over doxorubicin as a single agent. The 4T1.2 cells are highly metastatic to lungs (Eckhardt et al., 2005) and as such any anti-metastatic effects of the drug treatment may result in reduced lung weights. Furthermore, it has been demonstrated that the spleens of 4T1 tumour-bearing mice are typically enlarged (Kurt et al., 2003; Xanthopoulos et al., 2005), therefore, a reduction of spleen weight can be considered an indicator of reduced tumour burden. When the primary tumour, spleen, and lungs from the treated mice were weighed, no difference in the tissue weights were observed (Figure 5.17C), suggesting no anti-cancer advantage of the doxorubicin/AN-7 treatment relative to doxorubicin as a single agent.

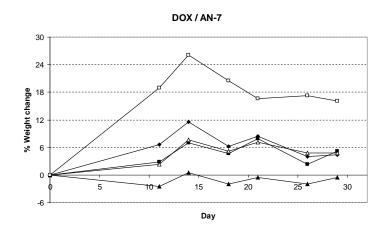
It was reasoned that the lack of anti-cancer benefit of the doxorubicin/AN-7 treatment may be due to insufficient formaldehyde reaching the tumour site, and as such DNA adduct levels may not have been high enough to result in a beneficial response. For this reason, the study was repeated with an additional dose of AN-7 (i.e. two doses of 100 mg/kg AN-7 administered orally following dosage of doxorubicin) in the prospect of increasing the level of formaldehyde at the tumour site. Once again, both the doxorubicin and doxorubicin/AN-7 treated groups tolerated the drug treatments with <10% weight loss recorded for all mice and no visible signs of distress observed throughout the duration of the study (Figure 5.18A-B). Upon culling, just as the previous study, no significant differences in the weights of the primary tumour, spleen, and lungs were observed between the two treatment groups (Figure 5.18C), indicating no advantage of the combination treatment. Furthermore, upon postmortem examination, lung metastases were evident in mice from both treatment groups.

Doxorubicin + intratumourally administered AN-9

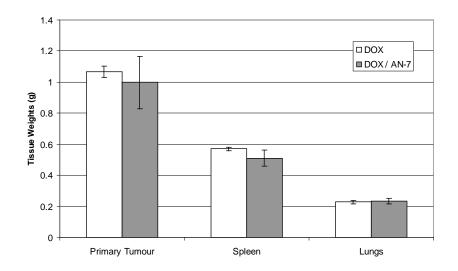
Based on the findings from the doxorubicin/AN-7 studies we decided to change the treatment modality of the formaldehyde-releasing prodrug. Instead of administering the AN-7 orally, where possibly only low levels of formaldehyde were reaching the tumour site, the prodrug AN-9 would be administered intratumourally. Intratumoural injections of AN-9 have been performed previously in an MDA-MB-231 mouse model, resulting in a reduction of tumour volume when combined with doxorubicin, relative to either prodrug or doxorubicin alone (see Figure 1.6, Cutts et al., unpublished data). By administering AN-9 directly into the tumour, this virtually guarantees high levels of formaldehyde at the tumour site, and thus can allow a conclusion to be made if doxorubicin-DNA adduct forming treatments have efficacy in this mouse model. For this experiment, mice were treated with either 2 mg/kg doxorubicin (intravenous tail vein), 100 mg/kg AN-9 (intratumoural injection), or the combination of both drugs. Because of several unexpected factors the mice only received four doses rather than the planned six, and one mouse in the combination treatment group did not develop a palpable tumour and was excluded from the treatment group. All the mice in the three treatment groups did not display >10% weight loss (Figure 5.19A-C) and showed no signs of distress for the duration of the experiment. Prior to culling, the primary tumour volumes were recorded and as shown in Figure 5.19D the doxorubicin/AN-9 treated mice possessed smaller tumour volumes relative to both the single agent groups. Likewise, upon post-mortem analysis, the primary tumour weights were lower for the doxorubicin/AN-9 treated mice (Figure 5.19E). There was no difference in the spleen and lung weights in all three groups, although visual analysis revealed greater levels of lung metastases in the AN-7 treated group relative to the other groups. Based on the findings of these preliminary mouse studies, there is some evidence to suggest that doxorubicin/AN-9 DNA adduct forming treatments have an efficacy advantage over both single agents in reducing primary tumour size, and as such may warrant further analysis in the future.







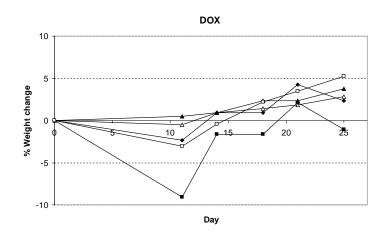




Α

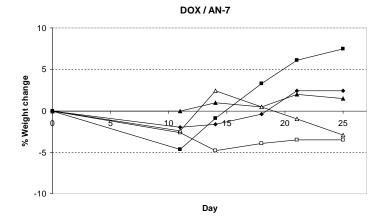
Figure 5.17. Tolerability and efficacy of doxorubicin in combination with orally administered AN-7 in a mouse model of spontaneous breast cancer.

Balb/c mice (two groups of five) were injected with 4T1.2/neo cells into the fourth mammary fat pad with treatment commencing seven days after implantation. Mice were treated with doxorubicin (2 mg/kg, 200 μ L intravenous tail vein injections in saline) alone and in combination with AN-7 (100 mg/kg, 200 μ L oral gavage in water, 30 min post doxorubicin injection), twice weekly for three weeks. Mice were treated on days 7, 11, 14, 18, 21, 26 and before each treatment the mice were weighed and evaluated for signs of distress. The percentage weight change for each individual mouse was recorded relative to the day of tumour cell implantation for both doxorubicin (A) and doxorubicin/AN-7 (B) treated mice. The mice were culled on day 32 and the average weight of the primary tumour, spleen, and lungs were recorded for each treatment group (C). Error bars in (C) represent the standard error of the mean recorded from the five mice per group.



В

Α



С

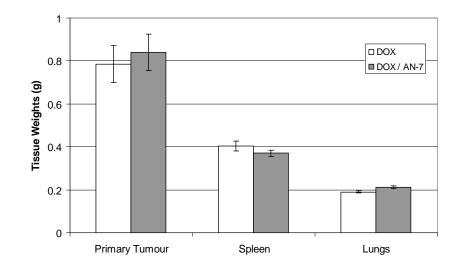
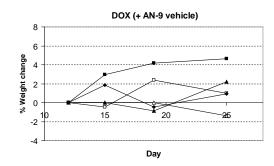
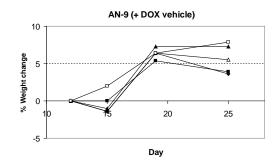
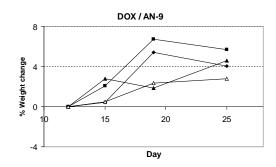


Figure 5.18. Tolerability and efficacy of doxorubicin in combination with a double dose of orally administered AN-7 in a mouse model of spontaneous breast cancer.

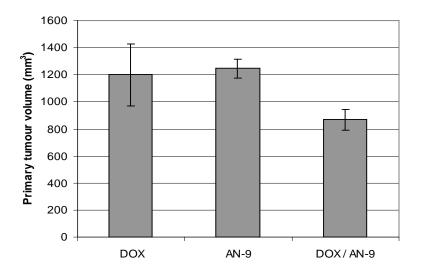
Balb/c mice (two groups of five) were injected with 4T1.2/neo cells into the fourth mammary fat pad with treatment commencing seven days after implantation. Mice were treated with doxorubicin (2 mg/kg, 200 μ L intravenous tail vein injections in saline) alone and in combination with a double dose of AN-7 (100 mg/kg, 200 μ L oral gavage in water, 30 min and 1 hr post doxorubicin injection), twice weekly for three weeks. Mice were treated on days 7, 11, 14, 18, 21, 25 and before each treatment the mice were weighed and evaluated for signs of distress. The percentage weight change for each individual mouse was recorded relative to the day of tumour cell implantation for both doxorubicin (A) and doxorubicin/AN-7 (B) treated mice. The mice were culled on day 27 and the average weight of the primary tumuor, spleen, and lungs were recorded for each treatment group (C). Error bars in (C) represent the standard error of the mean recorded from the five mice per group.







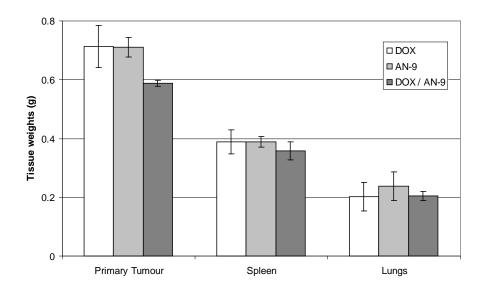
D



Α

В

С



Е

Figure 5.19. Tolerability and efficacy of doxorubicin in combination with intratumourally injected AN-9 in a mouse model of spontaneous breast cancer.

Balb/c mice (three groups of five) were injected with 4T1.2/neo cells into the fourth mammary fat pad with treatment commencing 12 days after implantation. Mice were treated with doxorubicin (2 mg/kg, 200 µL intravenous tail vein injections in saline), AN-9 (100 mg/kg, 20 µL intratumoural injection in DMSO, 30 min post doxorubicin injection), and the combination of both drugs twice weekly for two weeks (four treatments). The single agent treated mice also received a dose of the vehicle of the complimentary drug. Mice were treated on days 12, 15, 19, 25, and before each treatment the mice were weighed and evaluated for signs of distress. Note that one of the mice in the DOX/AN-9 group did not have a palpable tumour and as such was removed from the experiment. The percentage weight change for each individual mouse was recorded relative to the day of the first treatment for doxorubicin (A), AN-9 (B), and combination (C) treated mice. On day 27, the primary tumour volumes were measured (D), and on day 28 the mice were culled and the average weight of the primary tumour, spleen, and lungs was recorded for each treatment group (E). Error bars in (D) and (E) represent the standard error of the mean recorded from the mice in each treatment group.

5.3 **DISCUSSION**

5.3.1 The $\alpha\nu\beta$ 3 integrin is a highly suitable anti-cancer target

Cancer progression is considered to be a highly complex, multi-step process that differs for each individual, and it is essential to identify and understand the various proteins, complexes, and signalling pathways involved in order to develop specific drugs and targeting strategies against them. Several factors characterize a good anti-cancer target; 1) the target needs to be highly expressed on cancer cells with minimal expression on normal cells; 2) the target needs to have a well-defined role in promoting tumour growth and/or cancer progression; and 3) the target needs to possess features to make it easily amenable to targeting strategies. The $\alpha\nu\beta3$ integrin possesses such characteristics and as such has been identified as a key anti-cancer target.

The expression profile of the $\alpha\nu\beta3$ integrin is highly favourable, with low expression on most normal human tissues, and high expression on angiogenic endothelial cells and highly invasive tumour cells (Elicieri *et al.*, 1999; Wilder, 2002). Furthermore, cancer cells that possess a greater capacity to metastasize have been shown to express higher levels of the $\alpha\nu\beta3$ integrin (Wong *et al.*, 1998; Zheng *et al.*, 1999). This is observed with the cell models used in this project, since 4T1.2 cells which posses much greater metastatic potential than 66cl4 cells (Eckhardt *et al.*, 2005), expressed greater cell surface levels of $\beta3$ subunit (Figure 5.3; 4T1.2/pRS versus 66cl4/pBabe control cell lines), which in turn augments the levels of $\alpha\nu\beta3$ integrin heterodimers (Pereira *et al.*, 2004; Sloan *et al.*, 2006; Liu *et al.*, 2012).

While the main functions of integrins are as adhesion receptors that promote cell-cell and cell-matrix interactions, the downstream signalling events can regulate various cellular functions depending on the type of integrin and its ligand. In the case of the $\alpha\nu\beta3$ integrin (and other integrin types), evidence has shown that its downstream signalling plays a major role in promoting angiogenesis, cell migration, and invasion, all of which are key processes in tumour progression and metastasis (Brooks *et al.*, 1994a; Brooks *et al.*, 1994b; Brooks *et al.*, 1996; Sloan *et al.*, 2006). In this study it was observed that overexpression of the $\alpha\nu\beta3$

integrin (66cl4/ β 3 cells) promoted cancer cell adhesion to vitronectin (Figure 5.10A) and invasion through Matrigel (Figure 5.12), while knockdown of the $\alpha\nu\beta$ 3 integrin (4T1.2/sh β 3) reduced cancer cell adhesion to vitronectin (Figure 5.10B). While migration assays were not investigated in this study, previous studies have shown that in addition to promoting adhesion and invasion, the $\alpha\nu\beta$ 3 integrin also promoted migration (Eckhardt *et al.*, 2005; Sloan *et al.*, 2006). Considering that the processes of cell adhesion, migration, and invasion are implicated in angiogenesis and metastasis, it is evident that the $\alpha\nu\beta$ 3 integrin plays a definitive role in tumour progression.

The fact that integrins trigger the activation of so many molecules and pathways by the formation of focal adhesions means that they act as 'signalling hubs' that integrate a range of responses. This is another key feature that makes integrins such attractive targets, because although only the integrin itself is targeted, essentially a multitude of responses including pro-angiogenic or invasive cues can be inhibited concurrently. Therefore, while many anticancer targets affect only single pathways, the targeting of the $\alpha\nu\beta3$ integrin can result in a more pronounced inhibitory effect.

Many integrins including the $\alpha\nu\beta3$ integrin specifically bind to ligands possessing an RGD sequence, and this specificity has been exploited by designing RGD-containing peptides to target the $\alpha\nu\beta3$ integrin. This targeting strategy has proved to be successful to date as evident by the progression of the RGD peptide cilengitide to Phase II and III clinical trials (Mas-Moruno *et al.*, 2010). The use of RGD peptides for targeting and clinical applications will be discussed in greater detail in Section 5.3.5. Therefore, the $\alpha\nu\beta3$ integrin possesses all the necessary characteristics that make it an appealing anti-cancer target.

5.3.2 Doxorubicin-DNA adduct formation and resulting cytotoxicity is unaffected by $\alpha\nu\beta3$ integrin levels

While doxorubicin-DNA adduct forming treatments have been previously shown to induce synergistic levels of DNA adducts (Cutts et al., 2001; Cutts et al., 2005), and subsequently synergistic levels of cell death in a number of different cancer cell lines (Niitsu et al., 2000; Cutts et al., 2001; Cutts et al., 2005; Engel et al., 2006; Swift et al., 2006), the effect of high $\alpha v\beta 3$ integrin expression on doxorubicin-DNA adduct-forming treatments has not been investigated. If doxorubicin-DNA adduct forming treatments are to be successfully targeted to $\alpha v\beta \beta$ integrin expressing tumours, by RGD-based strategies or other means, then it is imperative that the cancer cells are susceptible to the mechanism of drug action, resulting in tumour-selective cytotoxicity. Two of the cell lines used in this project express high levels of $\alpha\nu\beta3$ integrin, either endogenously (4T1.2/pRS) or exogenously introduced (66cl4/ $\beta3$), and were used to assess if the presence of high $\alpha\nu\beta3$ integrin levels reduced the effectiveness of doxorubicin-DNA adduct forming treatments. Doxorubicin-DNA adduct formation appears to be unaffected by $\alpha\nu\beta3$ integrin levels with both overexpressing and knockdown cell lines displaying similar DNA adduct levels to control cell lines (Figure 5.4). The synergistic apoptotic response induced by the resultant doxorubicin-DNA adduct-formation was also unaffected by levels of $\alpha\nu\beta3$ integrin as observed in both the sub-G1 (Figure 5.6) and caspase-3 activation assays (Figure 5.8). Furthermore, the use of control compounds (AN-158 in combination with doxorubicin, and MEN-10755 in combination with AN-9) that do not result in DNA adduct formation, did not induce apoptosis (Figure 5.7). This highlights that the synergistic cell death response induced by doxorubicin in combination with either AN-9 or AN-7 is completely dependent on formaldehyde-mediated doxorubicin-DNA adduct formation. Therefore, while it was shown that high levels of $\alpha\nu\beta3$ integrin affect the degree of cancer cell adhesion (Figure 5.10) and invasion (Figure 5.12), it does not affect the ability of doxorubicin and formaldehyde-releasing prodrugs to enter cancer cells, form DNA adducts, and induce a synergistic apoptotic response.

5.3.3 RGD peptides can effectively inhibit $\alpha v\beta 3$ integrin function without affecting doxorubicin/AN-9 induced apoptosis

Since the $\alpha\nu\beta3$ integrin is now known to play an important role in angiogenesis and tumour progression, there has been considerable interest in inhibiting its function and developing anti- $\alpha\nu\beta3$ integrin tumour targeting strategies. The use of RGD peptides has proven to be successful in inhibiting the function of the $\alpha\nu\beta3$ integrin *in vitro* (Park *et al.*, 2008b), and *in vivo* by reducing angiogenesis and tumour growth (MacDonald *et al.*, 2001; Buerkle *et al.*, 2002). Since the primary action of integrins is to function as adhesion receptors to allow cells to adhere to the ECM and each other, it is expected that RGD peptide antagonists would impact on the cells adhesive capabilities.

Results from this study showed that the c(RGDfK) peptide affected the ability of the $\alpha\nu\beta3$ overexpressing 66cl4/ $\beta3$ cells to adhere to culture plates (Figure 5.13). Similar findings were observed in another study which showed that the RGD peptide cilengitide caused detachment of human endothelial and glioblastoma cells from culture vessels (Oliveira-Ferrer *et al.*, 2008). The c(RGDfK) peptide was also shown to affect the ability of 66cl4/ $\beta3$ cells to adhere to its endogenous ligand vitronectin (Figure 5.14). The c(RGDfK) peptide (500 μ M) was able to inhibit the adhesion of 66cl4/ $\beta3$ cells to vitronectin by approximately 75%, while the control c(RADfK) peptide had little effect on vitronectin adhesion, indicating an RGD sequence specific inhibitory effect. Therefore, it can be concluded that the RGD peptide is able to effectively bind to the $\alpha\nu\beta3$ integrin expressed on the surface of 66cl4/ $\beta3$ cells with sufficient affinity to competitively inhibit $\alpha\nu\beta3$ integrin adhesion to vitronectin. Previous studies have also shown that RGD peptides can effectively inhibit the adhesion of $\alpha\nu\beta3$ integrin expressing cells to ECM components, in the high nanomolar to low micromolar range (Kok *et al.*, 2002; Li *et al.*, 2007; Park *et al.*, 2008b).

In an *in vivo* setting, by inhibiting the adhesion of the $\alpha\nu\beta3$ integrin to vitronectin or other ECM ligands, RGD peptides can greatly affect the downstream events mediated by integrins. The lack of integrin ligation can prevent the formation of signalling hubs and the ability of the integrin to promote signalling events (outside-in signalling), thus preventing the induction of vital processes implicated in cancer progression such as migration and invasion.

Using concentrations of c(RGDfK) that caused 66cl4 cell detachment, it was demonstrated that the peptide did not affect the ability of doxorubicin/AN-9 treatment to induce apoptosis (Figure 5.15). This suggests that the RGD peptide is not interacting with the drugs, or affecting their entry into the cells, thus the doxorubicin/AN-9 combination is just as effectively able to kill 66cl4 cells in the presence of the peptide. The c(RGDfK) peptide itself did not induce apoptosis in the conditions used in these experiments, however, previous studies have shown that RGD peptides are able to induce caspase-dependent apoptosis in various cell lines (Maubant *et al.*, 2006; Oliveira-Ferrer *et al.*, 2008). This form of cell death termed anoikis, which results from detachment with the ECM, enables RGD peptides to kill av β 3 integrin expressing cancer cells in the absence of any targeted drugs/compounds. It is likely that if longer treatments times and/or higher c(RGDfK) peptide concentrations were used in this study, that apoptosis would be observed following detachment of 66cl4 cell lines.

5.3.4 Using a mouse model to evaluate the potential success of targeting doxorubicin-DNA adducts to $\alpha\nu\beta$ 3 integrin expressing tumours

Once it was established *in vitro* that doxorubicin/formaldehyde-releasing prodrug treatments induced synergistic cell kill in high $\alpha\nu\beta3$ integrin expressing cancer cells, a mouse model was used to determine if these treatments are tolerable and effective *in vivo*. A Balb/c syngeneic orthotopic mouse model of spontaneous breast cancer (Lelekakis *et al.*, 1999; Eckhardt *et al.*, 2005) was used for this study, which is a much better model compared to xenograft models. Most xenograft models of breast cancer are poorly metastatic to bone, and models of bone metastasis lack the presence of a primary tumour, and as such, many important tumour-host interactions are bypassed, including early stages of metastasis from the primary tumour (Eckhardt *et al.*, 2005; Sloan *et al.*, 2006). The use of the syngeneic orthotopic model allows both the effects on the primary tumour and metastases to be examined. Furthermore, the 4T1.2 cells used in this model closely mimic the metastatic distribution pattern of human breast cancer i.e. metastatic to bone, lung, and lymph nodes (Eckhardt *et al.*, 2005).

Treatments of doxorubicin (intravenous tail vein) as a single agent and in combination with both AN-7 (oral gavage) and AN-9 (intratumoural) were well tolerated with no weight loss greater than 10% being observed (Figures 5.17-5.19), and no visible signs of distress evident. Similar treatments were performed in a MDA-MB-231 breast cancer mouse model (see Section 1.7.2 and Figure 1.6) where both single agent (doxorubicin, AN-9, and AN-193) and combination treatments were also well tolerated (Cutts et al., unpublished data). The combination treatment of doxorubicin with the water soluble, orally administered AN-7 had no effect on primary tumour size and no evidence of an anti-metastatic advantage (based on lung and spleen weights and the presence of visible lung metastases in both treatment groups), relative to doxorubicin as a single agent (Figure 5.17C), even when a double-dose of AN-7 was administered to increase the amount of available formaldehyde (Figure 5.18C). Only when the formaldehyde-releasing prodrug AN-9 was administered intratumourally in combination with doxorubicin was there a reduction of primary tumour volume (Figure 5.19C) and primary tumour weight (Figure 5.19D), compared to both single agent treatment groups. This indicates that only when the formaldehyde-releasing prodrug is administered directly to the tumour that there is enough local formaldehyde release at the tumour site to enable sufficient doxorubicin-DNA adduct formation, and a resultant tumour size reduction. This was also observed in the MDA-MB-231 breast cancer mouse model (see Figure 1.6) where intratumoural but not intraperitoneal administration of the formaldehyde-releasing prodrugs AN-9 and AN-193 in combination with doxorubicin resulted in a reduction of primary tumour volume. Therefore, the results of both the MDA-MB-231 breast cancer model and this study suggest that unless the formaldehyde-releasing prodrugs are delivered to the tumour site, they become degraded by esterases in the bloodstream prior to reaching the tumour. Considering that intratumoural injections are not a clinically favourable method of drug administration, targeting strategies need to be developed to deliver sufficient formaldehyde to the tumour site (discussed further in Section 6.1.3).

In contrast, previous *in vivo* studies using a 4T1 mouse model have shown that the combination of doxorubicin with orally-administered AN-7 results in enhanced anticancer activity compared to single agent treatments (Tarasenko *et al.*, 2010; Tarasenko *et al.*, 2012). Even though the dose of AN-7 used in this present study was greater (100 mg/kg) compared to previous studies (25 and 50 mg/kg) to maximize formaldehyde release, no evidence of an anticancer benefit was observed with the combination treatment. This may be explained by

several differences between this study and previous studies, including the dose and route of administration of doxorubicin (intraperitoneal vs. intravenous) as well as the dosing schedules of both drugs. Therefore, fine-tuning the dosing and scheduling of both drugs may result in greater levels of DNA adduct formation at the tumour site, leading to greater anticancer efficacy.

Despite the fact that the results of the syngeneic orthotopic mouse model studies are preliminary, there is some evidence that the doxorubicin/AN-9 combination is effective against high $\alpha\nu\beta3$ integrin expressing primary tumours (Figure 5.19C-D). This anti-tumour advantage of the combination treatment over both single agents indicates that doxorubicin-DNA adduct formation is the major mechanism responsible for the tumour reduction. It should be noted that the mice only received four drug doses over two weeks rather than the planned six doses over three weeks, therefore, the anti-tumour effect seen may have been even more pronounced if the full dosing schedule was fulfilled. No anti-metastatic benefit, however, was observed with the doxorubicin/AN-9 combination. This may be due to the anti-tumour effects on the primary tumour occurring after the metastatic process was initiated, and for the same reason as to why intraperitoneal or oral administration of prodrugs were unsuccessful, not enough formaldehyde was able to reach the secondary metastatic sites to result in a beneficial response.

Overall, these mouse studies have shown some preliminary evidence to suggest that doxorubicin-DNA adduct-forming treatments can be potentially effective against high $\alpha\nu\beta3$ integrin expressing tumours, provided that the formaldehyde-releasing prodrugs are delivered to the tumour site. Therefore, these results warrant further studies with a larger cohort of mice to be conducted to investigate $\alpha\nu\beta3$ integrin targeting methods, for example with the use of RGD peptides, to allow sufficient DNA adduct formation specifically at the tumour site. Originally it was planned that RGD peptides linked to formaldehyde moieties would be tested in the mouse model in combination with doxorubicin, however, due to issues with the synthesis by collaborators, the RGD compounds did not get synthesized.

5.3.5 Clinical implications of RGD peptide-based targeting strategies

5.3.5.1 RGD peptides display a dual response

Studies have demonstrated that RGD peptides can have a dual response depending on the concentration of the peptide (Legler *et al.*, 2001; Reynolds *et al.*, 2009). It was discovered that low nanomolar doses of RGD peptides (including cilengitide) actually stimulated tumour angiogenesis and tumour growth in mouse models (Reynolds *et al.*, 2009), indicating that RGD antagonists exhibit a bell-shaped dose-response curve (Reynolds, 2010). Bell or U-shaped dose response curves have also been displayed by several other anti-angiogenic agents, reflecting a common clinical problem for anti-angiogenic therapy (Reynolds, 2010). When the mechanism behind this effect was investigated, evidence showed that RGD peptides at low nanomolar concentrations (but not micromolar concentrations) enhanced VEGF-mediated angiogenesis, which did not occur in the absence of VEGF (Reynolds *et al.*, 2009). Low RGD peptide doses induced an increase in VEGF receptor-2 (VEGFR2) and $\alpha\nu\beta3$ integrin recycling, thus, increasing cell migration to VEGF and subsequent angiogenesis (Reynolds *et al.*, 2009). Moreover, when VEGFR2 was inhibited with an antibody, this suppressed the ability of low doses of RGD peptides to promote tumour angiogenesis and tumour growth *in vivo* (Reynolds *et al.*, 2009).

These findings have important implications for the administration of RGD peptides since the plasma concentration of the RGD peptide can fall to nanomolar levels within a few hours and stimulate tumour growth (Reynolds *et al.*, 2009). Therefore, in clinical trials a relatively high concentration of RGD peptide must be administered or RGD peptides need to be co-administered with VEGF inhibitors to prevent this low-dose tumour stimulating effect (Strieth *et al.*, 2006; Reynolds, 2010). However, if the RGD peptide is used to target chemotherapeutics to $\alpha\nu\beta3$ integrin expressing tumours, then the low-dose tumour stimulating effect would be expected to be circumvented as long as the targeted chemotherapeutic is able to effectively kill the tumour cells.

5.3.5.2 RGD peptide-based targeting of chemotherapeutics

The targeting of chemotherapeutics to $\alpha\nu\beta3$ integrin expressing tumours poses a number of potential benefits that could lead to promising treatment outcomes in a clinical setting. First of all, targeting the $\alpha\nu\beta3$ integrin with RGD peptides inhibits the function of the integrin, thus preventing it from promoting adhesion (as observed in Figures 5.13-5.14), migration, invasion, and proliferation of tumour cells, hence minimizing tumour angiogenesis and metastasis. Furthermore, RGD peptides promote apoptosis (anoikis) in response to the integrin losing attachment to the surrounding ECM (Brooks *et al.*, 1994a; Frisch and Francis, 1994; Frisch and Screaton, 2001). Secondly, many chemotherapeutics, including doxorubicin, are associated with severe side-effects due to the exposure of normal cells to the drug. Therefore, by targeting the drug specifically to the tumour site its interactions with normal cells can be minimized, thus, reducing side-effects and increasing the clinical potential of the drug relative to systemic delivery.

Integrins undergo endocytosis and exocytosis (integrin recycling) and as such are able to internalize their ligands via clathrin dependent and independent processes (Bretscher, 1989; Memmo and McKeown-Longo, 1998; Dunehoo *et al.*, 2006; Sancey *et al.*, 2009; Ivaska and Heino, 2010). As such, studies have demonstrated that RGD peptides can become internalized (Cressman *et al.*, 2009a; Cressman *et al.*, 2009b; Sancey *et al.*, 2009). This internalization can allow RGD-targeted drugs to enter cells, thus, increasing the intracellular concentration of the drug and potentially increasing its efficacy.

Many RGD peptides are functionalized with various linker molecules to allow conjugation to chemotherapeutics, liposomes, radiolabels, and fluorescent probes (Dubey *et al.*, 2004; Dunehoo *et al.*, 2006; Desgrosellier and Cheresh, 2010). Most commonly used RGD peptides, including c(RGDfK) used in this study, contain a lysine residue, and the amino group on the lysine residue is an ideal site for chemical conjugation reactions (Chen and Chen, 2011). One major clinical application for RGD peptides is to deliver radiolabels and probes for cancer imaging and diagnostics (Chen *et al.*, 2004; Mitra *et al.*, 2005), and this has even been used to detect invasive $\alpha\nu\beta3$ integrin expressing tumours in humans (Haubner *et al.*, 2005; Bach-Gansmo *et al.*, 2006).

Several studies have demonstrated that the use of RGD peptide based targeting of chemotherapeutics to $\alpha\nu\beta3$ integrin expressing tumours can be a successful targeting strategy. Arap and colleagues (1998) coupled doxorubicin to an RGD-4C peptide and treated mice bearing human tumours derived from $\alpha\nu\beta3$ integrin expressing human breast cancer cells. Mice treated with the doxorubicin-RGD-4C conjugate displayed smaller tumours, less metastatic spread, and survived longer than mice treated with free doxorubicin. Furthermore, the doxorubicin-RGD-4C conjugate was less toxic to the heart and liver compared to free doxorubicin, indicating both a toxicity and efficacy advantage of targeting doxorubicin to $\alpha\nu\beta3$ integrin expressing tumour cells via RGD-peptides. In another study, Murphy and colleagues (2008) developed RGD-4C nanoparticles and used mouse models of $\alpha\nu\beta3$ integrin expressing tumours to demonstrate that doxorubicin-loaded RGD-nanoparticles reduced primary tumour growth, angiogenesis, and displayed a 15-fold increase in anti-metastatic activity compared to free doxorubicin.

Recently an RGD-peptide was identified that is able to penetrate into and disperse within tumour tissue far more effectively than conventional RGD-peptides (Sugahara *et al.*, 2009). This peptide termed iRGD (internalizing-RGD, CRGDK/RGPD/EC) binds to the $\alpha\nu\beta3$ integrin before becoming proteolytically cleaved, exposing a neuropilin-1 (co-receptor for VEGF receptors) binding motif which mediates entry into tumour tissue and cells. Treatment with the iRGD peptide causes a neuropilin-1 dependent increase in vascular permeability in the tumour, thus allowing enhanced tumour penetration of co-administered agents (Sugahara *et al.*, 2009; Sugahara *et al.*, 2010). It has been demonstrated that co-administration of iRGD with several agents including free doxorubicin, liposomal doxorubicin, abraxane, and the monoclonal antibody trastuzumab, markedly increased their tumour penetration in mouse models, thus increasing their efficacy (Sugahara *et al.*, 2010). The use of the tumour-penetrating iRGD-peptide has the advantage of not requiring any chemical conjugations with chemotherapeutics and due to the increased tumour penetration, can allow a lower dose of chemotherapeutics to be used to potentially minimize side-effects.

5.3.6 Conclusions

The $\alpha\nu\beta3$ integrin has been identified as a key player in promoting both angiogenesis and metastasis, and as such is a suitable candidate to target for the development of anti-cancer therapies. Using mouse mammary cancer cell lines it was shown that the $\alpha\nu\beta3$ integrin promotes cancer cell adhesion and invasion *in vitro*. This study also demonstrated that doxorubicin DNA adduct formation and resulting apoptosis induction are not affected by high levels of $\alpha\nu\beta3$ integrin, highlighting that highly invasive $\alpha\nu\beta3$ integrin expressing tumours may be sensitive to the effects of DNA adduct formation. Mouse studies provided some evidence that doxorubicin-DNA adduct formation can reduce the growth of $\alpha\nu\beta3$ integrin expressing tumours, provided that formaldehyde is readily available at the tumour site (via intratumoural injections of AN-9). Furthermore, the use of an RGD peptide was shown to inhibit $\alpha\nu\beta3$ integrin-mediated cancer cell adhesion, without affecting doxorubicin/AN-9 induced cytotoxicity. Taken together, these findings provide a preliminary framework to suggest that the targeting of doxorubicin-DNA adduct formation to $\alpha\nu\beta3$ integrin expressing tumours, via RGD peptides, may prove to be a promising anticancer targeting strategy. Chapter 6

GENERAL DISCUSSION & FUTURE DIRECTIONS

6.1 GENERAL DISCUSSION

The major aim of this research project was to investigate potential avenues for improving the anticancer potential of anthracycline-DNA adduct forming treatments. Over recent years, *in vitro* research in the Cutts/Phillips laboratory has demonstrated that anthracycline-DNA adduct formation can be a potentially promising anticancer treatment method, compared to doxorubicin as a single agent. In particular, the MDA-MB-231 mouse model studies (see Figure 1.6) have provided a proof of principle that when formaldehyde-releasing prodrugs are available in the vicinity of the tumour, the combined antitumour effect of doxorubicin and prodrug is profound due to the formation of DNA adducts at the tumour site.

The two major factors which could limit the therapeutic potential of any chemotherapeutic regimen are resistance and side effects, and it is a challenge to cancer research to be able to limit the effects of these factors in order to increase the efficacy of anticancer drugs. This project looked at Bcl-2 mediated resistance, which is a major form of intrinsic resistance in many cancer types, limiting the effectiveness of a wide range of chemotherapeutic drugs. This project also looked at using the $\alpha\nu\beta3$ integrin as a candidate to develop a targeting strategy to specifically direct doxorubicin-DNA adduct formation to high $\alpha\nu\beta3$ integrin expressing tumours, in order to limit side-effects and increase anticancer efficacy. This discussion will focus firstly on the advantages of anthracycline-DNA adduct formation as a potential anticancer therapy, before discussing how the findings from this project may enhance the anticancer efficacy of anthracycline-DNA adduct forming treatments.

6.1.1 Advantages of Anthracycline-DNA Adduct Formation

The formation of anthracycline-DNA adducts is a completely independent mechanism of action to topoisomerase-II poisoning, as has been demonstrated in this project using both doxorubicin/AN-9 (Figure 3.20) and doxazolidine (Figure 4.2), and offers some vital advantages which may be beneficial in a clinical setting. The combination of doxorubicin with formaldehyde-releasing prodrugs results in synergistic and highly cytotoxic DNA adducts (see Figure 3.23) which can allow much lower doses of doxorubicin to be used in

order to achieve comparable levels of cell kill to doxorubicin as a single agent. The use of lower doses of doxorubicin would be expected to reduce the severity of side-effects and improve quality of life for patients undergoing treatment. This is especially important considering that doxorubicin treatment is hampered by dose-limiting cardiotoxicity, so the use of lower doses can potentially reduce cardiotoxic effects and prolong treatment duration. Furthermore, the activation of doxorubicin to form DNA adducts allows new opportunities to localize DNA adduct formation to tumour cells by targeting the activating agents that release formaldehyde specifically to tumour cells (potential targeting mechanisms will be discussed in Section 6.1.3).

6.1.1.1 Cardiotoxicity

Formaldehyde-releasing prodrugs display low toxicity and are well tolerated in patients (Patnaik et al., 2002; Reid et al., 2004). Studies have shown that formaldehyde-releasing prodrugs display preferential toxicity against cancer cells compared to normal cells, including normal mononuclear cells (Rephaeli et al., 2006), normal astrocytes (Entin-Meer et al., 2005; Rephaeli et al., 2006; Tarasenko et al., 2010), and cardiomyocytes (Tarasenko et al., 2010), although the mechanism remains unclear. Further evidence indicates that formaldehyde-releasing prodrugs may reduce doxorubicin-induced cardiotoxic effects. The formaldehyde-releasing prodrugs AN-7 and AN-1 were shown to protect against doxorubicin-induced damage to rat cardiomyocytes in vitro and in a mouse model, while acetaldehyde-releasing prodrugs did not (Rephaeli et al., 2007). This implies that the formaldehyde released and subsequent doxorubicin-DNA adduct formation is critical in the protection of cardiomyocytes from doxorubicin toxicity. This may be explained by the notion that as DNA adducts are formed, less free drug is exposed to enzymes that catalyse redox cycling and thus less ROS are produced (Tarasenko et al., 2010), leading to a reduction in cardiotoxic effects. Furthermore, the doxorubicin-formaldehyde conjugate doxazolidine was shown to be more effective in inhibiting cancer cell growth, but not cardiomyocytes, relative to doxorubicin, indicating that the conjugate is not more cardiotoxic despite its greater anticancer activity (Kalet et al., 2007).

6.1.1.2 Resistance

The formation of doxorubicin-DNA adducts appears to overcome the two major mechanisms of resistance to doxorubicin. In cells that overexpress membrane efflux pumps (Cutts et al., 2005; Post et al., 2005; Engel et al., 2006; Cutts et al., 2007; Fenick et al., 1997), or have reduced topoisomerase-II levels (Cutts et al., 2005; Swift et al., 2006; Kalet et al., 2007), and thus are resistant to doxorubicin as a single agent, doxorubicin-formaldehyde conjugates or the combination of doxorubicin with formaldehyde-releasing prodrugs, are highly cytotoxic. When doxorubicin undergoes formaldehyde-mediated covalent-linkages to DNA it renders the drug less available as a substrate for membrane efflux pumps, therefore, as free drug continues to be pumped out of cells, covalently bound drug remains in the nucleus and is able to induce cell kill. Doxorubicin-formaldehyde conjugates are also more lipophilic and uncharged in comparison to doxorubicin making them less suitable substrates for membrane efflux pumps (Lampidis et al., 1997; Post et al., 2005). Furthermore, as DNA adduct formation is an independent mechanism of action to topoisomerase-II poisoning, unlike doxorubicin, doxorubicin-formaldehyde conjugates and the combination of doxorubicin with formaldehyde-releasing prodrugs, are able to induce cell kill in cells with low topoisomerase-II levels (Cutts et al., 2005; Swift et al., 2006; Kalet et al., 2007). The ability of DNA adduct formation to overcome conventional doxorubicin resistance mechanisms may allow high levels of cell kill to be achieved in tumours that were previously resistant to doxorubicin treatment, which is a major clinical advantage as it broadens the spectrum of cancers which doxorubicin may be used as a treatment.

6.1.2 Overcoming Bcl-2 Mediated Resistance

The overexpression of Bcl-2 and other anti-apoptotic proteins is one of the major factors contributing to inherent resistance of cancer cells to a wide range of cytotoxic agents, including doxorubicin as a single agent and the DNA adduct forming treatment of doxorubicin/AN-9 (see Figure 3.8). The BH3 mimetics ABT-737 and ABT-263 have proven to be the most successful compounds to date in overcoming Bcl-2 mediated resistance, and the data presented in Chapter 3 demonstrates that ABT-737 is able to overcome Bcl-2 mediated resistance to doxorubicin-DNA adduct forming treatments in HL-60 cells, with

high levels of synergistic cell kill being observed (see Figure 3.10). The findings from this project suggest that using ABT-737 as part of a triple treatment (ABT-737/doxorubicin/AN-9) would increase the clinical potential of DNA adduct forming treatments in Bcl-2 overexpressing cancer types that would otherwise be resistant to doxorubicin.

In response to doxazolidine treatment, the Bcl-2 mediated resistance in HL-60 cells, however, was shown to be only short-lived. Therefore, it appears that Bcl-2 is able to delay apoptotic cell death but not prevent it indefinitely. This short-lived Bcl-2 mediated resistance was also observed in this project in response to doxorubicin/AN-9 (Figure 4.11) and doxorubicin treatment (Figure 4.12), and previous studies have demonstrated similar findings using other drugs and other cell lines (Allouche *et al.*, 1997; Hoetelmans *et al.*, 2003; Huigsloot *et al.*, 2003; Liang *et al.*, 2010). Therefore, despite certain cancer cells displaying high levels of Bcl-2, it seems that the damage caused by certain drugs may overwhelm the cells ability to repair the damage, and eventually the cell is committed to death by apoptosis. The mechanism responsible for overcoming Bcl-2 resistance undoubtedly involves components of the Bcl-2 protein family, with the key factor most likely being changes in the relative ratios of individual pro- and anti-apoptotic family members, or changes in the levels of specific complexes such as the Bcl-2/Bax complex. The trigger point for apoptosis induction is very finely poised, and slight changes in the ratio of one protein to another may be sufficient to drive apoptosis.

The findings from this project raise the question of how much of a need is there for Bcl-2 inhibitors such as ABT-737 if certain drugs such as doxazolidine (in certain cancer cell types) are able to overcome resistance on their own? It would be an advantage if additional inhibitors were not required for therapy as the inclusion of extra compounds may lead to the induction of greater side-effects and dosing complications. However, the ability of drugs to overcome Bcl-2 mediated resistance may be limited to a narrow spectrum of cancer types. Furthermore, this effect is time dependent, as observed in this project with cell kill in response to doxazolidine treatment only observed ≥ 18 hr in HL-60/Bcl2 cells (Figure 4.6), and probably concentration dependent as well. Considering that one of the major goals for any anticancer therapy to be successful is to eradicate tumour cells as rapidly and efficiently as possible, any time delays in cancer cell death induction may be critical. An additional round of replication of cancer cells provides the opportunity for surviving cancer cells to

undergo mutations, potentially allowing invasion and metastasis to secondary sites in the body. Therefore, the inclusion of fast-acting Bcl-2 inhibitors such as ABT-737 may still be essential to enable the kill of as many cancer cells as possible, as quickly as possible, before they are able to invade and spread. Ultimately, extensive *in vivo* testing is required to determine if short-lived Bcl-2 mediated resistance also occurs in high Bcl-2 expressing tumour models, or whether anti-tumour effects are only observed with the inclusion of Bcl-2 inhibitors.

6.1.3 Targeting Anthracycline-DNA Adducts to Tumours

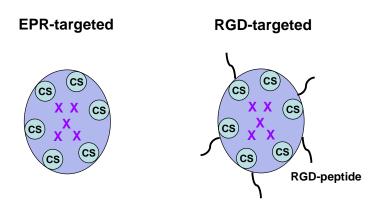
Targeting of anticancer agents specifically to tumour cells is a major focus of cancer research as it can potentially reduce side-effects and allow lower doses of drug to be used. In this project the $\alpha\nu\beta3$ integrin was examined as a potential target to deliver DNA adduct forming treatments to tumours via RGD-peptides. With the success of RGD-peptide based targeting of chemotherapeutics and radiolabels (Arap *et al.*, 1998; Chen *et al.*, 2004; Mitra *et al.*, 2005), and the high sensitivity of $\alpha\nu\beta3$ integrin expressing tumour cells to doxorubicin-DNA adduct forming treatments (Figure 5.6), the development of a strategy to target doxorubicin-DNA adducts to invasive, high $\alpha\nu\beta3$ integrin expressing tumours, may prove to be a promising anti-cancer therapy.

One such targeting approach would be to administer doxorubicin systemically while targeting formaldehyde specifically to $\alpha\nu\beta3$ integrin expressing tumours, thus, promoting the formation of high levels of DNA adducts only within tumour cells. The development of RGD-peptides (cyclic RGDfK) conjugated to multiple formaldehyde moieties was planned (Tad Koch, University of Colorado, Boulder, personal communication). It was proposed that these RGD-polyformaldehyde conjugates would bind to $\alpha\nu\beta3$ integrin expressing tumour cells, after which the formaldehyde oligomer would be hydrolysed, releasing several formaldehyde molecules, which together with systemically administered doxorubicin would allow the formation of doxorubicin-DNA adducts specifically at the tumour site (it should be noted that due to issues with the synthesis by collaborators, these conjugated RGD peptides were not synthesized). The success of this particular strategy may be limited by the same

reason that most likely prevented intraperitoneal (Cutts *et al.*, unpublished data) and orally administered (Figures 5.17-5.18) formaldehyde-releasing prodrugs, when combined with doxorubicin, from inducing anti-tumour effects in mouse models. There is a high likelihood that the polyformaldehyde group will be degraded by enzymes in the bloodstream before reaching the tumour site. Considering that intratumoural injections are not a clinically favourable method for drug administration, the encapsulation of formaldehyde-releasing prodrugs into nanoparticles may be a potential solution to overcome the problem of premature release of formaldehyde.

The use of nanoparticles for drug delivery is an effective method for preventing the interaction of drugs with normal cells to reduce systemic toxicities and side-effects. Furthermore, nanoparticles are able to passively accumulate at the tumour site due to the EPR effect (Maeda et al., 2000; Wang et al., 2012). One method that is currently being investigated in the Cutts/Phillips laboratory is the use of chitosan nanoparticles to covalently encapsulate and deliver formaldehyde-releasing prodrugs to the tumour site (Figure 6.1A). Chitosan possesses several favourable properties such as non-toxicity, low immunogenicity, can undergo self-assembly into nanoparticles, and is amenable to chemical conjugation (Park et al., 2010). Chitosan-based nanoparticles have been used to deliver the chemotherapeutic cisplatin to tumours via the EPR effect, thus increasing its efficacy and reducing toxicity (Kim et al., 2008). Furthermore, chitosan nanoparticles have been conjugated to a cyclic RGD-peptide, resulting in effective delivery of siRNA to $\alpha\nu\beta3$ integrin expressing tumours in vivo and subsequently causing inhibition of tumour growth (Han et al., 2010). Formaldehyde-releasing prodrugs have been conjugated to chitosan and subsequently encapsulated upon formation of chitosan-nanoparticles (stabilized by tripolyphosphate), and these loaded nanoparticles are approximately 150 nm in size (Masarudin et al., unpublished data), thus potentially allowing passive tumour targeting via the EPR effect. The formaldehyde-releasing prodrugs slowly become released from the nanoparticles over time (Masarudin et al., unpublished data), potentially allowing high levels of formaldehyde release and high levels of DNA adduct formation with systemically administered doxorubicin, at the tumour site.

The conjugation of RGD-peptides to chitosan-nanoparticles to allow specific targeting to $\alpha\nu\beta3$ integrin expressing tumour cells is also proposed (Figure 6.1B). These RGD-chitosan-



В

Α

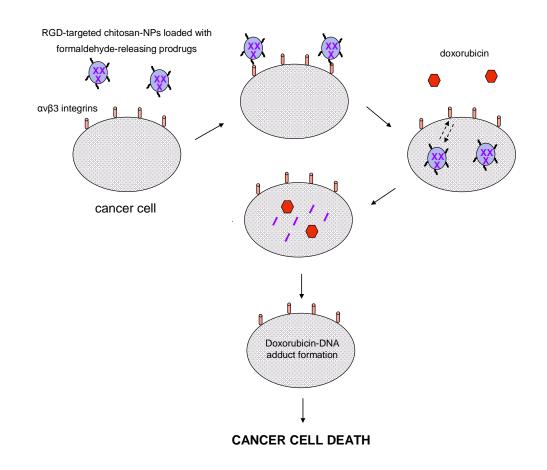


Figure 6.1. Model of targeting doxorubicin-DNA adduct formation to $\alpha\nu\beta$ 3 integrin expressing tumour cells via chitosan-loaded nanoparticles.

Chitosan nanoparticles are a promising delivery method for chemotherapeutics as they can accumulate at the tumour site via the EPR effect, but can also be modified to potentially link RGD-peptides to the surface of the nanoparticles (A). It is proposed that upon synthesis of RGD-targeted chitosan nanoparticles, formaldehyde-releasing prodrugs can be encapsulated following conjugation to chitosan and delivered to $\alpha\nu\beta3$ integrin expressing tumour cells (B). The RGD-peptide moiety can bind to $\alpha\nu\beta3$ integrins on the cell surface and the nanoparticles can subsequently become internalized via endocytosis as part of the integrin recycling process. Doxorubicin can be administered systemically and will passively enter cells and react with the released formaldehyde from the prodrugs to form DNA adducts in the nucleus. Therefore, this targeting method has the potential to specifically kill high $\alpha\nu\beta3$ integrin expressing tumour cells without affecting normal cells, leading to a potential reduction of side-effects.

nanoparticles can be loaded with formaldehyde-releasing prodrugs, and upon RGD-based binding with $\alpha\nu\beta3$ integrins expressed on the tumour cell surface, the nanoparticles can become internalized. This can allow high levels of formaldehyde release within the cancer cells, which together with systemically administered doxorubicin, can result in high levels of DNA adduct formation. Since the RGD-chitosan nanoparticles should not interact with most normal cells that express very low levels of $\alpha\nu\beta3$ integrin, it is proposed that this strategy will specifically result in high levels of tumour cell kill, thus potentially allowing lower doses of doxorubicin to be used, hence reducing adverse side-effects.

The design and synthesis of doxorubicin-formaldehyde conjugates, such as doxazolidine, has provided a more effective means of DNA adduct formation, leading to higher levels of cytotoxicity compared to doxorubicin/AN-9 and doxorubicin treatments (see Figure 4.2). This led to the further development of more stable conjugate compounds, including doxsaliform (Cogan et al., 2004), PPD (Burkhart et al., 2006), and GaFK-DOXAZ (Barthel et al., 2012) which are more suitable candidates to use in tumour targeting strategies. Burkhart and colleagues (2004) conjugated doxsaliform to RGD peptides and demonstrated that these targeted conjugates had a good binding affinity for the $\alpha\nu\beta\beta$ integrin and were as effective as untargeted doxsaliform in inhibiting breast cancer cell growth. Since doxsaliform displays a half-life of approximately 1 hr (Burke and Koch, 2004; Cogan et al., 2004), the RGD-targeted doxsaliform conjugates can potentially accumulate at the tumour site, bind to $\alpha\nu\beta3$ integrin expressing cancer cells, and result in high levels of DNA adducts. Furthermore, encapsulating the more stable doxorubicin-formaldehyde conjugates into RGD-nanoparticles may be an even more efficacious targeting strategy than using formaldehyde-releasing prodrugs and warrants future investigation. Moreover, it may be possible to link RGDpeptides directly to stable doxorubicin-formaldehyde conjugates, which would eliminate the need for nanoparticles.

6.2 CONCLUSIONS

This project aimed to investigate methods for enhancing the anti-cancer activity of anthracycline-DNA adduct forming treatments. Although anthracycline-DNA adduct forming treatments at this stage are not in clinical use, by carrying out extensive *in vitro* and *in vivo* research, the potential future clinical applications of such treatments may be enhanced. By tackling the two most important issues encountered in a clinical setting, namely resistance and side-effects, the potential clinical scope of anthracycline-DNA adduct forming treatments could be broadened.

This project demonstrated that cancer cells that express high levels of anti-apoptotic proteins such as Bcl-2, may be non-responsive to anthracycline-DNA adduct forming treatments, to a certain degree. The addition of the Bcl-2 inhibitor ABT-737 was able to overcome the resistance mediated by Bcl-2 in HL-60 cells, thus killing previously resistant cancer cells, which is a major clinical advantage. This project also showed that anthracycline-DNA adduct forming treatments were able to overcome Bcl-2 mediated resistance on their own accord, over longer treatment times. This suggests that under certain circumstances, Bcl-2 resistance may only be short-lived, and that cancer cells begin to die over time in response to the DNA damage sustained. This finding is also of clinical importance as it suggests that high Bcl-2 expressing tumours may still be (at least partially) responsive to anthracycline-DNA adduct forming treatments.

This project also demonstrated that targeting the $\alpha\nu\beta3$ integrin may be a successful strategy for delivering anthracycline-DNA adduct forming treatments specifically to tumour cells. Anthracycline-DNA adduct forming treatments were shown to kill high $\alpha\nu\beta3$ integrin expressing cancer cells and the combination of doxorubicin and intratumoural AN-9 was able to cause a reduction in tumour volume and weight, relative to single agent treatments in a mouse model. The use of RGD peptides which bind to and inhibit $\alpha\nu\beta3$ integrin function may provide a future means for delivering formaldehyde-releasing prodrugs loaded into nanoparticles, to tumour sites, enabling high levels of DNA adduct formation and high levels of tumour cell kill. Overall, the major findings from this project provide a foundation for overcoming Bcl-2 mediated chemoresistance as well as reducing side-effects in response to anthracycline-DNA adduct forming treatments. With continued research by the Cutts/Phillips laboratory, particularly in *in vivo* settings, it may be possible to consider anthracycline-DNA adduct forming treatments for clinical use, and therefore the findings from this project provide avenues for enhancing the anticancer potential for such drug treatments.

6.3 FUTURE DIRECTIONS

6.3.1 Overcoming Bcl-2 Resistance with ABT-737 / ABT-263

The main disadvantage with the potential use of ABT-737 in the clinic is that it possesses low aqueous solubility and a lack of oral bioavailability. The second generation inhibitor ABT-263 was designed to combat these issues and make the compound more amenable to clinical use (Park *et al.*, 2008a; Tse *et al.*, 2008). For this reason, ABT-737 could be replaced with ABT-263 to make the 'triple treatment' (doxorubicin/AN-9/ABT-737) more clinically favourable. Since ABT-263 functions via the same mechanism and has been shown to display a similar efficacy to ABT-737 (Tse *et al.*, 2008), it would be expected that the use of ABT-263 in the triple treatment would just as effectively overcome Bcl-2 mediated resistance to doxorubicin-DNA adduct forming treatments as ABT-737, however this remains to be tested.

Both ABT-737 and ABT-263 display a low affinity for Mcl-1 and as shown in Figure 3.31, knockdown of Mcl-1 in HCT116 cells resulted in increased sensitivity to ABT-737 as a single agent. To extend this finding further, the cells can be treated with the triple treatment following Mcl-1 knockdown to determine the success of doxorubicin-DNA adduct forming treatments when both Bcl-2 and Mcl-1 are neutralized. Therefore, if in the future a successful Mcl-1 inhibitor is developed this may then be added to the triple treatment to broaden its therapeutic potential to treat cancer cells which express high levels of both Bcl-2 and Mcl-1.

Ultimately, the triple treatment should be assessed *in vivo* in a Bcl-2 overexpressing mouse model. Therefore, it can be determined if Bcl-2 overexpression confers resistance to doxorubicin/AN-9 treatment *in vivo*, and if the addition of ABT-737 or ABT-263 is able to overcome this resistance. Positive responses to such *in vivo* studies would provide a strong case that the triple treatment may be a clinically viable treatment for Bcl-2 overexpressing cancers.

6.3.2 Short-Lived Bcl-2 Mediated Resistance

This study showed that Bcl-2 overexpressing HL-60 cancer cells become increasingly sensitive to doxazolidine (as well as doxorubicin/AN-9 and doxorubicin treatments) over time with classical apoptosis being observed. An important question that needs to be addressed is: how widely spread is this overcoming Bcl-2 resistance effect? By treating multiple cancer cell lines that overexpress Bcl-2 with doxazolidine, will allow a conclusion to be made if this effect is cell-type specific or a broader phenomenon. Also, chemotherapeutics that function via different mechanisms can be tested in HL-60/Bcl2 cells to determine if this effect is specific in response to DNA damaging agents or not. Therefore, a clearer picture can be gained as to what types of agents are able to overcome resistance and what types of agents do not.

More in-depth analysis can be performed to determine the exact mechanisms at play for overcoming Bcl-2 mediated resistance in response to doxazolidine. The mass spectrometry analysis performed to identify potential Bcl-2 binding partners was not completed until the very end of the experimental work for this thesis, therefore, experimental validation is required to gain a clearer understanding if any interactions are indeed responsible for overcoming resistance over time.

The pro-apoptotic protein Bim was identified by mass spectrometry as a potential Bcl-2 binding partner upon doxazolidine treatment, therefore this finding should be confirmed by the anti-FLAG co-IP assay. The regulation of any Bim/Bcl-2 interactions over time could also be investigated to determine if there are transcriptional or post-transcriptional factors at

play. Furthermore, anti-FLAG co-IP analysis could also be performed to determine if nucleophosmin or THRAP3 (also identified by mass spectrometry) interact with Bcl-2 at all in response to doxazolidine. Mass spectrometry could also be performed to identify potential Bcl-2 binding partners in response to doxorubicin/AN-9 and doxorubicin treatments that induce apoptosis over time. It is possible that different proteins are responsible for overcoming Bcl-2 resistance in response to different agents and types of DNA damage. A previous study identified an increase in the 14-3-3 σ protein as a possible mechanism for overcoming resistance in response to B1 treatment in HL-60/Bcl2 cells (Liang *et al.*, 2010), therefore, expression levels of this protein could also be determined over time in response to doxazolidine.

Ultimately, *in vivo* studies will provide a more meaningful picture to the overall significance of short-term Bcl-2 resistance. Using Bcl-2 overexpressing tumour mouse models, and treating the mice with doxazolidine will determine if any resistance is short-lived or long-term. Also, the addition of ABT-737/ABT-263 to doxazolidine as a treatment group, may allow a conclusion to be made as to the importance of using Bcl-2 inhibitors versus relying on chemotherapeutics to overcome resistance on their own.

6.3.3. RGD-Based Targeting of DNA Adduct Forming Treatments to αvβ3 Expressing Cancer Cells

In vitro

The RGD peptide used in this study was shown to inhibit the ability of the $\alpha\nu\beta3$ integrin to adhere to vitronectin, however, more in depth analysis could be performed to investigate other assays related to angiogenesis and metastasis. The RGD peptide could be incorporated into Matrigel-based cell invasion and migration assays using the 66cl4 and 4T1.2 cell lines to determine if the peptide inhibits the ability of the $\alpha\nu\beta3$ integrin to promote these processes as well.

Furthermore, other high $\alpha\nu\beta3$ integrin expressing cell lines could be used to assess the effectiveness of the combination of RGD peptides with doxorubicin/AN-9 treatment. For

example, human umbilical vein endothelial cells (HUVECs) have been shown to express high levels of $\alpha\nu\beta3$ integrin (Murphy *et al.*, 2008; Cressman *et al.*, 2009a) and when grown on Matrigel form tubule-networks which are characteristic of angiogenesis. Therefore, using RGD peptides in this assay to determine if tubule-network formation is inhibited is a good indicator that the peptide is affecting angiogenesis. HUVECs could then be co-treated with RGD peptides and doxorubicin/AN-9 to determine if any additive or synergistic cell kill is observed.

The development of RGD-targeted chitosan-nanoparticles is proposed. Chitosannanoparticles have already been shown to encapsulate formaldehyde-releasing prodrugs upon conjugation, and by linking RGD-peptides to the nanoparticles, this allows the nanoparticles to be targeted specifically to high $\alpha\nu\beta3$ expressing cancer cells. Once developed, the RGDchitosan-nanoparticles can be tested in 66cl4/ $\beta3$ and 4T1.2/pRS cells to determine if they inhibit binding of the cells to vitronectin. Ultimately, the RGD-chitosan-nanoparticles can be tested for their ability to encapsulate formaldehyde-releasing prodrugs, and can be used to treat high and low $\alpha\nu\beta3$ expressing 66cl4 and 4T1.2 cells, together with doxorubicin, and the levels of DNA adducts can be measured to determine the success of this potential targeting strategy.

In vivo

Preliminary *in vivo* experiments in this study showed some evidence that the combination of intravenous doxorubicin with intratumoural AN-9 displayed anti-tumour activity relative to the single agents (Figure 5.19C-D). In this experiment, the mice received only four of the scheduled six doses, therefore, repeating this experiment again with the full dosing schedule may reveal an even greater anti-tumour response with the combination treatment. The number of mice per group could also be increased (from 5 to 10) as well as including a vehicle control group. Furthermore, regular tumour size measurements could be performed during the course of the experiment to provide a more thorough analysis to monitor any anti-tumour effects more closely.

Since intratumoural injections are not a preferred clinical option, other means of administering sufficient formaldehyde levels at the tumour site need to be tested. If RGD-chitosan-nanoparticles are successfully developed and are able to encapsulate formaldehyde-

releasing prodrugs, the aim would be to test these nanoparticles in the Balb/c syngeneic orthotopic mouse model of spontaneous breast cancer used in this project. The prodrug-loaded RGD-chitosan-nanoparticles could be administered intravenously (instead of intratumourally), together with intravenously injected doxorubicin, and the effect of this targeting strategy can be assessed by analysis of tumour size, as well as angiogenesis (Matrigel plug assay) and metastasis assays (PCR for expression of tumour reporter gene in different organs).

Chapter 7

REFERENCES

- Ackler, S., Xiao, Y., Mitten, M. J., Foster, K., Oleksijew, A., Refici, M., et al. (2008) Mol Cancer Ther 7, 3265-3274
- Ackler, S., Mitten, M. J., Foster, K., Oleksijew, A., Refici, M., Tahir, S. K., et al. (2010) Cancer Chemother Pharmacol 66, 869-880
- Adair, B. D., Xiong, J. P., Maddock, C., Goodman, S. L., Arnaout, M. A., and Yeager, M. (2005) J Cell Biol 168, 1109-1118
- Adams, J. M., and Cory, S. (2007) Curr Opin Immunol 19, 488-496
- Albelda, S. M., Mette, S. A., Elder, D. E., Stewart, R., Damjanovich, L., Herlyn, M., *et al.* (1990) *Cancer Res* **50**, 6757-6764
- Allouche, M., Bettaieb, A., Vindis, C., Rousse, A., Grignon, C., and Laurent, G. (1997) Oncogene 14, 1837-1845
- Antonsson, B., Montessuit, S., Sanchez, B., and Martinou, J. C. (2001) J Biol Chem 276, 11615-11623
- Arap, W., Pasqualini, R., and Ruoslahti, E. (1998) Science 279, 377-380
- Arcamone, F., Cassinelli, G., Fantini, G., Grein, A., Orezzi, P., Pol, C., et al. (1969) Biotechnol Bioeng 11, 1101-1110
- Aslakson, C. J., and Miller, F. R. (1992) Cancer Res 52, 1399-1405
- Aviram, A., Zimrah, Y., Shaklai, M., Nudelman, A., and Rephaeli, A. (1994) Int J Cancer 56, 906-909
- Azmi, A. S., and Mohammad, R. M. (2009) J Cell Physiol 218, 13-21
- Bach-Gansmo, T., Danielsson, R., Saracco, A., Wilczek, B., Bogsrud, T. V., Fangberget, A., *et al.* (2006) *J Nucl Med* **47**, 1434-1439
- Bachur, N. R., Gee, M. V., and Friedman, R. D. (1982) Cancer Res 42, 1078-1081
- Bagchi, D., Bagchi, M., Hassoun, E. A., Kelly, J., and Stohs, S. J. (1995) Toxicology 95, 1-9
- Bakhshi, A., Jensen, J. P., Goldman, P., Wright, J. J., McBride, O. W., Epstein, A. L., *et al.* (1985) *Cell* **41**, 899-906
- Banno, A., and Ginsberg, M. H. (2008) Biochem Soc Trans 36, 229-234
- Bao, W., and Stromblad, S. (2004) J Cell Biol 167, 745-756
- Barthel, B. L., Torres, R. C., Hyatt, J. L., Edwards, C. C., Hatfield, M. J., Potter, P. M., *et al.* (2008) *J Med Chem* **51**, 298-304
- Barthel, B. L., Zhang, Z., Rudnicki, D. L., Coldren, C. D., Polinkovsky, M., Sun, H., *et al.* (2009) *J Med Chem* **52**, 7678-7688
- Barthel, B. L., Rudnicki, D. L., Kirby, T. P., Colvin, S. M., Burkhart, D. J., and Koch, T. H. (2012) *J Med Chem* 55, 6595-6607
- Basanez, G., and Hardwick, J. M. (2008) PLoS Biol 6, e154
- Bedikian, A. Y., Millward, M., Pehamberger, H., Conry, R., Gore, M., Trefzer, U., *et al.* (2006) *J Clin Oncol* **24**, 4738-4745
- Beglova, N., Blacklow, S. C., Takagi, J., and Springer, T. A. (2002) Nat Struct Biol 9, 282-287
- Beli, P., Lukashchuk, N., Wagner, S. A., Weinert, B. T., Olsen, J. V., Baskcomb, L., *et al.* (2012) *Mol Cell* **46**, 212-225
- Bellarosa, D., Ciucci, A., Bullo, A., Nardelli, F., Manzini, S., Maggi, C. A., et al. (2001) J Pharmacol Exp Ther 296, 276-283
- Bergelson, J. M., and Hemler, M. E. (1995) Curr Biol 5, 615-617
- Berman, E., and McBride, M. (1992) Blood 79, 3267-3273
- Bermudez, V. P., Lindsey-Boltz, L. A., Cesare, A. J., Maniwa, Y., Griffith, J. D., Hurwitz, J., *et al.* (2003) *Proc Natl Acad Sci U S A* **100**, 1633-1638
- Berry, G., Billingham, M., Alderman, E., Richardson, P., Torti, F., Lum, B., et al. (1998) Ann Oncol 9, 711-716

Bertino, A. M., Qi, X. Q., Li, J., Xia, Y., and Kuter, D. J. (2003) Transfusion 43, 857-866

- Bilardi, R. (2010) Cellular Processing and repair of anthracycline-DNA adducts, La Trobe University, Bundoora, Victoria
- Blank-Porat, D., Gruss-Fischer, T., Tarasenko, N., Malik, Z., Nudelman, A., and Rephaeli, A. (2007) *Cancer Lett* **256**, 39-48
- Blokhina, O., Virolainen, E., and Fagerstedt, K. V. (2003) Ann Bot 91 179-194
- Bogdanowich-Knipp, S. J., Chakrabarti, S., Williams, T. D., Dillman, R. K., and Siahaan, T. J. (1999) *J Pept Res* 53, 530-541
- Bonadonna, G., Monfardini, S., De Lena, M., Fossati-Bellani, F., and Beretta, G. (1970) *Cancer Res* **30**, 2572-2582
- Bonadonna, G., Moliterni, A., Zambetti, M., Daidone, M. G., Pilotti, S., Gianni, L., et al. (2005) BMJ 330, 217
- Boyle, P., and Maisonneuve, P. (1995) Lung Cancer 12, 167-181
- Bracken, C. P., Wall, S. J., Barre, B., Panov, K. I., Ajuh, P. M., and Perkins, N. D. (2008) *Cancer Res* 68, 7621-7628
- Bretscher, M. S. (1989) EMBO J 8, 1341-1348
- Brighton, D., and Wood, M. (2005) *The Royal Marsden hospital handbook of cancer chemotherapy : a guide for the multidisciplinary team* Elsevier Churchill Livingstone, Edinburgh, NY
- Brooks, P. C., Montgomery, A. M., Rosenfeld, M., Reisfeld, R. A., Hu, T., Klier, G., *et al.* (1994a) *Cell* **79**, 1157-1164
- Brooks, P. C., Clark, R. A., and Cheresh, D. A. (1994b) Science 264, 569-571
- Brooks, P. C., Stromblad, S., Klemke, R., Visscher, D., Sarkar, F. H., and Cheresh, D. A. (1995) *J Clin Invest* **96**, 1815-1822
- Brooks, P. C., Stromblad, S., Sanders, L. C., von Schalscha, T. L., Aimes, R. T., Stetler-Stevenson, W. G., et al. (1996) Cell 85, 683-693
- Brown, M. C., Cary, L. A., Jamieson, J. S., Cooper, J. A., and Turner, C. E. (2005) *Mol Biol Cell* **16**, 4316-4328
- Buensuceso, C., de Virgilio, M., and Shattil, S. J. (2003) J Biol Chem 278, 15217-15224
- Buerkle, M. A., Pahernik, S. A., Sutter, A., Jonczyk, A., Messmer, K., and Dellian, M. (2002) *Br J Cancer* **86**, 788-795
- Burke, P. A., DeNardo, S. J., Miers, L. A., Lamborn, K. R., Matzku, S., and DeNardo, G. L. (2002) *Cancer Res* **62**, 4263-4272
- Burke, P. J., and Koch, T. H. (2004) J Med Chem 47, 1193-1206
- Burkhart, D. J., Kalet, B. T., Coleman, M. P., Post, G. C., and Koch, T. H. (2004) *Mol Cancer Ther* **3**, 1593-1604
- Burkhart, D. J., Barthel, B. L., Post, G. C., Kalet, B. T., Nafie, J. W., Shoemaker, R. K., *et al.* (2006) *J Med Chem* **49**, 7002-7012
- Cabon, L., Galan-Malo, P., Bouharrour, A., Delavallee, L., Brunelle-Navas, M. N., Lorenzo, H. K., *et al.* (2012) *Cell Death Differ* **19**, 245-256
- Cai, W., and Chen, X. (2006) Anticancer Agents Med Chem 6, 407-428
- Calderwood, D. A., Zent, R., Grant, R., Rees, D. J., Hynes, R. O., and Ginsberg, M. H. (1999) *J Biol Chem* 274, 28071-28074
- Camaggi, C. M., Comparsi, R., Strocchi, E., Testoni, F., Angelelli, B., and Pannuti, F. (1988) *Cancer Chemother Pharmacol* **21**, 221-228
- Campbell, I. D., and Humphries, M. J. (2011) Cold Spring Harb Perspect Biol 3
- Candido, E. P., Reeves, R., and Davie, J. R. (1978) Cell 14, 105-113
- Cannistra, S. A., Ottensmeier, C., Niloff, J., Orta, B., and DiCarlo, J. (1995) *Gynecol Oncol* 58, 216-225

Capranico, G., Kohn, K. W., and Pommier, Y. (1990) Nucleic Acids Res 18, 6611-6619

- Carlson, T. R., Feng, Y., Maisonpierre, P. C., Mrksich, M., and Morla, A. O. (2001) J Biol Chem 276, 26516-26525
- Cartron, P. F., Gallenne, T., Bougras, G., Gautier, F., Manero, F., Vusio, P., et al. (2004) Mol Cell 16, 807-818
- Cary, L. A., Chang, J. F., and Guan, J. L. (1996) J Cell Sci 109 1787-1794
- Casanova, M., Morgan, K. T., Steinhagen, W. H., Everitt, J. I., Popp, J. A., and Heck, H. D. (1991) *Fundam Appl Toxicol* **17**, 409-428
- Castedo, M., Perfettini, J. L., Roumier, T., Andreau, K., Medema, R., and Kroemer, G. (2004) *Oncogene* 23, 2825-2837
- Certo, M., Del Gaizo Moore, V., Nishino, M., Wei, G., Korsmeyer, S., Armstrong, S. A., et al. (2006) Cancer Cell 9, 351-365
- Chakraborty, J., Banerjee, S., Ray, P., Hossain, D. M., Bhattacharyya, S., Adhikary, A., *et al.* (2010) *J Biol Chem* **285**, 33104-33112
- Chen, X., Park, R., Tohme, M., Shahinian, A. H., Bading, J. R., and Conti, P. S. (2004) Bioconjug Chem 15, 41-49
- Chen, L., Willis, S. N., Wei, A., Smith, B. J., Fletcher, J. I., Hinds, M. G., et al. (2005) Mol Cell 17, 393-403
- Chen, S., Dai, Y., Harada, H., Dent, P., and Grant, S. (2007) Cancer Res 67, 782-791
- Chen, Q., Manning, C. D., Millar, H., McCabe, F. L., Ferrante, C., Sharp, C., et al. (2008) Clin Exp Metastasis 25, 139-148
- Chen, K., and Chen, X. (2011) *Theranostics* **1**, 189-200
- Chi, K. C., Wallis, A. E., Lee, C. H., De Menezes, D. L., Sartor, J., Dragowska, W. H., et al. (2000) Breast Cancer Res Treat 63, 199-212
- Chia, J., Kusuma, N., Anderson, R., Parker, B., Bidwell, B., Zamurs, L., et al. (2007) Am J Pathol 170, 2135-2148
- Choong, P. F., and Nadesapillai, A. P. (2003) Clin Orthop Relat Res 415, S46-58
- Ciccia, A., and Elledge, S. J. (2010) Mol Cell 40, 179-204
- Cogan, P. S., Fowler, C. R., Post, G. C., and Koch, T. H. (2004) Lett Drug Design Dis 1, 247-255
- Cogliano, V. J., Grosse, Y., Baan, R. A., Straif, K., Secretan, M. B., and El Ghissassi, F. (2005) *Environ Health Perspect* **113**, 1205-1208
- Coldwell, K. E., Cutts, S. M., Ognibene, T. J., Henderson, P. T., and Phillips, D. R. (2008) *Nucleic Acids Res* 36, e100
- Coley, H. M., Amos, W. B., Twentyman, P. R., and Workman, P. (1993) Br J Cancer 67, 1316-1323
- Conus, S., Kaufmann, T., Fellay, I., Otter, I., Rosse, T., and Borner, C. (2000) *EMBO J* 19, 1534-1544
- Corbett, A. H., and Osheroff, N. (1993) Chem Res Toxicol 6, 585-597
- Cory, S. (1995) Annu Rev Immunol 13, 513-543
- Cotter, F. E., Johnson, P., Hall, P., Pocock, C., al Mahdi, N., Cowell, J. K., et al. (1994) Oncogene 9, 3049-3055
- Cowden Dahl, K. D., Robertson, S. E., Weaver, V. M., and Simon, M. C. (2005) *Mol Biol Cell* **16**, 1901-1912
- Craig, D., Gao, M., Schulten, K., and Vogel, V. (2004) Structure 12, 2049-2058
- Cressman, S., Sun, Y., Maxwell, J. E., Fang, N., Chen, D. D. Y., and Cullis, P. R. (2009a) *Int* J Pept Res Ther 15, 49-59
- Cressman, S., Dobson, I., Lee, J. B., Tam, Y. Y., and Cullis, P. R. (2009b) *Bioconjug Chem* **20**, 1404-1411

- Crown, J., O'Leary, M., and Ooi, W. S. (2004) Oncologist 9 Suppl 2, 24-32
- Cruet-Hennequart, S., Maubant, S., Luis, J., Gauduchon, P., Staedel, C., and Dedhar, S. (2003) Oncogene 22, 1688-1702
- Cullinane, C., and Phillips, D. R. (1990) Biochemistry 29, 5638-5646
- Cullinane, C., Cutts, S. M., van Rosmalen, A., and Phillips, D. R. (1994) *Nucleic Acids Res* 22, 2296-2303
- Cullinane, C., Cutts, S. M., Panousis, C., and Phillips, D. R. (2000) Nucleic Acids Res 28, 1019-1025
- Cummings, J., and McArdle, C. S. (1986) Br J Cancer 53, 835-838
- Cutts, S. M., and Phillips, D. R. (1995) Nucleic Acids Res 23, 2450-2456
- Cutts, S. M., Parsons, P. G., Sturm, R. A., and Phillips, D. R. (1996) *J Biol Chem* **271**, 5422-5429
- Cutts, S. M., Parker, B. S., Swift, L. P., Kimura, K. I., and Phillips, D. R. (2000) Anticancer Drug Des 15, 373-386
- Cutts, S. M., Rephaeli, A., Nudelman, A., Hmelnitsky, I., and Phillips, D. R. (2001) Cancer Res 61, 8194-8202
- Cutts, S. M., Swift, L. P., Rephaeli, A., Nudelman, A., and Phillips, D. R. (2003) *Mol Cancer Ther* **2**, 661-670
- Cutts, S. M., Nudelman, A., Pillay, V., Spencer, D. M., Levovich, I., Rephaeli, A., et al. (2005) Oncol Res 15, 199-213
- Cutts, S. M., Swift, L. P., Pillay, V., Forrest, R. A., Nudelman, A., Rephaeli, A., *et al.* (2007) *Mol Cancer Ther* **6**, 1450-1459
- Czabotar, P. E., Lee, E. F., van Delft, M. F., Day, C. L., Smith, B. J., Huang, D. C., et al. (2007) Proc Natl Acad Sci U S A 104, 6217-6222
- Dai, Y., and Grant, S. (2007) Cancer Res 67, 2908-2911
- Daniel, P., Brazier, M., Cerutti, I., Pieri, F., Tardivel, I., Desmet, G., et al. (1989) Clin Chim Acta 181, 255-263
- Davies, K. J., and Doroshow, J. H. (1986) J Biol Chem 261, 3060-3067
- de Jong, S., Zijlstra, J. G., de Vries, E. G., and Mulder, N. H. (1990) Cancer Res 50, 304-309
- Deffie, A. M., Batra, J. K., and Goldenberg, G. J. (1989) Cancer Res 49, 58-62
- Defilippi, P., Di Stefano, P., and Cabodi, S. (2006) Trends Cell Biol 16, 257-263
- Degterev, A., Lugovskoy, A., Cardone, M., Mulley, B., Wagner, G., Mitchison, T., et al. (2001) Nat Cell Biol 3, 173-182
- Degterev, A., Boyce, M., and Yuan, J. (2003) Oncogene 22, 8543-8567
- Degterev, A., Huang, Z., Boyce, M., Li, Y., Jagtap, P., Mizushima, N., et al. (2005) Nat Chem Biol 1, 112-119
- Del Gaizo Moore, V., Brown, J. R., Certo, M., Love, T. M., Novina, C. D., and Letai, A. (2007) *J Clin Invest* **117**, 112-121
- Del Gaizo Moore, V., Schlis, K. D., Sallan, S. E., Armstrong, S. A., and Letai, A. (2008) Blood 111, 2300-2309
- Delbaldo, C., Raymond, E., Vera, K., Hammershaimb, L., Kaucic, K., Lozahic, S., et al. (2008) Invest New Drugs 26, 35-43
- Den Boer, M. L., Pieters, R., and Veerman, A. J. (1998) Leukemia 12, 1657-1670
- Deng, X., Gao, F., Flagg, T., Anderson, J., and May, W. S. (2006) Mol Cell Biol 26, 4421-4434
- Denicourt, C., and Dowdy, S. F. (2004) Science 305, 1411-1413
- Desagher, S., Osen-Sand, A., Nichols, A., Eskes, R., Montessuit, S., Lauper, S., et al. (1999) J Cell Biol 144, 891-901
- Desgrosellier, J. S., and Cheresh, D. A. (2010) Nat Rev Cancer 10, 9-22

- DeVita, V. T., Hellman, S., and Rosenberg, S. A. (2005) *Cancer: principles and practice of oncology*, 7th edition ed., Lippincott-Raven, Philadelphia, PA
- DeVita, V. T., Hellman, S., and Rosenberg, S. A. (2008) Cancer: principles and practice of oncology, 8th edition ed., Wolters Kluwer / Lippincott Williams & Wilkins, Philadelphia, PA
- Di Marco, A., Gaetani, M., Orezzi, P., Scarpinato, B. M., Silvestrini, R., Soldati, M., et al. (1964) Nature 201, 706-707
- Di Marco, A., Gaetani, M., and Scarpinato, B. (1969) Cancer Chemother Rep 53, 33-37
- Didenko, V. V., Ngo, H., and Baskin, D. S. (2003) Am J Pathol 162, 1571-1578
- Dole, M. G., Jasty, R., Cooper, M. J., Thompson, C. B., Nunez, G., and Castle, V. P. (1995) *Cancer Res* 55, 2576-2582
- Domina, A. M., Vrana, J. A., Gregory, M. A., Hann, S. R., and Craig, R. W. (2004) Oncogene 23, 5301-5315
- Doroshow, J. H., Locker, G. Y., and Myers, C. E. (1980) J Clin Invest 65, 128-135
- Doroshow, J. H., and Davies, K. J. (1986) J Biol Chem 261, 3068-3074
- Doyle, L. A., Yang, W., Abruzzo, L. V., Krogmann, T., Gao, Y., Rishi, A. K., *et al.* (1998) *Proc Natl Acad Sci U S A* **95**, 15665-15670
- Drake, C. J., Cheresh, D. A., and Little, C. D. (1995) J Cell Sci 108 2655-2661
- Dubey, P. K., Mishra, V., Jain, S., Mahor, S., and Vyas, S. P. (2004) *J Drug Target* **12**, 257-264
- Dunehoo, A. L., Anderson, M., Majumdar, S., Kobayashi, N., Berkland, C., and Siahaan, T. J. (2006) *J Pharm Sci* **95**, 1856-1872
- Ebeler, S. E., Clifford, A. J., and Shibamoto, T. (1997) J Chromatogr B Biomed Sci Appl 702, 211-215
- Eckhardt, B. L., Parker, B. S., van Laar, R. K., Restall, C. M., Natoli, A. L., Tavaria, M. D., *et al.* (2005) *Mol Cancer Res* **3**, 1-13
- Eliceiri, B. P., and Cheresh, D. A. (1999) J Clin Invest 103, 1227-1230
- Elliott, M. J., Stribinskiene, L., and Lock, R. B. (1998) Cancer Chemother Pharmacol 41, 457-463
- Engel, D., Nudelman, A., Levovich, I., Gruss-Fischer, T., Entin-Meer, M., Phillips, D. R., et al. (2006) J Cancer Res Clin Oncol 132, 673-683
- Entin-Meer, M., Rephaeli, A., Yang, X., Nudelman, A., VandenBerg, S. R., and Haas-Kogan, D. A. (2005) *Mol Cancer Ther* **4**, 1952-1961
- Fadeel, B., and Orrenius, S. (2005) J Intern Med 258, 479-517
- Fairbairn, D. W., and O'Neill, K. L. (1995) In Vitro Cell Dev Biol Anim 31, 171-173
- Fearon, E. R., and Vogelstein, B. (1990) Cell 61, 759-767
- Felding-Habermann, B., O'Toole, T. E., Smith, J. W., Fransvea, E., Ruggeri, Z. M., Ginsberg, M. H., et al. (2001) Proc Natl Acad Sci U S A 98, 1853-1858
- Fenick, D. J., Taatjes, D. J., and Koch, T. H. (1997) J Med Chem 40, 2452-2461
- Ferlay, J., Shin, H. R., Bray, F., Forman, D., Mathers, C., and Parkin, D. M. (2010) Int J Cancer 127, 2893-2917
- Ferrara, N. (1999) Kidney Int 56, 794-814
- Ferreira, A. L., Matsubara, L. S., and Matsubara, B. B. (2008) Cardiovasc Hematol Agents Med Chem 6, 278-281
- Ford, D., Easton, D. F., Stratton, M., Narod, S., Goldgar, D., Devilee, P., *et al.* (1998) *Am J Hum Genet* **62**, 676-689
- Forrest, R. A. (2010) DNA damage responses elicited by anthracycline-DNA adducts, La Trobe University, Bundoora, Victoria

- Forrest, R. A., Swift, L. P., Rephaeli, A., Nudelman, A., Kimura, K. I., Phillips, D. R., *et al.* (2012) *Biochem Pharmacol* **83**, 1602-1612
- Friess, H., Langrehr, J. M., Oettle, H., Raedle, J., Niedergethmann, M., Dittrich, C., et al. (2006) BMC Cancer 6, 285-296
- Frisch, S. M., and Francis, H. (1994) J Cell Biol 124, 619-626
- Frisch, S. M., and Screaton, R. A. (2001) Curr Opin Cell Biol 13, 555-562
- Fulda, S., and Debatin, K. M. (2006) Oncogene 25, 4798-4811
- Gabizon, A., Shmeeda, H., and Barenholz, Y. (2003) Clin Pharmacokinet 42, 419-436
- Galluzzi, L., and Kroemer, G. (2008) Cell 135, 1161-1163
- Gandhi, L., Camidge, D. R., Ribeiro de Oliveira, M., Bonomi, P., Gandara, D., Khaira, D., *et al.* (2011) *J Clin Oncol* **29**, 909-916
- Gewirtz, D. A. (1999) Biochem Pharmacol 57, 727-741
- Ghaneh, P., Kawesha, A., Evans, J. D., and Neoptolemos, J. P. (2002) J Hepatobiliary Pancreat Surg 9, 1-11
- Giam, M., Huang, D. C., and Bouillet, P. (2008) Oncogene 27 S128-136
- Gigli, M., Doglia, S. M., Millot, J. M., Valentini, L., and Manfait, M. (1988) *Biochim Biophys Acta* **950**, 13-20
- Gingras, M. C., Roussel, E., Bruner, J. M., Branch, C. D., and Moser, R. P. (1995) J Neuroimmunol 57, 143-153
- Glaser, K. B., Staver, M. J., Waring, J. F., Stender, J., Ulrich, R. G., and Davidsen, S. K. (2003) *Mol Cancer Ther* **2**, 151-163
- Gobe, G., Rubin, M., Williams, G., Sawczuk, I., and Buttyan, R. (2002) Cancer Invest 20, 324-332
- Golden, R., Pyatt, D., and Shields, P. G. (2006) Crit Rev Toxicol 36, 135-153
- Goodman, J., and Hochstein, P. (1977) Biochem Biophys Res Commun 77, 797-803
- Gottesman, M. M., Fojo, T., and Bates, S. E. (2002) Nat Rev Cancer 2, 48-58
- Grant, C. E., Valdimarsson, G., Hipfner, D. R., Almquist, K. C., Cole, S. P., and Deeley, R. G. (1994) *Cancer Res* 54, 357-361
- Grisendi, S., Mecucci, C., Falini, B., and Pandolfi, P. P. (2006) Nat Rev Cancer 6, 493-505
- Gutheil, J. C., Campbell, T. N., Pierce, P. R., Watkins, J. D., Huse, W. D., Bodkin, D. J., *et al.* (2000) *Clin Cancer Res* **6**, 3056-3061
- Hacki, J., Egger, L., Monney, L., Conus, S., Rosse, T., Fellay, I., et al. (2000) Oncogene 19, 2286-2295
- Hammes, H. P., Brownlee, M., Jonczyk, A., Sutter, A., and Preissner, K. T. (1996) *Nat Med* 2, 529-533
- Han, W., Xie, J., Li, L., Liu, Z., and Hu, X. (2009) Apoptosis 14, 674-686
- Han, H. D., Mangala, L. S., Lee, J. W., Shahzad, M. M., Kim, H. S., Shen, D., et al. (2010) Clin Cancer Res 16, 3910-3922
- Hanahan, D., and Folkman, J. (1996) Cell 86, 353-364
- Hanahan, D., and Weinberg, R. A. (2000) Cell 100, 57-70
- Hanahan, D., and Weinberg, R. A. (2011) Cell 144, 646-674
- Hang, H., and Lieberman, H. B. (2000) Genomics 65, 24-33
- Harker, W. G., Slade, D. L., Drake, F. H., and Parr, R. L. (1991) Biochemistry 30, 9953-9961
- Harker, W. G., Slade, D. L., Parr, R. L., Feldhoff, P. W., Sullivan, D. M., and Holguin, M. H. (1995) *Cancer Res* 55, 1707-1716
- Harrison, L. B., Chadha, M., Hill, R. J., Hu, K., and Shasha, D. (2002) Oncologist 7, 492-508
- Haubner, R., Weber, W. A., Beer, A. J., Vabuliene, E., Reim, D., Sarbia, M., *et al.* (2005) *PLoS Med* **2**, e70

- Hauptmann, M., Lubin, J. H., Stewart, P. A., Hayes, R. B., and Blair, A. (2004) Am J Epidemiol 159, 1117-1130
- Haura, E. B., Williams, C. A., Chiappori, A. A., Adams, J., Northfelt, D. W., Malik, S. M., et al. (2008) J Clin Oncol 26, 19035
- Heist, R. S., Fain, J., Chinnasami, B., Khan, W., Molina, J. R., Sequist, L. V., *et al.* (2010) *J Thorac Oncol* **5**, 1637-1643
- Helt, C. E., Wang, W., Keng, P. C., and Bambara, R. A. (2005) Cell Cycle 4, 529-532
- Hersey, P., Sosman, J., O'Day, S., Richards, J., Bedikian, A., Gonzalez, R., et al. (2010) Cancer **116**, 1526-1534
- Hoetelmans, R. W., Vahrmeijer, A. L., Mulder, G. J., van de Velde, C. J., Nagelkerke, J. F., and van Dierendonck, J. H. (2003) *Chemotherapy* **49**, 309-315
- Hofmann, G. A., and Mattern, M. R. (1993) Cytotechnology 12, 137-154
- Hsu, C. Y., and Yung, B. Y. (2000) Int J Cancer 88, 392-400
- Huang, S., and Sinicrope, F. A. (2008) Cancer Res 68, 2944-2951
- Hughes, P. E., Diaz-Gonzalez, F., Leong, L., Wu, C., McDonald, J. A., Shattil, S. J., *et al.* (1996) *J Biol Chem* **271**, 6571-6574
- Huigsloot, M., Tijdens, R. B., and van de Water, B. (2003) Mol Pharmacol 64, 965-973
- Hwang, J. J., Kuruvilla, J., Mendelson, D., Pishvaian, M. J., Deeken, J. F., Siu, L. L., *et al.* (2010) *Clin Cancer Res* **16**, 4038-4045
- Hynes, R. O. (1992) Cell 69, 11-25
- Iliskovic, N., and Singal, P. K. (1997) Am J Pathol 150, 727-734
- Ishii, H., Inageta, T., Mimori, K., Saito, T., Sasaki, H., Isobe, M., et al. (2005) Proc Natl Acad Sci U S A **102**, 9655-9660
- Ivaska, J., and Heino, J. (2010) Cell Tissue Res 339, 111-120
- Iwamoto, F. M., and Fine, H. A. (2010) Arch Neurol 67, 285-288
- Jackson, S. P., and Bartek, J. (2009) Nature 461, 1071-1078
- Janssen, M. L., Oyen, W. J., Dijkgraaf, I., Massuger, L. F., Frielink, C., Edwards, D. S., et al. (2002) Cancer Res 62, 6146-6151
- Januszewicz, E., Rabizadah, E., Novogrodsky, A., and Shaklai, M. (1988) *Med Oncol Tumor Pharmacother* **5**, 259-263
- Jemal, A., Siegel, R., Xu, J., and Ward, E. (2010) CA Cancer J Clin 60, 277-300
- Jenab-Wolcott, J., and Giantonio, B. J. (2009) Expert Opin Biol Ther 9, 507-517
- John, K., Alla, V., Meier, C., and Putzer, B. M. (2011) Cell Death Differ 18, 874-886
- Johnston, S. R., and Gore, M. E. (2001) Eur J Cancer 37 S8-14
- Kalasz, H. (2003) Mini Rev Med Chem 3, 175-192
- Kalet, B. T., McBryde, M. B., Espinosa, J. M., and Koch, T. H. (2007) J Med Chem 50, 4493-4500
- Kalyanaraman, B., Sealy, R. C., and Sinha, B. K. (1984) Biochim Biophys Acta 799, 270-275
- Kamada, S., Shimono, A., Shinto, Y., Tsujimura, T., Takahashi, T., Noda, T., *et al.* (1995) *Cancer Res* **55**, 354-359
- Kang, M. H., Kang, Y. H., Szymanska, B., Wilczynska-Kalak, U., Sheard, M. A., Harned, T. M., et al. (2007) Blood 110, 2057-2066
- Kasof, G. M., Goyal, L., and White, E. (1999) Mol Cell Biol 19, 4390-4404
- Kasukabe, T., Rephaeli, A., and Honma, Y. (1997) Br J Cancer 75, 850-854
- Kato, S., Burke, P. J., Fenick, D. J., Taatjes, D. J., Bierbaum, V. M., and Koch, T. H. (2000) *Chem Res Toxicol* **13**, 509-516
- Kato, S., Burke, P. J., Koch, T. H., and Bierbaum, V. M. (2001) Anal Chem 73, 2992-2997
- Keller, A., Nesvizhskii, A. I., Kolker, E., and Aebersold, R. (2002) Anal Chem 74, 5383-5392

- Kerr, L. E., Birse-Archbold, J. L., Short, D. M., McGregor, A. L., Heron, I., Macdonald, D. C., et al. (2007) Oncogene 26, 2554-2562
- Kikuchi, Y., Niwano, M., Yajima, N., Nakamura, G., and Miyata, N. (1985) *J Antibiot* (*Tokyo*) **38**, 1670-1676
- Kim, H., Rafiuddin-Shah, M., Tu, H. C., Jeffers, J. R., Zambetti, G. P., Hsieh, J. J., et al. (2006) Nat Cell Biol 8, 1348-1358
- Kim, R., Emi, M., Matsuura, K., and Tanabe, K. (2007) Cancer Gene Ther 14, 1-11
- Kim, J. H., Kim, Y. S., Park, K., Lee, S., Nam, H. Y., Min, K. H., et al. (2008) J Control Release 127, 41-49
- Kimura, K., Nakayama, S., Koyama, T., Shimada, S., Kawaguchi, N., Miyata, N., et al. (1987) J Antibiot (Tokyo) 40, 1353-1355
- Kimura, K., Nakayama, S., Miyata, N., Takeshita, Y., and Kawanishi, G. (1988) J Antibiot (Tokyo) **41**, 411-414
- Kimura, K., Morinaga, T., Miyata, N., and Kawanishi, G. (1989) J Antibiot (Tokyo) 42, 1838-1843
- Kimura, K., Spencer, D. M., Bilardi, R., Swift, L. P., Box, A. J., Brownlee, R. T., et al. (2010) Anticancer Agents Med Chem 10, 70-77
- Kirkin, V., Joos, S., and Zornig, M. (2004) Biochim Biophys Acta 1644, 229-249
- Kitada, S., Miyashita, T., Tanaka, S., and Reed, J. C. (1993) Antisense Res Dev 3, 157-169
- Kitada, S., Leone, M., Sareth, S., Zhai, D., Reed, J. C., and Pellecchia, M. (2003) J Med Chem 46, 4259-4264
- Klasa, R. J., Gillum, A. M., Klem, R. E., and Frankel, S. R. (2002) Antisense Nucleic Acid Drug Dev 12, 193-213
- Kline, M. P., Rajkumar, S. V., Timm, M. M., Kimlinger, T. K., Haug, J. L., Lust, J. A., *et al.* (2007) *Leukemia* **21**, 1549-1560
- Kobayashi, S., Lee, S. H., Meng, X. W., Mott, J. L., Bronk, S. F., Werneburg, N. W., *et al.* (2007) *J Biol Chem* **282**, 18407-18417
- Koblinski, J. E., Ahram, M., and Sloane, B. F. (2000) Clin Chim Acta 291, 113-135
- Kok, R. J., Schraa, A. J., Bos, E. J., Moorlag, H. E., Asgeirsdottir, S. A., Everts, M., et al. (2002) Bioconjug Chem 13, 128-135
- Komatsu, K., Miyashita, T., Hang, H., Hopkins, K. M., Zheng, W., Cuddeback, S., et al. (2000) Nat Cell Biol 2, 1-6
- Konopleva, M., Contractor, R., Tsao, T., Samudio, I., Ruvolo, P. P., Kitada, S., et al. (2006) Cancer Cell 10, 375-388
- Konopleva, M., Watt, J., Contractor, R., Tsao, T., Harris, D., Estrov, Z., et al. (2008) Cancer Res 68, 3413-3420
- Koutinos, G., Stathopoulos, G. P., Dontas, I., Perrea-Kotsarelis, D., Couris, E., Karayannacos, P. E., et al. (2002) Anticancer Res 22, 815-820
- Kuroda, J., Puthalakath, H., Cragg, M. S., Kelly, P. N., Bouillet, P., Huang, D. C., *et al.* (2006) *Proc Natl Acad Sci U S A* **103**, 14907-14912
- Kurt, R. A., Bauck, M., Harma, S., Adler, E., Vitiello, P., Wisner, K. P., et al. (2003) Breast Cancer Res Treat 77, 225-232
- Kutuk, O., and Letai, A. (2008) Cancer Res 68, 7985-7994
- Kuwana, T., Bouchier-Hayes, L., Chipuk, J. E., Bonzon, C., Sullivan, B. A., Green, D. R., et al. (2005) Mol Cell 17, 525-535
- Lammers, T., Hennink, W. E., and Storm, G. (2008) Br J Cancer 99, 392-397
- Lampidis, T. J., Kolonias, D., Podona, T., Israel, M., Safa, A. R., Lothstein, L., *et al.* (1997) *Biochemistry* **36**, 2679-2685
- Lavrik, I. N., Golks, A., and Krammer, P. H. (2005) J Clin Invest 115, 2665-2672

Leder, A., and Leder, P. (1975) *Cell* 5, 319-322

- Lee, J. O., Rieu, P., Arnaout, M. A., and Liddington, R. (1995) Cell 80, 631-638
- Lee, M. W., Hirai, I., and Wang, H. G. (2003) Oncogene 22, 6340-6346
- Lee, K. M., Hsu Ia, W., and Tarn, W. Y. (2010) Nucleic Acids Res 38, 3340-3350
- Legler, D. F., Wiedle, G., Ross, F. P., and Imhof, B. A. (2001) J Cell Sci 114, 1545-1553
- Lei, X., Chen, Y., Du, G., Yu, W., Wang, X., Qu, H., et al. (2006) FASEB J 20, 2147-2149
- Lelekakis, M., Moseley, J. M., Martin, T. J., Hards, D., Williams, E., Ho, P., et al. (1999) Clin Exp Metastasis 17, 163-170
- Leng, F. F., Savkur, R., Fokt, I., Przewloka, T., Priebe, W., and Chaires, J. B. (1996) *Journal* of the American Chemical Society **118**, 4731-4738
- Lessene, G., Czabotar, P. E., and Colman, P. M. (2008) Nat Rev Drug Discov 7, 989-1000
- Letai, A., Bassik, M. C., Walensky, L. D., Sorcinelli, M. D., Weiler, S., and Korsmeyer, S. J. (2002) *Cancer Cell* **2**, 183-192
- Levine, A. J. (1997) Cell 88, 323-331
- Levovich, I., Nudelman, A., Berkovitch, G., Swift, L. P., Cutts, S. M., Phillips, D. R., et al. (2008) Cancer Chemother Pharmacol 62, 471-482
- Li, L., and Zou, L. (2005) J Cell Biochem 94, 298-306
- Li, Z. B., Cai, W., Cao, Q., Chen, K., Wu, Z., He, L., et al. (2007) J Nucl Med 48, 1162-1171
- Li, J., Viallet, J., and Haura, E. B. (2008) Cancer Chemother Pharmacol 61, 525-534
- Li, C. H., Cheng, Y. W., Hsu, Y. T., Hsu, Y. J., Liao, P. L., and Kang, J. J. (2010) *Toxicol Sci* **118**, 544-553
- Liang, X., Xu, Y., Xu, K., Liu, J., and Qian, X. (2010) Mol Cancer Res 8, 1619-1632
- Liddington, R. C., and Ginsberg, M. H. (2002) J Cell Biol 158, 833-839
- Lieberman, H. B. (2006) J Cell Biochem 97, 690-697
- Lieberman, H. B., Bernstock, J. D., Broustas, C. G., Hopkins, K. M., Leloup, C., and Zhu, A. (2011) *J Mol Cell Biol* **3**, 39-43
- Lin, X., Morgan-Lappe, S., Huang, X., Li, L., Zakula, D. M., Vernetti, L. A., et al. (2007) Oncogene 26, 3972-3979
- Lindsten, T., Ross, A. J., King, A., Zong, W. X., Rathmell, J. C., Shiels, H. A., et al. (2000) Mol Cell 6, 1389-1399
- Liu, L. F., Liu, C. C., and Alberts, B. M. (1980) Cell 19, 697-707
- Liu, L. F., Rowe, T. C., Yang, L., Tewey, K. M., and Chen, G. L. (1983) *J Biol Chem* 258, 15365-15370
- Liu, S., and Ginsberg, M. H. (2000) J Biol Chem 275, 22736-22742
- Liu, G., Kelly, W. K., Wilding, G., Leopold, L., Brill, K., and Somer, B. (2009) *Clin Cancer Res* **15**, 3172-3176
- Liu, H., Radisky, D. C., Yang, D., Xu, R., Radisky, E. S., Bissell, M. J., et al. (2012) Nat Cell Biol 14, 567-574
- Lock, R., Carol, H., Houghton, P. J., Morton, C. L., Kolb, E. A., Gorlick, R., *et al.* (2008) *Pediatr Blood Cancer* **50**, 1181-1189
- Loegering, D., Arlander, S. J., Hackbarth, J., Vroman, B. T., Roos-Mattjus, P., Hopkins, K. M., et al. (2004) J Biol Chem 279, 18641-18647
- Luo, B. H., Carman, C. V., and Springer, T. A. (2007) Annu Rev Immunol 25, 619-647
- Lurje, G., and Lenz, H. J. (2009) Oncology 77, 400-410
- MacDonald, T. J., Taga, T., Shimada, H., Tabrizi, P., Zlokovic, B. V., Cheresh, D. A., et al. (2001) Neurosurgery 48, 151-157
- Maeda, H., Wu, J., Sawa, T., Matsumura, Y., and Hori, K. (2000) *J Control Release* 65, 271-284

- Maiguel, D. A., Jones, L., Chakravarty, D., Yang, C., and Carrier, F. (2004) Mol Cell Biol 24, 3703-3711
- Manfait, M., Alix, A. J., Jeannesson, P., Jardillier, J. C., and Theophanides, T. (1982) *Nucleic Acids Res* **10**, 3803-3816
- Mansilla, S., Priebe, W., and Portugal, J. (2006) Cell Cycle 5, 53-60
- Marinelli, L., Lavecchia, A., Gottschalk, K. E., Novellino, E., and Kessler, H. (2003) J Med Chem 46, 4393-4404
- Martin, A. G., Trama, J., Crighton, D., Ryan, K. M., and Fearnhead, H. O. (2009) Aging (Albany NY) 1, 335-349
- Mas-Moruno, C., Rechenmacher, F., and Kessler, H. (2010) Anticancer Agents Med Chem 10, 753-768
- Mason, K. D., Carpinelli, M. R., Fletcher, J. I., Collinge, J. E., Hilton, A. A., Ellis, S., et al. (2007) Cell 128, 1173-1186
- Masters, S. C., Yang, H., Datta, S. R., Greenberg, M. E., and Fu, H. (2001) *Mol Pharmacol* **60**, 1325-1331
- Matter, M. L., and Ruoslahti, E. (2001) J Biol Chem 276, 27757-27763
- Maubant, S., Saint-Dizier, D., Boutillon, M., Perron-Sierra, F., Casara, P. J., Hickman, J. A., *et al.* (2006) *Blood* **108**, 3035-3044
- McCarter, M. D., and Fong, Y. (2001) Ann Surg Oncol 8, 38-43
- McDermott, D. F., and George, D. J. (2010) Cancer Treat Rev 36, 216-223
- McNeel, D. G., Eickhoff, J., Lee, F. T., King, D. M., Alberti, D., Thomas, J. P., *et al.* (2005) *Clin Cancer Res* **11**, 7851-7860
- McPherson, J. P., Sarras, H., Lemmers, B., Tamblyn, L., Migon, E., Matysiak-Zablocki, E., et al. (2009) Cell Death Differ 16, 331-339
- Melino, G., Bernassola, F., Ranalli, M., Yee, K., Zong, W. X., Corazzari, M., et al. (2004) J Biol Chem 279, 8076-8083
- Memmo, L. M., and McKeown-Longo, P. (1998) J Cell Sci 111 425-433
- Merino, R., Ding, L., Veis, D. J., Korsmeyer, S. J., and Nunez, G. (1994) *EMBO J* 13, 683-691
- Messori, L., Temperini, C., Piccioli, F., Animati, F., Di Bugno, C., and Orioli, P. (2001) Bioorg Med Chem 9, 1815-1825
- Mi, Z., Guo, H., Wai, P. Y., Gao, C., and Kuo, P. C. (2006) Carcinogenesis 27, 1134-1145
- Michels, J., Johnson, P. W., and Packham, G. (2005) Int J Biochem Cell Biol 37, 267-271
- Mihara, M., Erster, S., Zaika, A., Petrenko, O., Chittenden, T., Pancoska, P., et al. (2003) Mol Cell 11, 577-590
- Miller, A. A., Kurschel, E., Osieka, R., and Schmidt, C. G. (1987) *Eur J Cancer Clin Oncol* 23, 1283-1287
- Minotti, G., Menna, P., Salvatorelli, E., Cairo, G., and Gianni, L. (2004) *Pharmacol Rev* 56, 185-229
- Mitra, A., Mulholland, J., Nan, A., McNeill, E., Ghandehari, H., and Line, B. R. (2005) J Control Release **102**, 191-201
- Miyashita, T., and Reed, J. C. (1995) Cell 80, 293-299
- Mohammad, R. M., Wang, S., Aboukameel, A., Chen, B., Wu, X., Chen, J., *et al.* (2005) *Mol Cancer Ther* **4**, 13-21
- Monti, E., Prosperi, E., Supino, R., and Bottiroli, G. (1995) Anticancer Res 15, 193-197
- Morris, M. J., Tong, W. P., Cordon-Cardo, C., Drobnjak, M., Kelly, W. K., Slovin, S. F., *et al.* (2002) *Clin Cancer Res* **8**, 679-683
- Motoyama, N., Wang, F., Roth, K. A., Sawa, H., Nakayama, K., Negishi, I., *et al.* (1995) *Science* **267**, 1506-1510

- Mott, J. L., Bronk, S. F., Mesa, R. A., Kaufmann, S. H., and Gores, G. J. (2008) Mol Cancer Ther 7, 2339-2347
- Moufarij, M. A., Cutts, S. M., Neumann, G. M., Kimura, K., and Phillips, D. R. (2001) Chem Biol Interact 138, 137-153
- Mukherji, S. K. (2010) AJNR Am J Neuroradiol 31, 235-236
- Mulgrew, K., Kinneer, K., Yao, X. T., Ward, B. K., Damschroder, M. M., Walsh, B., et al. (2006) Mol Cancer Ther 5, 3122-3129
- Mullamitha, S. A., Ton, N. C., Parker, G. J., Jackson, A., Julyan, P. J., Roberts, C., et al. (2007) Clin Cancer Res 13, 2128-2135
- Murphy, E. A., Majeti, B. K., Barnes, L. A., Makale, M., Weis, S. M., Lutu-Fuga, K., *et al.* (2008) *Proc Natl Acad Sci U S A* **105**, 9343-9348
- Myers, C. E., McGuire, W. P., Liss, R. H., Ifrim, I., Grotzinger, K., and Young, R. C. (1977) *Science* **197**, 165-167
- Myers, C. E., Gianni, L., Simone, C. B., Klecker, R., and Greene, R. (1982) *Biochemistry* **21**, 1707-1712
- Nabors, L. B., Mikkelsen, T., Rosenfeld, S. S., Hochberg, F., Akella, N. S., Fisher, J. D., *et al.* (2007) *J Clin Oncol* 25, 1651-1657
- Nakano, K., and Vousden, K. H. (2001) Mol Cell 7, 683-694
- Nakayama, K., Negishi, I., Kuida, K., Shinkai, Y., Louie, M. C., Fields, L. E., *et al.* (1993) *Science* **261**, 1584-1588
- Nakayama, K., Negishi, I., Kuida, K., Sawa, H., and Loh, D. Y. (1994) *Proc Natl Acad Sci U S A* **91**, 3700-3704
- Nash, T. (1953) Biochem J 55, 416-421
- Nesvizhskii, A. I., Keller, A., Kolker, E., and Aebersold, R. (2003) Anal Chem 75, 4646-4658
- Neuberger, A. (1981) *The metabolism of glycine and serine*, Elsevier, Amsterdam, The Netherlands
- Niitsu, N., Kasukabe, T., Yokoyama, A., Okabe-Kado, J., Yamamoto-Yamaguchi, Y., Umeda, M., et al. (2000) Mol Pharmacol 58, 27-36
- Niland, S., and Eble, J. A. (2011) J Oncol 2012, 125278
- Nudelman, A., Ruse, M., Aviram, A., Rabizadeh, E., Shaklai, M., Zimrah, Y., *et al.* (1992) *J Med Chem* **35**, 687-694
- Nudelman, A., Gnizi, E., Katz, Y., Azulai, R., Cohen-Ohana, M., Zhuk, R., et al. (2001) Eur J Med Chem 36, 63-74
- Nudelman, A., Levovich, I., Cutts, S. M., Phillips, D. R., and Rephaeli, A. (2005) *J Med Chem* 48, 1042-1054
- O'Brien, M. E., Wigler, N., Inbar, M., Rosso, R., Grischke, E., Santoro, A., et al. (2004) Ann Oncol 15, 440-449
- O'Brien, S. M., Cunningham, C. C., Golenkov, A. K., Turkina, A. G., Novick, S. C., and Rai, K. R. (2005) J Clin Oncol 23, 7697-7702
- O'Brien, S., Moore, J. O., Boyd, T. E., Larratt, L. M., Skotnicki, A., Koziner, B., *et al.* (2007) *J Clin Oncol* 25, 1114-1120
- Oda, E., Ohki, R., Murasawa, H., Nemoto, J., Shibue, T., Yamashita, T., *et al.* (2000) *Science* **288**, 1053-1058
- Olive, P. L. (1989) Radiat Res 117, 79-92
- Oliveira-Ferrer, L., Hauschild, J., Fiedler, W., Bokemeyer, C., Nippgen, J., Celik, I., et al. (2008) J Exp Clin Cancer Res 27, 86
- Oltersdorf, T., Elmore, S. W., Shoemaker, A. R., Armstrong, R. C., Augeri, D. J., Belli, B. A., *et al.* (2005) *Nature* **435**, 677-681

- Opferman, J. T., Letai, A., Beard, C., Sorcinelli, M. D., Ong, C. C., and Korsmeyer, S. J. (2003) *Nature* **426**, 671-676
- Opferman, J. T., Iwasaki, H., Ong, C. C., Suh, H., Mizuno, S., Akashi, K., et al. (2005) Science **307**, 1101-1104
- Panaretakis, T., Pokrovskaja, K., Shoshan, M. C., and Grander, D. (2002) J Biol Chem 277, 44317-44326
- Pandita, R. K., Sharma, G. G., Laszlo, A., Hopkins, K. M., Davey, S., Chakhparonian, M., et al. (2006) Mol Cell Biol 26, 1850-1864
- Papahadjopoulos, D., Allen, T. M., Gabizon, A., Mayhew, E., Matthay, K., Huang, S. K., et al. (1991) Proc Natl Acad Sci U S A 88, 11460-11464
- Papajik, T., Jedlickova, K., Kriegova, E., Jarosova, M., Raida, L., Faber, E., et al. (2001) Neoplasma 48, 501-505
- Parikh, S. A., Kantarjian, H., Schimmer, A., Walsh, W., Asatiani, E., El-Shami, K., et al. (2010) Clin Lymphoma Myeloma Leuk 10, 285-289
- Park, C. M., Bruncko, M., Adickes, J., Bauch, J., Ding, H., Kunzer, A., et al. (2008a) J Med Chem 51, 6902-6915
- Park, K., Kim, Y. S., Lee, G. Y., Park, R. W., Kim, I. S., Kim, S. Y., et al. (2008b) Pharm Res 25, 2786-2798
- Park, J. H., Saravanakumar, G., Kim, K., and Kwon, I. C. (2010) *Adv Drug Deliv Rev* **62**, 28-41
- Parker, B. S., Cullinane, C., and Phillips, D. R. (1999) Nucleic Acids Res 27, 2918-2923
- Parrilla-Castellar, E. R., Arlander, S. J., and Karnitz, L. (2004) DNA Repair (Amst) 3, 1009-1014
- Patnaik, A., Rowinsky, E. K., Villalona, M. A., Hammond, L. A., Britten, C. D., Siu, L. L., et al. (2002) Clin Cancer Res 8, 2142-2148
- Pawlicki, M., Rolski, J., Zaluski, J., Siedlecki, P., Ramlau, C., and Tomzak, P. (2002) Oncologist 7, 205-209
- Pepper, C., Hoy, T., and Bentley, P. (1998) Leuk Lymphoma 28, 355-361
- Pereira, J. J., Meyer, T., Docherty, S. E., Reid, H. H., Marshall, J., Thompson, E. W., *et al.* (2004) *Cancer Res* **64**, 977-984
- Perez-Galan, P., Roue, G., Villamor, N., Campo, E., and Colomer, D. (2007) Blood 109, 4441-4449
- Perrin, L. C., Cullinane, C., Kimura, K., and Phillips, D. R. (1999) Nucleic Acids Res 27, 1781-1787
- Peto, J. (2001) Nature 411, 390-395
- Petros, A. M., Olejniczak, E. T., and Fesik, S. W. (2004) Biochim Biophys Acta 1644, 83-94
- Planchard, D. (2011) Expert Rev Anticancer Ther 11, 1163-1179
- Plow, E. F., Haas, T. A., Zhang, L., Loftus, J., and Smith, J. W. (2000) *J Biol Chem* 275, 21785-21788
- Post, G. C., Barthel, B. L., Burkhart, D. J., Hagadorn, J. R., and Koch, T. H. (2005) *J Med Chem* **48**, 7648-7657
- Prasad, K. N. (1980) Life Sci 27, 1351-1358
- Puthalakath, H., Huang, D. C., O'Reilly, L. A., King, S. M., and Strasser, A. (1999) *Mol Cell* 3, 287-296
- Rabizadeh, E., Shaklai, M., Nudelman, A., Eisenbach, L., and Rephaeli, A. (1993) *FEBS Lett* **328**, 225-229
- Rabizadeh, E., Bairey, O., Aviram, A., Ben-Dror, I., Shaklai, M., and Zimra, Y. (2001) Eur J Haematol 66, 263-271
- Rahman, A. M., Yusuf, S. W., and Ewer, M. S. (2007) Int J Nanomedicine 2, 567-583

- Reardon, D. A., Fink, K. L., Mikkelsen, T., Cloughesy, T. F., O'Neill, A., Plotkin, S., *et al.* (2008) *J Clin Oncol* **26**, 5610-5617
- Reid, T., Valone, F., Lipera, W., Irwin, D., Paroly, W., Natale, R., et al. (2004) Lung Cancer 45, 381-386
- Rephaeli, A., Rabizadeh, E., Aviram, A., Shaklai, M., Ruse, M., and Nudelman, A. (1991) *Int* J Cancer 49, 66-72
- Rephaeli, A., Blank-Porat, D., Tarasenko, N., Entin-Meer, M., Levovich, I., Cutts, S. M., et al. (2005) Int J Cancer 116, 226-235
- Rephaeli, A., Entin-Meer, M., Angel, D., Tarasenko, N., Gruss-Fischer, T., Bruachman, I., et al. (2006) Invest New Drugs 24, 383-392
- Rephaeli, A., Waks-Yona, S., Nudelman, A., Tarasenko, I., Tarasenko, N., Phillips, D. R., et al. (2007) Br J Cancer 96, 1667-1674
- Reynolds, A. R., Hart, I. R., Watson, A. R., Welti, J. C., Silva, R. G., Robinson, S. D., et al. (2009) Nat Med 15, 392-400
- Reynolds, A. R. (2010) Dose Response 8, 253-284
- Rice, A. M. (1997) Nurs Stand 12, 49-54
- Rifkin, R. M., Gregory, S. A., Mohrbacher, A., and Hussein, M. A. (2006) *Cancer* **106**, 848-858
- Rinkenberger, J. L., Horning, S., Klocke, B., Roth, K., and Korsmeyer, S. J. (2000) Genes Dev 14, 23-27
- Roos, W. P., and Kaina, B. (2006) Trends Mol Med 12, 440-450
- Roos-Mattjus, P., Hopkins, K. M., Oestreich, A. J., Vroman, B. T., Johnson, K. L., Naylor, S., *et al.* (2003) *J Biol Chem* **278**, 24428-24437
- Rosenbaum, D. M., Degterev, A., David, J., Rosenbaum, P. S., Roth, S., Grotta, J. C., *et al.* (2010) *J Neurosci Res* 88, 1569-1576
- Ross, W. E., Glaubiger, D. L., and Kohn, K. W. (1978) Biochim Biophys Acta 519, 23-30
- Ross, W. E., and Bradley, M. O. (1981) Biochim Biophys Acta 654, 129-134
- Ruddon, R. W. (2007) *Cancer biology*, 4th edition ed., Oxford University Press, Oxford, New York
- Rudin, C. M., Kozloff, M., Hoffman, P. C., Edelman, M. J., Karnauskas, R., Tomek, R., *et al.* (2004) *J Clin Oncol* **22**, 1110-1117
- Salti, G. I., Das Gupta, T. K., and Constantinou, A. I. (2000) Anticancer Res 20, 3189-3193
- Samant, R., and Gooi, A. C. (2005) Can Fam Physician 51, 1496-1501
- Sancey, L., Garanger, E., Foillard, S., Schoehn, G., Hurbin, A., Albiges-Rizo, C., et al. (2009) Mol Ther 17, 837-843
- Saraste, A., and Pulkki, K. (2000) Cardiovasc Res 45, 528-537
- Scatena, M., Almeida, M., Chaisson, M. L., Fausto, N., Nicosia, R. F., and Giachelli, C. M. (1998) *J Cell Biol* 141, 1083-1093
- Schimmer, A. D., O'Brien, S., Kantarjian, H., Brandwein, J., Cheson, B. D., Minden, M. D., et al. (2008) Clin Cancer Res 14, 8295-8301
- Schlaepfer, D. D., Jones, K. C., and Hunter, T. (1998) Mol Cell Biol 18, 2571-2585
- Schlagbauer-Wadl, H., Klosner, G., Heere-Ress, E., Waltering, S., Moll, I., Wolff, K., et al. (2000) J Invest Dermatol 114, 725-730
- Schmitt, C. A., Rosenthal, C. T., and Lowe, S. W. (2000) Nat Med 6, 1029-1035
- Schwartz, M. A., and Assoian, R. K. (2001) J Cell Sci 114, 2553-2560
- Seyffart, G. (1991) *Drug dosage in renal insufficiency*, Kluwer Academic Publishers, Dordrecht, The Netherlands
- Shaham, J., Bomstein, Y., Meltzer, A., Kaufman, Z., Palma, E., and Ribak, J. (1996) *Carcinogenesis* 17, 121-125

- Shoemaker, A. R., Oleksijew, A., Bauch, J., Belli, B. A., Borre, T., Bruncko, M., et al. (2006) Cancer Res 66, 8731-8739
- Shoemaker, A. R., Mitten, M. J., Adickes, J., Ackler, S., Refici, M., Ferguson, D., et al. (2008) Clin Cancer Res 14, 3268-3277
- Shteynberg, D., Deutsch, E. W., Lam, H., Eng, J. K., Sun, Z., Tasman, N., *et al.* (2011) *Mol Cell Proteomics* **10**, M111 007690
- Shuker, S. B., Hajduk, P. J., Meadows, R. P., and Fesik, S. W. (1996) Science 274, 1531-1534
- Siegel, R., Naishadham, D., and Jemal, A. (2012) CA Cancer J Clin 62, 10-29
- Simunek, T., Sterba, M., Popelova, O., Adamcova, M., Hrdina, R., and Gersl, V. (2009) *Pharmacol Rep* **61**, 154-171
- Singh, R., and Lillard, J. W., Jr. (2009) *Exp Mol Pathol* 86, 215-223
- Sinha, B. K. (1980) Chem Biol Interact 30, 67-77
- Sinha, B. K., and Gregory, J. L. (1981) Biochem Pharmacol 30, 2626-2629
- Sinha, B. K., Trush, M. A., Kennedy, K. A., and Mimnaugh, E. G. (1984) *Cancer Res* 44, 2892-2896
- Siu, L. L., Von Hoff, D. D., Rephaeli, A., Izbicka, E., Cerna, C., Gomez, L., et al. (1998) Invest New Drugs 16, 113-119
- Siveski-Iliskovic, N., Hill, M., Chow, D. A., and Singal, P. K. (1995) Circulation 91, 10-15
- Sloan, E. K., Pouliot, N., Stanley, K. L., Chia, J., Moseley, J. M., Hards, D. K., et al. (2006) Breast Cancer Res 8, R20
- Slovak, M. L., Hoeltge, G. A., Dalton, W. S., and Trent, J. M. (1988) *Cancer Res* 48, 2793-2797
- Smith, P. J., Morgan, S. A., Fox, M. E., and Watson, J. V. (1990) *Biochem Pharmacol* 40, 2069-2078
- Soldi, R., Mitola, S., Strasly, M., Defilippi, P., Tarone, G., and Bussolino, F. (1999) *EMBO J* 18, 882-892
- Solomons, K., and Cochrane, J. W. (1984) S Afr Med J 66, 103-106
- Spanel, P., Smith, D., Holland, T. A., Al Singary, W., and Elder, J. B. (1999) Rapid Commun Mass Spectrom 13, 1354-1359
- Spencer, D. M., Bilardi, R. A., Koch, T. H., Post, G. C., Nafie, J. W., Kimura, K., et al. (2008) *Mutat Res* 638, 110-121
- Speyer, J. L., Green, M. D., Zeleniuch-Jacquotte, A., Wernz, J. C., Rey, M., Sanger, J., *et al.* (1992) *J Clin Oncol* **10**, 117-127
- Stathopoulos, G. P., Stergiou, G. S., Golematis, B., Thalassinos, N., and Fillipakis, M. (1995) Oncology **52**, 306-309
- Steinherz, L., and Steinherz, P. (1991) *Pediatrician* 18, 49-52
- Stellman, S. D., and Resnicow, K. (1997) *IARC Sci Publ* **138**, 229-250
- Strieth, S., Eichhorn, M. E., Sutter, A., Jonczyk, A., Berghaus, A., and Dellian, M. (2006) *Int J Cancer* **119**, 423-431
- Stupack, D. G., Puente, X. S., Boutsaboualoy, S., Storgard, C. M., and Cheresh, D. A. (2001) *J Cell Biol* **155**, 459-470
- Subramanian, R. R., Masters, S. C., Zhang, H., and Fu, H. (2001) Exp Cell Res 271, 142-151
- Sugahara, K. N., Teesalu, T., Karmali, P. P., Kotamraju, V. R., Agemy, L., Girard, O. M., *et al.* (2009) *Cancer Cell* **16**, 510-520
- Sugahara, K. N., Teesalu, T., Karmali, P. P., Kotamraju, V. R., Agemy, L., Greenwald, D. R., *et al.* (2010) *Science* **328**, 1031-1035
- Swain, S. M., Whaley, F. S., Gerber, M. C., Ewer, M. S., Bianchine, J. R., and Gams, R. A. (1997) J Clin Oncol 15, 1333-1340

Swain, S. M., and Vici, P. (2004) J Cancer Res Clin Oncol 130, 1-7

- Swerlick, R. A., Brown, E. J., Xu, Y., Lee, K. H., Manos, S., and Lawley, T. J. (1992) *J Invest Dermatol* **99**, 715-722
- Swift, L. P., Rephaeli, A., Nudelman, A., Phillips, D. R., and Cutts, S. M. (2006) *Cancer Res* 66, 4863-4871
- Taatjes, D. J., Gaudiano, G., Resing, K., and Koch, T. H. (1996) J Med Chem 39, 4135-4138
- Taatjes, D. J., Gaudiano, G., and Koch, T. H. (1997a) Chem Res Toxicol 10, 953-961
- Taatjes, D. J., Gaudiano, G., Resing, K., and Koch, T. H. (1997b) J Med Chem 40, 1276-1286
- Taatjes, D. J., Fenick, D. J., and Koch, T. H. (1998) J Med Chem 41, 1306-1314
- Taatjes, D. J., and Koch, T. H. (1999a) Anticancer Res 19, 1201-1208
- Taatjes, D. J., Fenick, D. J., and Koch, T. H. (1999b) Chem Res Toxicol 12, 588-596
- Tahir, S. K., Yang, X., Anderson, M. G., Morgan-Lappe, S. E., Sarthy, A. V., Chen, J., *et al.* (2007) *Cancer Res* 67, 1176-1183
- Takada, Y., Ye, X., and Simon, S. (2007) *Genome Biol* 8, 215
- Takaishi, M., Makino, T., Morohashi, M., and Huh, N. H. (2005) J Biol Chem 280, 4696-4703
- Tan, C., Tasaka, H., Yu, K. P., Murphy, M. L., and Karnofsky, D. A. (1967) *Cancer* **20**, 333-353
- Tan, C., Etcubanas, E., Wollner, N., Rosen, G., Gilladoga, A., Showel, J., et al. (1973) Cancer 32, 9-17
- Tanackovic, G., Ransijn, A., Thibault, P., Abou Elela, S., Klinck, R., Berson, E. L., *et al.* (2011) *Hum Mol Genet* **20**, 2116-2130
- Tarasenko, N., Nudelman, A., Tarasenko, I., Entin-Meer, M., Hass-Kogan, D., Inbal, A., et al. (2008) Clin Exp Metastasis 25, 703-716
- Tarasenko, N., Kessler-Icekson, G., Boer, P., Inbal, A., Schlesinger, H., Phillips, D. R., et al. (2010) Invest New Drugs 30, 130-143
- Tarasenko, N., Cutts, S. M., Phillips, D. R., Inbal, A., Nudelman, A., Kessler-Icekson, G., et al. (2012) PLoS One 7, e31393
- Teng, S., Beard, K., Pourahmad, J., Moridani, M., Easson, E., Poon, R., *et al.* (2001) *Chem Biol Interact* **130-132**, 285-296
- Tewey, K. M., Rowe, T. C., Yang, L., Halligan, B. D., and Liu, L. F. (1984) Science 226, 466-468
- Thompson, J., Finlayson, K., Salvo-Chirnside, E., MacDonald, D., McCulloch, J., Kerr, L., et al. (2008) Apoptosis 13, 394-403
- Thorndike, J., and Beck, W. S. (1977) Cancer Res 37, 1125-1132
- Tolcher, A. W., Chi, K., Kuhn, J., Gleave, M., Patnaik, A., Takimoto, C., *et al.* (2005) *Clin Cancer Res* **11**, 3854-3861
- Toscani, A., Soprano, D. R., and Soprano, K. J. (1988) Oncogene Res 3, 223-238
- Touzeau, C., Dousset, C., Bodet, L., Gomez-Bougie, P., Bonnaud, S., Moreau, A., et al. (2011) Clin Cancer Res 17, 5973-5981
- Trikha, M., Zhou, Z., Nemeth, J. A., Chen, Q., Sharp, C., Emmell, E., et al. (2004) Int J Cancer 110, 326-335
- Trudel, S., Li, Z. H., Rauw, J., Tiedemann, R. E., Wen, X. Y., and Stewart, A. K. (2007a) *Blood* **109**, 5430-5438
- Trudel, S., Stewart, A. K., Li, Z., Shu, Y., Liang, S. B., Trieu, Y., et al. (2007b) Clin Cancer Res 13, 621-629
- Tse, C., Shoemaker, A. R., Adickes, J., Anderson, M. G., Chen, J., Jin, S., *et al.* (2008) *Cancer Res* **68**, 3421-3428

Tsou, R., and Isik, F. F. (2001) Mol Cell Biochem 224, 81-89

- Tsujimoto, Y., Finger, L. R., Yunis, J., Nowell, P. C., and Croce, C. M. (1984) Science 226, 1097-1099
- Tsujimoto, Y., Cossman, J., Jaffe, E., and Croce, C. M. (1985) Science 228, 1440-1443
- Tzung, S. P., Kim, K. M., Basanez, G., Giedt, C. D., Simon, J., Zimmerberg, J., et al. (2001) Nat Cell Biol 3, 183-191
- Uchida, T., Imoto, M., Takahashi, Y., Odagawa, A., Sawa, T., Tatsuta, K., et al. (1988) J Antibiot (Tokyo) 41, 404-408
- Ueda, K., Cardarelli, C., Gottesman, M. M., and Pastan, I. (1987) *Proc Natl Acad Sci U S A* 84, 3004-3008
- Ulisse, S., Baldini, E., Sorrenti, S., and D'Armiento, M. (2009) *Curr Cancer Drug Targets* 9, 32-71
- Uren, R. T., Dewson, G., Chen, L., Coyne, S. C., Huang, D. C., Adams, J. M., et al. (2007) J Cell Biol 177, 277-287
- Vaclavikova, R., Kondrova, E., Ehrlichova, M., Boumendjel, A., Kovar, J., Stopka, P., et al. (2008) *Bioorg Med Chem* 16, 2034-2042
- Vairo, G., Innes, K. M., and Adams, J. M. (1996) Oncogene 13, 1511-1519
- Vakifahmetoglu, H., Olsson, M., and Zhivotovsky, B. (2008) Cell Death Differ 15, 1153-1162
- van Delft, M. F., Wei, A. H., Mason, K. D., Vandenberg, C. J., Chen, L., Czabotar, P. E., *et al.* (2006) *Cancer Cell* **10**, 389-399
- van Rosmalen, A., Cullinane, C., Cutts, S. M., and Phillips, D. R. (1995) *Nucleic Acids Res* 23, 42-50
- Vaux, D. L., Cory, S., and Adams, J. M. (1988) *Nature* 335, 440-442
- Veronese, F. M., and Pasut, G. (2005) Drug Discov Today 10, 1451-1458
- Vidali, G., Boffa, L. C., Bradbury, E. M., and Allfrey, V. G. (1978) *Proc Natl Acad Sci U S A* **75**, 2239-2243
- Vlahakis, N. E., Young, B. A., Atakilit, A., Hawkridge, A. E., Issaka, R. B., Boudreau, N., et al. (2007) J Biol Chem 282, 15187-15196
- Vogler, M., Dinsdale, D., Sun, X. M., Young, K. W., Butterworth, M., Nicotera, P., et al. (2008) Cell Death Differ 15, 820-830
- Vogler, M., Dinsdale, D., Dyer, M. J., and Cohen, G. M. (2009) Cell Death Differ 16, 360-367
- Von Hoff, D. D., Layard, M. W., Basa, P., Davis, H. L., Jr., Von Hoff, A. L., Rozencweig, M., et al. (1979) Ann Intern Med 91, 710-717
- Vuori, K., Hirai, H., Aizawa, S., and Ruoslahti, E. (1996) Mol Cell Biol 16, 2606-2613
- Walensky, L. D., Kung, A. L., Escher, I., Malia, T. J., Barbuto, S., Wright, R. D., et al. (2004) Science 305, 1466-1470
- Walensky, L. D., Pitter, K., Morash, J., Oh, K. J., Barbuto, S., Fisher, J., et al. (2006) Mol Cell 24, 199-210
- Walker, J. R., Sharma, A., Lytwyn, M., Bohonis, S., Thliveris, J., Singal, P. K., *et al.* (2011) *J Am Soc Echocardiogr* 24, 699-705
- Wang, A. H., Gao, Y. G., Liaw, Y. C., and Li, Y. K. (1991) Biochemistry 30, 3812-3815
- Wang, J. C. (1996) Annu Rev Biochem 65, 635-692
- Wang, J. L., Liu, D., Zhang, Z. J., Shan, S., Han, X., Srinivasula, S. M., et al. (2000) Proc Natl Acad Sci U S A 97, 7124-7129
- Wang, G. W., Klein, J. B., and Kang, Y. J. (2001) J Pharmacol Exp Ther 298, 461-468
- Wang, A. Z., Langer, R., and Farokhzad, O. C. (2012) Annu Rev Med 63, 185-198
- Warr, M. R., and Shore, G. C. (2008) Curr Mol Med 8, 138-147

- Watanabe, J., Kushihata, F., Honda, K., Mominoki, K., Matsuda, S., and Kobayashi, N. (2002) *Int J Oncol* **21**, 515-519
- Waters, J. S., Webb, A., Cunningham, D., Clarke, P. A., Raynaud, F., di Stefano, F., *et al.* (2000) *J Clin Oncol* **18**, 1812-1823
- Webb, C. D., Latham, M. D., Lock, R. B., and Sullivan, D. M. (1991) *Cancer Res* **51**, 6543-6549
- Weiss, R. B. (1992) Semin Oncol 19, 670-686
- Wilder, R. L. (2002) Ann Rheum Dis 61 ii96-99
- Willis, S. N., Chen, L., Dewson, G., Wei, A., Naik, E., Fletcher, J. I., *et al.* (2005) *Genes Dev* 19, 1294-1305
- Willis, S. N., Fletcher, J. I., Kaufmann, T., van Delft, M. F., Chen, L., Czabotar, P. E., *et al.* (2007) *Science* **315**, 856-859
- Wilson, J. W., Nostro, M. C., Balzi, M., Faraoni, P., Cianchi, F., Becciolini, A., *et al.* (2000) *Br J Cancer* **82**, 178-185
- Wilson, W. H., O'Connor, O. A., Czuczman, M. S., LaCasce, A. S., Gerecitano, J. F., Leonard, J. P., *et al.* (2010) *Lancet Oncol* **11**, 1149-1159
- Wolf, D., and Rotter, V. (1985) Proc Natl Acad Sci U S A 82, 790-794
- Wolter, K. G., Hsu, Y. T., Smith, C. L., Nechushtan, A., Xi, X. G., and Youle, R. J. (1997) *J Cell Biol* **139**, 1281-1292
- Wong, N. C., Mueller, B. M., Barbas, C. F., Ruminski, P., Quaranta, V., Lin, E. C., et al. (1998) Clin Exp Metastasis 16, 50-61
- Working, P. K., and Dayan, A. D. (1996) Hum Exp Toxicol 15, 751-785
- Wu, H. L., Hsu, C. Y., Liu, W. H., and Yung, B. Y. (1999) Int J Cancer 81, 923-929
- Wu, M. H., Chang, J. H., and Yung, B. Y. (2002) Carcinogenesis 23, 93-100
- Wu, Z., Meyer-Hoffert, U., Reithmayer, K., Paus, R., Hansmann, B., He, Y., et al. (2009) J Invest Dermatol 129, 1446-1458
- Xanthopoulos, J. M., Romano, A. E., and Majumdar, S. K. (2005) *J Biomed Biotechnol* **2005**, 10-19
- Xiong, J. P., Stehle, T., Zhang, R., Joachimiak, A., Frech, M., Goodman, S. L., *et al.* (2002) *Science* **296**, 151-155
- Xu, G., Zhang, W., Ma, M. K., and McLeod, H. L. (2002) Clin Cancer Res 8, 2605-2611
- Yamada, K. M., and Even-Ram, S. (2002) Nat Cell Biol 4, E75-76
- Yang, T., Kozopas, K. M., and Craig, R. W. (1995) J Cell Biol 128, 1173-1184
- Ye, K. (2005) Cancer Biol Ther 4, 918-923
- Yin, J., Brocher, J., Fischer, U., and Winkler, C. (2011) Mol Neurodegener 6, 56
- Yuan, L., Kawada, M., Havlioglu, N., Tang, H., and Wu, J. Y. (2005) J Neurosci 25, 748-757
- Zaidel-Bar, R., Itzkovitz, S., Ma'ayan, A., Iyengar, R., and Geiger, B. (2007) Nat Cell Biol 9, 858-867
- Zeman, S. M., Phillips, D. R., and Crothers, D. M. (1998) Proc Natl Acad Sci U S A 95, 11561-11565
- Zhai, D., Jin, C., Satterthwait, A. C., and Reed, J. C. (2006) Cell Death Differ 13, 1419-1421
- Zhang, L., Ming, L., and Yu, J. (2007) Drug Resist Updat 10, 207-217
- Zhang, H., Wu, S., and Xing, D. (2011) Apoptosis 16, 808-821
- Zheng, D. Q., Woodard, A. S., Fornaro, M., Tallini, G., and Languino, L. R. (1999) *Cancer Res* 59, 1655-1664
- Zhong, Q., Gao, W., Du, F., and Wang, X. (2005) Cell 121, 1085-1095
- Ziegler, U., and Groscurth, P. (2004) News Physiol Sci 19, 124-128
- Zimra, Y., Wasserman, L., Maron, L., Shaklai, M., Nudelman, A., and Rephaeli, A. (1997) J Cancer Res Clin Oncol 123, 152-160

Zong, W. X., Lindsten, T., Ross, A. J., MacGregor, G. R., and Thompson, C. B. (2001) Genes Dev 15, 1481-1486

Zou, L., Cortez, D., and Elledge, S. J. (2002) Genes Dev 16, 198-208